MOUSE MAST CELL PROTEASE 4 PROTECTS AGAINST ULTRAVIOLET-B INDUCED SKIN TUMOURIGENESIS

A thesis submitted in partial fulfillment of the PhD degree

in

School of Biological Sciences

Faculty of Science

The University of Adelaide

by

Houng Huy Taing

February 2017

Table of contents

Declaration

This work contains no material which has been accepted for the award of any other degree or diploma in any university or other tertiary institution to **Houng Huy Taing** and, to the best of my knowledge and belief, contains no material previously published or written by another person, except where due reference has been made in the text. I give consent to this copy of my thesis, when deposited in the University Library, being made available for loan and photocopying according to the provisions of the Copyright Act 1968. I also give permission for the digital version of my thesis to be made available on the web, via the digital research repository of the University of Adelaide, the Library catalogue, the Australasian Digital Theses Program and also through web search engines, unless permission has been granted by the University to restrict access for any unforeseen reasons. I acknowledge the support I have received for my research through the provision of an Australian Government Research Training Program Scholarship.

Houng Huy Taing

Abbreviations

1,2-DMH: 1,2-Dimethylhydrazine

Ab: antibody

Ag: antigen

αIIβ3: integrin and glycoprotein IIB

αMβ2: macrophage-1 antigen

α-MSH: alpha-melanocyte stimlating hormonse

APC: adenomatous polyposis coli

APS: ammonium persulphate

BCC: basal cell carcinoma

bFGF: basic fibroblast growth factor

BM: bone marrow

BMCMC: bone marrow-derived cultured MCs

BME: β-mercaptoethanol

BSA: bovine serum albumin

CCL: CC-chemokine ligand

cdh11: cadherin 11

cDNA: complementary DNA

CGRP: calcitonin-gene related peptide

CHS: contact hypersensitivity

CMP: common myeloid progenitor

col12α1: collagen XII

CPA3: carboxypeptidase A3

CTMC: connective tissue mast cell

DAG: diacylglycerol

DMBA: dimethylbenz[a]anthracene

DMEM: Dulbecco's modified eagle medium

DMSO: dimethyl sulphoxide

DNP-HSA: dinitrophenol-human serum albumin

DSC2: desmocollin2

DSG2: desmoglein2

ECL: enhance chemiluminescence

ECM: extracellular matrix

EGF: epidermal growth factor

EIA: enzyme immunoassays

ELISA: enzyme-linked immunosorbent assay

EMT: epithelial-mesenchymal transition

ERK: extracellular regulated kinase

EtOH: ethanol

fbln2: fibulin2

FBS: fetal bovine serum

FcERI: high afftinity IgE receptor

FGF: fibroblast growth factor

GAB2: GRB2-associated binding protein 2

GM-CSF: granulocyte macrophage-colony stimulating factor

GMP: granulocyte myeloid progenitor

H&E: Haemotoxylin and Eosin

HIV: human immunodeficiency virus

HPV: human papillomavirus

HRP: horse radish peroxidase

HSC: haematopoietic stem cells

i.d..: intradermal

i.p.: intraperitoneal

i.v.: intravenous

IFN: interferon

Ig: immunoglobulin

IL: interleukin

IP3: inositol-1,4,5-triphosphate

ITAM: immunoreceptor tyrosine-based activation motifs

JNK: c-Jun N-terminal kinase

KO: knockout

LAT: link for activation of T cells

LEC: lymphatic endothelial cell

LN: lymph node

LN_2: liquid nitrogen

Lox: lysyl oxidase

LT: leukotriene

LYVE-1 : lymphatic vessel endothelial hyaluronan receptor-1

mAb: monoclonal anitbody

MAPK: mitogen activated protein kinase

MC: mast cell

MC-CPA3: MC-derived carboxypeptidase A3

MC-IL-10: MC-dervied IL-10

MCP: mast cell progenitor

MC_T: tryptase expressing human MCs

MC_{TC}: tryptase and chymase expressing human MCs

MDSC: myeloid-derived supressor cells

MEK: MAPK kinase

MMC: mucosal mast cell

mMCP: mouse mast cell protease

MMP: matrix metalloproteinase

MQ: MilliQ

NF-κB: nuclear factor-κB

NGF: nerve growth factor

NK: natural killer

NMSC: non-melanoma skin cancer

O/N: overnight

PAF: platelet activating factor

PBS: phosphate buffered saline

PCA: passive cutaneous anaphylaxis

PDGF: platelet-dervied growth factor

Pen/Strep: Penicillin/Streptomycin

PG: prostaglandin

PI3K: phosphoinostitol 3-kinase

PKB: protein kinase B (AKT)

PKC: protein kinase C

PLA2: phospholipase A_2

PLCγ: phospholipase Cγ

PMA: phorbol-12 myristate-13 acetate

p-NAG: P-Nitrophenyl-N-acetyl-Beta-D-glucosaminide

Ptd(3,4,5)P3: phosphatidylinositol-3,4,5-triphophate

qRT-PCR: quantitative real-time PCR

RANTES: regulated on activation normal T cell expressed and secreted

rm: recombinant mouse

ROS: reactive oxygen species

RT-PCR: real-time polymerase chain reaction

SCC: squamous cell carcinoma

SCF: stem cell factor

SDS-PAGE: Sodium dodecyl sulfate polyacrylamide gel electrophoresis

Sl: steel

SMA: smooth muscle actin

SNP: single nucleotide polymorphism

SP: substance P

Srg: serglycin

TBST: tris-buffered saline

TEMED: Tetramethylethylenediamine

TGF: transforming growth factor

TLR: toll-like receptor

TNF: tumour necrosis factor

TPA: 12-O-tretradecanoylphorbol-13-acetate

TRAMP: transgenic adenocarcinoma of the mouse prostate

Treg: T regulartory cells

TSP-1: thrombospondin-1

UCA: urocanic acid

UV: ultraviolet

VCAM: vascular cell adhesion molecule

Vcan: versican

VEGF: vascular endothelial growth factor

VIP: vasoactive intestinal peptide

W: white spotting

WT: wild-type

Acknowledgements

First and foremost, I would like to thank my supervisors, A/Prof. Michele Grimbaldeston and A/Prof. Natasha Harvey for their constant guidance and support throughout my PhD study, especially Michele for offering me such a stimulating and challenging project and for demonstrating to me personally what scientific research is really about. A big thanks also goes to my postgraduate coordinator Prof. Shaun McColl for assistance toward the end of my PhD.

Thank you to the Pitson lab, especially Prof. Stuart Pitson and Dr. Briony Gliddon for taking me in, when no one else would. You gave me a second chance to experience research in a different environment, for that I am most grateful and appreciate all you have done for me. I wish you both as well as the lab all the best for the future.

Thank you to the current and past lab members of the Mast Cell lab; Dr. Anastasia Yu, Dr. Boris Fedoric, Dr Dave Yip, Dr Natasha Kolesnikoff, Nicholas Hauschild, Alicia Chenoweth, and Viera Stanekova, for the ongoing support and help when needed. Thank you again to A/Prof Natasha Harvey and the rest of the lymphatic development lab; Dr. Kelly Betterman, Dr. Genevieve Secker, Jan Kasenwadel and Dr. Drew Sutton for teaching me all that there is to know about lymphatics but also for the ongoing support and providing me help when I needed it the most. I'd also like to say thank you to our neighbouring lab, Dr. Michael Samuel for providing me advice but I'd like to say a big thank you especially to Dr. Anthony Pollard, Natasha Pyne and Dr. Jasreen Kular for always watching out for me, listening to me but most of all being extra supportive throughout my PhD candidature.

To the LSU ladies, Geraldine and Marianne, thank you both for always checking on me and seeing how my day was. You are both an indispensable team and I wouldn't know how the Centre for Cancer Biology would survive without the both of you. Thank you to the many current and past members of the CCB. Many of you have provided ongoing support for me and I appreciate every moment, thank you all again for looking out for me.

To my family, thank you mum and dad for putting up with me for the last 6 years. I know I may not have been the most appreciative son in the world, but thank you both for

supporting me and my career. Thank you both for working so hard and doing the long hours at the restaurant. You are both an inspiration and I'll never know anyone else that will work as hard as the both of you. Thank you both for allowing me to do what I needed to do, without the both of you I wouldn't be here but most importantly I wouldn't be the person I am today. Thank you to my older sister and brother Seay and Hieng for giving me advice when I needed it, thank you for cheering me up during the worst times but thank you most of all for supporting me but also bringing me up since I was young. I love you all for all you have done for me and will never forget your encouragement and advice. I will never forget our times at the restaurant, even though it was never the most peaceful place to be, I know in my heart it was our only way to spend time together and I will never forget it.

A big shout out also goes to our regular customers of Phuket Thai Resaturant, I cannot remember everyones names, but thank you to Geoff and Carol Lambert, Darryl and Moreene, Clive and Gloria, Bruce and Pauline and many others, thank you all for the ongoing support and always, always checking up on me.
I would also like to acknowledge my grandfather, grandmother, and auntie, who had passed away during my candidature. I miss you all, and wish you all eternal bliss and happiness in the afterlife, thank you for watching over me.

Lastly, to my partner Layla. It has been a rough journey for the both of us during our PhD's but we've finally almost made it. Thank you for always being by my side, for giving advice, for listening but most of all for being my partner. Without you, I would have never found my love for science and without you I would have never continued my studies in research. Thank you for all that you have done for me in the last 7 years, you will always be an inspiration in my eyes and I am so proud of you and what you have achieved for your career. I look forward to many more happy years together.

Thesis Summary

Excessive exposure to ultraviolet (UV)-B radiation (290-320 nm), a component of sunlight, is considered the major etiological factor in skin cancer, causing detrimental alterations in the patterns of tissue remodelling processes, inflammation, angiogenesis and lymphangiogenesis. An accumulation of mast cells (MCs) in the peri-tumoural stroma is typically a hallmark feature; this has given rise to the important question of whether MCs at the peri-lesional interface function to provide a permissive tumourigenic environment or to guard against rapid neoplastic progression.

Recently, we discovered that MCs can negatively regulate inflammatory responses caused by chronic low-dose UVB irradiation of the skin (levels which cause skin damage and not induce tumours), via a pathway involving the immunomodulatory agent vitamin D_3 and MC-derived interleukin (MC-IL)-10. Our current studies highlight that mouse mast cell protease 4 (mMCP4), the functional homologue of human MC chymase, is an important MC-specific mediator that can provide an additional protective mechanism against detrimental UVB-induced skin pathology. By implementing chronic high doses and excessive exposures of UVB that cause skin tumourigenesis, we demonstrate that MC-deficient c-*kit* mutant *Kit*$^{W/W\text{-}v}$ mice engrafted with bone marrow-derived cultured mast cells (BMCMCs) from *mMCP4*$^{-/-}$ mice yield higher rates of UVB-induced ear ulceration and *in situ* SCCs than wild-type BMCMC-engrafted *Kit*$^{W/W\text{-}v}$ mice.

Interestingly, in response to extensive chronic UVB irradiation, not only *mMCP4*$^{-/-}$ BMCMC→*Kit*$^{W/W\text{-}v}$ mice, but also our non-pigmented *Tyr*$^{c\text{-}2j}$–*mMCP4*$^{-/-}$ mice, exhibit extensive lymphatic vessel dilation in their UVB-exposed ears compared to the experimental wild-type counterparts, thereby suggesting a potential role of mMCP4 and its substrates in governing protection against pathological lymph vessel dysfunction at critical stages during skin tumourigenesis. Moreover, microarray studies demonstrated that the loss of mMCP4 causes global changes in mRNA expression in multiple pathways especially upregulation of genes involved in cell migration and in the extracellular matrix (ECM)

Taken together, our data provides an important mechanistic insight into the beneficial function of dermal MCs and mMCP4 at distinct checkpoints in a setting of UVB irradiation driven epidermal neoplasia.

Chapter 1

LITERATURE REVIEW

1.1 Mast cell biology

Mast cells (MC) were first discovered in human tissue by Paul Ehrlich in 1878 and named "mastzellen" due to their abundance of large electron dense granules with metachromatic staining properties[1,2]. In addition to their staining characteristics and morphological features, MCs are identified by their cell surface expression of the high-affinity receptor, FcεRI (high affinity for immunoglobulin [Ig]E) and c-*kit* (CD117; receptor for stem cell factor [SCF]). Since their discovery, our knowledge of MCs has expanded dramatically. MCs are found throughout the body particularly at sites that are exposed to the environment and they exhibit heterogeneity and plasticity depending on the environmental cues they are exposed to. What has also been of great interest is their roles and involvement in both physiological and pathophysiological conditions, particularly in IgE-dependent diseases settings such as asthma, atopic dermatitis and anaphylaxis[3]. Although the contribution of MCs in allergic settings is well recognised, their roles in prominent diseases like cancer are less well understood[4]. Historically, MCs have gained notoriety due to their ability to exacerbate immune responses in certain pathological settings such as anaphylaxis. Interestingly, recent developments in the MC field suggest that MCs also exhibit anti-inflammatory functions in numerous disease models[5-7]. Our recent study has demonstrated the role of MCs and their mediators[8-10] in suppressing inflammation, and these studies have opened a new field of research to understand and utilise and even manipulate MCs functions for therapeutic use.

1.1.1 MC progeny and tissue distribution

Human MC progenitors are derived from $CD34^+$ haematopoietic stem cells (HSC) in the bone marrow (BM) and are found as immature MC progenitors (MCP; $CD34^+CD117^+CD13^+CD14^-$) in circulation[11]. Once human MCPs reach their specific anatomical location they will mature and differentiate into MCs that exhibit specific phenotypes with distinct expression profiles of mediators, receptors and other features that reflect the environmental milieu[12,13].

In mice, mast cell development progresses through the following stages. The myeloid lineage of Kit^+Sca1^+ HSCs differentiate into $Kit^+Sca1^{lo}FcγRII^{lo}FcγRIII^{lo}$ common myeloid progenitor (CMP) and then to the $Kit^+Sca1^-FcγRIII/III^{hi}$ granulocyte monocyte progenitor (GMP), which gives rise to all granulocytes, neutrophils, basophils,

eosinophils and macrophages. Mouse MCPs were initially suggested to be only originated from GMPs[14,15]. Later studies, however, have demonstrated that MCPs originate directly from either HSCs, or CMPs[16-18]. Interestingly, Chen *et al.*, discovered a megakaryocytic/erythrocyte MCP lineage ($Lin^{-}c\text{-}kit^{+}Sca\text{-}1^{-}Ly6c^{-}Fc\varepsilon RI^{-}CD27^{-}\beta7^{+}T1/ST2^{+}$) in the BM of adult C57BL/6 mice[13], and this lineage was found to originate from the $Kit^{+}Sca^{lo}$ CMP population. A follow-up study by Franco *et al*., redefined this population and confirmed that MC progenitors could indeed be independently derived from the CMPs rather than just the GMPs[19].

As explained above, mouse and human MCPs circulate as immature progenitors in the blood until they reach the specific anatomical location[18]. Typically, mature MCs are localised in areas of connective tissue, mucosal sites, and vascularised organs in which they will ultimately reside (including skin, peritoneum, airway and gastrointestinal tract), where they are in close proximity to blood and lymphatic vessels as well as exposed to the environment[3,18]. At these sites, growth factors like SCF and interleukin (IL)-3 play a crucial role for the growth and development of MCPs into mature MCs[20]. To facilitate the migration of MCPs to their specific anatomical sites, they are normally guided by chemotactic factors, and bind to adhesion molecules such as vascular cell adhesion molecule (VCAM-1) and E-selectin expressed by specific tissues[21-23].

1.1.2 MC homing and trafficking

1.1.2.1 MC progenitor homing

Due to the low numbers of progenitor cells *in situ*, the exact mechanisms of how these MCPs localise to various sites of tissues is still under investigation[24,25]. It is understood that, like leukocytes, the homing of MCPs is dependent on chemokines and integrins, and the requirements of these chemotactic factors and their receptors may vary depending on the organ of interest[26,27,28].

The migration of MCPs toward the intestine requires the chemokine receptor CXCR2, as suggested by a significant decrease in the number of MCPs observed in the intestines of CXCR2-deficient mice[23]. Recent studies have also implicated that α4β7 integrin is required for MCP migration. This is consistent with observations that both the loss of α4β7 and blocking the binding of α4β7-specific ligands MadCAM-1 and VCAM-1 result in a deficiency in MCP populations in the intestine[21,29]. Furthermore, human MCPs

require expression of α4β1 integrin to facilitate adhesion to VCAM-1 and E-selectin expressing endothelial cells of the mucosa[30].

Although homing of MCPs to the skin is not yet clearly understood, recent findings demonstrate that homing of MCPs to the peritoneum is dependent on integrins such as macrophage-1 antigen (αMβ2) integrin and glycoprotein IIb (αIIbβ3). Mice lacking these specific integrins show a significant reduction (~50-70%) in peritoneal MCs, while the number of peritoneal MCs in the spleens and intestine were not affected[31-33]. Additional factors including MC-derived tumour necrosis factor (TNF)α are also crucial in the up-regulation of the adhesion molecule VCAM-1 and facilitate binding to α4β7 integrins[34]. Furthermore, intradermal (*i.d.*) injected leukotriene (LT) B4, can recruit MCPs to peripheral tissues, via its receptor LTB1a that is not expressed on mature MCs[24].

Once reaching their specific anatomical site in which they will reside, MCPs mature and differentiate, and exhibit different phenotypic characteristics. This process is highly influenced by the localisation and the surrounding environmental cues of these cells[35,36].

1.1.2.2 Mature MC trafficking

Mature and differentiated MCs are rarely found in the circulation of healthy individuals, but they have been found present in the blood stream of patients suffering from systemic mastocytosis[37], a condition where MCs have attained activating mutations in the *c-kit* receptor that promote uncontrollable proliferation, activation and degranulation of MCs[38,39]. Recent studies indicate that MCs can migrate to distant sites via the guidance of certain mediators. These include chemokines such as monocyte chemotactic factor (MCP-1/CC-chemokine ligand [CCL]2)[40,41] and Regulated on Activation Normal T cell Expressed and Secreted (RANTES/CCL5)[41,42]. Other mediators involved in MC trafficking include anaphylatoxins C3a and C5a[43,44], prostaglandins (PG)D2 and PGE2[45,46] as well as cytokines such as transforming growth factor (TGF)β[47,48] and SCF[49,50]. Blocking of the TNFα and IL-6 receptors expressed on rat peritoneal MCs also inhibited the TNFα and IL-6 induced chemotaxis of MCs[51,52]. In addition, a more recent study has shown the CXCR4 antagonist AMD3100 is able to block the migration of dermal MCs from the skin to the draining lymph nodes following chronic UVB irradiation[53,54].

1.1.3 MC heterogeneity

MCs exhibit different phenotypes depending on the localisation and environmental cues they are exposed. In mice, there are two subsets of MCs; connective tissue mast cells (CTMC), which are generally found in the dermis of the skin or peritoneum[55,56] and mucosal MCs (MMC), which are typically localised in the mucosa linings of the lungs or gut[55]. In addition to their distinct anatomical site, these two subsets of MCs can also be differentiated by the expression profile of their granular content, such as MC-specific neutral proteases (mMCP). CTMCs express α– and β–chymases (mMCP4 and 5, mMCP9 [only in uterine localised MCs]), and β-tryptase mMCP6 as well as MC-carboxypeptidase A (MC-CPA3), while MMCs predominantly express tetrameric β-tryptases (mMCP6 and mMCP7) and β–chymases (mMCP1 and mMCP2)[57,58]. In addition, MMCs typically produce cysteinyl leukotrienes LTD4 and LTB4 and prostanoids PGD2[59], whereas CTMCs primarily produce prostanoids[60].

Similar to mice, human MCs also exhibit a degree of heterogeneity. The two subsets of human MCs are classified by their protease composition. MCs found in the skin or intestinal mucosa are classified as MC_{TC}, and they express two classes of (α & β) tryptase, one (β) chymase and one MC-CPA3[61-63]. The other subtype, which are normally present in mucosal surfaces in the lung and gut, expresses only (α & β) tryptase but not chymase. Hence these cells are classified as MC_T[63]. Furthermore, like mouse MCs, MC_T appear to express only leukotrienes[64], while MC_{TC} express prostanoids[65].

As stated above, MC heterogeneity is conferred by their ability to express certain profiles of proteases according to the particular environmental cues they encounter in their residential tissues[66]. This was further supported by a study demonstrating that when mouse BM-derived cultured MCs (BMCMC) and cultured peritoneal MCs from (WB/ReJ×C57BL/6)F_1 (WBB6F_1) wild-type (WT) mice (both expressing mMCP1, 2, 4, 5, and 6) were transplanted into the stomach wall of MC-deficient WBB6F_1-*Kit*$^{W/W\text{-}v}$ mice, they appeared in both mucosa (with down-regulated mMCP1, 4, 5 and 6) and muscularis propria (with down-regulated mMCP1 and 2). On the other hand, when fully differentiated peritoneal MCs from WT mice (expressing mMCP2, 4, 5 and 6) were transplanted, they adopted the stomach mucosa profile by down-regulating mMCP4, 5 and 6[67].

1.1.4 MC development and maturation

MCs mature and differentiate into distinct subtypes depending on the growth factors present in their residential environment. One of the main factors that directs their development and maturation is SCF, a growth factor that plays crucial roles in haematopoiesis[68]. The dependency of SCF for MC development and maturation is crucial not only in humans but also in mice[68-70]. This is supported by the *in vivo* findings that mutations of SCF or c-*kit* receptor (mutations in both *steel* (*Sl)* and *white spotting* (*W) locus in mice)* have significant effects on MC populations, among other deficiencies such as gametogenesis, melanogenesis, and haematopoiesis[71-74]. In humans, mutations in the c-*kit* gene is associated with abnormalities in pigmentation, such as piebladism[75,76]. Other studies have also reported associations between c-*kit* mutations and rare disease of mastocytosis[77] and tumour growth and gastric and lung cancers[78,79].

A number of other cytokines are also important for MC development and/or maturation. In mice, the T cell-derived cytokine IL-3 is important for the proliferation of mouse BMCMC populations from the spleen, intestine and bone marrow[13,17,55]. In comparison, MCs that exhibit a more connective tissue like phenotype *in vitro* require other factors such as SCF and/or IL-4[80-82]. It is worth noting that IL-10, a well-known anti-inflammatory cytokine, is also an enhancer for the growth of MCs. Although IL-10 by itself does not promote proliferation of MCs, it has synergistic effects with IL-3, SCF, or IL-4 in the proliferation of mouse BMCMCs[82]. On the other hand, culturing human MCs *in vitro* requires SCF and IL-6. In the presence of these cytokines, MCs populations can be cultured from human cord blood-derived mononuclear cells, $CD34^+$ HSCs and also peripheral blood MCPs[20,69,82-84].

1.1.5 MC activation/degranulation

MCs can be activated by a variety of means, but the most well-known and characterised route is through the antigen (Ag) + IgE-dependent pathway. The majority of MCs in the body are sensitised by circulating IgE bound to the high affinity receptor FcεRI[3]. When FcεRI-bound IgE encounters specific multivalent Ag, this leads to crosslinking of the IgE molecules and aggregation of the FcεRI receptors. Ultimately, this results in MC activation and degranulation, which is a highly controlled release of its granular contents[85]. Depending on the type but also the magnitude of the stimulus, MCs can release

all of their granular contents via exocytosis or gradually and selectively through piecemeal degranulation[86]. Furthermore, MCs are capable of participating in multiple cycles of activation and degranulation.

MCs express a wide array of receptors, hence can be activated by a variety of other stimuli, including SCF[49,87], cytokines such as IL-1, IL-3 and granulocyte macrophage-colony stimulating factor (GM-CSF)[88,89], and chemokines such as CCL3[90]. Other factors that can activate MCs include bacterial-induced anaphylatoxins such as C3a and C5a[91,92], neuropeptides such as substance P (SP) and calcitonin gene-related peptide (CGRP)[93-95], as well as pathogen-derived Ags that signal through toll-like receptors (TLR)s, TLR-2, -3, -4, -7 and -9[96-98]. Unlike IgE + surface Ag-mediated activation, activation of MC by non-IgE-related stimuli does not always lead to a complete degranulation and release of all mediators. Instead, selective and differential release of mediators can occur. In human MCs, IL-1α can induce the degranulation-independent release of IL-6[99]. PGE2 has also been reported to promote release of the chemokine CCL2[100]. Other factors like the neuropeptide CGRP triggers piecemeal secretion of the MC-specific protease mMCP-1 from mouse BMCMCs[95]. Furthermore, monomeric IgE, in the absence of surface Ag stimulation, can also activate mouse BMCMCs and induce the production of pro-inflammatory cytokines, such as TNFα, IL-6, IL-4 and IL-13[101].

1.1.6 MC mediators

The mediators released upon MC activation and degranulation fall into three categories; 1) pre-formed mediators, 2) lipid derived mediators and 3) cytokines, chemokines and growth factors.

1.1.6.1 Preformed MC mediators

Preformed MC mediators are packed into the cytoplasmic granules and are the first to be released upon MC activation, especially in the IgE-dependent pathways. These mediators include biogenic amines, neutral proteases and proteoglycans. Notably, the expression profile of pre-formed mediators differs depending on the residential localisation and phenotype of the MCs.

1.1.6.1.1 Biogenic amines

Serotonin and histamine are both the most well characterised biogenic amines released by MCs. Both of these mediators are not only involved in MC-mediated signalling to nerve endings, they also exhibit their own unique roles. Histamine is well known to be involved in regulating inflammatory responses by promoting vasodilation of blood vessels, contraction of smooth muscle, but also induces immunosuppression of contact hypersensitivity responses[102-105]. Serotonin, on the other hand, is suggested to be involved in immunological processes via promoting proliferation and function of T cells as well as other immune cell types[106].

1.1.6.1.2 Proteases

Proteases constitute another group of preformed mediators found in the dense granules of MCs. The MC-specific neutral proteases are of interest due to their complexity and significance in a number of disease settings[57], and they can be divided into three categories which include tryptases, chymases, and the zinc-dependent matrix metalloproteinase MC-CPA3; reviewed in[85]. In addition to MC-specific neutral proteases, non MC-specific proteases such as granzymes, cathepsins, lysozymes and the family of Zn^{+} and Ca^{2+} - dependent matrix metalloproteinases (MMP)[107] can also be found in the granules of MCs.

1.1.6.1.3 Tryptases

Mast cell tryptases are tetrameric serine proteases that have trypsin-like cleavage specificity (Lysine/Arginine residues). Human MCs primarily express two classes of secreted tryptases (α and β) and three subtypes of β tryptases exist (βI, βII and βIII)[108]. Another class of tryptase (γ) has also been found to be expressed on the surface of human MCs after degranualation[109]. In mice, CTMCs express two types of tryptases, mMCP6 and mMCP7. Like that observed in human MCs, an additional γ–tryptase that is expressed on the cell surface of mouse MCs. To study the biological function of tryptase, many approaches have been utilised including usage of purified or recombinant tryptases and also the use of tryptase inhibitors in animal disease models[63,110]. Recently, Thakurdas *et al*., generated an mMCP6-deficient mouse model, which provides a more specific approach for defining the role of mast cell tryptases *in vivo*.

1.1.6.1.4 Chymase

Chymases are monomeric enzymes that exhibit chymotrypsin-like activities (cleave aromatic residues) and they are the most well characterised MC-specific proteases. The chymase protein is synthesised as a precursor that is inactive due to the binding of acidic dipeptide. Cleavage of the acidic dipeptide by depeptidylpeptidase results in conformational change and the subsequent activation of the chymase[111]. The activated chymase is then stored in granules. As stated previously, only one α-chymase is expressed in human MCs. By contrast, mouse MCs express four different kinds of β-chymases; mMCP1, mMCP2, mMCP4 and mMCP9 (only expressed in uterus) and one α-chymase; mMCP5. Among the different subtypes of mMCPs, mMCP4 is considered the functional mouse homologue of human chymase, based on the expression profile and substrate specificities[57,61,62,112].

1.1.6.1.5 MC-CPA3

MC-CPA3 exhibits exopeptidase-like activity (cleaves amino acid on the C-terminal ends)[63] and it is the least known member in the three classes of MC-specific proteases. MC-CPA3 has been shown to play a role in regulating innate immune responses by degrading toxins such as endothelin-1 and snake venom[113]. In addition, increasing expression of MC-CPA3 has been associated with tumour progression in a mouse model of chemical-induced skin carcinogenesis[114]. Notably, only one CPA3 has been identified so far across all species, and the expression profile, as well as structural and functional properties of MC-CPA3 are conserved between human and mice[115,116]. Therefore, it is less of an issue to compare the function of MC-CPA3 between mice and humans, in contrast to chymases and tryptases. Interestingly, although basophils exhibit a distinct expression profile of proteases (preferentially mMCP8 and 11) compared to MCs, they can also express CPA3[117-119].

1.1.6.1.6 Proteoglycans

Proteoglycans are core proteins with glycoaminoclycan side chains, and they constitute another class of preformed MC mediators, which are normally released in conjunction with other mediators such as neutral MC proteases. Proteoglycans are expressed by most cell types, and they are localised either on the cell surface where they act as co-receptors (syndecan, glypican), or exist in extracellular compartments such as the cartilage or

basement membranes (aggrecan, perlican)[35,120-122]. Serglycin (Srg), an intracellular proteoglycan highly expressed by MCs[36,123] has been implicated to be critical in mediating the storage of MC granules and MC-protease function[36]. Srg can be released upon MC degranulation, or exist in complex with other mediators including MC-chymase, MC-CPA3 and also granzyme B[124]. The attachment of proteases to Srg is thought to be required to prevent them from diffusing away from the site of degranulation, hence improving presentation of cytokines/chemokines to targeted cells. Srg can also potentially bind to inflammatory compounds that exhibit heparin binding properties and allow more advantageous targeting by bound proteases[35,36].

Interestingly, TNFα is another preformed mediator that is stored in the granules of MCs. When released, TNFα can serve as an immediate source of cytokine to promote inflammatory responses efficiently and effectively, particularly in IgE-dependent responses[125].

1.1.6.2 Lipid derived mediators

In addition to the release of preformed mediators, the *de novo* generation of lipid-derived mediators can also occur in MCs, typically within min to hr after IgE + surface Ag activation[126,127]. Through the cleavage of arachidonic acids from membrane phospholipids, two types of lipid-derived mediators are generated. These include prostaglandins PGD2 and leukotrienes (including LTC4 and LTB4). The production of prostaglandins begins with metabolism of arachidonic acids by cyclooxygenase enzymes. This produces PGH2, which then serves as a substrate for the production of either prostaglandin or thromboxane. Upon activation, MCs typically express the enzyme prostaglandin D synthase, which then produces PGD2 in large quantities to promote chemotaxis of leukocytes in allergy[128,129] and vasodilation in asthma[130]. The production of leukotrienes follows a similar pathway but through different enzymes. Cytosolic phospholipase A2, 5-lipoxygenase and LTA4 enzymes are capable of generating all leukotrienes including LTB4 and LTC4, which undergo further processing by LTC4 synthase[131]. LTB4 is a potent chemoattractant that can recruit leukocytes, macrophages, eosinophils, macrophages and monocytes[132-134]. As previously mentioned, LTB4 can also recruit immature MCPs to peripheral tissues[24].

1.1.6.3 Cytokines/chemokines

Within one hour of MC activation, following the production of leukotrienes and prostaglandins, *de novo* synthesis of cytokines, chemokines and growth factors can occur. Cytokines are immunomodulatory mediators secreted by specific cells that carry functional signals locally to other cells via engagement of cytokine receptors on target cells. Chemokines, on the other hand, exhibit chemotactic properties and regulate recruitment of specific cell types that express the corresponding surface receptors. MCs are capable of producing an array of different cytokines, chemokines and growth factors that stimulate a plethora of different functions; these factors include, but are not limited to, IL-2, IL-3, IL-4, IL-6, IL-8, IL-10, IL-13, interferon (IFN)-γ, TGF-β, GM-CSF, basic fibroblast growth factor (bFGF) and nerve growth factor (NGF)[135-137]. Production of growth factors, such as IL-3 and IL-4, is crucial for MC development both *in vivo* and *in vitro*[80,138]. MCs can also express chemokines such as CCL2 and CCL5[40-42], which are capable of recruiting macrophages and monocytes, while IL-8 recruits neutrophils[139]. The production of the anti-inflammatory cytokine IL-10 has also been shown to be important in limiting inflammatory responses[8,9]. The complexity of MC mediators reflects its differential roles in regulating the immune responses, suggesting that MCs are capable of eliciting distinct functions in different disease settings via the release of specific mediators. However, the exact mechanism of this complicated system is yet to be further investigated.

1.1.7 Mast cell signalling

1.1.7.1 FcεRI signalling

FcεRI receptors are composed of one α-subunit, one β-subunit and two γ-subunits. Of these subunits the α-subunit permits specific binding to IgE, while the β- and γ-subunits contain immunoreceptor tyrosine-based activation motifs (ITAM). Upon crosslinking and aggregation of the FcεRI receptors, ITAMs undergo autophosphorylation, as well as recruitment, and phosphorylation of other tyrosine kinases Fyn, Lyn and Syk[140]. As a result, this leads to phosphorylation of adaptor proteins, link for activation of T cells (LAT) and GRB2-associated binding protein 2 (GAB2), followed by the activation of phospholipase Cγ (PLCγ) and phosphoinositol 3-kinase (PI3K)[141]. Subsequent phosphorylation events result in the production of diacylglycerol (DAG), inositol-1,4,5-

triphosphate (IP3) and phosphatidylinositol-3,4,5-triphosphate (Ptd(3,4,5)P3) which leads to Ca^{2+} mobilisation and the activation of protein kinase C (PKC), which ultimately results in degranulation and the release of MC granular contents[142,143].

In addition, phosphorylated Syk can also initiate the RAS-mitogen-activated protein kinase (MAPK) signalling cascade[140,144,145]. The RAS-MAPK pathway, consisted of RAS, RAF, MAPK kinase (MEK) and MAPKs (e.g. extracellular signal regulated kinase [ERK]1/2, c-Jun N-terminal kinase [JNK] and p38), activates a variety of transcription factors as well as phospholipase A_2 (PLA_2, which participates in arachidonic acid metabolism), thereby regulating the synthesis of protein and lipid-derived mediators, respectively[141,146,147]. Furthermore, production of Ptd(3,4,5)P3 can also regulate other proteins such as Bruton's tyrosine kinase (Btk) and protein kinase B (PKB, [AKT]) which are important in the direct or indirect activation of nuclear factor-κB (NF-κB) and transcription of pro-inflammatory cytokines[148,149].

1.1.7.2 c-kit signalling

In addition to FcεRI signalling, MCs are also dependent on the *c-kit* receptor for growth, development survival activation, as well as immune regulatory function[150,151]. The c-*kit* receptor is a type III tyrosine kinase receptor, and it is a member of the tyrosine kinase superfamily[152]. Engagement of the c-*kit* receptor by its ligand SCF leads to dimerisation of the receptor, which results in activation of the split tyrosine kinase domain in the C-terminus[152]. Upon activation of c-*kit*, phosphorylated residues in the C-terminal domain provide docking sites for associating signalling molecules, similar to the FcεRI signalling pathway. These include PLCγ, the p85 subunit of PI3K, Fyn, Lyn[152-155], AKT, MAPK and BTK[156,157]. Furthermore, this important role of *c-kit* receptor is also supported by the synergistic effect of SCF and IgE + surface Ag activation in enhancing MC responses[157]. It is important to note that since the IgE bound Ag is not required in c-*kit* signalling, this pathway can be activated and play crucial roles in disease settings such as cancer[49,158,159] (**Figure 1.1**). In the context of UVB irradiation, it is known that UVB can also activate the SCF/c-kit signalosome[160], including activating PLCγ in human lymphocytes[161], p38 MAPK pathway[162,163] and PI3K/AKT pathway[164].

Figure 1.1 FcεRI and c-*kit* receptor signalling in mast cells.
Cross-linking of FcεRI receptors results in phosphorylation of tyrosine kinases Fyn, Lyn and Syk. Phosphorylation of these tyrosine kinases activates downstream signalling molecules such as PLCγ, MAPK and PLA_2. IgE-independent c-*kit* receptor activation results in similar activation of signalling molecules. See text for more details. Adapted from Gilfillan *et al*[159].

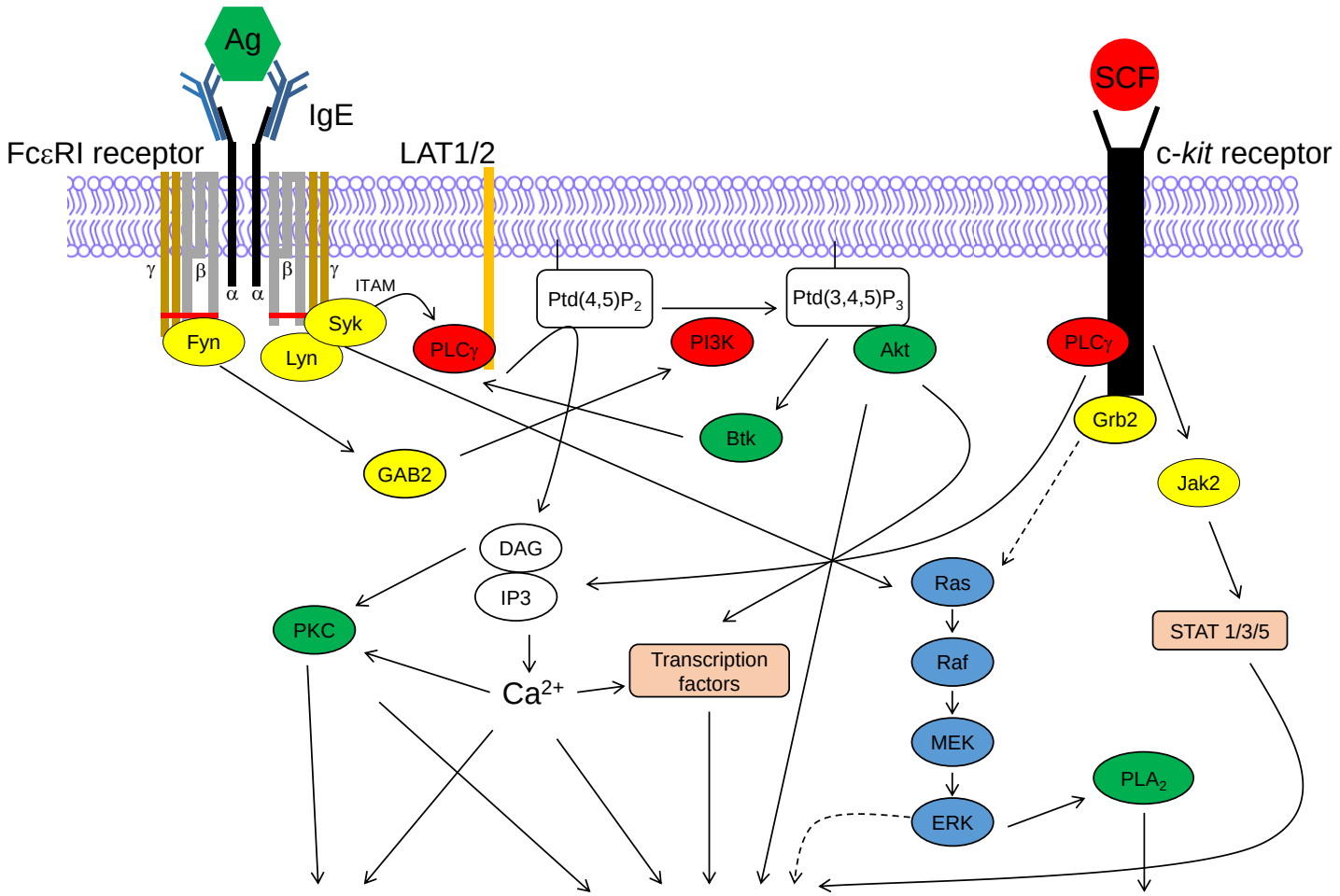

DEGRANULATION
- Preformed Mediators
- Biogenic amines
- Proteases
- TNF, IL-15

GENE TRANSCRIPTION
-Cytokine synthesis
-Chemokine synthesis
-MC growth/survival
-MC migration/adhesion

ARACHADONIC ACID METABOLISM
- Prostanoids
- Leukotrienes
-Platelet-derived factors

1.1.8 Tools used to investigate MC function *in vitro*

The advancement of technologies and research techniques has allowed better understanding of MCs. However, this process is typically labour intensive and the procedures of MC extraction and enrichment can at times change the phenotype of the MCs and, more importantly, disrupt their interactions with other cell types. To overcome some of these issues, numerous MC cell lines have been generated, including human cell lines such as HMC-1, LAD1 and LAD2[66]. The HMC-1 cell line was established from the peripheral blood of patients diagnosed with MC leukaemia[165]. However, this cell line exhibits non-physiological characteristics including SCF-independent growth, lack of well-formed granules and dysfunctional IgE receptors, and they are more similar to immature MCs[165]. LAD-1 and LAD-2 cell lines were derived from bone marrow aspirates of a patient diagnosed with MC sarcoma/leukaemia[166]. These cells lines exhibit more physiological characteristics including; numerous well-formed granules, respond and activate in response to IgE-dependent stimuli and are SCF-factor dependent for cell growth and survival[166]. Cell lines from rats (RBL-2H3) and mice (MC-9 and Cl.MC/C57.1) have also been developed to determine the biological roles of MCs[66,167]. It is important to note that cell lines are prone to phenotypic alterations due to accumulated mutations, following long-term culturing in the laboratory. MCs derived from bone marrow and other tissues of mice can be cultured using conditioned media. Within the conditioned media, one of the most critical factors required for mouse MC proliferation is T-cell-derived IL-3[168]. Mouse BMCMCs cultured in IL-3 were initially thought to attain a MMC-like phenotype. However, it is now understood that these MCs are more heterogeneous and are actually immature. It was also found that their phenotype could still be altered when co-cultured with fibroblasts in the presence of IL-3[169]. It was later discovered that the fibroblast-derived factor SCF was a critical MC survival factor in mice, and also the key to driving BMCMCs to attain a more connective tissue like phenotype[170-172].

1.1.8 Tools employed to investigate MC functions *in vivo*

The role of MCs in the development and progression of a particular human disease is generally assessed by comparing the number of MCs and/or the level of their released mediators between normal and pathological tissues. Mouse models have also been developed to investigate the contribution of MCs to the pathology of various diseases.

The use of *c-kit* mutant mice that have a profound reduction in MC populations, together with the ever-increasing number of other mouse models of human diseases, has enabled the *in vivo* assessment of MCs[73,173]. There are currently two widely used MC deficiency models: the (WB/ReJ×C57BL/6)F_1-*Kit*$^{W/W\text{-}v}$ (*i.e.* WBB6F_1-*Kit*$^{W/W\text{-}v}$) mice and the C57BL/6-*Kit*$^{W\text{-}sh/W\text{-}sh}$ mice[174]. WBB6F_1- *Kit*$^{W/W\text{-}v}$ mice have multiple mutations in the (W) white spotting locus on chromosome 5 which encodes the CD117 (c-*kit*) receptor. *Kit*^{W} corresponds to a heterozygous mutation causing exon skipping and the resulting cell surface expression of a truncated c-*kit*, while *Kit*$^{W\text{-}v}$ corresponds to mutations in the tyrosine kinase domain of c-*kit* which causes reduced c-kit signalling. On the other hand, C57BL/6-*Kit*$^{W\text{-}sh/W\text{-}sh}$ mice contain an inversion mutation that affects the transcriptional regulatory element upstream of the *c-kit* transcription start site on chromosome 5. Both strains are severely MC-deficient due to the specific mutations in the c-*kit* receptors, but they display distinct additional abnormalities. WBB6F_1-*Kit*$^{W/W\text{-}v}$ mice have a deficiency in melanocyte populations, and are known to have macrocytic anaemia, sterility, reduced numbers of BM and blood neutrophils, and lack of interstitial cells of Cajal as well as T cell receptor (TCR)γδ cells in the small intestine; and, for the latter, enlarged spleen, mild cardiomegaly, and increased numbers of BM and blood neutrophils[174]. In comparison, C57BL/6-*Kit*$^{W\text{-}sh/W\text{-}sh}$ mice are not anaemic, and have normal populations of $TCR_{\gamma\delta}$ cells in the intestine. Adoptive cell transfer is a powerful method commonly utilised to assess the function of MCs or MC-specific mediators by introducing *in vitro*-derived, genetically compatible WT BMCMCs or genetically altered BMCMCs[174-176]. By engraftment of BMCMCs via systemic intravenous (*i.v.*) or local intraperitoneal (*i.p.*) and intradermal (*i.d.*) route, the so-called "MC knock-in" mice differ from their c-*kit* mutant counterparts solely based on the presence of MCs, or variation of a particular MC component, offering an invaluable tool in the field of MC research[177]. Many MC-related studies today employ both of these MC-deficient mouse strains to confirm the specific MC-dependent function(s) of interest *in vivo* irrespective of their individual genetic background and additional abnormalities. However, based on limitations of the c-*kit* mutant models, other mouse models have been generated to overcome some of these phenotypic abnormalities, which may affect our interpretation of the role of MCs in the disease settings being studied.

Recent studies have also sought to develop new mouse models that do not exhibit phenotypic abnormalities that relate to the structure or expression of the c-*kit* receptor.

One example is a mouse model generated via the crossing of CPA3-Cre (Cre recombinase expressed under the CPA3 [MC and basophil-associated protease] promoter) and mice encoding a floxed version of myeloid cell leukaemia sequence-1 (Mcl-1)[178,179]. By conditionally removing the MC survival factor Mcl-1 from MCs or even basophils that predominantly express the protease CPA3, these mice show a ~92%-100% reduction in both CTMC and MMC populations at anatomical sites of the skin, trachea, lung, peritoneum and stomach. A marked reduction in basophil populations (58% in spleen, 74% in blood and 75% in bone marrow) was also observed, but, as expected, no effects was seen on other immune cell populations[178]. Similarly, the 'Cre-Master' mice have been developed by expressing Cre under the control of CPA3 promoter via knock-in strategy, along with deletion of the first 28 nucleotides of exon 1 of CPA3. As a result, this modification led to a virtual loss of MCs, MC-associated proteases, as well as all MC gene expression signature in the peritoneal cavity and the skin[180,181]. Notably, both of these newly developed mouse models exhibited similar phenotypes as the *Kit*$^{W/W\text{-}v}$ and *Kit*$^{W\text{-}sh/W\text{-}sh}$ mouse models when the classic MC-dependent responses (i.e. IgE-dependent passive cutaneous anaphylaxis [PCA]) were assessed.

It is worth noting that this newly developed MC-specific Cre system could also be utilised to develop mouse models that specifically target MC-derived mediators such as the mast cell proteases. This would be advantageous as it would provide a more specific targeting of mediators that are expressed in specific tissues. One example of such model is the *mMCP5*-Cre; *il-10*$^{fl/fl}$ mice. In essence, this mouse model uses a Cre recombinase that is expressed under the mast cell specific mMCP5 promoter and crossed with a mouse encoding a floxed version of the anti-inflammatory mediator IL-10. This conditional knockout deletes the *il-10* gene specifically in MCs that predominantly express mMCP5. In this case, it is likely to target MCs that typically reside in the skin and peritoneal cavity[182,183]. Moreover, *mMCP5*-Cre mice have been utilised in numerous studies including understanding the role of MCs in contact hypersensitivity responses[183], bladder infections[184], anaphylaxis[185], bacterial infections[186] and also autoimmunity[187,188].

1.2 MCs in health and disease

As stated previously, MCs are normally localised in close proximity to nerve fibres as well as blood and lymphatic vessels. Since their mediators have various influences on the vasculature and the surrounding environment, MCs play multiple roles in both physiological and pathological processes (**Figure 1.2**).

1.2.1 MCs in homeostasis

It is well understood that MCs are involved in the wound healing process by promoting inflammation via the recruitment of inflammatory cells[189]. MCs are also able to promote inflammation by inducing angiogenesis through the release of angiogenic factors such as vascular endothelial growth factor (VEGF), platelet-derived growth factor (PDGF) and NGF[190-192]. However, recent studies by Willenborg *et al*[193] demonstrate that the role of MCs in wound healing may not be as crucial as previously thought. Utilisation of mice with genetically ablated MC populations showed that, in an excisional wounding model, MCs show no effect on the re-epithelialisation, formation of vascularised granulation tissue, or scar formation. In addition, a previous study reported increased deposition of glycoaminoglycans and extracellular matrix in the ears of naive mMCP4-deficient mice, also suggesting a role for MCs and mMCP4 in homeostatic tissue remodelling[194].

1.2.2 MCs in allergy

Allergy is an abnormal immune response directed against non-infectious environmental substances called allergens[3]. Allergic disorders include anaphylaxis, hay fever, atopic dermatitis, allergic asthma and some food allergies, and most, if not all, of these reactions are triggered by allergens (e.g. pollens, house-dust-mite faecal particles, animal dander, certain foods (e.g. peanuts, fish, milk and eggs, latex and insect venoms) that induce IgE production and subsequent "sensitisation" of host MCs[144,195].

The degranulation of MCs plays an essential role in the early-phase allergic reaction, which is a type I hypersensitivity response immediately following exposure to allergens. Known as a hallmark of allergic response, the release of preformed mediators such as histamine and lipid-derived mediators prostanoids and leukotrienes (histamine, PGD2 LTB4) are responsible for the commonly known features of vasodilation, increased vascular permeability and bronchoconstriction during the allergic airway inflammation[130,195,196]. In the meantime, other MC-mediators such as TNFα and

Figure 1.2 Positive and negative regulatory functions of MCs in disease settings.
MCs are capable of releasing mediators that can elicit either beneficial or detrimental functions. (Green box: beneficial; Red box: detrimental; Blue box: potentially beneficial and detrimental) . The stage of the disease and the environmental cues MCs are predisposed to will determine how MCs respond in the specific context.

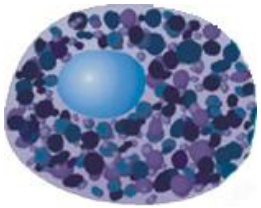

POSITIVE

HOST DEFENCE AGAINST BACTERIAL INFECTIONS ← TNF, Protease

HOST DEFENCE AGAINST PARASITIC INFECTIONS ← TNF, IL-4, Protease

ALLERGIC AIRWAY INFLAMMATION ← TNF, CCL2, CCL5, Protease

ARTHRITIS ← IL-1, Protease

ALLERGIC RHINITIS ← TSLP

NEGATIVE

Histamine → UVB-INDUCED SUPPRESSION OF CHS AND DTH RESPONSES

IL-10 → LIMITS INFLAMMATORY RESPONSE IN CHS

IL-10 → LIMITS CHRONIC LOW DOSE UVB IRRADIATION RESPONSE

IL-10 → PERIPHERAL TOLERANCE TO SKIN ALLOGRAFTS

IL-10 → LOCALISED TOLERANCE IN CHRONIC BLADDER INFECTION

Proteases → DEGRADATION OF TOXINS AND VENOMS

chemotactic factors PGD2, CCL2, CCL3 and CCL5, can promote recruitment of other immune cells to the affected site to promote further inflammation, vasodilation, vascular permeability, smooth muscle contraction, and bronchoconstriction[3,144,197,198]. This suggests that MCs are key to providing and sustaining not only the recruitment but also the activation of these immune cells when exposed to allergen.

1.2.3 MCs in parasitic infections

An increase in the number of MCs upon infection with parasites has been previously reported[199-202]. In addition, MC-deficient *Kit*$^{W/W-v}$ mice exhibit longer duration of *T. Spiralis* infection compared to both WT and MC 'knock in' mice. The release of MC-derived TNFα and IL-4 was required for clearance of *T. spiralis*[203]. Since IL-4 and IL-13 mediators derived from cell populations such as basophils, T cell and eosinophils have been implicated in host defence from helminth infections[204], it would be worthwhile to investigate whether MC-derived IL-13 (MC-IL-13) also exhibits a similar function[205]. Other MC-derived mediators such as mast cell proteases have also been shown to be involved in host defence against parasites. For example, mMCP1 was suggested to be involved in the expulsion of parasites by regulating epithelial barrier function and vascular permeability[206,207]. mMCP6 was also shown to be required to initiate immune responses against *T. spiralis* by promoting the recruitment of eosinophils to the site of infection, although it was not required for clearance of *T. spiralis*[208]. Furthermore, studies suggest that IL-3 is critical for expansion of haematopoietic effector cells such as MCs and basophils against parasitic infections[201,202]

1.2.4 MC in bacterial and viral infections

There has been a significant amount of evidence demonstrating the involvement of MCs in host defence against both bacterial and viral infections. Studies using the *Kit*$^{W/W-v}$ mouse model have demonstrated a protective role for MCs in both *E.coli* and *helicobacter felis* infection[199,209]. Like that observed in parasitic infections, MC hyperplasia has also been reported by many studies upon bacterial infections[199,200], and MCs can be activated by bacterial Ag through TLR4, phagocytosis of bacterial particles and bacteria-induced anaphylatoxins. More importantly, MC-derived TNFα, LTC4 and LTB4 were found to be crucial for the recruitment of neutrophils to the site of infection, and the release of anti-

microbial mediators[210,211]. The release of the antimicrobial peptide cathecidin from MCs is also implicated in protection against *Streptococcus* infection[212].

MCs are known to have both beneficial and detrimental effects in viral infection. It has been demonstrated that both human and mouse MCs could be activated by a virus-like polyI:C molecule which can promote the production of anti-viral mediators (such as IFNβ) and also the release of CCL5 to regulate anti-viral T cell function and the recruitment of cytotoxic T cells[213-215]. Furthermore, upon Dengue virus infection, MCs are important in providing a functional innate immune response by producing TNFα, IFNα, CCL5, CXCL12 and promoting the recruitment of natural killer (NK) and NKT cells to enhance host defence and viral clearance[216]. On the other hand, MCs have also been reported to assist in viral infection. One prime example is during human immunodeficiency virus (HIV) infection. MCPs and mature MCs can be infected by HIV and act as a viral reservoir for latent infection[217-219].

1.2.5 Negative regulatory functions of MCs in inflammation

Coinciding with the well-recognised pro-inflammatory roles, there have been instances where MCs are also capable of promoting negative immunomodulatory functions. One such example includes the ability of MCs to assist in suppressing the sensitisation of contact hypersensitivity (CHS) responses to the hapten 2,4,6-trinitrochlorobenzene in (C57BL/6 × DBA/2)-F1-*Kit*$^{W\text{-}f/W\text{-}f}$ (dermal MC-deficient) mice through the production of chronic UVB-induced histamine[105]. In addition, MCs are also involved in promoting peripheral tolerance to skin allografts by recruiting $CD4^+CD25^+FoxP3^+$ regulatory T cells (Treg). MCs are also capable of secreting IL-9 which can suppress allo-reactive functions of $CD8^+$ T cells[220,221]. Interestingly, it has also been found that IgE-dependent MC degranulation can inhibit Treg function and promote a T cell-dependent acute rejection of established skin allografts[222].

In addition to the above mentioned immune-suppressive functions of MCs, our recent studies demonstrated the ability of MCs to limit inflammatory responses via MC-derived IL-10 (MC-IL-10) in models of chronic CHS and chronic low-dose UVB irradiation[8-10]. It was found that, in chronic CHS responses, IgG1-FcγRI signalling was involved in mediating the suppression of CHS inflammatory responses by MC-IL-10[8]. In response to chronic UVB, however, our study showed that MC-IL-10 required the vitamin D

receptor-signalling pathway to mediate its protection against UVB induced skin inflammation[8,9]. Chacon-Salinas *et al.*, showed that MC-IL-10 can inhibit the formation of germinal centre and follicular T cell and hence limit the humoral response associated with regional lymph nodes (LN)[223], further supporting the role of MC-IL-10 in supressing the immune response. It is interesting to note that, depending on the context of the disease, the immune-suppressive function of MC-IL-10 can also have detrimental effects. For example, MC-IL-10 was shown to drive localised tolerance in chronic bladder infection by limiting the recruitment of Ag presenting DCs and Ig class switching in B cells[184]. It is important to note that IL-10 derived from other sources has also been reported to play a detrimental role in cancer by promoting a tumour suppressive microenvironment[224].

1.2.6 MCs in cancer

Cancer is a disease promoted by the dysregulation of essential pathways which results in uncontrolled proliferation of tissue cells and the eventual tumour formation[225]. So far, almost all cell types have been shown to play a role in dysregulating some of the essential pathways that are required to keep tumour outgrowth at bay[226]. MCs have been suggested by multiple studies to be involved in various cancer types[227,228]. It has been shown by numerous studies that during tumourigenesis, MCs are one of the most abundant inflammatory cells that infiltrate into the stroma of the microenvironment and this has been shown to be directly correlated with poor prognosis of patients suffering from cancers such as squamous cell carcinomas (SCCs)[229-231]. However, their actual roles in cancer remains controversial as MCs have been reported to play both protective and detrimental roles in a context-dependent manner, as summarised in **Table 1.1**[4]. Although still at an early stage, studies have used MC-deficient mice to assess the contribution and function of MCs at different stages of neoplastic development/tumourigenesis. For example, in WBB6F$_1$-*Kit*$^{W/W\text{-}v}$ mice, MCs have been shown to promote the tumour formation and lung metastasis of B16-Bl6 melanoma cells[232], and 1,2-DMH-induced colonic epithelial neoplasms[233]. MCs have also been found to promote the development of Myc-induced pancreatic islet tumours[234] and prostate adenocarcinoma[235].

Table 1.1 Role of MCs in mouse models.

Cancer model	Mouse model	Main findings	Reference
Transplant model of B16-BL6 melanoma cells.	WBB6F$_1$-*Kit*$^{W/W\text{-}v}$	MCs **contribute to tumour formation** by promoting angiogenic and metastatic response.	232
HPV16-induced skin carcinogenesis model.	WBB6F$_1$-*Kit*$^{W/W\text{-}v}$	MCs **contribute to tumour development and invasiveness** by release of pro-angiogenic and ECM degrading proteases.	236
1,2-DMH-induced colonic epithelial neoplasms.	WBB6F$_1$-*Kit*$^{W/W\text{-}v}$	MCs (an potentially other haematopoietic cells [due to c-kit mutation]) **contribute to growth of chemically induced tumours.**	233
Myc-induced pancreatic islet tumours.	C57BL/6-*Kit*$^{W\text{-}sh/W\text{-}sh}$ Cromolyn treatment of WT mice	MCs and MC-derived mediators **promote tumour development** through angiogenesis and proliferation of Myc-induced tumours.	234
Transplant of well differentiated prostate adenocarcinomas from TRAMP mice	C57BL/6-*Kit*$^{W\text{-}sh/W\text{-}sh}$	MCs **contribute to development of well differentiated prostate adenocarcinomas** through release of MC-derived MMP9.	235
Two-stage chemical carcinogenesis model (DMBA and TPA)	WBB6F$_1$-*Kit*$^{W/W\text{-}v}$	MCs **limit development of chemical induced skin papillomas.**	6
Trangenic C57BL/6J-APC$^{Min/+}$: model of intestinal carcinomas	C57BL/6J-APC$^{Min/+}$ crossed onto WT and C57BL/6-*Kit*$^{W\text{-}sh/W\text{-}sh}$	MCs play a **protective role against tumour growth** by promoting apoptosis.	237
Transgenic TRAMP mice: model of early prostate cancer	TRAMP-C57BL/6-*Kit*$^{W\text{-}sh/W\text{-}sh}$	MCs and release of mediators **protect against prostate tumourigenesis.**	235

HPV, human papilomavirus; ECM, extracellular matrix; 1,2-DMH, 1,2-Dimethylhydrazine; TRAMP, transgenic adenocarcinoma of the mouse prostate; MMP, matrix metalloproteinase; DMBA, dimethylbenz[a]anthracene; TPA, 12-O-tretradecanoylphorbol-13-acetate; APC, adenomatous polyposis coli.

On the flip side, MCs can also elicit protective functions in some tumourigenesis models. For example, the deficiency of MCs resulted in enhanced tumour growth of intestinal carcinoma in a transgenic C57BL/6J$^{APCMin/+}$ mouse model, suggesting a protective role of MCs against tumour growth by potentially promoting apoptosis[237]. Further supporting the tumour-suppressing function of MCs, using the transgenic TRAMP mouse model of prostate adenocarcinoma, Pittoni *et al*., demonstrated that either removal of MCs or inhibition of MC degranulation resulted in higher incidence of anaplastic tumours[235].

Due to the plasticity and complexity of MCs, it is not surprising that they are capable of exhibiting differential functions in cancers depending on the tumour type and stage of tumour development. However, further work is still required to fully clarify this complicated involvement of MCs in cancer.

1.2.7 MC-mediators in cancer

MCs can promote tumourigenesis through releasing pro-inflammatory and angiogenic mediators such as TNFα, IL-6, VEGFs and matrix degrading enzymes[49,238]. MCs can also contribute to cancer development by promoting tumour invasion. This is supported by the study by Coussens *et al.,* which demonstrated a role for MCs in assisting the progression and invasion of human papillomavirus (HPV)16-induced SCC via chymase- and tryptase-mediated re-modelling of tissue architecture[236,239]. In parallel, MCs can contribute to tumour development by promoting immunosuppression through MC-IL-10 and TGFβ, as well as through enhancing Foxp3$^+$ Treg cells, which ultimately lead to suppression of T cells and NK cells[49]. There has also been *in vitro* and *in vivo* evidence suggesting a role of other MC mediators such as histamine in promoting tumour growth via immune suppression[105,240-244].

On the other hand, MC mediators have also been reported to mediate anti-cancer functions. For example, MC-derived tryptases have been shown to disrupt tumour formation[245]. MC-derived heparin can interfere with the growth of human breast cancer cells[246]. Other factors such as histamine can inhibit the proliferation of human primary melanoma cells and suppress the ability of CD11b$^+$Ly6G$^+$ immature myeloid cells to promote growth of tumour allografts[247]. Interestingly, IL-6 release can recruit NK and CD3$^+$ cells and promote tumour regression[248,249]. The addition of IL-6 can also enhance the anti-tumour functions of histamine[250]. Recently, we have found that, in response to chronic low-dose UVB irradiation, MCs can produce the active form of vitamin D_3,

1,25dihydroxyvitamin D_3[9,10], which has been shown by various studies to exert photo-protective functions in UVB-induced skin tumourigenesis[251-257].

1.3 Non-melanoma skin cancers

Australia has the highest incidence of non-melanoma skin cancers (NMSCs) worldwide. NMSCs are categorised into basal cell carcinomas (BCCs) and squamous cell carcinomas (SCCs). Unlike BCCs, SCCs are less common and tend to metastasise. UVB radiation, a component of sunlight, is one of the major factors in promoting the development of cutaneous SCCs, which is often thought to be a multistep process. A single dose of UVB irradiation (2 kJ/m^2) on neonatal transgenic TPras mice was shown to predispose the mice to development of melanoma due to a significant reduction in Langerhan cells in the neonatal epidermis but also potentially due to the development of an immunosuppressive microenvironment[258,259]. Based on the current findings, one of the key mutations that drive the development of cutaneous SCCs is thought to be through mutations of the tumour suppressor gene *p53*[260-262]. Therefore, it was hypothesised that mutations in *p53* could promote precancerous lesions and serve as a risk marker for SCC development[263,264]. In addition to UVB, other factors such as HPV and chemical carcinogens can also play crucial roles in the development of cutaneous SCCs[6,265-268].

1.3.1 Human papillomavirus (HPV)-induced skin carcinogenesis

HPV belongs to the papillomaviridae family which is consisted of a highly diverse group of viruses that has a tendency to infect areas of the skin (β genus) and mucosal epithelia (α genus). The αHPV subtype (including high risk HPV 16 and 17) is predominantly (99%) responsible for cervical cancers, which is a result of integration of papillomaviral DNA genome into the chromosome of the host cervical epithelial cells[269,270]. On the other hand, the βHPV subtype typically responsible for the development of cutaneous SCCs, and this predominantly occurs at the area of skin that is exposed to the sun[265].

Similar to cervical cancer-inducing HPV, the E6 and E7 proteins of βHPV are considered to be the most prominent oncogenes. However, despite the ability of these proteins to transform keratinocytes, they have not been proved to directly drive tumourigenesis in cutaneous SCCs[271,272]. Studies have demonstrated that cells expressing HPV E6 and E7 proteins showed compromised DNA repair mechanisms and mRNA synthesis recovery[265,273,274]. UVB is known to suppress apoptosis of keratinocytes by

downregulating the expression of Fas ligand[275,276]. Hence it is likely that the anti-apoptotic and DNA-damaging effect of UVB can further promote the accumulation of DNA damage in HPV-infected keratinocytes, leading to an increased likelihood of tumourigenesis over a long period of time.

Inflammatory cells, including $CD4^+$ T cells and $Gr\text{-}1^+$ granulocytes, have been found in premalignant lesions and cancers associated with HPV[277,278]. Interestingly, MCs have also been thought to promote HPV16-induced skin carcinogenesis[41,236,267]. A study by Coussens *et al*., demonstrated that in a mouse model of HPV16-induced cutaneous SCC, MCs are required for the remodelling of tissue architecture through the release of chymases and tryptases, allowing tumours to progress and invade into the neighbouring tissue[236]. Additionally, MCs have been shown to be recruited by CCL2 and CCL5 produced by E7-expressing epithelial cells, which can promote an immunosuppressive environment and allow the persistence of E7-induced skin lesions[41].

1.3.2 Chemical-induced skin carcinogenesis

Chemical carcinogens can promote genetic and epigenetic changes in cells which ultimately lead to neoplastic transformation. The two-stage carcinogenesis model is the most common model utilised to study chemically-induced skin carcinogenesis[268,279-281]. The first stage of this model involves a single sub-carcinogenic dose of 7,12-dimethylbenz[a]anthracene (DMBA), which induces an A→T mutation of codon 61 of H-Ras[282]. This is then followed by repeated topical application of chemical agents like 12-O-tretradecanoylphorbol-13-acetate (TPA)[283], which promotes many pathways including stimulation of PKC, epidermal growth factor (EGF), MAPK signalling[284-286], increased production of growth factors (e.g. EGF)[286-288], oxidative stress[289,290] and tissue inflammation[291-294]. These outcomes, in turn, result in clonal expansion of mutated cells leading to sustained epidermal hyperplasia which can be observed by an increase in nucleated cell layers and an overall increase in the thickness of the epidermis[295,296].

This two-stage carcinogenesis model is widely used as it causes the outgrowth of papillomas, and can lead to the conversion from papilloma to invasive SCCs, depending on the mouse strain[297-299]. However, it is important to note that mutations in *p53* have been suggested to be the main initiating factor for the development of non-melanoma skin cancers[263], while only 10-20% of BCC and SCC cases are related to *ras* mutations[300-302]. This poses the question as to whether it truly imitates UV-induced skin carcinogenesis.

Nevertheless, interestingly, individuals diagnosed with UV-induced xenoderma pigmentosum have been found to show a higher frequency of *N-ras* mutations[303].

It is well understood that infiltrating immune cells as well as local inflammatory responses are critical in contributing to tumour development and growth[304,305]. MCs are also a key cell population that accumulate at the site of tumour microenvironment[114,306,307]. Using the two-stage carcinogenesis model, recent studies have demonstrated that, in response to TPA and DMBA treatment, MC-deficient *Kit*$^{W/W-v}$ mice develop greater number of tumours compared to MC knock in mice, suggesting that MCs can also limit the development of chemical-induced skin carcinogenesis[6].

1.4 UVB-induced skin carcinogenesis

1.4.1 Solar spectrum

Chronic sun exposure remains the main etiological factor for the development and pathogenesis of SCCs[263,308]. Within the solar spectrum, the ultraviolet component (wavelength: 280-400 nm) consists of UVA (320-400 nm), UVB (280-320 nm), and UVC (<280 nm). Both UVA and UVB are only partially filtered by the ozone layer, and they are responsible for the acute and chronic effects on sun exposed skin, such as photoaging and sunburn[309-312]. In comparison, UVC, although being the most harmful component of UV radiation, is completely filtered out by the ozone layer.

1.4.2 UVB exposure to the skin

Chromophores, such as *trans*-urocanic acid (UCA), melanin [313], 7-dehydrocholesterol (precursor to vitamin D_3)[314] and DNA[264,309], are a group of molecules that have an absorption spectra similar to UVB radiation. Due to the ubiquitous expression of chromophores in the skin[315], UVB can be readily absorbed by the skin, even though it is partly filtered out by the ozone layer.

Depending on the amount or 'threshold' of UVB the skin is exposed to, UVB exposure of the skin can be either beneficial or detrimental. Exposure to low doses of UVB leads to the production of vitamin D3 and melanogenesis, which may protect from further cutaneous damage caused by subsequent UVB exposure[256,316,317]. Alternatively, higher doses of UVB exposure can promote detrimental effects including oxidative stress, genetic mutations and chronic inflammation[309]. The threshold of UVB dosage is highly dependent on the phototype of an individual's skin. For example; 10-15 min of sun

exposure is considered a low dose for individuals with darker pigmented skin (Type II → IV), but a medium dose for individuals with pale/fair skin (Type I).

Due to the short wavelength of UVB, most of the damage is elicited in the epidermis of the skin, particularly in keratinocytes in response to UVB exposure. Keratinocytes have been reported to produce reactive oxygen species (ROS)[318,319] and undergo apoptosis[275] in response to UVB. In addition, the generation of ROS has also been shown to deplete anti-oxidant molecules such as vitamin C and E, leaving the skin susceptible to further deleterious effects including cellular damage, DNA damage, lipid peroxidation and protein damage[309,320]. In parallel, nitrogen oxide species are also produced, which, similarly to ROS, can also promote DNA damage[321-323].

In addition to production of ROS, UVB can also cause direct DNA damage and mutations via the generation of DNA cyclobutane pyrimidine dimers and pyrimidine pyrimidone photoproducts[309,324], which together can generate UVB-induced lesions[325-327]. In response to UVB-induced mutations, cells will respond efficiently by up-regulating the tumour suppressor gene *p53*, which initiates cell cycle arrest and DNA repair[328,329]. Interestingly, numerous studies have shown that both the active and analogues of vitamin D_3 can provide photo-protection against UVB-induced DNA damage by potentiating *p53* expression[251-253,256]. Moreover, keratinocytes with non-repairable DNA will undergo apoptosis via ROS- and *p53*-dependent pathways[319,330]. Mutations often occur in *p53* and these are considered to be the 'initiating' mutations that promote the pathogenesis of SCCs[331-333]. An accumulation of non-repairable mutations, particularly in *p53*, can disrupt cell cycle arrest and DNA damage repair mechanisms which can consequently lead to the dysregulated proliferation of DNA damaged cells and ultimately impending tumour development[334].

In addition to DNA damage and generation of ROS, inflammation is also another key factor in promoting the development of UVB-induced skin cancer. As a result of chronic UVB exposure, persistent chronic inflammation can cause significant alterations to the skin, which include edema and erythema[313]. These features are often seen when tissue undergoes a series of changes referred to as the 'metaplasia-dysplasia-carcinoma' process. This common theme is represented as atypical epithelial tissue organisation (metaplasia), followed by increasing disorganisation of tissue architecture (dysplasia) and the

development of neoplastic *in situ* cancer cells (carcinoma) that have the potential to become invasive[226,335].

1.4.3 UVB-induced angiogenesis and lymphangiogenesis

As stated previously, UVB can promote edema and erythema, which are characterised by fluid accumulation and swelling. The vascular system is comprised of blood and lymphatic vessels. The blood vessels play crucial roles in providing nutrients and oxygen under homeostatic conditions, while they can also mediate inflammatory responses by providing chemotactic mediators and assisting the recruitment of cells to the sites of inflammation[336]. On the other hand, the lymphatic vasculature returns fluid, immune cells and proteins back to the circulation to maintain tissue homeostasis and facilitates immune surveillance by mediating the mobilisation and trafficking of immune cells to and from sites of inflammation[337,338]. Although both blood and lymphatic vessels are particularly important in tissue homeostasis, when dysregulated they can promote both tumourigenesis and metastasis[339].

Angiogenesis is primarily promoted by VEGF-A acting through VEGFR-1,-2 receptors, and its role in cancer has been documented extensively over the past decade[336,339]. VEGF-A is crucial in regulating angiogenesis and is central to tumour development due to its ability to promote inflammation and recruitment of inflammatory cells[167,340-345]. In humans, UVB irradiation has been reported to induce dermal angiogenesis which results in a dramatic increase in the number of enlarged vessels and profound proliferation of endothelial cells[346,347]. This is correlated with an up-regulation of VEGF-A and a down-regulation of the angiogenic inhibitor thrombospondin-1 (TSP-1). Moreover, chronic UVB irradiation can also cause dilation and leakage of blood vessels and facilitates an infiltration of extracellular matrix (ECM) degrading neutrophils, both of which can subsequently contribute to exacerbated skin damage[346,348].

Current studies suggest neo-lymphangiogenesis to be a causal factor in promoting tumour metastasis[349]. Elevated levels of the pro-lymphangiogenic factors VEGF-C and –D have been shown to promote metastasis of various types of cancers, including SCCs[350-354]. However, the role of lymphangiogenesis in the setting of chronic UVB-irradiation has only recently been reported[339]. To date, few studies have examined the effects of UVB exposure on lymphangiogenesis in the skin. Studies by Kajiya *et al.*, demonstrated that exposure to both acute (single dose; 40 mJ/cm^2) and chronic (cumulative dose; 5.46 J/cm^2)

UVB irradiation can impair lymphatic function by causing lymphatic vessels to become enlarged and leaky by a VEGF-A mediated process, consequently disrupting their ability to drain the inflammatory infiltrate from the site of inflammation[353,355,356].

Currently, there is no link between MCs and lymphatic vessels in the pathology associated with UVB irradiation. Since MCs can synthesise VEGFs, it is plausible[344,357,358] that MCs could also regulate lymphangiogenesis as well as angiogenesis in UVB-irradiated settings. Interestingly, a study by Schweintzger *et al*, demonstrate that UVB-induced dermal angiogenesis was MC independent[359].

1.5 UVB-induced activation of MCs and MC-mediators in cancer

1.5.1 UVB-induced activation of MCs

Resident immune surveillance cells, such as MCs, are the first to initiate inflammatory responses. Since UVB radiation has limited potential to transmit to the dermal layer of the skin due to its short wavelength, it is thought that UVB can activate dermal MCs through indirect pathways[307]. Studies have proposed that upon UVB-irradiation, the chromophore *trans*-UCA is isomerised to *cis*-UCA[242], which can activate c-sensory never fibres that extend from the epidermis to the dermis[360]. This can lead to the activation of MCs via the production of the neuropeptides SP and CGRP[360,361]. Other UVB-induced mediators such as IL-33[362] keratinocyte-derived NGF[243], SCF[49], alpha-melanocyte stimulating hormone (α-MSH)[363], platelet activating factor (PAF)[364], and vitamin D_3[9] can also induce MC activation (**Figure 1.3**)[307] in the skin.

1.5.2 UVB-induced MC mediators

It is known that following UVB irradiation, MCs can be activated and release mediators that are involved in limiting pathology and promoting immunosuppression and inflammation[8,9]. However, many of the mediators that might be released by MCs in the tumourigenic setting are undefined, particularly at critical stages of incipient neoplasia. Based on studies using adoptive cell transfer in c-*kit* (MC-deficient) mutant mice, MCs can release mediators including IL-8[365], IL-10[8,9], TNFα[366] and histamine[367], in response to acute UVB exposure.

UVB irradiation can also induce VEGF-A production, primarily from keratinocytes[368] but also MCs[343,344]. In addition, MMP9, another well-known mediator involved in ECM

Figure 1.3 Ultraviolet-B induced activation of mast cells.
Mast cell activation is thought to be indirect when skin is exposed to UVB radiation. Chromophores such as urocanic acid (UCA) are one of the main mediators that can promote activation of MCs through the production of neuropeptides. Other UVB-induced mediators are also known to promote MC activation. See text for more details. Adapted from Ch`ng *et al*[306].

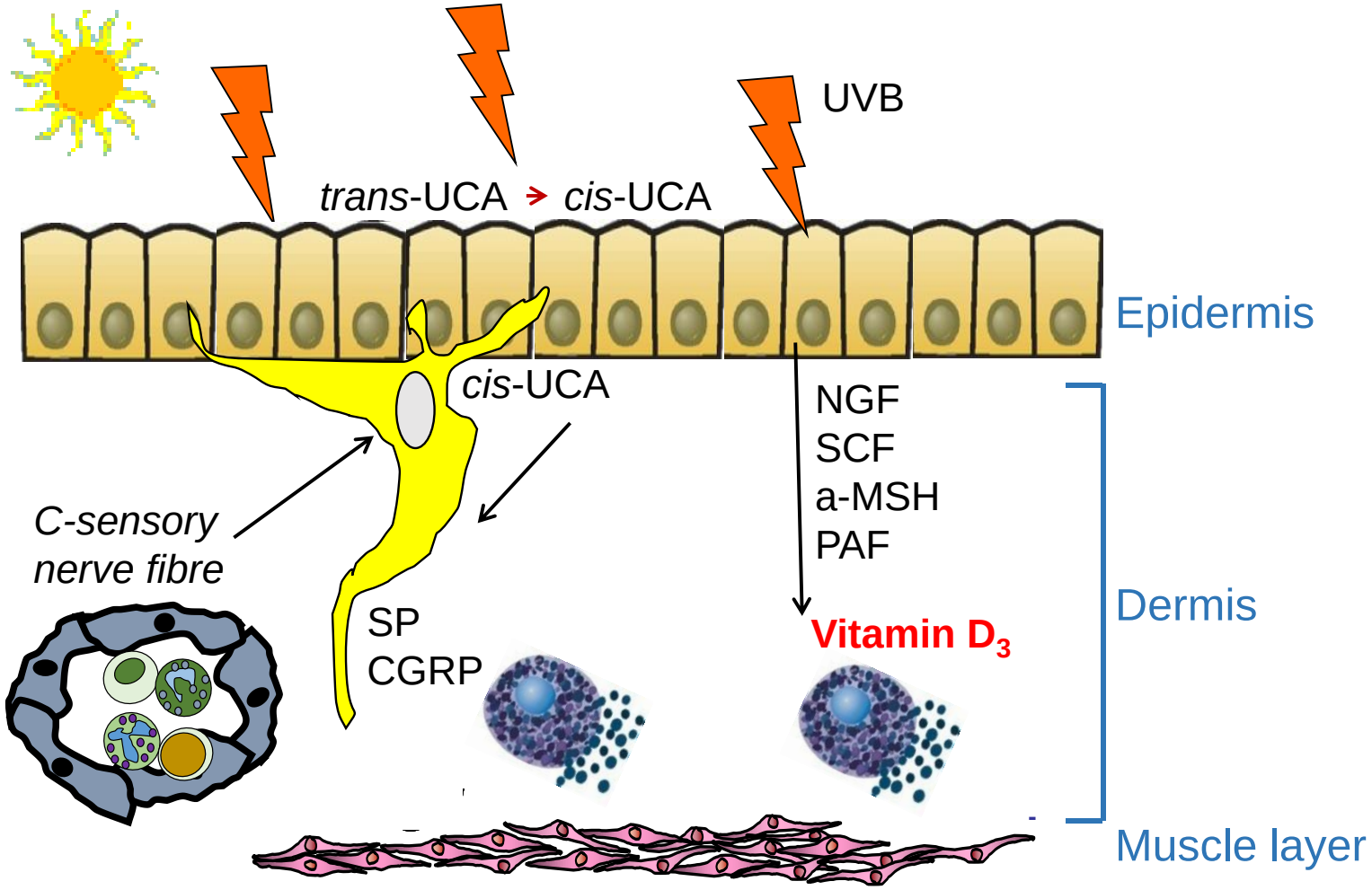
UVB
trans-UCA → cis-UCA
Epidermis
cis-UCA
NGF
SCF
a-MSH
PAF
C-sensory
nerve fibre
SP
CGRP
Vitamin D3
Dermis
Muscle layer

remodelling, tumour angiogenesis and tumourigenesis[236,] can also be released by MCs following UVB irradiation[369].

1.6 MC Proteases in physiological and pathological settings

1.6.1 Tryptase

Tryptase has been reported to be involved in a wide range of biological processes under both physiological and pathological conditions. The ability of human tryptase to generate the bioactive vascular dilating peptide bradykinin from prekallikrein has also been suggested to be involved in vascular permeability[370]. In addition, tryptase has been shown to degrade bronchodilating neuropeptides vasoactive intestinal peptide (VIP) and CGRP[371,372] to increase bronchial responsiveness. In mice, mMCP6 can exhibit anticoagulating functions through degradation of the coagulating factor fibrinogen[373]. Furthermore, mMCP6 has also been implicated in disease settings of bacterial and parasite infection as well as arthritis[58,208,374]. It is worth noting that mMCP7 is another tryptase expressed in mice. However, studies have demonstrated that by knocking out mMCP6, expression of mMCP7 is also compromised, suggesting that the differential function of these two enzymes requires further investigation[374]

1.6.2 MC-CPA3

Studies using the MC-CPA3-deficient mice found that this enzyme plays an important role in degradation and clearance of toxic peptides such as bacteria-derived endothelin-1[375]. This was further supported by the use of MC-CPA3 'knock in' mice, which demonstrated the involvement of MC-CPA3 in the clearance of endothelin-1 and snake venom[113,376].

1.6.3 Chymase

The generation of chymase-deficient mouse strains (reviewed by Wernersson *et al* 2014)[85] has provided major new insight to the biological functions of chymases under different physiological and pathophysiological settings. mMCP1 has been shown to be important in assisting host defence and clearance of *T. spiralis* parasites[206]. Mice lacking mMCP5 have been shown to exhibit reduced ischemia reperfusion injury in skeletal muscle[377]. It is important to note that, since the loss of mMCP5 can also cause a deficiency in MC-CPA3 storage in the MC granules, whether the reported effect was also related to the alteration of MC-CPA3 is yet to be clarified.

mMCP4 is the most well-characterised mouse chymase due to its functional similarities with human chymase (**Figure 1.4**). Numerous studies demonstrate the protective role of mMCP4 in settings including allergic airway inflammation[7], poly-microbial sepsis[5], degradation of toxins[378], post-traumatic brain inflammation[379], spinal cord damage[380], ureteral obstruction[381] and chemical carcinogenesis[114]. Interestingly, mMCP4 has also been shown to have detrimental effects including potentiating epidermal burns[382] and HPV-induced skin tumourigenesis[236]. However, the role of mMCP4 in UVB-induced skin tumourogenesis is yet to be delineated.

1.7 Rationale for this study

Our previous studies have demonstrated a protective role of MCs and MC-IL-10 in limiting chronic low dose UVB-induced inflammation in the skin, via limiting pro-inflammatory cytokines, leukocyte recruitment, and UVB-induced skin pathology[8]. More recently, we have also identified a similar role for mMCP4 in the same setting (data unpublished). However, it is important to note that the low dosage of UVB irradiation utilised in these studies is not considered to be tumourigenic. Based on our previous studies and the preliminary findings that suggest mMCP4 to be protective in a range of diseases, this study aims to further investigate whether MCs and mMCP4 could retain their protective function following chronic high dose UVB irradiation, and are able to protect against the development of UVB-induced skin carcinogenesis.

Like many other cancer types, the multi-step development and progression of UVB-induced skin carcinogenesis also involves the hallmark capabilities/features of cancer including pathological angiogenesis and lymphangiogenesis. UVB irradiation is known to promote angiogenesis, though not much is known regarding its effects on lymphatics. More importantly, the role of MCs in lymphangiogenesis is yet to be defined. In this study, we will assess how MCs and mMCP4 are involved in the pathological angiogenesis and lymphangiogenesis induced by chronic UVB irradiation.

1.8 Hypothesis

Mast cells and the MC-specific protease mMCP4 are protective against chronic UVB-induced skin tumourigenesis.

Figure 1.4 Dual roles of MC proteases in disease.
Mast cell proteases have been reported to both promote inflammation and protect against inflammatory responses. Adapted from Pejler *et al*[57].

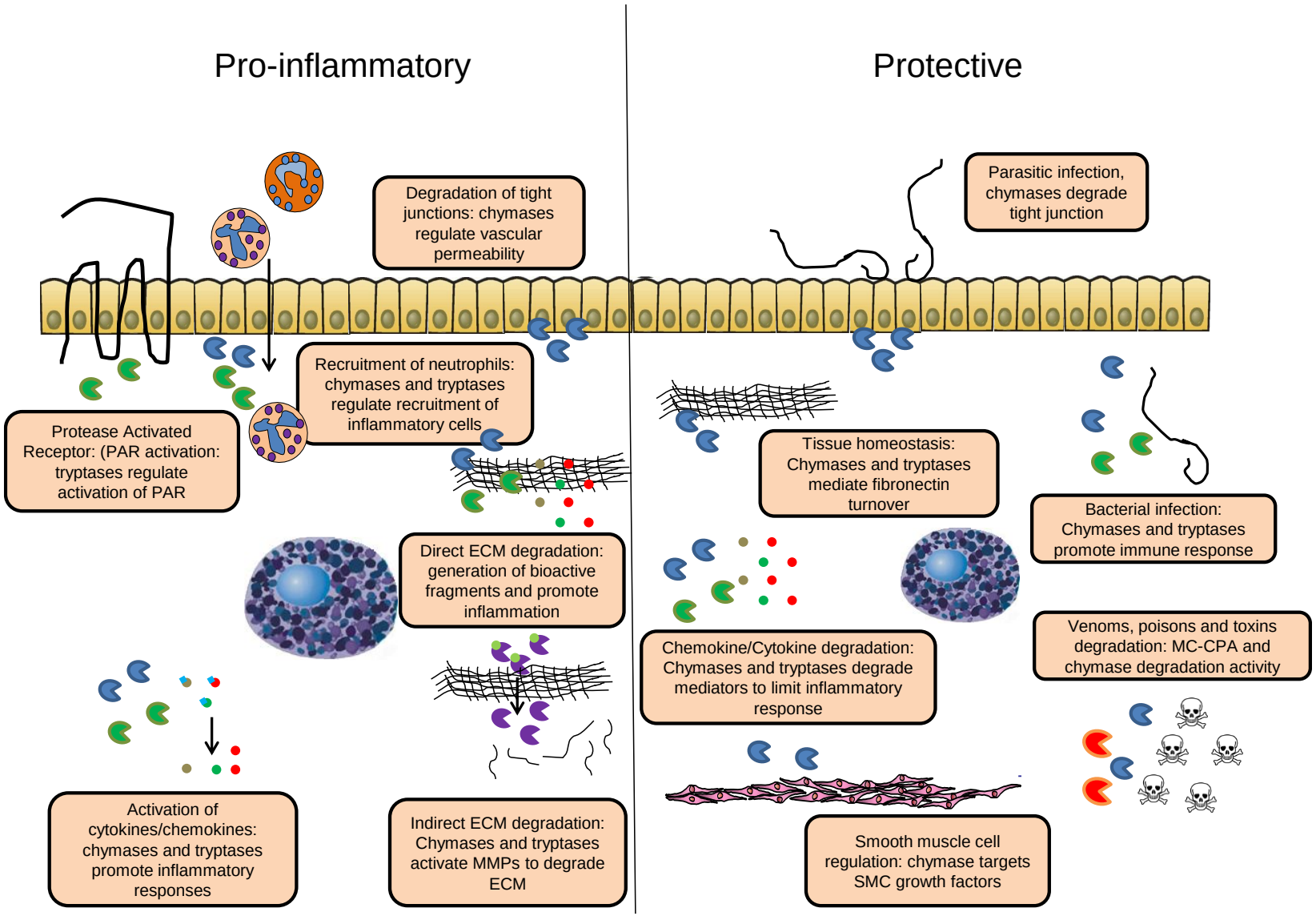
Pro-inflammatory
Protective
Degradation of tight junctions: chymases regulate vascular permeability
Recruitment of neutrophils: chymases and tryptases regulate recruitment of inflammatory cells
Protease Activated Receptor: (PAR activation: tryptases regulate activation of PAR
Direct ECM degradation: generation of bioactive fragments and promote inflammation
Activation of cytokines/chemokines: chymases and tryptases promote inflammatory responses
Indirect ECM degradation: Chymases and tryptases activate MMPs to degrade ECM
Parasitic infection, chymases degrade tight junction
Tissue homeostasis: Chymases and tryptases mediate fibronectin turnover
Bacterial infection: Chymases and tryptases promote immune response
Chemokine/Cytokine degradation: Chymases and tryptases degrade mediators to limit inflammatory response
Venoms, poisons and toxins degradation: MC-CPA and chymase degradation activity
Smooth muscle cell regulation: chymase targets SMC growth factors

1.9 Aims

1.9.1 Aim 1: Characterisation of BMCMC derived from *mMCP4*$^{-/-}$ mice

The first aim of the project is to investigate the effect of mMCP4 deficiency on the morphological features and functional characteristics of MCs. This part of the study aims to ensure that *mMCP4*$^{-/-}$ MCs are viable to be used in engraftment studies, and to thoroughly investigate the phenotype of *mMCP4*$^{-/-}$ mice, thereby allowing us to assess the protective function of mMCP4 in chronic UVB-induced skin tumourigenesis in both WBB6F$_1$-*Kit*$^{W/W\text{-}v}$ and *mMCP4*$^{-/-}$ mouse models.

1.9.2 Aim 2: Assessing the role of MCs and mMCP4 in chronic UVB-induced skin carcinogenesis

In order to assess the *in vivo* function of MCs and mMCP4 in UVB-induced skin carcinogenesis, we will implement a MC 'knock in' model (MC-deficient WBB6F$_1$-*Kit*$^{W/W\text{-}v}$ engrafted with wild-type or *mMCP4*$^{-/-}$ BMCMCs) treated with a chronic high-dose UVB regime (12 x 4 kJ/m^2 + 13 x 8 kJ/m^2; cumulative dose: 152 kJ/m^2) and assess the early phases of non-melanoma skin cancer development, such as ear thickening, skin damage and necrosis. To further validate our findings, we will also compare the effects of this UVB regime in pigmented *mMCP4*$^{-/-}$ mice and non-pigmented *Tyr*$^{c\text{-}2j}$-*mMCP4*$^{-/-}$ mice.

1.9.3 Aim 3: Investigating the role of MCs and mMCP4 in UVB-irradiation induced angiogenesis and lymphangiogenesis

To investigate the role of MCs and mMCP4 in UVB-induced angiogenesis and lymphangiogenesis, the consequences of exposure to chronic UVB irradiation on the number and calibre of blood vessels and lymphatic vessels will be assessed in WBB6F$_1$-*Kit*$^{W/W\text{-}v}$ engrafted and also pigmented *mMCP4*$^{-/-}$ mice and non-pigmented *Tyr*$^{c\text{-}2j}$-*mMCP4*$^{-/-}$ mice. The levels of pro-angiogenic and pro-lymphangiogenic growth factors VEGF-A and –D will be compared and the functional integrity of lymphatic vessels will be assessed by the draining efficiency of injected Evan's blue dye, as well as composition of the inflammatory infiltrates, will also investigated.

1.9.4 Aim 4: Identifying potential mediators of mMCP4 in chronic UVB irradiation

In order to identify potential direct or indirect targets of mMCP4 in chronic UVB initiated skin tumourigenesis, microarrays will be performed using tissue from MC-deficient *Kit*$^{W/W\text{-}v}$ and *mMCP4*$^{-/-}$ BMCMC→*Kit*$^{W/W\text{-}v}$ mice, as well as their corresponding controls, following 12 UVB exposures. This approach will identify global changes in signalling pathways induced by chronic UVB irradiation that are different between control, mast cell deficient, and *mMCP4*$^{-/-}$ BMCMC→*Kit*$^{W/W\text{-}v}$ mice. Potential target genes identified by microarray will be further validated by qRT-PCR.

Chapter 2

METHODS AND MATERIALS

2.1 Commercial Reagents

2.1.1 Tissue culture reagents

Dulbecco's modified eagle medium (DMEM): Life Technologies.

Penicillin (10,000 U/mL)/Streptomycin (10,000 µg/mL) (Pen/Strep): Life Technologies.

β-mercaptoethanol; 1000X (BME): Life Technologies.

Fetal bovine serum (FBS): Bovogen.

Albumin solution from bovine serum; 35% (BSA): Sigma Aldrich.

Dulbecco's phosphate buffered saline; 10X (PBS): Life Technologies.

Dimethyl sulphoxide (DMSO): BDH.

Human Serum Albumin, dinitrophenol (DNP-HSA): Sigma Aldrich.

Water for irrigation: Baxter.

Trypan blue: BDH.

Monoclonal α-DNP (mouse IgE; clone SPE-7 [cat# D8406]): Sigma-Aldrich.

2.1.2 Cytokines and recombinant protein

Recombinant mouse (rm)IL-3: Shenandoah Biotech.

rmSCF: Made in house and gift from Prof. Angel Lopez.

2.1.3 Hybridomas

WEHI-3B Hybridoma: Gift from Stanford University, California, U.S.A.

SPE-7 Hybridoma: Gift from Stanford University, California, U.S.A.

2.1.4 β-Hexosaminidase degranulation assay reagents

Phorbol-12 myristate-13 acetate (PMA): Sigma Aldrich.

Calcium ionophore A23187: Sigma Aldrich.

P-Nitrophenyl-N-acetyl-Beta-D-glucosaminide (p-NAG): Sigma Aldrich.

2.1.5 Enzyme-Linked Immunosorbent Assay (ELISA)/ Enzyme Immunoassays (EIA) kits/reagents

BD OptEIA™ mouse IL-6 ELISA Set (≥ 15.63 pg/mL): BD Biosciences.

BD OptEIA™ mouse IL-10 ELISA Set (≥ 31.25 pg/mL): BD Biosciences.

BD OptEIA™ mouse TNFα ELISA Set (≥ 15.63 pg/mL): BD Biosciences.

Mouse TNF ELISA Ready-SET-Go!® (≥ 15.63 pg/mL): eBioscience.

Mouse IL-6 ELISA Ready-SET-Go!® (≥ 15.63 pg/mL): eBioscience.

Duokit VEGF-D ELISA kit (≥ 31.25 pg/mL) : R&D Systems.

Quantikine VEGF-A ELISA kit (≥ 3.096 pg/mL): R&D Systems.

3,3',5,5'-tetramethyl-benzidine liquid substrate: Sigma Aldrich.

Tween-20: Sigma Aldrich.

2.1.6 Reagents for flow cytometry

2.1.6.1 Mast cell surface receptor labelling

FITC-conjugated α-mouse FcεRIα (Armenian hamster IgG; MAR-1 [cat# 17-5898]): eBioscience.

PE-conjugated α-mouse CD117 (c-*kit*; rat IgG_{2b} ;2B8 [cat# 12-1171]): eBioscience.

Purified α-mouse CD16/32 (2.4G2 [cat# 553142]): BD Bioscience.

PE-conjugated Rat IgG_{2b} (rat IgG; [cat# 124321]): eBiosciences.

FITC-conjugated Armenian hamster IgG isotype control (eBio299Arm [cat# 11-4888]): eBioscience.

2.1.6.2 Reagents for characterising cell populations

Liberase CTL: Roche.

Fixation & Permeabilization Kit: eBioscience.

Live/dead AQUA stain: eBioscience.

2.1.6.3 Antibodies for characterising cell populations

2.1.6.3.1 T cell populations

APC-conjugated α–mouse CD4 (RM4-5 [cat# 553051]): BD Biosciences.

PE-conjugated α–mouse CD8b (H35-17:2 [cat# 12-0083]): BD Biosciences.

FITC-conjugated α–mouse CD3e (145-2C11 [cat# 12-0031]): BD Biosciences.

2.1.6.3.2 B cell populations

PE-conjugated α–mouse CD3e (145-2C11 [cat# 12-0031]): BD Biosciences.

FITC-conjugated α–mouse B220 (RA3-6B2 [cat# 553087]): BD Biosciences.

PerCy5.5-conjugated α–mouse NK1.1 (PK136 [cat#561082]): BD Biosciences.

APC-conjugated α–mouse CD4 (RM4-5 [cat# 553051]): BD Biosciences.

APC-Cy7-conjugated α–mouse CD45 (30-F11 [cat# 557659): BD Biosciences.

2.1.6.3.3 Granulocyte populations

PE-conjugated α–mouse Gr-1 (RB6-8C5 [cat# 553128]): BD Biosciences.

PerCy5.5-conjugated α–mouse CD11b (M1/70 [cat# 550993]): BD Biosciences.

APC-conjugated α–mouse F4/80 (BM8 [cat# 17-4801]): eBiosciences.

2.1.6.3.4 Treg cell populations

PE-conjugated α–mouse/rat FoxP3 (FJK-16s [cat# 00-5523]): eBiosciences.

Alexa Fluor 488-conjugated α–mouse CD25 (PC61.5 [cat# 53-0251]): BD Biosciences.

APC-conjugated α–mouse CD4 (RM4-5 [cat# 553051]): BD Biosciences.

2.1.7 Histochemistry reagents

Accustain Giemsa and May-Grunwald stains: Sigma Aldrich.

Toluidine blue O: Sigma Aldrich.

DePex mounting medium: BDH.

2.1.8 Immunofluorescence staining reagents

Paraformaldehyde: Sigma Aldrich.

Mounting medium (anti-fade reagent): ProSciTech.

Blocking reagent: Roche.

Sucrose: BDH.

Newborn FCS: Invitrogen.

Goat α-mouse CCL21/6kine: R&D Systems.

Rabbit α-mouse Ki67 : Abcam.

Rat α-mouse CD31 (PECAM-1; MEC13.3 [cat# 102501]): BioLegend.

Rabbit α-mouse lymphatic vessel endothelial hyaluronan receptor (LYVE-1; [cat#11-034]): AngioBio.

Cy3-conjugated α-mouse smooth muscle actin (SMA; 1A4 [cat# C6198]): Sigma Aldrich.

Alexafluor488-conjugated Donkey α-rat IgG: Invitrogen.

Alexafluor 555-conjugated Donkey α-goat: IgG: Invitrogen.

Alexafluo647-conjugated Donkey α-rabbit IgG: Invitrogen.

2.1.9 Sodium dodecyl sulfate polyacrylamide gel electrophoresis (SDS-PAGE) and western blot reagents

Horse radish peroxidase (HRP)-conjugated α-rabbit: Cell Signaling.

Horse radish peroxidase (HRP)-conjugated α-mouse: Cell Signaling.

Bio-Rad D_c protein assay: Bio-Rad.

BSA standard: New England Biolabs.

Precision Plus Protein^{TM} standards-Kaleidoscope: Bio-Rad.

Nitrocellulose membrane: Pall Corporation.

Amersham enhance chemiluminescence (ECL) Plus Western Blotting Detection System: GE Healthcare.

40% Acrylamide: Bio-Rad.

Rabbit α-mouse mMCP4 serum antibody: Gift from Prof. Gunnar Pejler, Sweden.

Rabbit polyclonal α-mouse MMP9 antibody: Millipore.

Mouse monoclonal α-β-actin antibody: Cell Signaling.

Tetramethylethylenediamine (TEMED): Bio-Rad.

Ammonium Persulphate (APS): Sigma Aldrich.

2.1.10 PCR reagents

Proteinase K: Roche.

GoTaq® Green master 2X master mix: Promega.

1Kb+ Ladder Marker: Life Technologies.

GelRed™ Nucleic Acid Gel Stain; 10,000X: Biotium.

TRIzol® reagent: Invitrogen.

QuantiTect® reverse transcription kit: QIAGEN.

QuantiTect® SYBR® Green real-time polymerase chain reaction (RT-PCR) master mix: QIAGEN.

Amplifuor Single Nucleotide Polymorphisms (SNP) genotyping kit: Millipore

2.1.11 Primers: Geneworks

All primers were designed using primer3 program and Oligocalc was used to confirm self-complmentarity of primer pairs. For quantitative real-time PCR primers, forward and reverse primers were designed to span exon-exon junctions. Primers were produced by Geneworks.

2.1.11.1 Mouse Genotyping primers

Mouse genotyping Primers (forward and reverse primers used at 20 μg/mL) (5`→ 3`):

mMCP4 genotyping:

mMCP4 Forward: CAAGGTCCAACTAACTCCCTTTGTGCTCC.

mMCP4 Neo Reverse: GGGCCAGCTCATTCCTCCCACTCATGATCT.

mMCP4 exon2 Reverse: GGTGATCTCCAGATGGGCCATGTAAGGGCG.

Tyrosinase genotyping:

Tyrosinase Forward: GACCTCAGTTCCCCTTCAAAG.

Tyrosinase Reverse: ACCCATGAAGTTGCCTGAG.

2.1.11.2 Quantitative Real-time PCR primers

Quantitative Real-time PCR (qRT-PCR) primers (Both forward and reverse primers used at 5 μg/mL) (5`→3`):

Table 2.1. List of primers used for qRT-PCR

Gene	Forward (5`→3`)	Reverse (5`→3`)
GAPDH	ACTTGGCAGGTTTCTCCAG	ACATCATCCCTGCATCCACT
mMCP4	GTGAACCCTCTCTCAGTGGTG	TGACCGACACTGGCAAGAT
VEGF-A	TGAGACCCTGGTGGACATCT	TATGTGCTGGCTTTGGTGAG
VEGF-C	GCAGCTAACAAGACATGTCCAA	CCACAACTAGATGGCCGAAG
VEGF-D	TGCAAGACGAGACTCCACTG	GCAGCAGCTCTCCAGACTTT
Desmocollin2	GAGGGTGGGTCACTGTTAATG	ATTCCCAGAGTTCCAGTACAGC
Fibulin 2	CATGCTCTCCTGCTGTGAAG	TATTGGGCAGTTCAGCCTCT
Collagen IV	GAGGTTGGAATGATGGGCTA	TTCCTTTCTCTCCTCGTTCG
Lysyl oxidase	AGGGCGGATGTCAGAGACTA	CCATGCTGTGGTAATGTTGG
CCL3	ACTGCCTGCTGCTTCTCCTACA	AGGAAAATGACACCTGGCTGG
CCL12	CCACACTTCTATGCCTCCTG	GCTGCTTGTGATTCTCCTGT

Versican	CTGATAGCAGATTTGATGCCTACTGC	GTGGTTCTTTGGATAAACTGGGTGATG
Collagen XII	ATAACTTGGGCACCTGTTGG	CAGGTCCTCGCTTTCAGACT
Cadherin 11	CCAACAGCCCAATAAGGTAT	TGAATTTCTGCTGCGAAGAC
CXCL11	AGGAAGGTCACAGCCATAGC	CGATCTCTGCCATTTTGACG

2.1.12 *In vivo* experimental materials and reagents

T-PER tissue protein extraction reagent: Thermo Scientific.

Complete mini EDTA-free (protease inhibitor cocktail tablets): Roche.

Evan's Blue Dye: Gurr-Searle Diagnostic.

Component D lysis buffer: Anaspec.

UVX-31 spectrophotometer sensor: UV products

Micrometre: Ozaki MFG. CO., LTD

2.2 Solutions and Buffers

2.2.1 Tissue culture medium and reagents

Flushing Medium:

2% Pen/strep, 0.1% BME in 1X DMEM.

Complete DMEM:

10% FBS, 2% Pen/strep, 0.1% BME in DMEM.

Bone marrow-derived MC survival media (3 ng/mL IL-3):

10% FBS, 2% Pen/strep, 0.1% BME, 20% WEHI-3B medium, 1X DMEM up to 500 mL. Addition of rmIL-3 to a final concentration of 3 ng/mL and filter sterilised prior to use.

Bone marrow-derived MC expansion media (4 ng/mL IL-3):

10% FBS, 2% Pen/strep, 0.1% BME, 20% WEHI-3B medium in 1X DMEM up to 500 mL. Addition of rmIL-3 to a final concentration of 4 ng/mL and filter sterilised prior to use.

Connective tissue MC Bone marrow-derived MCs survival media (3 ng/mL IL-3 + 50 ng/mL SCF):

10% FBS, 2% Pen/strep, 0.1% BME, 20% WEHI-3B medium in 1X DMEM up to 500 mL. Addition of rmIL-3 to a final concentration of 3 ng/mL and 50 ng/mL SCF. Filter sterilised prior to use.

Connective tissue MC Bone marrow-derived MCs expansion media (4 ng/mL IL-3 media + 50 ng/mL SCF):

10% FBS, 2% Pen/strep, 0.1% BME, 20% WEHI medium in 1X DMEM up to 500mL. Addition of rmIL-3 to a final concentration of 4 ng/mL and 50 ng/mL SCF filter sterilised prior to use. Filter sterilised prior to use.

Phosphate buffered saline:

PBS (10X) in MQ H_2O to 1L

Starvation Media:

1% Pen/strep, 0.1% BME, 0.1% BSA in 1X DMEM.

Hybridoma freezing medium

90% FBS and 10% DMSO.

2.2.2 β-Hexosaminidase degranulation assay

HEPES buffer:

1M HEPES in MQ H_2O to 100 mL, pH adjusted to 7.4.

Tyrode's Buffer:

10 mM HEPES buffer, 129 mM sodium chloride, 5 mM potassium chloride, 1.4 mM calcium chloride, 1 mM magnesium chloride, 8.4 mM D-glucose, 0.1% BSA in MQ H_2O, filter sterilised, and pH adjusted to 7.4.

0.5% Triton X-100:

0.5% triton X-100 in 1X Tyrode's buffer.

Substrate Buffer:

155 mM Disodium hydrogen phosphate, 88 mM citric acid, pH adjusted to 4.5

p-NAG solution:

4 mM p-NAG, substrate buffer in MQ H_2O, heating is applied until p-NAG is completely dissolved. Filter sterilised.

0.2M Glycine:

0.2M Glycine in MQ H_2O, pH adjusted to 10.7

2.2.3 ELISA/EIA kit buffer

Blocking buffer:

10% heat inactivated FBS in 1X PBS.

Or

1% BSA in 1X PBS.

ELISA WASH (PBS-TWEEN):

0.05% Tween-20 in 1X PBS.

Stop solution:

2N (1M) sulphuric acid in MQ H_2O.

2.2.4 Flow cytometry

FACS washing buffer:

2% heat inactivated FBS in 1X PBS.

FACS fixation buffer:

0.1% Formaldehyde, 2% glucose, 0.02% sodium azide in 1X PBS.

2.2.5 Histology/Immunohistochemistry solutions

10% neutral buffered formalin:

37% (v/v) Formaldehyde in 1X PBS.

1% aqueous toluidine blue:

1% toluidine blue in MQ H_2O.

0.1% acidic toluidine blue:

0.1% aqueous toluidine blue, 1N hydrochloric acid, pH adjusted to 1.0.

Haematoxylin stain: Sigma Aldrich.

Eosin Stain: Sigma Aldrich.

2.2.6 SDS-PAGE and Western Blotting buffers

Lower gel buffer:

1.5M Tris, 0.4% SDS in MQ H_2O, pH adjusted to 8.8.

Upper gel buffer:

0.5M Tris, 0.4% SDS in MQ H_2O, pH adjusted 6.8.

10% Ammonium persulphate (APS):

10% APS in MQ H_2O.

10X SDS-PAGE running buffer:

Tris 0.25M, 2M glycine, 1% SDS in MQ H_2O, pH adjusted to 8.3.

Transfer buffer:

25 mM Tris, 0.2M Glycine, 20% MeOH.

5% skim milk (blocking buffer):

5% (w/v) skim milk in 1X TBST.

10X Tris-buffered saline (TBST):

0.5M Tris, 1.54M sodium chloride, 1% Tween-20, H_2O, pH adjusted to 7.4.

Primary Antibody Buffer:

5% (w/v) BSA, 0.02% sodium azide in 1X PBS.

Lysis Buffer:

50 mM Tris, 0.1M sodium chloride, 5 mM EDTA, 1% NP-40, 67 mM Sodium pyrophosphate. pH adjusted to 7.5 and 1X complete protease inhibitor prior to use.

6X SDS sample loading buffer:

375 mM Tris, 10% SDS, 50% glycerol, 0.03% bromophenol blue.

2.2.7 PCR and genotyping buffers

1 M Tris-HCl:

1M Tris in MQ H_2O, pH adjusted to 8.0.

Tail lysis buffer:

100 mM Tris-HCl, 5 mM EDTA, 0.2% SDS, 200 mM sodium chloride in MQ H_2O, Proteinase K added (1:100 dilution).

TE (Tris-EDTA) buffer:

10 mM Tris-HCl (pH 7.5), 1 mM EDTA (pH 8) in MQ H_2O.

Diethylpyrocarbonate (DEPC)-H_2O (RNAase-free):

0.01% DEPC in MQ H_2O, bottles are incubated O/N at room temperature (RT) and autoclaved the next day.

50X TAE:

1.6M Tris, 800 mM sodium acetate, 40.27 mM EDTA in MQ H_2O, pH adjusted to 7.4.

2% agarose gel:

2% (w/v) Agarose in 1X TAE.

GelRed™ nucleic acid gel stain:

GelRed (10000X stock), 0.1M sodium chloride.

2.2.8 *In vivo* experimental reagents

EDTA-free TPER lysis buffer:

1 tablet of EDTA-free protease inhibitors in 10 mL of TPER buffer.

1% Evan's blue dye:

1% (v/v) Evan's blue dye in 0.9% Saline.

2.2.9 Immunofluorescence staining reagents.

Maelic acid buffer:

100 mM Maelic acid, 150 mM sodium chloride in MQ H_2O. pH adjusted to 7.5 and filter sterilised.

Blocking reagent:

20% NewBorn Heat inactivated FBS, 10% Blocking reagent, 60% Maelic acid buffer and filter sterilised.

TBST Washing buffer:

50 mM Tris-HCl, 150 mM NaCl in MQ H_2O and 0.1% Tween-20; pH adjusted to 7.6.

2.3 Mice

C57BL/6 (B6), C57BL/6-*Tyr*$^{c\text{-}2j}$ (*Tyr*$^{c\text{-}2j}$) and c-*kit* mutant, genetically mast cell-deficient (WB/ReJ-*Kit*$^{W/+}$ x C57BL/6-*Kit*$^{W\text{-}W/+}$)F_1-*Kit*$^{W/W\text{-}v}$ were obtained from Jackson Laboratories (Bar Harbor, ME). To produce genetically MC-deficient mice, WB/ReJ-*Kit*$^{W/+}$ heterozygote (het) and C57BL/6-*Kit*$^{W\text{-}W/+}$ (het) were paired together to generate WBB6F_1-*Kit*$^{W/W\text{-}v}$ (*Kit*$^{W/W\text{-}v}$) mice and their wild-type (WT) littermates (WBB6F_1-*Kit*$^{+/+}$ [*Kit*$^{+/+}$]). B6-*mMCP4*-deficient (*mMCP4*$^{-/-}$) mice were a generous gift from Prof. Gunnar Pejler (Swedish University of Agricultural Sciences, Sweden) and were generated by gene trapping techniques as previously explained[194]. Genetically *mMCP4*-deficient non-

pigmented mice were generated by crossing B6-*mMCP4*$^{-/-}$ (pigmented) with B6-tyrosinase mutant (B6-*Tyr*$^{c\text{-}2j}$ [non-pigmented]) mice to produce *Tyr*$^{c\text{-}2j}$–*mMCP4*$^{-/-}$ (*mMCP4*-deficient non-pigmented mice). Age-matched female and male mice of at least 9 weeks of age were used for *in vivo* experiments as explained in **section 2.10**. All mice were bred in house at the Institute of Medical and Veterinary Science (IMVS) animal care facility (Adelaide, Australia). All experiments were performed in compliance with the ethical guidelines of the National Health and Medical Research Council of Australia and with approval from the Institute of Medical and Veterinary Science and University of Adelaide animal ethics committee (Univeristy of Adelaide ethics approval number: S-2012-244).

2.4 Tissue culture methods

2.4.1 Generating and culturing BMCMCs

To generate BMCMCs, mice were humanely sacrificed by CO_2 inhalation. Following CO_2 inhalation, the hind legs of the sacrificed mice were surgically removed and were further processed in a Class 2 Biosafety hood. Bone marrow-derived cells were collected by flushing the femurs and tibias with flushing medium. Once collected, bone marrow-derived cells were cultured in BMCMC 3 ng/mL IL-3 media for a period of 2-3 weeks to selectively promote survival of MCs. The cells were subsequently cultured in BMCMC 4 ng/mL IL-3 media to promote proliferation. MC populations were identified by staining for their granular morphology through May-Grunwald Giemsa staining **(Section 2.7.1)**. Additionally, MC-specific cell surface marker expression (c-*kit*$^{+}$FcεRI^{+}) was assessed by flow cytometry **(Section 2.6.2)** to confirm and determine the percentage of the MC population. After 4-6 weeks of culturing, >95% of the cell population were found to be generally c-*kit*$^{+}$ and FcεRI^{+} BMCMCs.

To generate a population of connective tissue-like BMCMCs (CTMCs), cells were collected as stated above, but, cultured in media containing 3 or 4 ng/mL IL-3 + 50 ng/mL SCF media. To confirm the generation of CTMCs, Western blot analysis of mMCP4 was performed as CTMCs typically express higher levels of endogenous of mMCP4 compared to BMCMCs cultured in IL-3 only.

2.4.2 Generating and culturing WEHI-3B hybridomas

Frozen and stored aliquots of WEHI-3B hybridomas were thawed and cultured in cDMEM medium in the first 2 weeks, until all cells appeared healthy and viable. To generate IL-3 containing medium from WEHI-3B hybridomas, cells were seeded at 1.5 x 10^5 cells/ml and incubated at 37°C/5% CO_2 over 5 days, until the cell concentration reached ~10^6 cells/ml. Cells were centrifuged (250 *g*, 15 min at 4°C) and supernatant was collected and centrifuged again (350 *g*, 20 min at 4°C). After the final spin, harvested supernatant was filter sterilised using a Millipore® Steritop^{TM} (0.22μm) filter in a Class 2 Biosafety hood. In addition, a small aliquot of the harvested supernatant was collected to assess IL-3 concentration by ELISA and the remaining was stored at -20°C. Typically, the concentration of IL-3 in WEHI-3B conditioned medium ranged from 8-12ng/ml of IL-3. To store WEHI-3B hybridomas, cells were cultured to ~50% confluence and resuspended in WEHI freezing medium (90% FBS, 10% DMSO) slowly in a drop-wise fashion, the cells would then be stored in a Mr Frosty freezing container (Nalgene) at -80°C and ultimately stored in the IMVS liquid nitrogen storage facility.

2.5 *In vitro* procedures/assays

2.5.1 β-hexosaminidase degranulation assay

To measure IgE-dependent activation of BMCMCs, 5-8 week old BMCMCs were seeded to a concentration of 10^6 cells/mL and sensitised with SPE-7 α–DNP IgE at 2 μg/mL in BMCMC 3 ng/mL media and incubated at 37°C/5% CO_2 overnight (O/N). Following O/N incubation, cells were counted and washed with 1X Tyrode's buffer, resuspended at a concentration of 6.25 x 10^6 cells/mL and plated in a 96 V-well plate (Costar). Once plated, cells were stimulated with DNP-HSA at 1-1000 ng/mL or with PMA (50 ng/mL)/A23187 (10 μM) as a positive control for 1 h at 37°C/5% CO_2. After 1 h incubation, the plate was centrifuged (250 *g* for 5 min at 4°C), cell supernatants were collected and cell pellets were lysed with 0.5% Triton X-100. Harvested cell supernatants and lysates were incubated with p-NAG substrate solution for 1 h at 37°C/5% CO_2. β–hexosaminidase degranulation activity was assessed after the addition of 0.2M glycine and the optical density reading was recorded at a wavelength of 405nm on an EPOCH ELISA plate reader (BioTek). Degranulation activity was presented as % degranulation and was calculated by dividing the activity from culture supernatant by total degranulation activity (cell lysates + supernatant) x 100%.

To examine the BMCMCs ability to degranulate through non-IgE dependent stimulation, BMCMCs were also stimulated with SP (1 μM-200 μM) and with PMA (50 ng/mL)/A23187 (10 μM) as a positive control for a period of 1 and 24 h at 37°C/5% CO_2. β–hexosaminidase degranulation activity was assessed as explained above.

2.5.2 Measuring cytokine concentration by ELISA or EIA analysis

To determine the level of cytokine release from BMCMCs, 5-8 week old cultured BMCMCs were seeded at 10^6 cells/mL and preloaded with SPE-7 α–DNP IgE at 2 μg/mL in BMCMC 3 ng/mL IL-3 medium at 37°C/5% CO_2 O/N as explained in **section 2.5.1**. Following O/N incubation, cells were washed and resuspended in starvation medium at a concentration of 10^6 cells/mL and were plated out (in triplicate) in a 48 well plate and stimulated with 20 ng/mL DNP-HSA or untreated for 6 h at 37°C/5% CO_2. After 6 h of incubation, cell supernatants were harvested and used for ELISA or EIA analysis.

To determine the cytokine levels released from BMCMCs, cell supernatants from IgE + Ag treated BMCMCs were applied to ELISA analysis following the manufacturer's protocols. Prior to measurement of cytokines, depending on the instructions, certain ELISA kits required an incubation of specific-cytokine capture Ab with its corresponding coating buffer onto high affinity binding 96 well plates (Costar) O/N at 4°C. Following the O/N incubation, the coated plate(s) were washed 3 times with PBS-Tween and blocked with ELISA blocking buffer prepared according to manufacturer's protocol for 1 h at RT. Following the 1 hr incubation, the plate was washed 3 times and incubated for 2 h with neat/diluted sample and ELISA standards with serial dilutions. Following incubation with samples/standards, the plate was washed 3 times and incubated with detection antibody and streptavidin-HRP for 1 h at RT (in darkness); For ELISA/EIA kits from eBioscience or R&D systems, the plate was incubated for 1 h with detection antibody at RT, and an additional 30 min with streptavidin-HRP with washing in between. After incubation with secondary/strep-HRP, plates were washed three times, and 3,3',5,5'-tetramethyl-benzidine liquid substrate was added to all wells for colour development and the reaction was stopped using stop solution when the top standards displayed maximum colour intensity (usually blue precipitates would be observed at the bottom of the wells). The optical density readings were obtained at 450 with a reference wavelength of 570nm using an EPOCH ELISA plate reader (BioTek).

2.6 Flow cytometry

2.6.1 Cell-surface receptor labelling

To characterise the expression profile of cell surface markers of the BMCMCs, 10^6 cells were washed with FACS wash buffer, centrifuged (250 *g* for 5 min at 4°C) and were resuspended with 100 μL of FACS buffer and Fc receptor binding was blocked by incuabting with Fc receptor blocking antibody (Ab)(1:100) on ice for 15 min. BMCMCs were stained with PE-conjugated α-mouse CD117 (c-*kit*) (1:100) and FITC-conjugated FcεRI (1:200) for 30 min on ice (in the dark). Following the labelling of cell surface markers, cells were washed with FACS buffer, centrifuged (100 *g* for 5 min; 4°C) and resuspended in 500 μL of FACS buffer and analysed freshly on the day of staining. Surface-labelled BMCMCs were processed on a FCS 500 Flow Cytometer (Beckman Coulter) at the Detmold Imaging Facility (IMVS). Data was analysed on FCS Express (version 4.1).

2.6.2 Assessing cell population by flow cytometry

The leukocyte populations in the ears and draining lymph nodes of UVB-treated mice and no UVB treated mice were analysed as previously described (Grimbaldeston *et al* 2007 and 2010)[8,9]. The skin on the ears were split parallel with the cartilage into two halves, cut into fine pieces and incubated in RPMI containing 0.5 mg/ml of Liberase CI (Roche) for 2 h at 37°C. A single cell suspension was obtained using a 70 μm nylon cell strainer to separate undigested tissue. Single cell suspensions were incubated with α-mouse CD16/CD32 mAb (eBioscience) on ice for 15 min for FcR blocking. Leukocytes were then incubated on ice for 40 min with antibodies for cell populations of T cells, B cells, NKT cells, Treg cells and granulocytes **(Abs listed in 2.1.6.3)**. All antibodies were diluted 1:100 (Gates for sub populations were based on single colour staining of the cells to assess compensation and non-specific fluorescence). Live dead AQUA stain was used to detect dead cells. Only cells negative for AQUA Live/Dead stain were analysed. To calculate the number of lives cells of a particular cell type recovered per ear (determined by gating on AQUA-negative cells), the following calculation was applied for each population quantified: lives cells recovered per ear in a particular subset of leukocytes = (% gated of the total cell population in that ear) x (total number of cells recovered form that ear [counted using a hemocytometer after tissue digestion and single cell suspension]). All

cell population data was analysed on a Gallios Flow Cytometer and data was assessed and extrapolated from FACS express 4.

2.6.3 Intracellular marker staining

For intracellular staining of FoxP3$^+$ Treg cells, the single cell suspension, was fixed with the IC fixation buffer (Fixation & Permeabilization Kit) for 20 min at RT. Cells were then washed with and resuspended in 1x permeabilization buffer (diluted with H_2O from 10X Permeabilization Buffer, Fixation & Permeabilization Kit), and incubated with primary Ab(s) α-CD3, α-CD4 and α-CD25 for 30 min on ice and then incubated with α-mouse FOXP3-PE according to manufacturer's instructions (eBioscience). When unconjugated primary Abs were used, cells were washed with 1x permeabilization buffer following the first incubation and subsequently labelled with corresponding fluorochrome-conjugated secondary Ab(s) for a further 30 min on ice. In all cases, labelled cells were finally washed with 1x permeabilization buffer, resuspended in FACS buffer and analysed on a Gallios Flow Cytometer (Beckman Coulter). Flow data was extrapolated and assessed on FACS express 4.

2.7 Cell staining

2.7.1 May-Grunwald Giemsa staining

Once BMCMCs were cultured for 4-6 weeks, at least 2.5 x 10^5 cells were taken and loaded onto a cytospin funnel following manufacturer's instructions. Cells were centrifuged at 100 *g* at high acceleration for 5 min. After centrifugation, slides containing cytospun cells were stained with May-Grunwald stain for 5 min and washed in PBS for 90 seconds. The slides were then stained in Giemsa stain (1:20 in MQ H_2O) for 20 min and were briefly washed under tap water and air dried for 30 min. After air drying, coverslips were mounted on with DePex mounting medium and left to dry O/N. Images of cells were taken on an Olympus BX45 microscope.

2.8 PCR and genotyping procedures

2.8.1 Genotyping of WT and *mMCP4*$^{-/-}$ mice

Prior to any experimentation, to ensure the correct genotype of the mice, genomic (g)DNA was extracted from tail tips of the mice and applied to PCR analysis. Tail tips were taken from 2 week-old mice and were lysed in tail lysis buffer containing Proteinase K (1:100) O/N at 55°C with gentle rocking/agitation. Tubes containing the lysates were

centrifuged (13,000 *g* for 10 min at 4°C) and lysates were transferred to new Eppendorf tubes containing 500 μL of 100% isopropanol. Precipitate was formed with gentle inversion and centrifuged at 17,000 *g* for 5 min at 4°C. Following centrifugation, the supernatant was removed and the DNA pellet was washed with 70% EtOH and subsequently centrifuged again (17,000 *g* for 5 min at 4°C). Following the spin, the supernatant was removed and the DNA pellet was air-dried at RT. gDNA pellets were then redissolved at 65°C in 300 μL of TE buffer for 30 min and stored at 4°C or -20°C.

After gDNA extraction, GoTaq Master mix cocktails containing GoTaq master mix (6.25 μL/sample), nuclease-free H_2O (4.85 μL/sample), and a primer set consisting of primers specific for exon 1 of the *mMCP4* gene B6-*mMCP4*$^{+/+}$, a common primer, and a primer specific for the Neomycin cassette, (which was used to replace exon 1 of *mMCP4* and generate B6-*mMCP4*$^{-/-}$ mice; primer concentration 20 μM; 0.3 μL/primer/sample). In 0.2 mL PCR tubes, 12 μL of the GoTaq cocktail was mixed with 0.5 μL of tail-extracted gDNA and subjected to thermocycling as listed below:

Step 1: 94°C 3 min

Step 2: 94°C 15sec

Step 3: 58°C 20 sec

Step 4: 72°C 20 sec

Repeat steps 2-4 for 34 cycles

Step 5: 72°C 2 min

Step 6: 8°C hold

To visualise the PCR products, 5 μL of PCR reaction was loaded onto a 2% agarose gel and subjected to electrophoresis at 90V for 30 min. The gel was stained with Gel-Red (1:10000 in 0.1M NaCl) for 10 min and PCR products were visualised at 320 nm UV light (UviTech). A PCR product at 900bp indicated a WT, 320bp indicated a knockout (KO), and both indicated as a het.

2.8.2 Genotyping of *Tyr*$^{c\text{-}2j}$ mice

Following the protocol from **2.8.1**, extracted gDNA from *Tyr*$^{c\text{-}2j}$ mice was mixed with Amplifuor SNPS genotyping (Millipore) reagents following the manufacturer's instructions. Customised primer sequences specific for *Tyr*$^{c\text{-}2j}$ mice were used and these PCR reactions were subjected to thermocycling as listed below:

Step 1: 95°C 5 min

Step 2: 94°C 30 sec

Step 3: 60°C 30 sec

Step 4: 72°C 40 sec

Repeat steps 2-4 for 39 cycles

Step 5: 72°C 2 min

Step 6: 10°C hold

Following the PCR, to determine the genotype of these mice, fluorescent end point analysis was done using the ABI PRISM 7500 thermocycler. PCR reactions using gDNA from WT and het mice were used as controls to determine the genotype of mice.

2.8.3 RNA extraction

To determine mRNA expression of specific genes, RNA was extracted from tissues, cDNA generated from which was analysed using quantitative real-time RT-PCR. Tissues were harvested and process as explained in **section 2.10.6** and sonicated with 500 μL TRIzol reagent. After the sonication step, an additional 500 μL of TRIzol reagent was added to the tubes and the same samples were snap-frozen in liquid nitrogen (LN_2) and stored at -80°C. Samples were later thawed at RT and allowed to equilibrate for 5 min. The samples were then centrifuged (12,000 *g* for 15 min at 4°C) to pellet the tissue and debris and the remaining supernatant was transferred to a clean RNase-free Eppendorf tube. 200 μL of chloroform was added to the tubes and the tubes were vigorously shaken for 15 sec and allowed to rest for 5 min. Samples were centrifuged (12,000 *g* for 15 min at 4°C) and 200 μL of the aqueous layer was carefully transferred to a new Eppendorf tube containing 500 μL of 100% isopropanol. The tubes were then briefly vortexed and left on ice for 1 h to allow RNA precipitation. Following RNA precipitation the samples were centrifuged (12,000 *g* for 15 min at 4°C), washed with 75% RNase-free EtOH, centrifuged again (7,500 *g* for 5 min at 4°C), and supernatant was aspirated, while the RNA pellet was allowed to air dry for 30 min at RT. The air-dried RNA pellet was re-dissolved in 20 μL DEPC-treated H_2O and RNA concentration was quantified using a Nanodrop 1000 spectrophotometer. After quantification, RNA was either stored at -80°C or immediately used for complementary DNA (cDNA) synthesis.

2.8.4 Complementary DNA synthesis

To measure the relative expression of specific genes, cDNA was generated using the QIAGEN Quantitect reverse transcription kit. 1 µg of RNA (adjusted to 12 µL with DEPC-H_2O) was incubated with 2 µL of gDNA Wipeout Buffer for 2 min at 42°C. After 2 min, the mixture was added to a RT mixture containing 1 µL reverse transcription enzyme, 1 µL primer mix and 4 µL of (5x) RT buffer; and incubated for 30 min at 42°C followed by 3 min at 95°C. All of the incubation steps were done in a Bio-Rad thermocycler. Synthesised cDNA were either stored at -20°C or immediately used for qRT-PCR.

2.8.5 Quantitative real-time RT-PCR

qRT-PCR was performed in triplicate with cDNA samples at an appropriate dilution ranging from 1/6 (samples) to 1/20 (calibrator). Each final reaction (10 µL) consisted of 2 µL of diluted cDNA, 5 µL of QuantiTech SYBR green master mix, 1 µL of RNase-free H_2O, and 1 µL of each of the designated forward and reverse primer pair (5 µM diluted working stock). The level of GAPDH was assessed in all cases as the housekeeping gene to allow normalisation of results. Reactions containing RNase-free H_2O instead of cDNA dilution were also included for each primer pair as negative controls. All RT-PCR reactions were carried out in the Rotor-Gene 6000 Real-time Rotary Analyzer (Corbett) using conditions as follows:

Step 1: 95°C 15 min

Step 2: 95°C 20 secs

Step 3: 57-60°C 25 secs

Step 4: 72°C 20 secs

Steps 2-4 for 50 cycles

Step 5: 72°C 60 secs

Step 5: 72°C 90 secs (Melting)

72°C - 99°C at 5 sec/°C

The relative quantity of the PCR product was analysed using the "Comparative Quantitation" method of the Rotor-Gene 6000 Series Software (version 1.7).

2.8.6 mRNA microarray

Tissue RNA from UVB and untreated ears were extracted as described in **2.8.3**. RNA integrity was determined with the Agilent BIOANALYZER. 1 μg of RNA was processed for use on the microarray by using the Affymetrix GeneChip one-cycle target labeling kit (Affymetrix, Santa Clara, CA) according to the manufacturer's recommended protocols. All protocols and data analysis were conducted by the Centre for Cancer Biology Genomics Facility.

2.9 SDS-PAGE and Western Blot analysis

2.9.1 Preparation of whole cell lysates

Cultured BMCMCs (2-3 x 10^6 cells/sample) were washed twice with cold PBS, and supernatant was removed as thoroughly as possible. Each cell pellet was subsequently lysed in ~100 μL of lysis buffer on ice for 20 min, and centrifuged (17,000 *g*, 10 min, 4°C) to obtain the clarified cell lysate. The protein content of resultant total cell lysates were quantified using Bio-Rad D_c protein assay following the manufacturer's instructions. Once total protein was measured cell lysates were snap frozen using LN_2 and stored at -20 °C until analysed.

2.9.2 SDS-PAGE

Cell lysate samples were thawed, mixed with 6X SDS-PAGE sample loading buffer (i.e. in a 5:1 ratio), and boiled for 5 min before being subjected to SDS-PAGE (10% SDS-PAGE; 20-100 μg of protein/lane) at 100 V for 60-90 min in SDS-PAGE running buffer. Precision Plus Protein™ standards-Kaleidoscope markers were loaded in parallel as a reference for protein sizes.

2.9.3 Protein transfer and western blot analysis

Following SDS-PAGE, proteins were transferred onto a nitrocellulose membrane 300 V for 90 min in transfer buffer. The membrane was blocked with 5% skim milk for 1 h at RT, and subsequently blotted with designated primary Ab ([rabbit anti-mMCP4 serum, 1:500, mouse anti-β-actin, 1:3000, rabbit anti-mouse MMP-9, 1:500] all diluted in 5% BSA, 0.02% sodium azide) O/N at 4°C, followed by the corresponding HRP-conjugated secondary Ab(s) (anti-rabbit HRP, 1:3000 and anti-mouse, 1:3000) for 1 h at RT. Three 5 min washes with 1X TBST were carried out after each blotting step. The blots were

developed using Amersham ECL Plus Western Blotting Detection System and detected using LAS-4000 Luminescence Analyser, and analysed using the Multi Gauge software (version 3.1). In cases where membranes needed to be re-probed with another primary Ab, they were first briefly washed with 1X TBST and stripped with the stripping solution.

2.10 *In vivo* experiments and tissue sample analysis

2.10.1 Adoptive transfer of BMCMCs into mice

BMCMCs derived from WT B6-*mMCP4*$^{+/+}$ (WT BMCMCs) or B6-*mMCP4*$^{-/-}$ (*mMCP4*$^{-/-}$ BMCMCs) were cultured as explained in section **2.4.1**. Once cultured BMCMCs were analysed and determined as >95% c-*kit*$^{+}$ and FcεRI^{+} mast cell population, they were resuspended in normal DMEM media and were intradermally injected (*i.d.*; 2 injections into each ear of mice, 2 x 10^6 cells in 25 μL DMEM/injection) into at least 4-6 week old *Kit*$^{W/W\text{-}v}$ mice. For physiological relevance, we allowed 4-6 weeks for the injected BMCMCs to localise to their pathophysiological locations.

2.10.2 Chronic UVB irradiation of mice

For UVB irradiation of mice, a bank of 6 Philips FS40T12 lamps (Ultraviolet Resources International) emitting a broad 270–380 nm band of UV, with peak emission at 310 nm comprising ~65% of the energy emitted, was used to irradiate mice in individual compartments of Perspex cages. The intensity and spectral output of the UVB lamps was measured before each irradiation using a UVX spectrophotometer with a UVX-31 sensor (UV products). A new sheet of clear PVC plastic film (0.23 mm thick) was taped to the top of each perspex cage before irradiation to screen wavelengths <290 nm. The lamps were held 15 cm above the cages. 9-13 week-old mice were conscious and had full range of movement during irradiation. For chronic exposures the entire mouse (including both ears) was irradiated with doses of 4 kJ/m^2 to 8 kJ/m^2 of UVB every 2 days for a total of 5, 12 or 25 exposures (total cumulative dose = 20 kJ/m^2, 60 kJ/m^2 or 152 kJ/m^2 UVB, respectively). Ear thickness was measured using a micrometer (Ozaki MFG. CO., LTD) prior to each UVB irradiation. At the end of each experiment mice were sacrificed by CO_2 inhalation 3 or 24 h after the final UVB exposure and samples of ear were taken for histology (**Section 2.10.3**), FACS analysis (**Section 2.6.2**), immunofluorescence staining (**Section 2.10.7**) and cytokine production (ELISA) (**Section 2.10.6**).

2.10.3 Ear tissue histology and numeration of tissue MCs

Samples of ear pinnae (1 mm-wide strips through the centre) were fixed in 10% buffered formalin and embedded in paraffin (with care to ensure a cross-section orientation). Paraffin ear sections were cut in a transverse orientation at 4μm thickness using a Microtome (Leica) and left to air-dry O/N. Ear sections were dewaxed by being immersed sequentially in Xylene (twice; 5 min each), 100% EtOH (twice; 3 and 2 min), 70% EtOH (3 min), 50% EtOH (2 min), and H_2O (5 min) (until staining); and stained with 0.1% acidic toluidine blue (**Section 2.10.4**) for detection of MCs (cytoplasmic granules appear purple).

2.10.4 Toluidine blue staining

For toluidine blue staining of ear tissue MCs, dewaxed ear sections (Section 2.10.3) were stained with 0.1% acidic (pH 1) toluidine blue solution for exactly 90 sec, thoroughly rinsed with H_2O, air-dried and then mounted in DePex mounting medium. After toluidine blue staining, images were taken on a Hamamatsu NanoZoomer Virtual Microscopy System at 40x magnification. Ear pinna MCs and horizontal length of ear cartilage were counted and measured on Nanozoomer image software. MC numbers were expressed as number of MCs per horizontal length of ear cartilage (mm).

2.10.5 Haematoxylin and Eosin (H&E) staining

To examine the presence of *in situ* SCCs in tissue. Sections taken from UVB-treated and no-UVB treated mice were processed and stained in H&E stain. Formalin fixed tissue was dewaxed and rehydrated as explained in **section 2.10.3**. Dewaxed sections were stained in Haematoxylin for 6 min and washed in MQ H_2O for 10 min. Slides were then washed in 0.25% acid alcohol for 3 sec and rinsed under running tap water for 5 min. Following the wash, slides were immersed in Lithium Carbonate for 3 sec, rinsed in MQ H_2O and then counterstained in Eosin for 15 sec. After staining, slides were dehydrated in 95% EtOH (2 times, 3 min), 100% EtOH (2 times, 2 min) and rinsed in xylene. Coverslips were mounted on slides using DePex mounting medium. Sections were scored by SA Pathology dermatopathologist Dr. Jan Ibbetson and A/Prof Michele Grimbaldeston.

2.10.6 Ear tissue lysate preparation and cytokine analysis

To measure the cytokine levels in ear tissues, the ears were finely cut up on an ice cold surface, sonicated in 250 µL of Tper lysis buffer containing EDTA-free protease inhibitors or PBS containing EDTA-free protease inhibitors and snap frozen with LN_2 and immediately stored at –80 ºC until analysis After thawing at RT, samples were centrifuged at 17,000 *g* (10 min, 4 ºC) and the supernatants were collected. Concentrations of VEGF-A, VEGF-D, TNFα, IL-6 and IL-10 in the supernatants were measured by ELISA (eBioscience), according to the manufacturer's instructions (detection limit for each ELISA is indicated in **section 2.1.5**). Data is normalised with protein concentration in each sample and expressed as pg/mg (cytokine concentration/protein concentration), where total protein concentrations in the supernatants were measured by a Bio-Rad D_c protein assay, according to the manufacturer's instructions.

2.10.7 Immunofluorescence staining of tissue

UVB-treated and untreated ears were fixed in 4% paraformaldehyde O/N at 4°C with gentle rocking. Following fixation, tissues were washed extensively in PBS and cryoprotected in 30% sucrose O/N at 4°C with gentle agitation, then frozen in TissueTek® Optimal Cutting Temperature (OCT) compound on dry ice and stored at -80°C. Sections were cut at -20°C to -25°C using a cryostat (Leica). Cryosections were cut in a transverse orientation at 10 µm thickness and embedded on superfrost slides. The cryosections were stored at -20°C until analysis. Cryosections were blocked in 50 µL (per section) blocking solution for 1 h at RT in a humidifying chamber, and stained with 50 µL of rat α-mouse CD31 (1:500) and rabbit α-mouse LYVE-1 (1:1000) diluted in blocking solution O/N at RT. The stained sections were then washed 3 times in Tris-buffered Saline containing 0.1% tween-20 and incubated with respective antibodies, α-mouse smooth muscle actin (SMA)-Cy3 (1:1000), donkey α-rat Alexafluor488 (1:500) and donkey α-rabbit Alexfluor647 (1:500) for 3 h at RT. The sections were mounted in mounting medium containing an anti-fade reagent. The Immunofluorescently stained sections were analysed using a Carl Zeiss LSM700 confocal microscope (Carl Zeiss). Quantification of data was done using ImageJ software.

To assess $Ki67^+$ cell proliferation markers, tissues were processed as explained above and the primary antibodies that were used are the following: rat α-mouse CD31 (1:500), rabbit α-mouse Ki67 (1:250) and goat α-mouse CCL21/6kine (1:250); all of which were diluted in blocking solution and stained O/N in a humidifying chamber. After O/N incubation, slides were washed as explained above and incubated with respective secondary antibodies: Alexafluor488-conjugated Donkey α-rat IgG, Alexafluor555-conjugated Donkey α-goat: IgG and Alexafluor647-conjugated Donkey α-rabbit IgG (all secondary Abs were diluted 1:500) in a humidifying chamber for 3 h at RT. Following incubation, all slides were processed and analysed as explained in **section 2.10.6**. $Ki67^+$ cells in lymphatic vessels were counted and normalised to the number of enlarged lymphatic vessels per field of view.

2.10.8 Evan's blue dye injection

To determine the functionality of lymphatic vessels, 24 h after the final UVB exposure, mice were injected with 10 μL 1% Evan's blue dye via *i.d.* ear injection and incubated for 1 h at RT. Following the incubation, mice were sacrificed and photos of the ears and draining superficial lymph nodes were taken. The ears and draining lymph nodes were harvested, weighed and processed similar to that described to section **2.10.6**. Following processing, the ears and LNs were incubated with 300 μL of formamide at 55°C with gentle rocking/agitation O/N to extract the Evan's blue dye. Following the O/N incubation, 100 μL of the extracted Evan's blue dye was plated on to 96 well plates (in duplicate) and the absorbance was measured at 610nm. Data was represented as absorbance/g of tissue.

2.11 Statistical analysis

All data shown in were tested for statistical significance using the unpaired, two-tailed, Student's *t*-test or the Mann Whitney U test (GraphPad Software, version 5.04) between each pair of different treatments. Analysis of variance (ANOVA) for repeated measures was used to assess differences in ear thickening among mouse groups in all chronic UVB experiments, and other experiments that involved repeated measurements on the same animal over a period of time. In all cases, *P* values less than 0.05 were considered statistically significant, and data are presented as either "mean + SEM", "mean + SD" or "median" or "median ± range" as indicated.

Chapter 3

CHARACTERISATION OF BONE MARROW-DERIVED CULTURED MAST CELLS FROM *mMCP4*$^{-/-}$ MICE

3.1 Introduction

It is well understood that MCs can promote inflammatory responses, but more studies are now demonstrating their ability to negatively regulate responses through the release of mediators such as IL-10[8], histamine[383] and mast cell proteases[5], particularly mMCP4. Our preliminary data (unpublished) suggests that mMCP4 could also be protective in a model of chronic low-dose (non-tumourigenic) UVB irradiation, similar to what we have previously demonstrated in regards to the protective function of MC-IL-10[8,9]. Hence, this project aims to determine whether mMCP4 is still protective under carcinogenic doses of chronic UVB irradiation.

The most well-known method of determining the function of mMCP4 at either physiological or pathological conditions is utilising genetically modified B6-*mMCP4*$^{-/-}$ mice, which were generated by gene targeting which removes exon 1 of the mMCP4 gene by homologous recombination[194]. By substituting exon 1 for a neomysin cassette this prevented further translation of the *mMCP4* gene.

The generation of genetically-modified mice can exhibit distinct pathologies under homeostatic conditions. Studies have shown that B6-*mMCP4*$^{-/-}$ mice are generally phenotypically normal under physiological conditions, with the exception of increased collagen and hydroxyproline deposition in the skin, suggesting that mMCP4 is critical for homeostatic tissue remodelling[194,384]. However, when this homeostasis is disrupted, the B6-*mMCP4*$^{-/-}$ mice do exhibit differential pathology when challenged in experimental models such as spinal cord damage[380], traumatic brain inflammation[379], poly-microbial sepsis[5], and allergic airway inflammation[7].

Prior to assessing the roles of mMCP4 in our chronic UVB model, it is critical to assess if the absence of mMCP4 could influence the function and characterisation of MCs. Hence, for this part of the study, the morphological features and basic functions of B6-*mMCP4*$^{+/+}$ and B6-*mMCP4*$^{-/-}$ BMCMCs were characterised. The morphological features of BMCMCs were assessed by May-Grunwald giemsa stain and expression of MC-specific cell surface markers by flow cytometric analysis.

In terms of activation and functionality of MCs, it is well understood that binding and cross-linking of antigen with IgE-bound FcεRI can induce degranulation and *de novo* synthesis, with the subsequent release of an array of mediators such as proteases,

chemokines and cytokines (**section 1.1.6**) from MCs[3]. Whilst the activation and functional significance of MCs is well characterised in IgE-dependent situations, our understanding of MC activation in conditions associated with UVB exposure remains to be clarified. However, there is evidence that UVB-induced mediators such as PAF, vitamin D_3[9,10], *cis*-UCA[360], α-MSH[363], SP[360,385] and CGRP[360] can activate MCs.

Therefore B6-*mMCP4*$^{+/+}$ and B6-*mMCP4*$^{-/-}$ BMCMCs were first assessed by the well-defined IgE-dependent mode of activation and measured for degranulation (β-hexosaminidase release) and *de novo* synthesis of pro-inflammatory cytokines IL-6 and TNFα. Subsequently these MCs were also activated in an IgE-independent manner through stimulation with the neuropeptide SP, which is known to activate MCs in response to UVB exposure[360,385].

3.2 Results

3.2.1 *mMCP4*$^{+/+}$ *and mMCP4*$^{-/-}$ *mice and BMCMCs are functionally and phenotypically comparable.*

To confirm that the gene trapping technique did remove the presence of mMCP4 both at the mRNA transcript and protein level, we assessed the mRNA expression by quantitative real-time RT-PCR and endogenous protein expression level by western blot analysis. qRT-PCR revealed a complete absence of mRNA transcript in B6-*mMCP4*$^{-/-}$ mice compared to B6-*mMCP4*$^{+/+}$ (WT) mice (**Figure 3.1a**). mMCP4 is a ~26kDa protein. Western blot analysis also confirmed a complete absence of endogenous mMCP4 protein expression in B6-*mMCP4*$^{-/-}$ tissue lysates as no band could be identified at ~26kDa compared to B6-WT mice (**Figure 3.1b**). Additionally, B6-*mMCP4*$^{-/-}$ mice did not exhibit any distinguishable phenotypic characteristics with respect to appearance of hair, body weight and size, and exhibit normal fertility similar to B6-WT mice (**Figure 3.1c**). Phenotypically, studies have demonstrated a complete absence of chymotrypsin-like activity in the skin of *mMCP4*$^{-/-}$ mice consequently promoting an increase in collagen and hydroxyproline deposition in the tissue of the mice suggesting a homeostatic role in tissue remodelling[194,384].

Skin pigmentation is typically composed of melanin, which is known to have a critical role in photoprotection against the generation of UVB-induced photoproducts[386,387,313,388] hence their associated detrimental effects that can contribute to the induction of non-

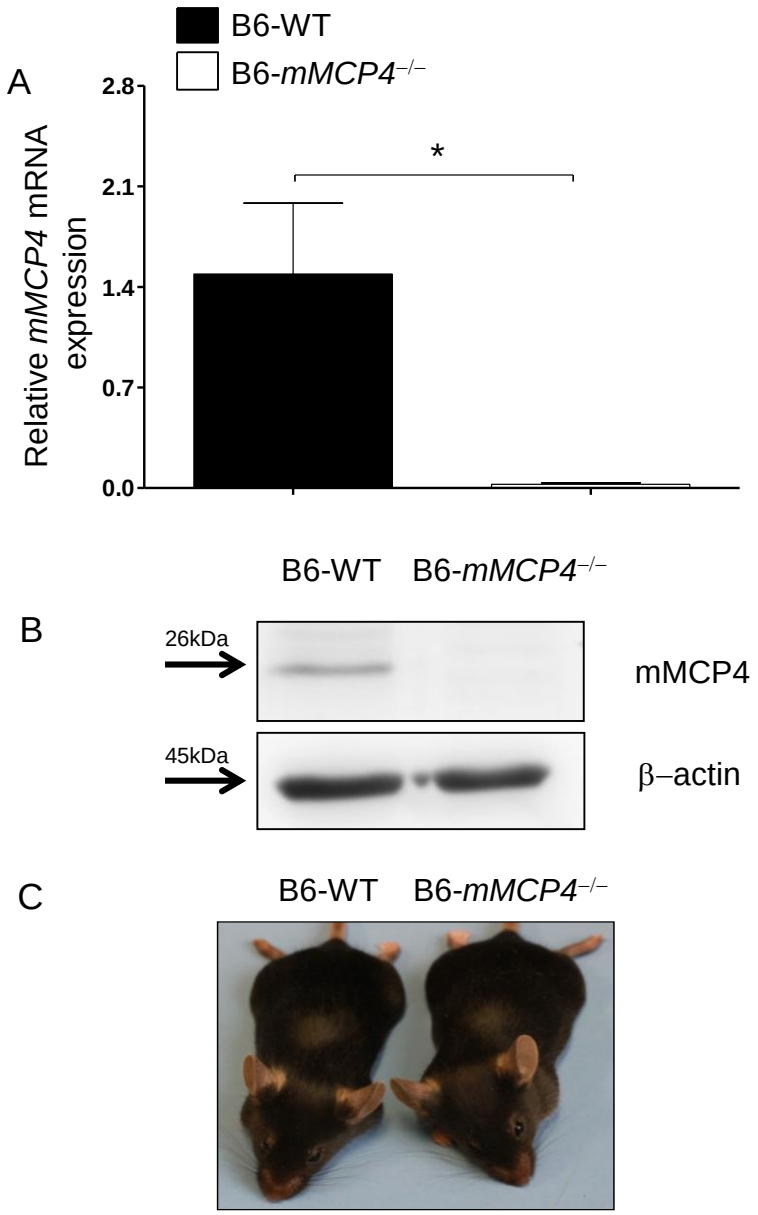

Figure 3.1 Pigmented B6-*mMCP4*$^{-/-}$ do not express mMCP4 at the mRNA or protein level. Absence of mMCP4 does not promote any detrimental phenotypes under homeostatic conditions. (A) RNA isolated from naïve B6-WT and B6-*mMCP4*$^{-/-}$ ear tissue was assessed for relative *mMCP4* mRNA expression and was normalised to the house keeping gene mouse *GAPDH*. Data represented as mean + SEM from 2 independent experiments (n=5-6 mice/genotype). Student's T test *p<0.05. **(B)** Tissue lysates from B6-WT and B6-*mMCP4*$^{-/-}$ ear tissue were assessed for endogenous mMCP4 protein by western blot analysis**.** Representative immunoblot from 2 independent experiments; β–actin was used as a loading control **(C)** B6-*mMCP4*$^{+/+}$ and B6-*mMCP4*$^{-/-}$ exhibit normal size, coating and viable phenotype.

melanoma skin cancers. Particularly, loss of the enzymatic activity of tyrosinase, the rate limiting enzyme for melanin biosynthesis, has been linked to development of NMSCs[13,389,390,391]. In addition to utilising pigmented *mMCP4*$^{-/-}$ mice derived from C57BL/6 background, non-pigmented *mMCP4*$^{-/-}$ mice were also generated by crossing albino B6-*Tyr*$^{c\text{-}2j}$ mice with pigmented B6-*mMCP4*$^{-/-}$ mice. To confirm the absence of mMCP4 in *mMCP4*$^{-/-}$ mice, we again assessed the presence of mRNA transcript and endogenous protein expression. We confirmed *Tyr*$^{c\text{-}2j}$-*mMCP4*$^{-/-}$ mice do not express the mRNA transcript of mMCP4 (**Figure 3.2a**) and also demonstrated a complete absence of mMCP4 endogenous protein expression (**Figure 3.2b**). Similar to pigmented B6-*mMCP4*$^{-/-}$ mice, *Tyr*$^{c\text{-}2j}$-*mMCP4*$^{-/-}$ mice do not exhibit any distinguishable characteristics, except for a complete absence of pigment in the skin, hair and eyes (**Figure 3.2c**).

3.2.2 Absence of mMCP4 does not influence or alter the morphology or cell surface expression of mouse bone marrow-derived cultured MCs

Although there are no additional detrimental phenotypic abnormalities of *mMCP4*$^{-/-}$ mice, we needed to characterise the role of mMCP4 in MCs and see whether it affects the morphological features of MCs as well as the cell surface expression of receptors FcεRI and c-*kit*. To establish if WT and *mMCP4*$^{-/-}$ BMCMCs from both pigmented and non-pigmented genetic backgrounds of mice exhibit similar intrinsic morphological, phenotypical and functional properties, BMCMCs were generated from these mice. Irrespective of *Tyr* expression, after 5-8 weeks of culturing, no distinct differences were observed between WT and *mMCP4*$^{-/-}$ BMCMCs in their granular morphology, size or shape as seen by May-Grunwald geimsa staining, supporting previous reports[85,194] (**Figure 3.3a**). We then investigated whether the absence of mMCP4 could influence the cell surface expression of mature BMCMC receptors FcεRI and c-*kit*, double positive expression of both receptors will indicate the presence of MC populations. Following flow cytometric analysis, after 5 weeks of culturing, WT and *mMCP4*$^{-/-}$ BMCMCs exhibited greater than 90% FcεRI^{+} and c-*kit*$^{+}$ populations and no noticeable differences in the expression of c-*kit* and FcεRI were observed between WT and *mMCP4*$^{-/-}$ BMCMCs derived from mice of both backgrounds (**Figure 3.3b**). In addition, after 5-6 weeks of culturing, a similar number of BMCMCs was attained after they reached >95% purity (**Figure 3.3c**).

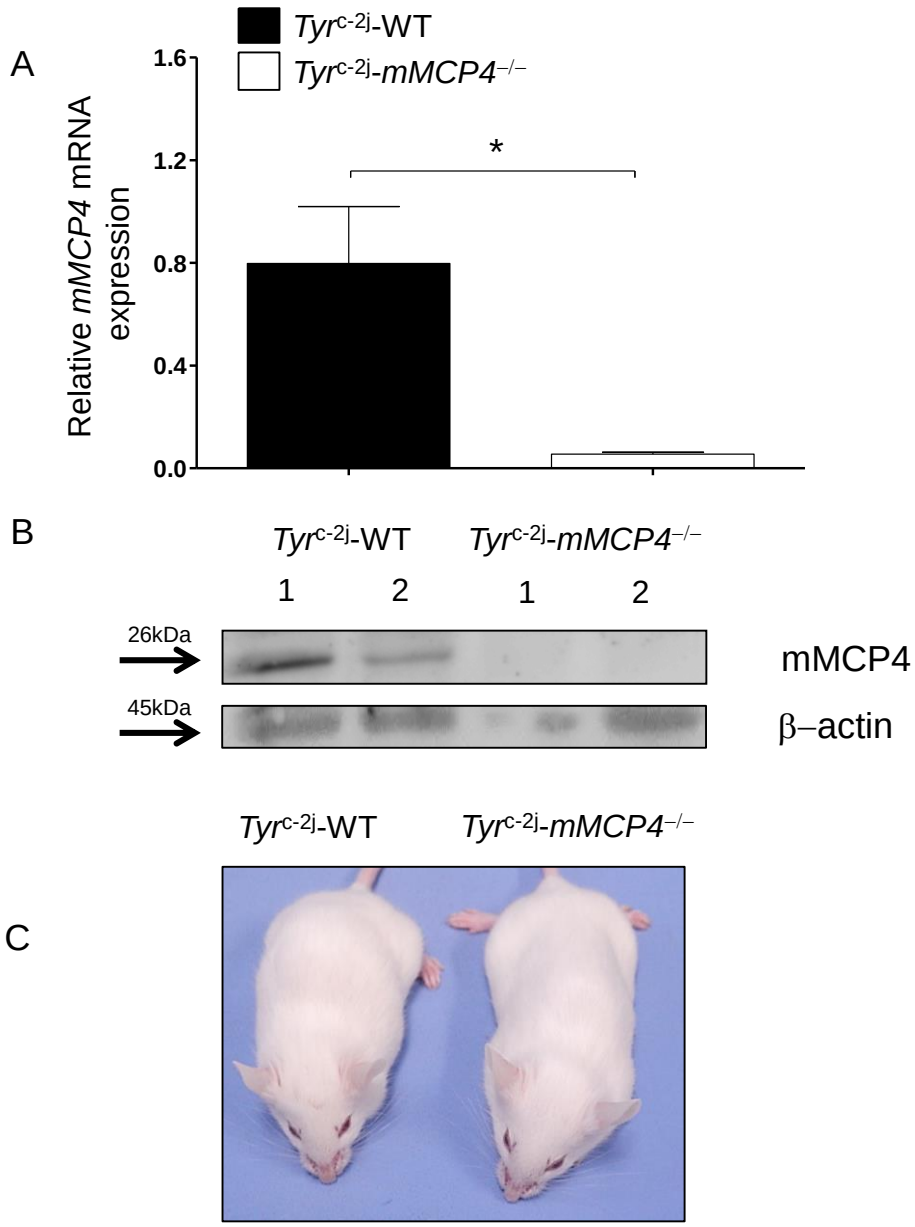

Figure 3.2. Non-pigmented *Tyr*$^{c\text{-}2j}$-*mMCP4*$^{-/-}$ do not express any mMCP4 at the mRNA or protein level. The absence of mMCP4 does not promote any detrimental phenotypes under homeostatic conditions. (A) RNA isolated from naïve *Tyr*$^{c\text{-}2j}$-WT and *Tyr*$^{c\text{-}2j}$-*mMCP4*$^{-/-}$ ear tissue was assessed for relative *mMCP4* mRNA expression and was normalised to the house keeping gene mouse *GAPDH*. Data represented as mean + SEM from 2 independent experiments (n=5-7 mice/genotype). Students T test *p<0.05. **(B)** Tissue lysates from *Tyr*$^{c\text{-}2j}$-WT and *Tyr*$^{c\text{-}2j}$-*mMCP4*$^{-/-}$ ear tissue were assessed for endogenous mMCP4 protein by Western blot analysis**.** Representative immunoblot from 2 independent experiments; β–actin was used as a loading control. Representative Immunoblot from 1 experiment (n=2) **(C)** *Tyr*$^{c\text{-}2j}$-WT and *Tyr*$^{c\text{-}2j}$-*mMCP4*$^{-/-}$ exhibit normal size, coating and viable phenotype.

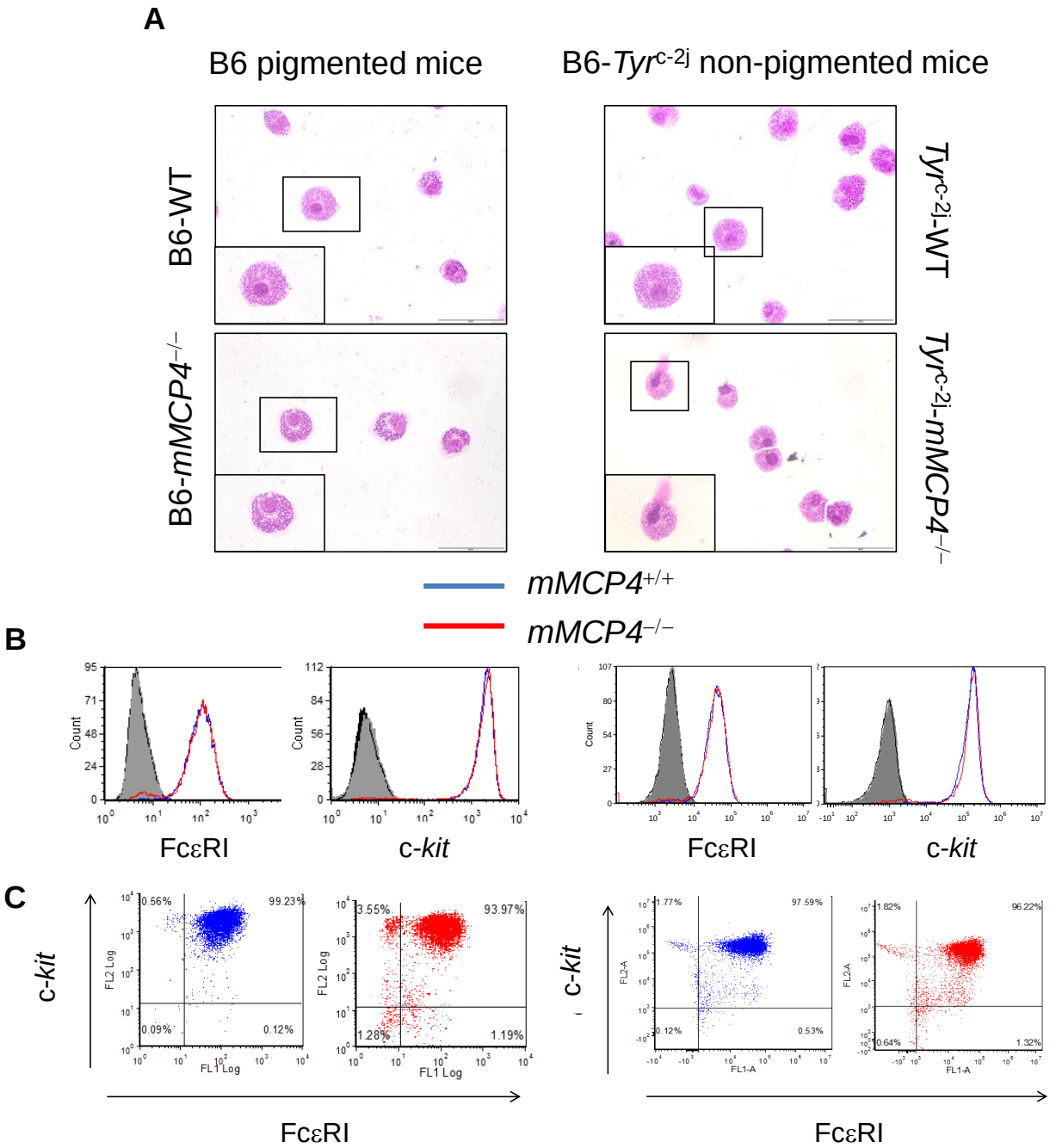

Figure 3.3 Absence of mMCP4 does not contribute to any changes in morphological features or expression of cell-surface markers c-*kit* or FcεRI in mast cells. (A) WT and *mMCP4*$^{-/-}$ BMCMCs derived from pigmented B6 and non-pigmented B6-*Tyr*$^{c\text{-}2j}$ mice were stained with May-Grunwald geimsa stains to assess cell and granular morphology after 6 weeks of culture; scale bar = 200 μm. **(B)** After 6 weeks of culturing, c-*kit* and FcεRI cell-surface expression on WT and *mMCP4*$^{-/-}$ BMCMCs derived from pigmented B6 and non-pigmented B6-*Tyr*$^{c\text{-}2j}$ mice was assessed by flow cytometry; Blue: *mMCP4*$^{+/+}$, Red: *mMCP4*$^{-/-}$, Grey: IgG2 isotype control, Black line: unstained cells **(C)** Double positive c-*kit* and FcεRI expressing WT and *mMCP4*$^{-/-}$ BMCMCs were assessed for overall purity after 6 weeks of culturing, MC populations have reached at least ~95% purity.

3.2.3 BMCMCs cultured in IL-3 and SCF express higher endogenous levels of mMCP4

Due to the phenotypic heterogeneity of MCs in human and mice, the differences in MC subtypes are not only differentiated by their ability to express specific classes of MC-derived proteases but also the localisation and environment they are found in[18,85]. To ensure our work was physiologically relevant to our disease setting of chronic UVB exposure of the skin, it was critical to ensure that the BMCMCs we generated exhibited a connective tissue phenotype (cultured in presence of IL-3 and SCF)[170-172]. These BMCMCs were also compared to BMCMCs cultured in IL-3 only, which normally exhibit a mucosal-like MC phenotype[66].

It is well understood that BMCMCs cultured in IL-3 exhibit a mature phenotype based on high expression levels of FcεRI and c-*kit*, but they also express a range of proteases. However, depending on the anatomical location of these cells and different factors they are exposed to will influence the phenotype of MCs and their mediator expression profile. In the case of protease expression profile, BMCMCs that are primarily exposed to IL-3 will typically express mMCP5, 6, 7 and MC-CPA3[63]. On the other hand BMCMCs that are exposed to both in IL-3 and SCF express endogenous mMCP4[67] in addition to the above proteases. Consistent with the literature, our Western blot analysis confirmed that BMCMCs cultured in IL-3 and SCF did express higher levels of endogenous mMCP4 protein compared to BMCMCs cultured in IL-3 only. Furthermore, Western blot analysis revealed no endogenous mMCP4 protein in *mMCP4*$^{-/-}$ BMCMCs from both backgrounds (**Figure 3.4**).

3.2.4 The function of BMCMCs is not affected or influenced by the absence of mMCP4.

Activating MCs via crosslinking of IgE bound FcεRI by cognate antigen is a routine test that determines if MCs function normally. Hence, to assess the functionality of WT and *mMCP4*$^{-/-}$ BMCMCs, we first investigated the activation of these cells through the IgE-dependent activation pathway. Typically, MCs are sensitized with the IgE α-dinitrophenol (DNP) mAb (SPE7 clone; 2 μg/mL) overnight, followed by stimulation with α-DNP-human serum albumin (DNP-HSA; 1 ng/mL – 1000 ng/mL). As a typical test of degranulation, the release of the granule stored mediator β-hexosaminidase was

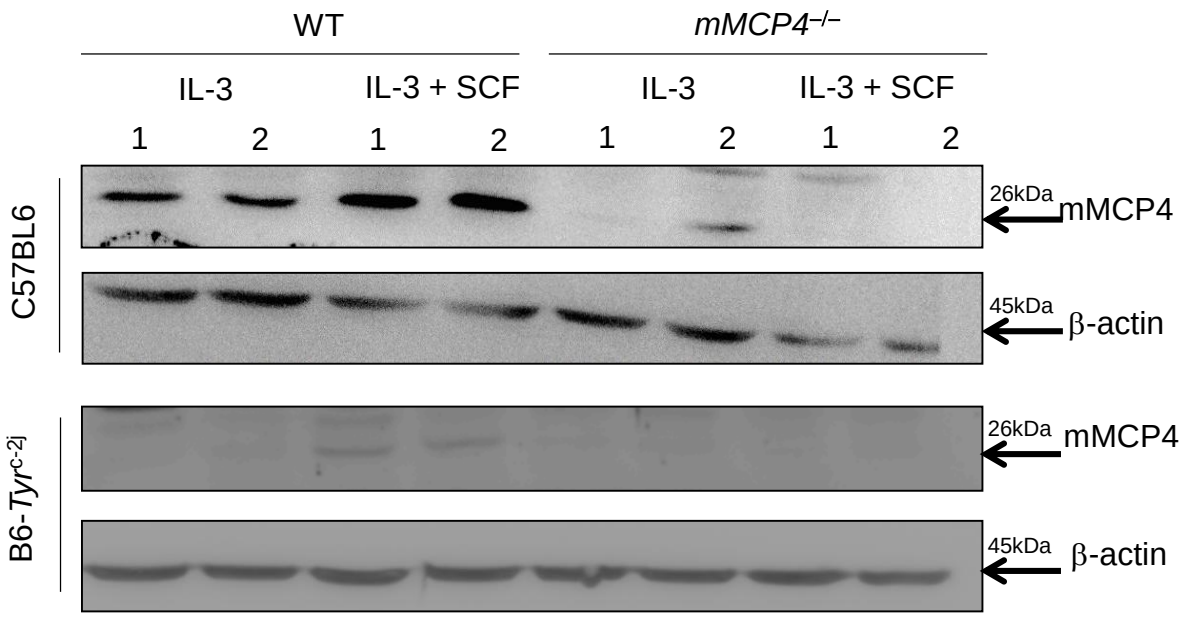

Figure 3.4 WT BMCMCs cultured in IL-3 and SCF express higher level of endogenous mMCP4 protein compared to WT BMCMCs cultured in IL-3 only. After 6 weeks of culture, cell lysates were generated from WT and *mMCP4*$^{-/-}$ BMCMCs cultured in IL-3 (4 ng/mL) or IL-3 (4 ng/mL) and SCF (50 ng/mL). To assess endogenous mMCP4 protein expression, cell lysates were loaded onto 10% SDS-PAGE gels and probed for mMCP4. β-actin was used as a loading control. Representative immunoblot from 2 independent experiments.

assessed. Both B6-WT and B6-*mMCP4*$^{-/-}$ BMCMCs cultured in IL-3 only exhibited a peak degranulation response of ~30-40% β-hexosaminidase release at 10-100 ng/mL DNP-HSA. However, no difference in degranulation was observed in the absence of mMCP4 (**Figure 3.5a**). Similarly, when stimulated, BMCMCs cultured in IL-3 (4 ng/mL) and SCF (50 ng/mL) showed a similar trend with a peak degranulation response at 10-100 ng/mL DNP-HSA. However, this peak response was ~20% lower compared to BMCMCs cultured in IL-3. Additionally, no difference in β-hexosaminidase degranulation was evident between both B6-WT and B6-*mMCP4*$^{-/-}$ BMCMCs either (**Figure 3.5b**). Similar results were observed in BMCMCs derived from *Tyr*$^{c\text{-}2j}$-WT and *Tyr*$^{c\text{-}2j}$-*mMCP4*$^{-/-}$ mice (**Figure 3.5c, d**). No difference in degranulation between WT and *mMCP4*$^{-/-}$ BMCMCs of mice from both backgrounds was observed in response to the positive controls PMA and the calcium ionophore A23187, was detected irrespective of *Tyr* genotype from which the BMCMCs were generated.

In addition to their ability to degranulate preformed and granule stored mediators, we also assessed the ability of BMCMCs to *de novo* synthesise proinflammatory cytokines IL-6 and TNFα. IgE sensitised BMCMCs were stimulated with 20 ng/mL DNP-HSA for 6 h, which typically allows enough time for cytokine production at detectable levels. As shown by ELISA, following 6 h of stimulation, BMCMCs from pigmented mice cultured in IL-3 only or IL-3 + SCF released more IL-6 and TNFα. No differences were observed in the absence of mMCP4 (**Figure 3.6a, b**). In comparison, a similar trend was observed in stimulated BMCMCs from non-pigmented mice cultured in IL-3. No difference was observed in the absence of mMCP4. Interestingly, although *Tyr*$^{c\text{-}2j}$-WT and *Tyr*$^{c\text{-}2j}$-*mMCP4*$^{-/-}$ BMCMCs cultured in IL-3 + SCF also released more IL-6 and TNFα following stimulation, their response appeared to be lower compared to BMCMCs cultured in IL-3 only. Similarly, no difference was observed in the absence of mMCP4 (**Figure 3.6c, d**). It was also interesting to see that IgE (SPE7 clone) alone could promote cytokine release but at lower levels compared to IgE + Ag stimulation, which support previously published studies[101]. Based on this data, absence of mMCP4 does not appear to affect the morphology or IgE-dependent stimulatory responses *in vitro*.

Figure 3.5 The absence of mMCP4 does not influence the functional characteristics of BMCMC degranulation in response to IgE-dependent activation. To assess β-hexosaminidase release as a measure of degranulation, WT and *mMCP4*$^{-/-}$ BMCMCs derived from pigmented B6 and non-pigmented B6-*Tyr*$^{c\text{-}2j}$ mice were cultured in **(A and C)** IL-3 (4 ng/mL) or **(B and D)** IL-3 (4 ng/mL) and SCF (50 ng/mL). After 6 weeks of culture, BMCMCs were pre-sensitized with IgE anti-DNP mAb (2 μg/mL) overnight. Pre-sensitized BMCMCs were then stimulated with specific antigen DNP-HSA (1-1000 ng/mL) for 1h and assessed for β-hexosaminidase release. PMA (10 ng/mL) and A23187 (10 μM) stimulation was used as a positive control. All experimental data shown as mean % β-hexosaminidase release + SEM from 3-5 independent experiments. One-Way ANOVA with Bonferroni's post test $^{\#/*}p<0.05$, $^{\#\#/**}p<0.01$, $^{\#\#\#/***}p<0.001$, $^{\#\#\#\#/****}p<0.001$ (treatment vs control). No significance between genotypes observed.

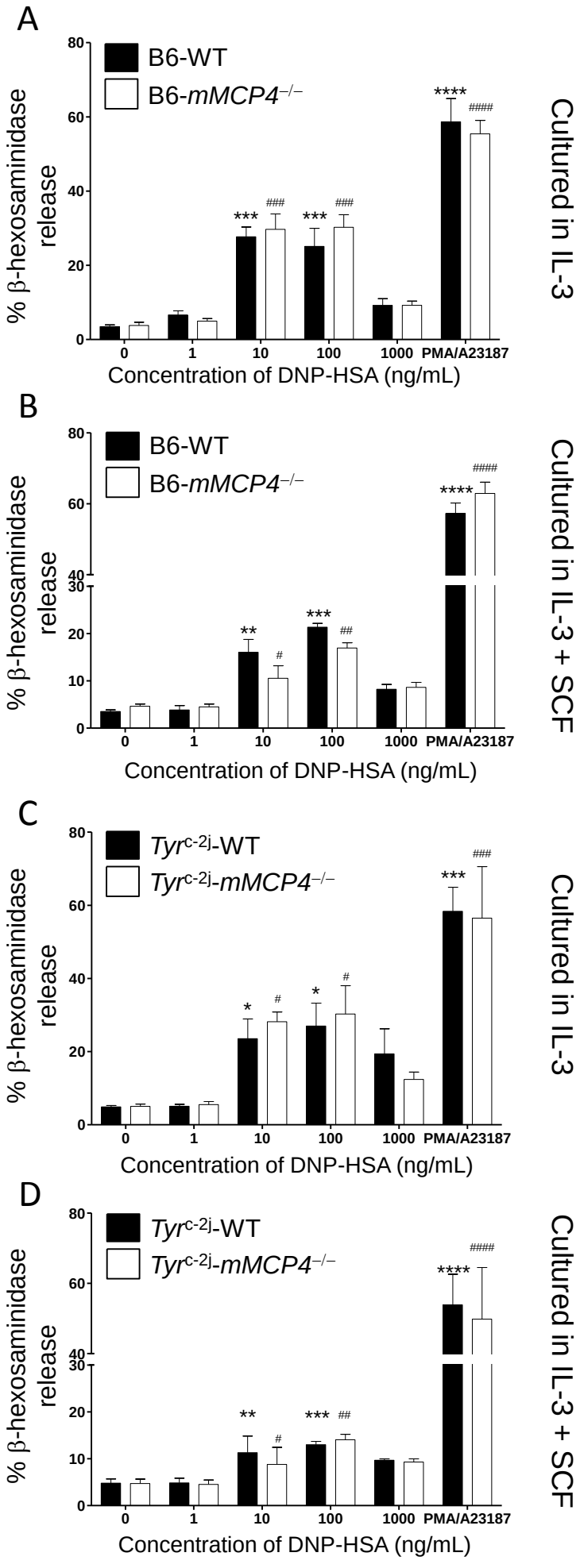
A
B6-WT
B6-mMCP4−/−
% β-hexosaminidase release
Concentration of DNP-HSA (ng/mL)
0
1
10
100
1000
PMA/A23187
Cultured in IL-3
B
B6-WT
B6-mMCP4−/−
% β-hexosaminidase release
Concentration of DNP-HSA (ng/mL)
Cultured in IL-3 + SCF
C
Tyrc-2j-WT
Tyrc-2j-mMCP4−/−
% β-hexosaminidase release
Concentration of DNP-HSA (ng/mL)
Cultured in IL-3
D
Tyrc-2j-WT
Tyrc-2j-mMCP4−/−
% β-hexosaminidase release
Concentration of DNP-HSA (ng/mL)
Cultured in IL-3 + SCF

Figure 3.6 The absence of mMCP4 does not influence the functional characteristics of BMCMC *de novo* cytokine synthesis in response to IgE-dependent activation. To assess *de novo* synthesis of cytokines IL-6 and TNFα, WT and *mMCP4*$^{-/-}$ BMCMCs derived from pigmented B6 and non-pigmented B6-*Tyr*$^{c\text{-}2j}$ mice were cultured in IL-3 (4 ng/mL) or IL-3 (4 ng/mL) and SCF (50 ng/mL). After 6 weeks of culture, BMCMCs were pre-sensitized with IgE anti-DNP mAb (2 μg/mL) overnight. Pre-sensitized BMCMCs were then stimulated with specific antigen DNP-HSA (20 ng/mL) for 6 h. After 6 h of stimulation, supernatants were harvested and **(A and C)** IL-6 and **(B and D)** TNFα release was assessed by ELISA. All experimental data shown as mean + SEM from 3-6 independent experiments. One-Way ANOVA with Bonferroni's post test $^{\#/*}p<0.05$, $^{**}p<0.01$, $^{***}p<0.001$, $^{****}p<0.001$ (treatment vs control; and between groups).

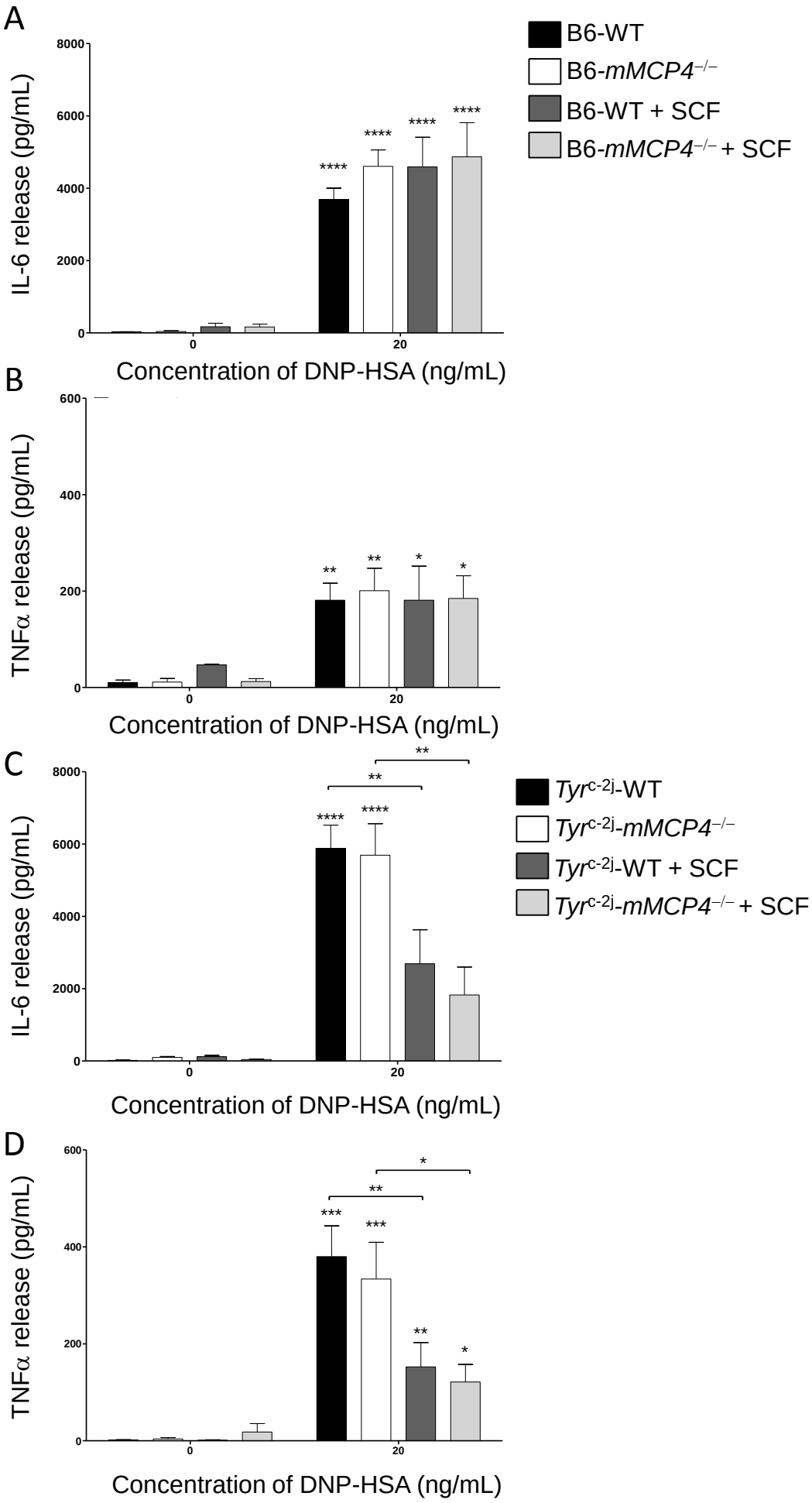
A
IL-6 release (pg/mL)
8000
6000
4000
2000
0
****
****
****
****
0
20
Concentration of DNP-HSA (ng/mL)
B6-WT
B6-mMCP4−/−
B6-WT + SCF
B6-mMCP4−/− + SCF
B
TNFα release (pg/mL)
600
400
200
0
**
**
*
*
0
20
Concentration of DNP-HSA (ng/mL)
C
IL-6 release (pg/mL)
8000
6000
4000
2000
0
**
**
****
****
0
20
Concentration of DNP-HSA (ng/mL)
Tyrc-2j-WT
Tyrc-2j-mMCP4−/−
Tyrc-2j-WT + SCF
Tyrc-2j-mMCP4−/− + SCF
D
TNFα release (pg/mL)
600
400
200
0
*
**
***
***
**
*
0
20
Concentration of DNP-HSA (ng/mL)

3.2.5 Substance P can induce β-hexosaminidase release in CTMCs

Although studies have shown that MCs can be activated by UVB induced-mediators such as neuropeptides SP and CGRP[360]. The direct activation of MCs by chronic UVB requires further investigation. Interestingly, the secretagogue receptor for SP has been recently discovered and was only found to be expressed on MCs that exhibit a connective-tissue phenotype[93]. For the final aspect of characterising these BMCMCs, we aimed to confirm if SP can activate BMCMCs with a connective tissue phenotype (cultured in IL-3 and SCF) *in vitro*, and assess if loss of mMCP4 affects this process.

Connective-tissue type BMCMCs were stimulated with 10 μM – 200 μM of SP as previously reported[93]. Typically, the release of β-hexosaminidase is measured within 1 h of stimulation as IgE mediated Passive Cutaneous Anaphylaxis (PCA) studies exhibit maximal ear swelling responses within the first 30 min[392]. In addition, McNeil *et al* demonstrated that when stimulated with 200 μM of SP, mouse peritoneal MCs showed a full degranulation response as measured by a rise in intracellular calcium. Therefore, we attempted to activate the BMCMCs for 1 h but very minimal degranulation was observed at 200 μM of SP (**Figure 3.7a**). We extended the stimulation to 24 h when only started to observe a small increase in degranulation of β–hexosaminidase between 10 - 200 μM of SP (**Figure 3.7b**). A viable cell count was carried out after 24 h of stimulation to assess if cell death was associated with minimal degranulation observed. The viability of WT and *mMCP4*$^{-/-}$ BMCMCs were both ~90%, suggesting that cell death is not responsible for the minimal degranulation response.

3.3 Discussion

For this chapter, we have confirmed that both pigmented and non-pigmented *mMCP4*$^{-/-}$ mice show an absence of mMCP4 at the transcript and protein levels. Consistent with the literature, phenotypically, these mice appear normal compared to their WT littermates[194]. Therefore these mice were phenotypically comparable, but the basic function of MCs in these mice was not known and needed to be investigated.

Consistent with previous studies, the loss of mMCP4 showed no effects on the size, granularity and staining characteristics of BMCMCs[194]. Additionally, the absence of mMCP4 in both pigmented and non-pigmented backgrounds of mice, had no influence on cell surface receptor expression of FcεRI and c-*kit*.

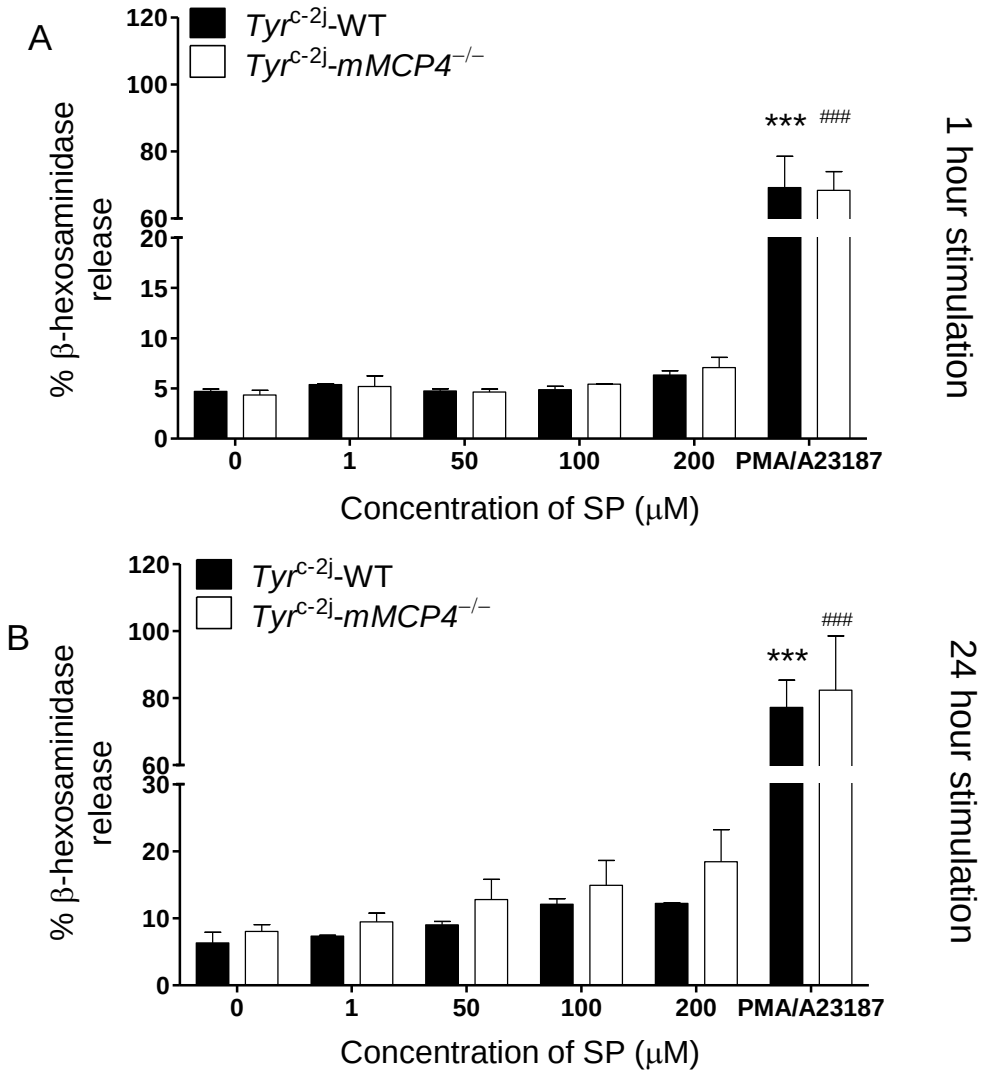

Figure 3.7 Stimulation of connective tissue MCs with neuropeptide SP induces degranulation via an IgE-independent mode of activation. To assess β-hexosaminidase release as a measure of degranulation via an IgE-independent mode of activation, BMCMCs derived from *Tyr*$^{c\text{-}2j}$-WT and *Tyr*$^{c\text{-}2j}$*-mMCP4*$^{-/-}$ mice were cultured in IL-3 (4 ng/mL) + SCF (50 ng/mL) were incubated with SP (1-200 μM) for **(A)** 1 h and **(B)** 24 h**.** PMA (10 ng/mL) and A23187 (10 μM) stimulation was used as a positive control. All data shown as mean % β-hexosaminidase release + SD from 1 experiment (2 mice/genotype). One-Way ANOVA with Bronferroni's post test ###/***p<0.001 (treatment vs control). No significance between genotypes were observed.

As previously outlined, to ensure our studies were physiologically relevant, our BMCMCs were cultured in IL-3 + SCF to allow them to differentiate into a connective tissue-like MC phenotype. As a comparison, we also cultured BMCMCs in IL-3 promotes a mucosal-like phenotype. Other additional growth factors that assist in this differentiation include IL-10 and IL-4[82,393]. In agreement with the literature, we observed that from both pigmented B6 and non-pigmented B6-*Tyr*$^{c\text{-}2j}$ mice, BMCMCs cultured in IL-3 and SCF did express much higher levels of endogenous mMCP4 protein compared to BMCMCs cultured in IL-3 only. This low level of mMCP4 in BMCMCs cultured in IL-3 only is consistent with the literature that suggests these cells are more likely to express tryptases rather than chymases (mMCP4)[67,85].

In order to characterise any effect of mMCP4 on the functionality of BMCMCs, we first assessed the IgE-dependent MC activation response by measuring degranulation of β-hexosaminidase, and *de novo* synthesis of IL-6 and TNFα cytokines. In response to DNP-HSA, we observed a peak degranulation response at a concentration ranging 10-100 ng/mL in BMCMCs cultured in IL-3 and IL-3 and SCF. This peak response suggests that within this concentration range, there is optimal cross-linking of antigen (DNP-HSA) with IgE-bound FcεRI, thereby allowing optimal signal transduction and subsequent degranulation. Additionally, no difference was observed in the degranulation response between *mMCP4*$^{-/-}$ and WT BMCMCs. Although the level of β-hexosaminidase release is lower compared to our previous reports[9], this likely due to the use of H1-ε26 IgE, compared to SPE-7 IgE used in this study, which may lead to different level of responses from MCs.

In addition to degranulation, MCs can also *de novo* synthesise a range of cytokines. We assessed the release of IL-6 and TNFα as a measurement of this pathway. As the ELISA data suggests BMCMCs cultured in IL-3 or IL-3 and SCF were responsive to antigen stimulation at 20 ng/mL (within optimal concentration range) as shown by enhanced release of IL-6 and TNFα. In addition, no difference was observed in BMCMCs derived from pigmented B6 and non-pigmented B6-*Tyr*$^{c\text{-}2j}$ mice, in the *de novo* synthesis pathway in the absence of mMCP4. The responses observed as described above were consistent with documented responses of functionally normal MCs as previously reported[125,394-396].

It is worth nothing that BMCMCs cultured in IL-3 and SCF showed reduced degranulation and *de novo* synthesis of IL-6 and TNFα (very obvious in B6-*Tyr*$^{c\text{-}2j}$

BMCMCs, and does not happen in the B6 BMCMCs). This is consistent with previous studies demonstrating that prolonged exposure of BMCMCs to SCF can down-regulate the *Src* kinase Hck which results in ineffective cytoskeletal reorganisation, leading to a reduction in MC-mediator release[397]. In addition, since the experiments on the pigmented B6 BMCMCs and the non-pigmented B6-*Tyr*$^{c\text{-}2j}$ BMCMCs were performed at least two years apart, different culturing conditions due to batch-to-batch variations in critical tissue culture reagents (e.g. FBS, WEHI-3B, and recombinant SCF) are likely to be a contributing factor to the discrepancies observed. Hence it will be ideal to confirm this observation by culturing and analysing these BMCMCs from both genetic background simultaneously. Moreover, non-pigmented B6-*Tyr*$^{c\text{-}2j}$ mice may exhibit subtle differences in genetic background compared to pigmented B6 mice arising from the crossing procedure, which could also potentially influence the MC response. Alternatively, it is also likely that this difference observed represents a real phenomenon which could suggest that non-pigmented BMCMCs from B6-*Tyr*$^{c\text{-}2j}$ mice are functionally different from pigmented B6 BMCMCs.

Piliponsky *et al*[5] reported, using a model of Poly-microbial sepsis, that mMCP4 is required to degrade TNFα and prevent further inflammation and detrimental mortality *in vivo* and *in vitro*. This study showed that in response to IgE and antigen stimulation, *mMCP4*$^{-/-}$ BMCMCs exhibit elevated levels of TNFα release, which is not consistent with our observations (**Figure 3.6**). These differences observed may be due to utilisation of alternative reagents and protocols. In this study, BMCMCs were stimulated for a total of 18 h, whilst our stimulation was only 6 h. It is possible that other mediators could potentiate TNFα production in the absence of mMCP4 during this 18 h period[5]. In addition, a different clone of IgE was utilised in this study (H1-ε26)[398] compared to SPE-7 used in our study. It is likely that the use of a different clone of IgE may influence the responses of BMCMCs[5].

Following characterisation of the IgE-dependent activation of WT and *mMCP4*$^{-/-}$ BMCMCs, we showed no difference in degranulation and cytokine production between these cells, indicating that in the absence of mMCP4, BMCMCs function normally in this setting.

Since UVB irradiation indirectly activates MCs through an IgE-independent mode of activation via a number of mediators. We next investigated an IgE-independent activation

of BMCMCs with the neuropeptides. Studies using CGRP and SP agonists show that presence of these neuropeptides are required to promote at least >50% histamine release from peritoneal MCs derived from rats[360,385]. Furthermore, it was shown that removal of neuropeptide producing-C-sensory nerve fibres are crucial for the degranulation of rat peritoneal MCs[360]. More importantly, Rychter *et al*. have suggested that the stimulation of mucosal MCs with the neuropeptide CGRP can induce piecemeal degranulation of the chymase, mMCP1[95]. Since connective tissue MCs have recently been reported to express the secretagogue receptor Mrgprb2 (human orthologue to MRGPRX2), which is a receptor specific to another neuropeptide SP[93], we hypothesise that SP may induce degranulation and release of mMCP4.

Based on our results, in response to 24 h of stimulation with SP, BMCMCs cultured in IL-3 and SCF showed a small increase in degranulation. No difference was observed in the absence of mMCP4, suggesting that mMCP4 does not affect this particular IgE-independent mode of activation. Interestingly we observed no degranulation following 1 h of stimulation with up to 200 μM of SP. However, the study by McNeil *et al* demonstrated a full degranulation response following 200 μM SP simulations within 30 min. Additionally, another study by van der Kleij *et al.* also showed a high degranulation response of β-hexosaminidase within 30 min. One possible explanation for this discrepancy in observations is that the MCs used in both of these studies may exhibit a more well-defined phenotype due to their anatomical site for development, which might have provided a higher expression of the Mrgprb2 receptor. For example; McNeil *et al*. utilised peritoneal-derived MCs, whilst van der Kleij *et al.* cultured BMCMCs with IL-3, IL-4 and SCF[393,399]. It is noteworthy to add that pre-sensitisation of MCs with IgE is critical for priming MCs IgE-independent activation. This experiment did not utilise this feature hence this could also be the reason why we did not observe any noticeable degranulation after 1 h stimulation with SP[400].

Taken together, we have shown that in the absence of mMCP4, there is no effect on the gross phenotype of the mice. No influence on the MC morphology and cell surface receptor expression was observed either. Furthermore, the functional characteristics of MCs in both IgE-dependent and –independent activation pathways are normal in the absence of mMCP4. Based on these observations, we now have the tools to further assess the role of mMCP4 in our chronic UVB irradiation model.

Chapter 4

mMCP4 IS A CRITICAL TUMOUR SUPPRESSOR IN RESPONSE TO CHRONIC UVB IRRADIATION

4.1 Introduction

Among the ultraviolet components of the solar spectrum (UVA, 320-400 nm; UVB, 280-320 nm; and UVC, <280 nm), earlier studies have suggested UVB to be the main contributor of skin carcinogenesis[401]. Recently, evidence has emerged to suggest a complicated scenario where, even at subinflammatory doses, UV exposure (including both UVB and UVA) is able to induce skin carcinogenesis in animal models[402].

UVB exposure of the skin can be either beneficial or detrimental, depending on the amount or 'threshold' of UVB the skin is being exposed to. In response to low doses of UVB exposure (10-15 min exposure under the sun), it can be quite beneficial and promote production of vitamin D_3 and melanogenesis[316] which is protective against UVB and its deleterious effects[256,317]. Alternatively, higher doses of UVB exposure (constant exposure, >15 min) can promote detrimental side effects including oxidative stress, genetic mutations and chronic inflammation[309].

Chronic UVB exposure is a key factor in promoting DNA mutations, physical cutaneous injury, inflammation, immune suppression and eventually the development of SCCs[307]. There are many hallmark features of SCC development and is typically diagnosed and seen through a series of changes in the skin, which is often referred to as the 'metaplasia-dysplasia-carcinoma' process[335]. This common theme is represented as atypical epithelial tissue organisation (metaplasia), followed by increasing disorganisation of tissue architecture (dysplasia) and the development of neoplastic *in situ* cancer cells (carcinoma) which have the potential to become invasive[335]. Coinciding with these changes an influx of inflammatory infiltrate and an accumulation of MCs to the site of injury is an additional hallmark feature[230,307,403,404].

MCs are known to play an important role in mediating the development and progression of multiple cancers. The role of MCs in cancer continues to be a dilemma as both cancer-supportive and suppressive functions have been reported and this appears to be cancer type-specific. Similarly, in the skin, MCs have also been reported to show both positive and negative influence in carcinogenesis[245,405].

Despite the growing evidence pointing towards a protective function of MCs in skin carcinogenesis, the mechanism involved is yet to be further elucidated. The regulatory function of MCs are facilitated through the release of MC-derived mediators. Recently,

we have demonstrated that MCs and MC-IL-10 can limit UVB-induced inflammation and skin pathology, which are the factors that are responsible for the development of cutaneous malignancies like SCCs[8]. We later showed that MCs can convert $25OHD_3$ into the active form of vitamin D_3 1α25-dihydroxyvitaminD3 via a CYP27B1-dependent manner and the 1α25-dihydroxyvitaminD3 generated in turn activates MCs to produce the anti-inflammatory cytokine IL-10[9]. Interestingly, our recent unpublished study also suggests that another MC-derived mediator, mMCP4, also possesses protective functions similar to MC-IL-10 in response to chronic low-dose UVB (non-tumour promoting; data not shown).

Based on these findings, since our preliminary studies showed similar protective function between mMCP4 and MC-IL-10 in response to non-carcinogenic chronic low-dose UVB, we propose to assess if mMCP4 retains its protective function when exposed to chronic high-dose UVB irradiation and limit the development of UVB-induced skin carcinogenesis.

4.2 Results

4.2.1 MCs and mMCP4 are crucial in limiting development of UVB-induced in situ SCCs

To determine the function of MCs and mMCP4 in response to chronic high-dose UVB irradiation and investigate if mMCP4 and MC-IL-10 retain similar protective function that was previously observed in the chronic low-dose UVB setting, adoptive transfer of BMCMCs was first utilised.

BMCMC cultured from syngeneic mice were intra-dermally (*i.d.)* engrafted into the ears of MC-deficient *Kit*$^{W/W\text{-}v}$ mice. In order to achieve UVB-induced skin damage and consequent characteristics that could further lead to the development of skin cancer, the ears of WBB6F$_1$-*Kit*$^{+/+}$ (WT), mast cell-deficient WBB6F$_1$-*Kit*$^{W/W\text{-}v}$ mice, WBB6F$_1$-*Kit*$^{W/W\text{-}v}$ mice engrafted with genetically compatible *ex vivo*-derived WT BMCMCs (WT BMCMCs→WBB6F$_1$-*Kit*$^{W/W\text{-}v}$ mice) or *mMCP4*$^{-/-}$ BMCMCs (*mMCP4*$^{-/-}$ BMCMCs→WBB6F$_1$-*Kit*$^{W/W\text{-}v}$ mice) were then exposed to (12 × 4 kJ/m^2 +13 × 8 kJ/m^2) UVB every 2 days for a total of 25 exposures (cumulative dose 152 kJ/m^2).

We first investigated whether the pathology in mice lacking MC, MC-IL-10 or mMCP4 could lead to hallmarks that could drive tumour development by H&E staining (**Figure**

4.1a). H&E staining revealed increased levels of full-thickness epidermal necrosis, which comprises of infiltration of inflammatory cells into the epidermal layer, in the ears of *Kit*$^{W/W-v}$ and *mMCP4*$^{-/-}$ BMCMCs→WBB6F$_1$-*Kit*$^{W/W-v}$ mice as indicated by red arrowheads, compared to WT and WT BMCMCs→ WBB6F$_1$-*Kit*$^{W/W-v}$ mice (**Figure 4.1a**). More importantly, these characteristics observed in *Kit*$^{W/W-v}$, *mMCP4*$^{-/-}$ BMCMCs→WBB6F$_1$-*Kit*$^{W/W-v}$ and *IL-10*$^{-/-}$ BMCMCs→WBB6F$_1$-*Kit*$^{W/W-v}$ mice also correlate with the presence of *in situ* SCC's is indicated by black arrowheads (**Figure 4.1a**). Furthermore, quantification of *in situ* SCC free survival also suggests an earlier onset of *in situ* SCC in *Kit*$^{W/W-v}$, *mMCP4*$^{-/-}$ BMCMCs→WBB6F$_1$-*Kit*$^{W/W-v}$ and *IL-10*$^{-/-}$ BMCMCs→WBB6F$_1$-*Kit*$^{W/W-v}$ mice after 5 exposures to chronic UVB (**Figure 4.1b**).

Although the observations using the *Kit*$^{W/W-v}$ model confirmed that the protective function of both MC-IL-10 and mMCP4 are also retained even against chronic high-dose UVB irradiation and they are both able to delay the onset of UVB-induced *in situ* SCC, the rest of the chapter will focus on investigating the role of mMCP4 due to its novelty.

In order to confirm the successful BMCMC engraftment into the ears of *Kit*$^{W/W-v}$ mice, and to determine whether a difference in MC number contributes to pathologies observed in response chronic UVB irradiation, MC counts were performed on the Toluidine blue stained ear sections (**Figure 4.2**). Based on the analysis, prior to UVB irradiation, *Kit*$^{W/W-v}$ mice showed a complete lack of tissue MC populations in the ears, while 20-40 MCs/mm was observed in the ears of WT, WT BMCMCs→WBB6F$_1$-*Kit*$^{W/W-v}$, *mMCP4*$^{-/-}$ BMCMCs→WBB6F$_1$-*Kit*$^{W/W-v}$, and *IL-10*$^{-/-}$ BMCMCs→WBB6F$_1$-*Kit*$^{W/W-v}$ mice, confirming a successful BMCMC engraftment into the ears (**Figure 4.2**). Over 25 UVB exposures, a gradual increase in the MC number was observed in WT, WT BMCMCs→WBB6F$_1$-*Kit*$^{W/W-v}$, *mMCP4*$^{-/-}$ BMCMCs→WBB6F$_1$-*Kit*$^{W/W-v}$, and *IL-10*$^{-/-}$ BMCMCs→WBB6F$_1$-*Kit*$^{W/W-v}$ mice, and an increase was also observed in the ears of *Kit*$^{W/W-v}$ mice (**Figure 4.2**). Most importantly, no significant difference was observed in the MC number between WT BMCMCs→WBB6F$_1$-*Kit*$^{W/W-v}$, *mMCP4*$^{-/-}$ BMCMCs→WBB6F$_1$-*Kit*$^{W/W-v}$, and *IL-10*$^{-/-}$ BMCMCs→WBB6F$_1$-*Kit*$^{W/W-v}$ mice, suggesting that the difference in pathology observed in these mice are more likely due to the release of MC-derived mediators (**Figure 4.2**). In order to confirm the protective function of mMCP4 against the development of UVB-induced *in situ* SCCs,

Figure 4.1. Mast cells, mMCP4, and MC-IL-10 are required to limit UVB-induced *in situ* SCC development in WBB6F$_1$ mice (A) Representative images of H&E stained cross sections obtained from WT, WBB6F$_1$-*Kit*$^{W/W\text{-}v}$, WT BMCMC→WBB6F$_1$-*Kit*$^{W/W\text{-}v}$, *mMCP4*$^{-/-}$ BMCMC→WBB6F$_1$-*Kit*$^{W/W\text{-}v}$, and *IL-10*$^{-/-}$ BMCMC→WBB6F$_1$-*Kit*$^{W/W\text{-}v}$ mice 24 h after the final exposure to 4 kJ/m^2 (5 exposures) and 4 kJ/m^2 + 8 kJ/m^2 (25 exposures). All images were taken using an Nanozoomer technology microscope and digitised using Nanozoomer Digital Pathology software. Scale bar: 1000 μm; inset scale: 500 μm, *in situ* scale: 200 μm **(B)** H&E stained cross sections from UVB-treated WT, WBB6F$_1$-*Kit*$^{W/W\text{-}v}$, WT BMCMC→WBB6F$_1$-*Kit*$^{W/W\text{-}v}$, *mMCP4*$^{-/-}$ BMCMC→WBB6F$_1$-*Kit*$^{W/W\text{-}v}$ and *IL-10*$^{-/-}$ BMCMC→WBB6F$_1$-*Kit*$^{W/W\text{-}v}$ mice were blindly scored for pathological hallmarks of *in situ* SCC development. Red arrows indicate full-thickness epidermal necrosis; Black arrows indicate *in situ* SCC. **p*<0.008 Two-way ANOVA with Bonferroni's-corrected threshold multiple comparisons: WT vs WBB6F$_1$-*Kit*$^{W/W\text{-}v}$; WT vs WT BMCMC→WBB6F$_1$-*Kit*$^{W/W\text{-}v}$; WT vs *mMCP4*$^{-/-}$ BMCMC→WBB6F$_1$-*Kit*$^{W/W\text{-}v}$; WT BMCMC→WBB6F$_1$-*Kit*$^{W/W\text{-}v}$ vs *mMCP4*$^{-/-}$ BMCMC→WBB6F$_1$-*Kit*$^{W/W\text{-}v}$; WT vs *IL-10*$^{-/-}$ BMCMC→WBB6F$_1$-*Kit*$^{W/W\text{-}v}$; WT BMCMC→WBB6F$_1$-*Kit*$^{W/W\text{-}v}$ vs *IL-10*$^{-/-}$ BMCMC→WBB6F$_1$-*Kit*$^{W/W\text{-}v}$ and WT BMCMC→WBB6F$_1$-*Kit*$^{W/W\text{-}v}$ vs WBB6F$_1$-*Kit*$^{W/W\text{-}v}$ Data from 2-5 independent experiments. Dr Jan Ibbetson (dermatopathologist) performed the blind scoring of *in situ* SCC, A/Prof Michele Grimbaldeston performed H&E staining on the ear sections.

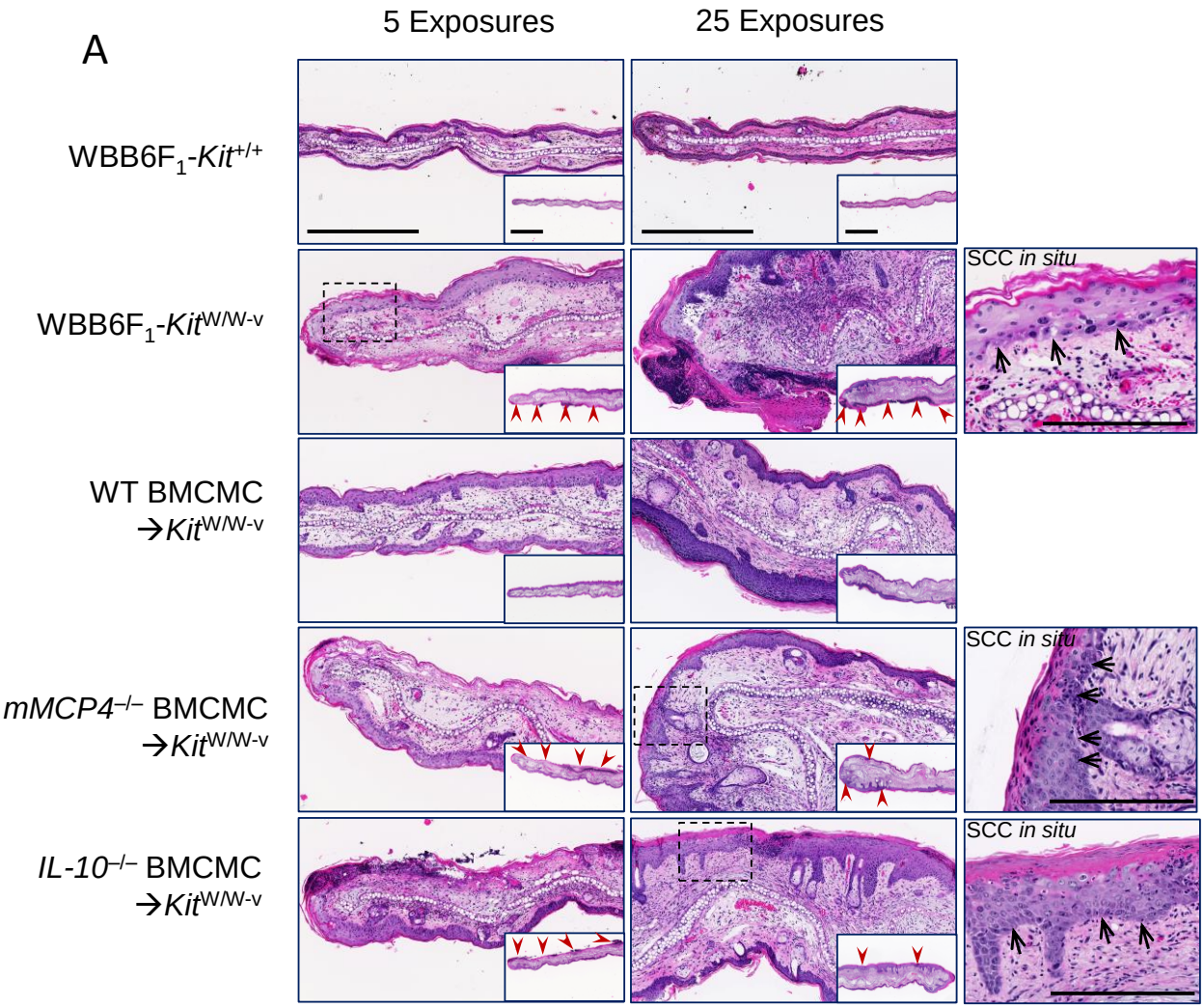
A
5 Exposures
25 Exposures
WBB6F1-Kit+/+
WBB6F1-KitW/W-v
WT BMCMC →KitW/W-v
mMCP4–/– BMCMC →KitW/W-v
IL-10–/– BMCMC →KitW/W-v
SCC in situ
SCC in situ
SCC in situ

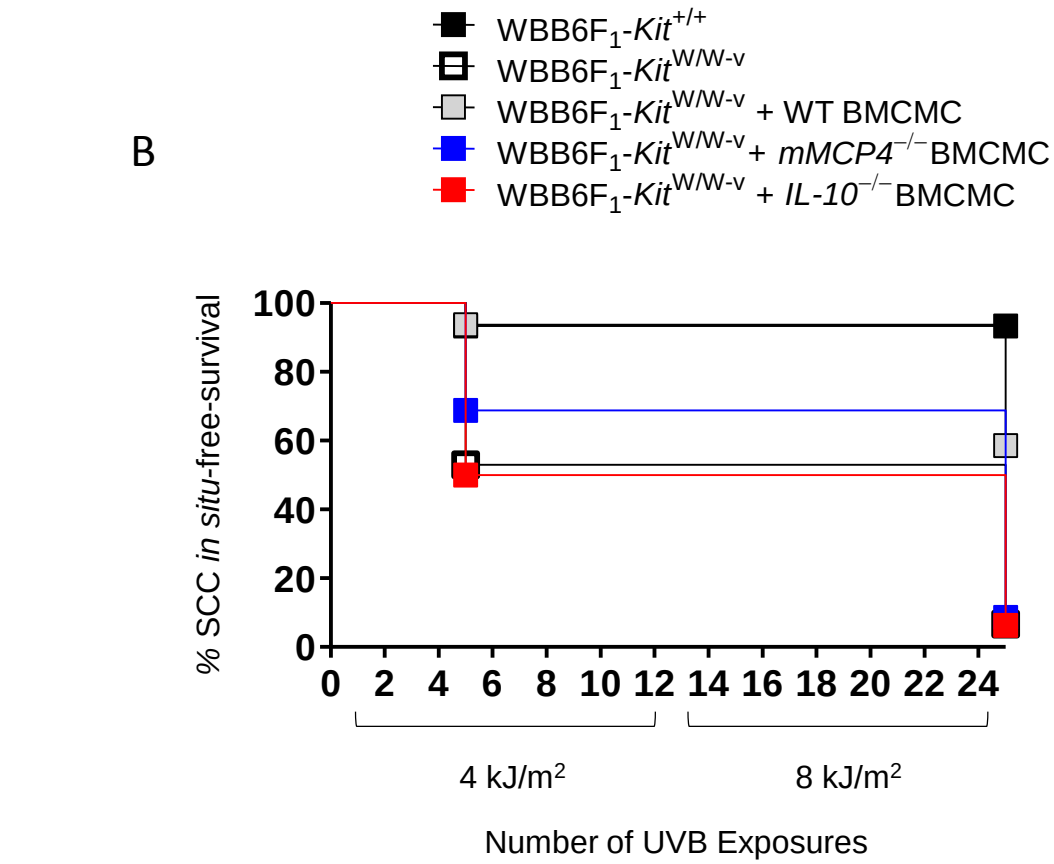
B
WBB6F1-Kit+/+
WBB6F1-KitW/W-v
WBB6F1-KitW/W-v + WT BMCMC
WBB6F1-KitW/W-v + mMCP4–/– BMCMC
WBB6F1-KitW/W-v + IL-10–/– BMCMC
% SCC in situ-free-survival
100
80
60
40
20
0
0 2 4 6 8 10 12 14 16 18 20 22 24
4 kJ/m2
8 kJ/m2
Number of UVB Exposures

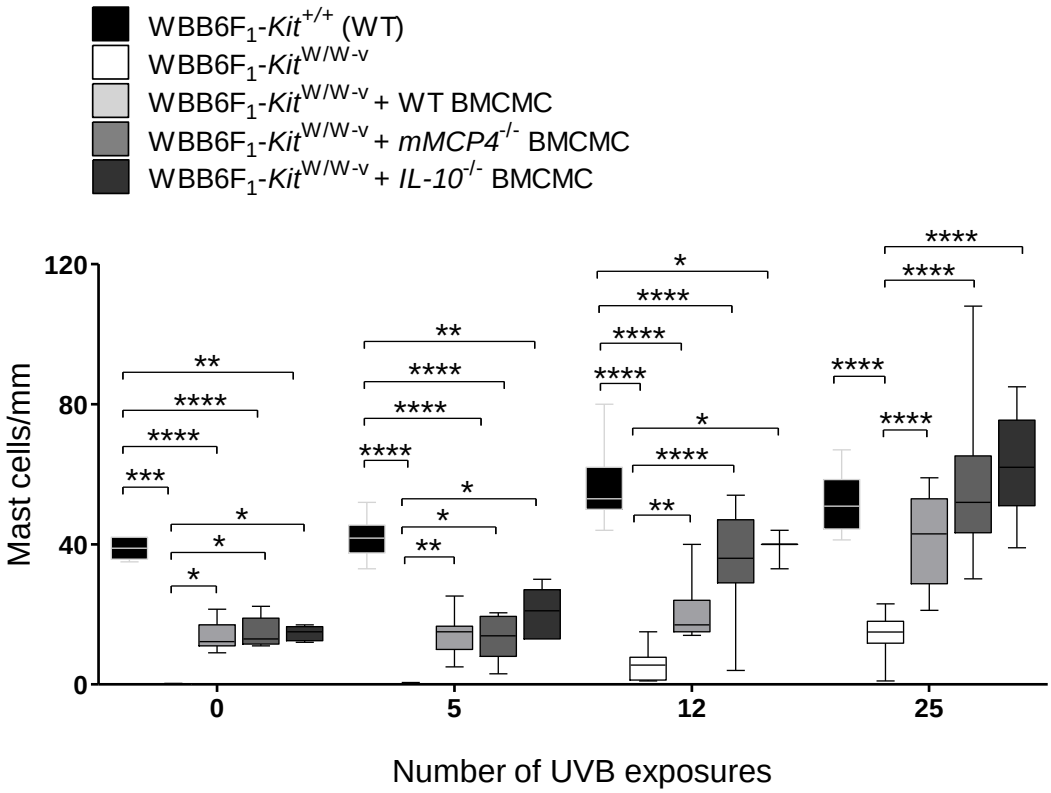

Figure 4.2. Mast cells numbers do not contribute to UVB-induced skin pathology associated with the loss of MCs and mMCP4 (A) Mast cell numbers were quantified from Toluidine blue stained cross sections of the ear pinnae of untreated and UVB-treated WT, WBB6F$_1$-*Kit*$^{W/W-v}$, WT BMCMC→WBB6F$_1$-*Kit*$^{W/W-v}$, *mMCP4*$^{-/-}$ BMCMC→WBB6F$_1$-*Kit*$^{W/W-v}$, and *IL-10*$^{-/-}$ BMCMC→WBB6F$_1$-*Kit*$^{W/W-v}$ mice (5, 12 [at 4 kJ/m^2] and 25 exposures [at 8 kJ/m^2]). Mast cell counts were normalised to length of the cartilage. Data represented as median; Mann-Whitney U test. *$p<0.05$. **$p<0.01$, ***$p<0.001$, ****$p<0.0001$. Data from 2-3 experiments. Images were taken on an Nanozoomer Technology microscope and visualised using Nanozoomer Digital Pathology software.

the non-pigmented *mMCP4*$^{-/-}$ (*Tyr*$^{c\text{-}2j}$-*mMCP4*$^{-/-}$) mice were also applied to the same UVB irradiation regime as the *Kit*$^{W/W\text{-}v}$ mice. Similar to engrafted-WBB6F$_1$-*Kit*$^{W/W\text{-}v}$ mice, H&E staining of UVB-treated ears of *Tyr*$^{c\text{-}2j}$-WT and *Tyr*$^{c\text{-}2j}$-*mMCP4*$^{-/-}$ mice revealed dramatic differences in the tissue architecture, with higher incidences of parakeratoses and disorganisation of the epithelial layer as well as full-thickness epidermal necrosis, particularly in *Tyr*$^{c\text{-}2j}$-*mMCP4*$^{-/-}$ mice (**Figure 4.3b**, **Table 4.1**). Furthermore, based on blind scoring analysis, the data suggests that *Tyr*$^{c\text{-}2j}$-*mMCP4*$^{-/-}$ mice have a greater incidence of *in situ* SCC development compared to *Tyr*$^{c\text{-}2j}$-WT mice after 25 exposures of chronic UVB irradiation (**Figure 4.3b**). Similar to that observed in the engrafted-*Kit*$^{W/W\text{-}v}$ mice, no difference in the MC counts was observed in the *Tyr*$^{c\text{-}2j}$ mice between genotypes (**Figure 4.4**). This further confirms that the UVB-induced skin pathology observed in these mice is associated with the absence of mMCP4, and not MCs themselves. Notably, no *in situ* SCC development was observed in pigmented B6 mice.

Table 4.1 UVB-treated non-pigmented *Tyr*$^{c\text{-}2j}$-*mMCP4*$^{-/-}$ mice exhibit higher incidence of full-thickness epidermal necrosis

Mice	Mice with full–thickness epidermal necrosis		
	5 exp	12 exp	25 exp
Tyr$^{c\text{-}2j}$-WT	4/15	0/10	7/25
Tyr$^{c\text{-}2j}$-*mMCP4*$^{-/-}$	15/18**	0/19$^{\#\#\#}$	15/34$^{\#\#}$

Quantification of full-thickness epidermal necrosis in H&E stained ear cross-sections of UVB-treated *Tyr*$^{c\text{-}2j}$-WT and *Tyr*$^{c\text{-}2j}$-*mMCP4*$^{-/-}$ mice after 5, 12 and 25 exposures. Values indicate mice whose ears showed evidence of full-thickness epidermal necrosis and, in some cases, ulcers, as assessed by histology at the end of the period of UVB exposure (mice with necrosis/total mice). $^{**}p< 0.01$ *Tyr*$^{c\text{-}2j}$-WT 5 UVB exposures versus the corresponding *Tyr*$^{c\text{-}2j}$-*mMCP4*$^{-/-}$ mice; or $^{\#\#}p< 0.01$; or $^{\#\#\#}p< 0.001$ 5 UVB exposures versus 12 or 25 exposures in the same genotype using Fisher's exact test. A/Prof Michele Grimbaldeston performed scoring on the ear sections.

4.2.2 MCs and mMCP4 are protective against UVB-induced ear thickening and skin pathology

In order to denote the level of inflammation and damage, ear-thickening and gross damage was monitored prior to each exposure. After 25 exposures of UVB irradiation, a

Figure 4.3. UVB-treated non-pigmented *Tyr*$^{c\text{-}2j}$-*mMCP4*$^{-/-}$ mice exhibit earlier onset of *in situ* SCCs (A) Representative images of H&E stained ear cross sections from UVB-treated *Tyr*$^{c\text{-}2j}$-WT and *Tyr*$^{c\text{-}2j}$-*mMCP4*$^{-/-}$ mice (after 5 and 25 exposures). Images were taken using an Nanozoomer technology microscope and digitised using Nanozoomer Digital Pathology software. Scale bar: 200μm; inset:1mm. **(B)** H&E stained images from UVB-treated *Tyr*$^{c\text{-}2j}$-WT and *Tyr*$^{c\text{-}2j}$-*mMCP4*$^{-/-}$ mice were blindly scored for pathological hallmarks of *in situ* SCC development. Black arrows indicate the presence of *in situ* SCC. 2-Way ANOVA with Bonferroni's post-test *$p<0.01$ *Tyr*$^{c\text{-}2j}$-WT vs *Tyr*$^{c\text{-}2j}$-*mMCP4*$^{-/-}$. Data from 2-5 independent experiments. Dr Jan Ibbetson (dermatopathologist) performed the blind scoring of *in situ* SCC, A/Prof Michele Grimbaldeston performed H&E staining on the ear sections.

A

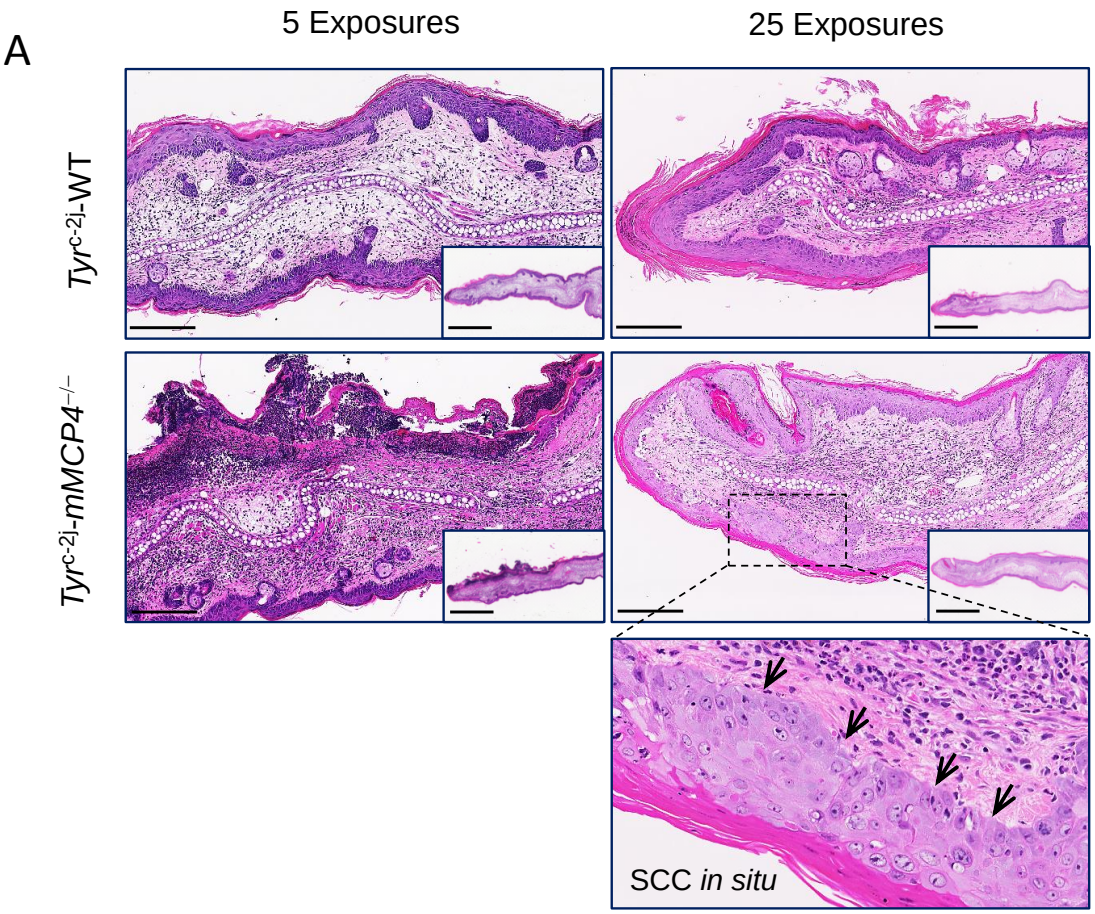
5 Exposures
25 Exposures
Tyrc-2j-WT
Tyrc-2j-mMCP4−/−
SCC in situ

B

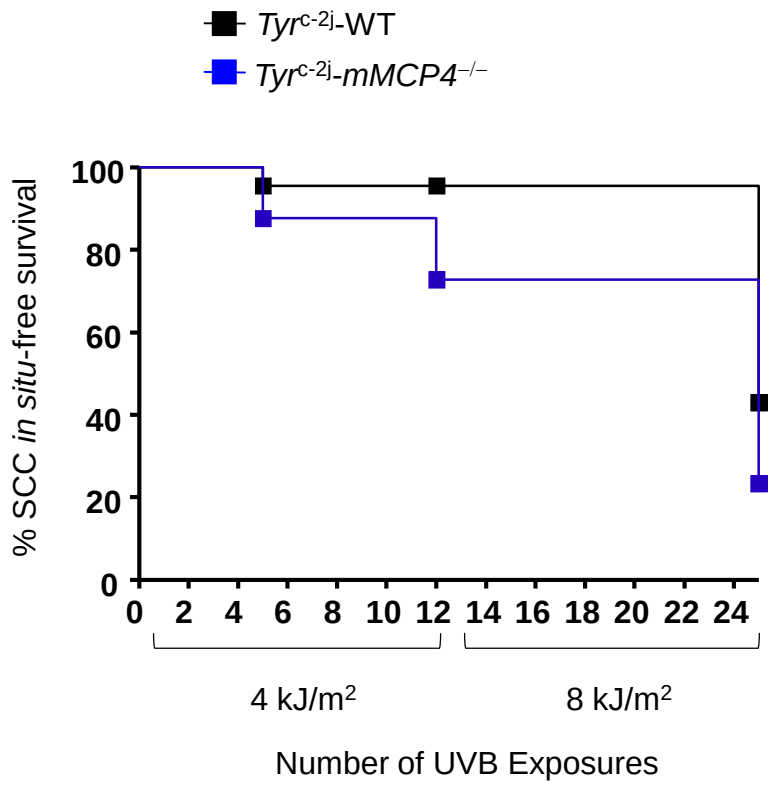
Tyrc-2j-WT
Tyrc-2j-mMCP4−/−
% SCC in situ-free survival
100
80
60
40
20
0
0 2 4 6 8 10 12 14 16 18 20 22 24
4 kJ/m2
8 kJ/m2
Number of UVB Exposures

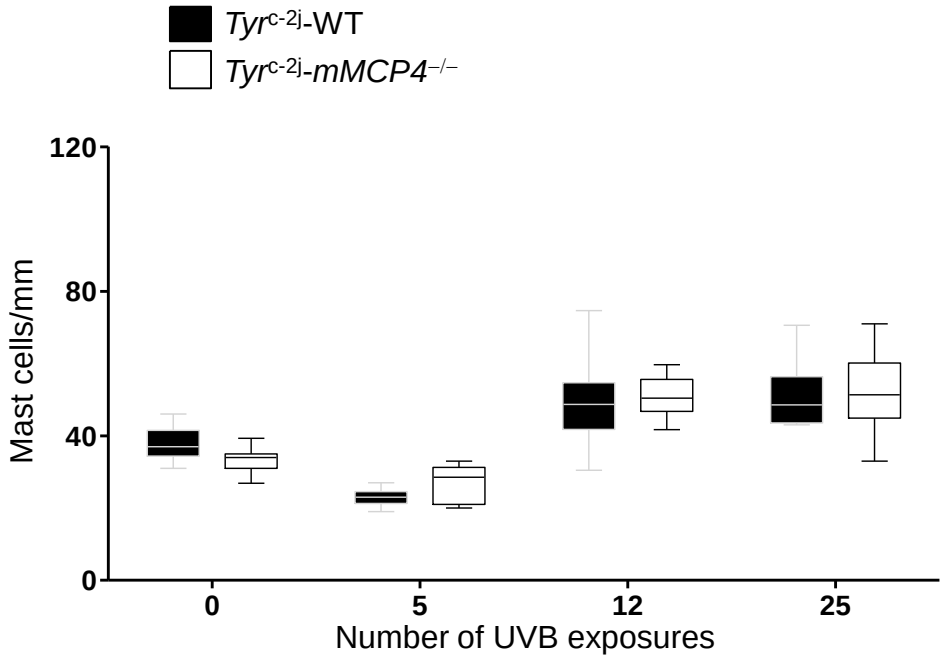

Figure 4.4. Mast cells numbers do not change in the absence of mMCP4 in response to chornic UVB irradiation. Mast cell numbers were quantified from Toluidine blue stained cross sections of the ear pinnae of untreated and UVB-treated non-pigmented *Tyr*$^{c\text{-}2j}$, WT and *mMCP4*$^{-/-}$ mice (5, 12 [at 4 kJ/m^2] and 25 exposures [at 8 kJ/m^2]). Mast cell counts were normalised to length of the cartilage. Data represented as median from 2-3 experiments. Images were taken on an Nanozoomer Technology microscope and visualised using Nanozoomer Digital Pathology software.

significantly more exacerbated ear thickening response was observed in *Kit*$^{W/W\text{-}v}$, *mMCP4*$^{-/-}$ BMCMCs→WBB6F$_1$-*Kit*$^{W/W\text{-}v}$, and *IL-10*$^{-/-}$ BMCMCs→WBB6F$_1$-*Kit*$^{W/W\text{-}v}$ mice compare to WT and WT BMCMCs→ WBB6F$_1$-*Kit*$^{W/W\text{-}v}$ counterparts (**Figure 4.5a**). Associated with the ear thickening response, a high degree of damage was also observed in the ears of *Kit*$^{W/W\text{-}v}$, *mMCP4*$^{-/-}$ BMCMCs→WBB6F$_1$-*Kit*$^{W/W\text{-}v}$, and *IL-10*$^{-/-}$ BMCMCs→WBB6F$_1$-*Kit*$^{W/W\text{-}v}$ mice and this includes ulcerations and scabbing, particularly at the tips of the ears where the skin was most exposed to UVB (**Figure 4.5b**). On the contrary, minimal signs of damage was observed in the ears of WT and WT BMCMCs→ WBB6F$_1$-*Kit*$^{W/W\text{-}v}$ mice (**Figure 4.5b**). Coinciding with the *in situ* SCC findings, this observation further supports the protective functions of both mMCP4 and MC-IL-10 in response to chronic high-dose UVB.

Due to the short wavelength of UVB, keratinocytes are typically the first layer of cells to be affected by chronic UVB exposure, leading to proliferation of keratinocytes and subsequent thickening of the epidermis[320,324]. Dermal MCs can secrete regulators of skin inflammation i.e. chymases and tryptases, therefore, we wanted to assess for any pathological changes in the epidermis associated with the lack of MCs or mMCP4, due to the significant degree of gross damage observed in the ears of *Kit*$^{W/W\text{-}v}$, and *mMCP4*$^{-/-}$ BMCMCs→WBB6F$_1$-*Kit*$^{W/W\text{-}v}$ mice (**Figure 4.5b**). Epidermal thickness of the UVB-treated ears was measured from Toluidine blue stained sections (**Figure 4.6**). After 25 exposures of chronic UVB, an overall increase in thickening of the epidermis was observed in all groups of mice. Notably, *Kit*$^{W/W\text{-}v}$ mice that lacked MCs or mMCP4 showed significantly more epidermal thickening in the ears compared to WT and WT BMCMCs→ WBB6F$_1$-*Kit*$^{W/W\text{-}v}$ counterparts, particularly after 12 and 25 exposures. Whilst after 5 exposures, the lack of mMCP4 did not seem to influence epidermal thickening compared to *Kit*$^{W/W\text{-}v}$ mice (**Figure 4.7**).

Similar to the observation in the *Kit*$^{W/W\text{-}v}$ mice, the ear thickening response from *Tyr*$^{c\text{-}2j}$-*mMCP4*$^{-/-}$ compared to *Tyr*$^{c\text{-}2j}$-WT mice showed small, but no significant differences after 25 exposures at 8 kJ/m^2 but a peak response in *Tyr*$^{c\text{-}2j}$-*mMCP4*$^{-/-}$ was observed after the 5 exposures (**Figure 4.8a**). Furthermore, a similar degree of gross damage was observed in both *Tyr*$^{c\text{-}2j}$-WT and *Tyr*$^{c\text{-}2j}$-*mMCP4*$^{-/-}$ mice (**Figure 4.8b**).

Prior to usage of the non-pigmented *Tyr*$^{c\text{-}2j}$ mice, pigmented B6-*mMCP4*$^{-/-}$ mice were also applied to the same chronic high-dose UVB irradiation regime to attempt to confirm

Figure 4.5. Mast cells, mMCP4, and MC-IL-10 protect and limit exacerbated ear thickening and skin pathology responses following chronic high-dose UVB irradiation (A) WT, WBB6F$_1$-*Kit*$^{W/W\text{-}v}$, WT BMCMC→WBB6F$_1$-*Kit*$^{W/W\text{-}v}$, *mMCP4*$^{-/-}$ BMCMC→WBB6F$_1$-*Kit*$^{W/W\text{-}v}$, and *IL-10*$^{-/-}$ BMCMC→WBB6F$_1$-*Kit*$^{W/W\text{-}v}$ mice were exposed to chronic high-doses of UVB (12 x 4 kJ/m^2 +13 x 8 kJ/m^2) every 2 days for a total of 25 exposures (cumulative dose 152 kJ/m^2). Data represented as mean + SEM from 4-8 independent experiments. 2-WAY ANOVA *p<0.05, **p<0.01, ***p<0.001 for the indicated comparisons. **(B)** Representative Images of gross ear pathology after 25 exposures of chronic UVB irradiation.

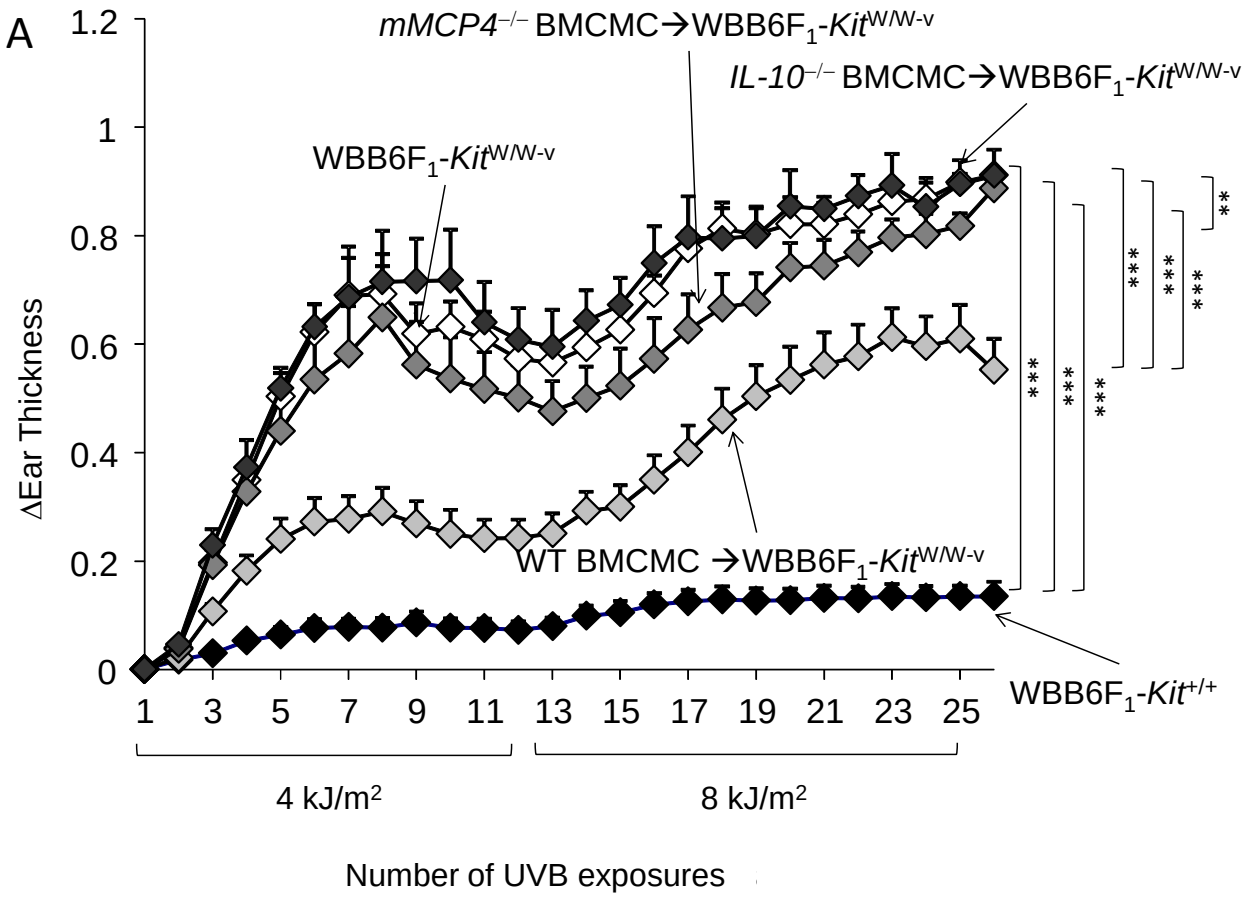
A
mMCP4−/− BMCMC→WBB6F1-KitW/W-v
IL-10−/− BMCMC→WBB6F1-KitW/W-v
WBB6F1-KitW/W-v
WT BMCMC →WBB6F1-KitW/W-v
WBB6F1-Kit+/+
ΔEar Thickness
1.2
1
0.8
0.6
0.4
0.2
0
1 3 5 7 9 11 13 15 17 19 21 23 25
4 kJ/m2
8 kJ/m2
Number of UVB exposures
***
**

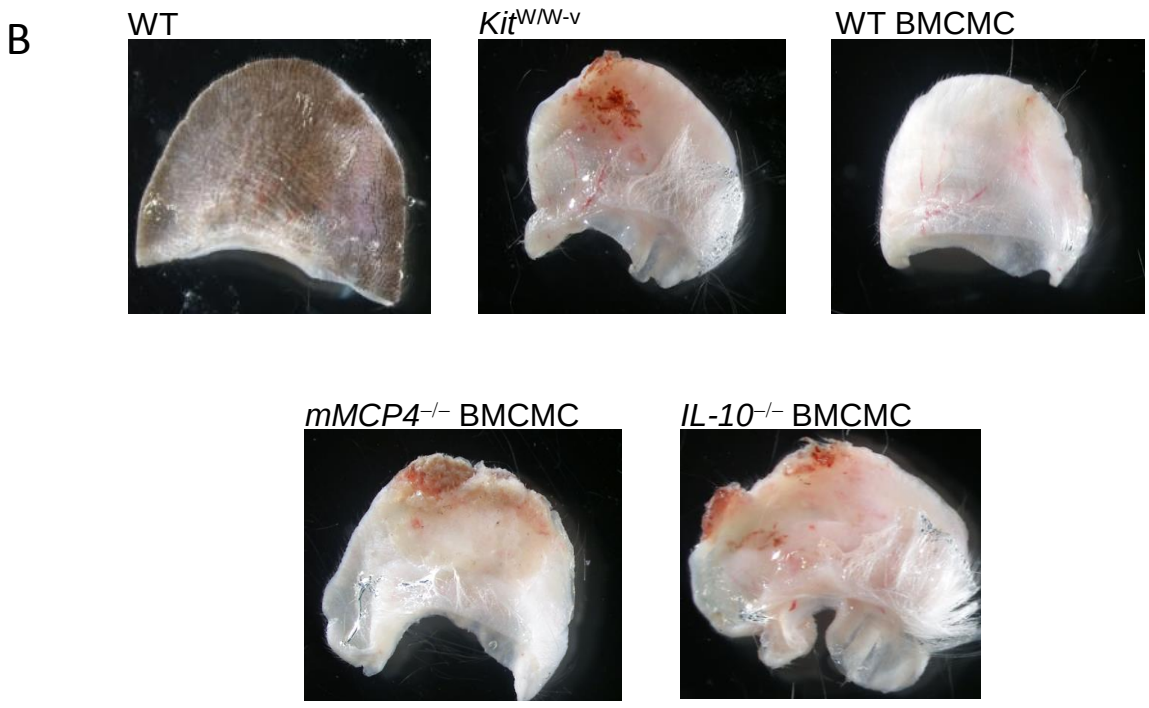
B
WT
KitW/W-v
WT BMCMC
mMCP4−/− BMCMC
IL-10−/− BMCMC

Figure 4.6. Toluidine blue stained-cross sections of UVB-treated engrafted-WBB6F$_1$-*Kit*$^{W/W\text{-}v}$ mice (A) Representative images of Toluidine blue stained-cross sections of untreated (no UVB) and UVB-treated ears from WT, WBB6F$_1$-*Kit*$^{W/W\text{-}v}$, WT BMCMC→WBB6F$_1$-*Kit*$^{W/W\text{-}v}$, *mMCP4*$^{-/-}$ BMCMC→WBB6F$_1$-*Kit*$^{W/W\text{-}v}$, and *IL-10*$^{-/-}$ BMCMC→WBB6F$_1$-*Kit*$^{W/W\text{-}v}$ mice at 24 hours after the final exposure to 4 kJ/m^2 (12 exposures) and 4 + 8 kJ/m^2 (25 exposures). Scale bar: 600 μm; inset: 2 mm; Red arrows indicate mast cells. Images were taken on an Nanozoomer Technology microscope and visualised using Nanozoomer Digital Pathology software.

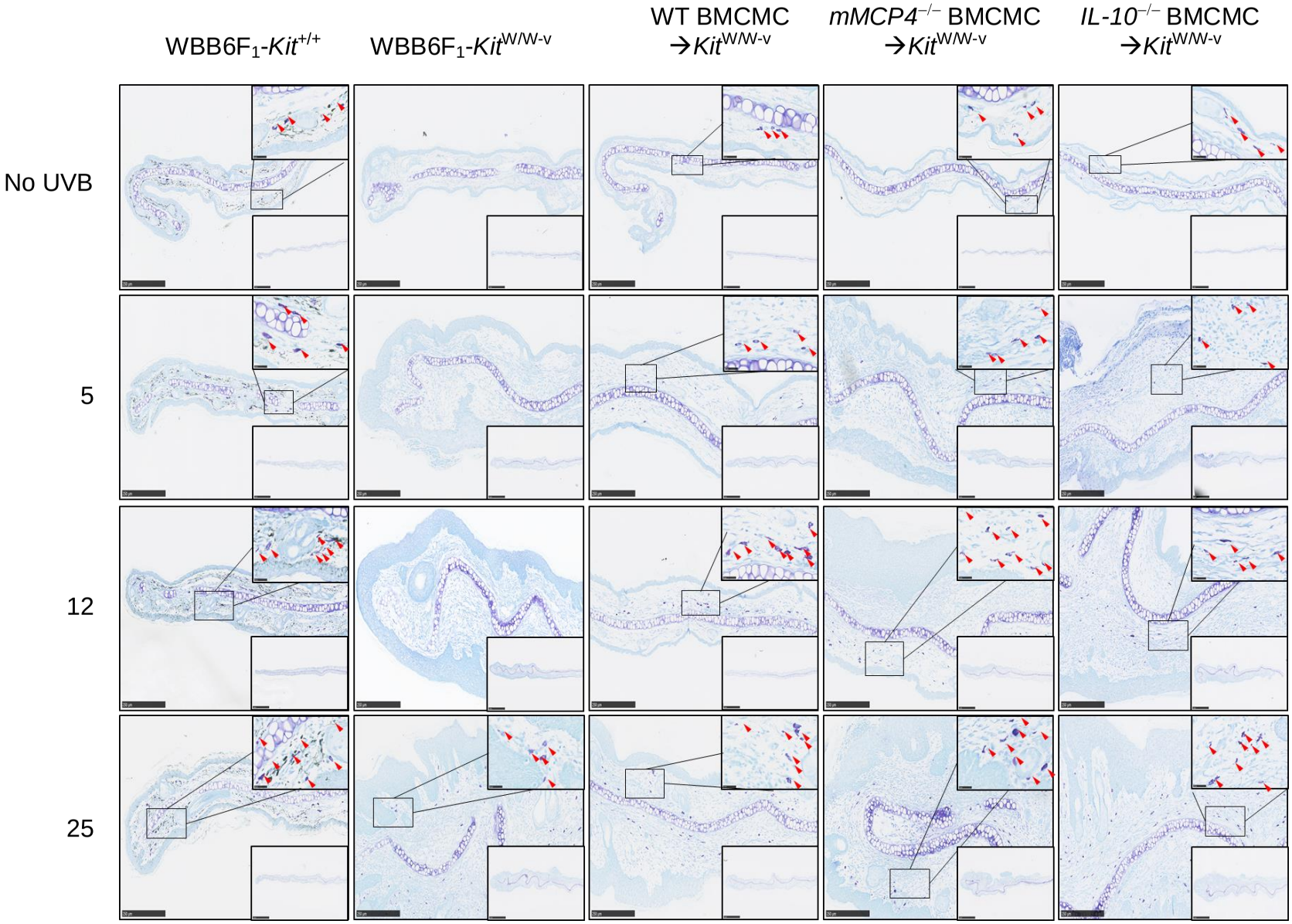
WBB6F1-Kit+/+
WBB6F1-KitW/W-v
WT BMCMC →KitW/W-v
mMCP4−/− BMCMC →KitW/W-v
IL-10−/− BMCMC →KitW/W-v
No UVB
5
12
25

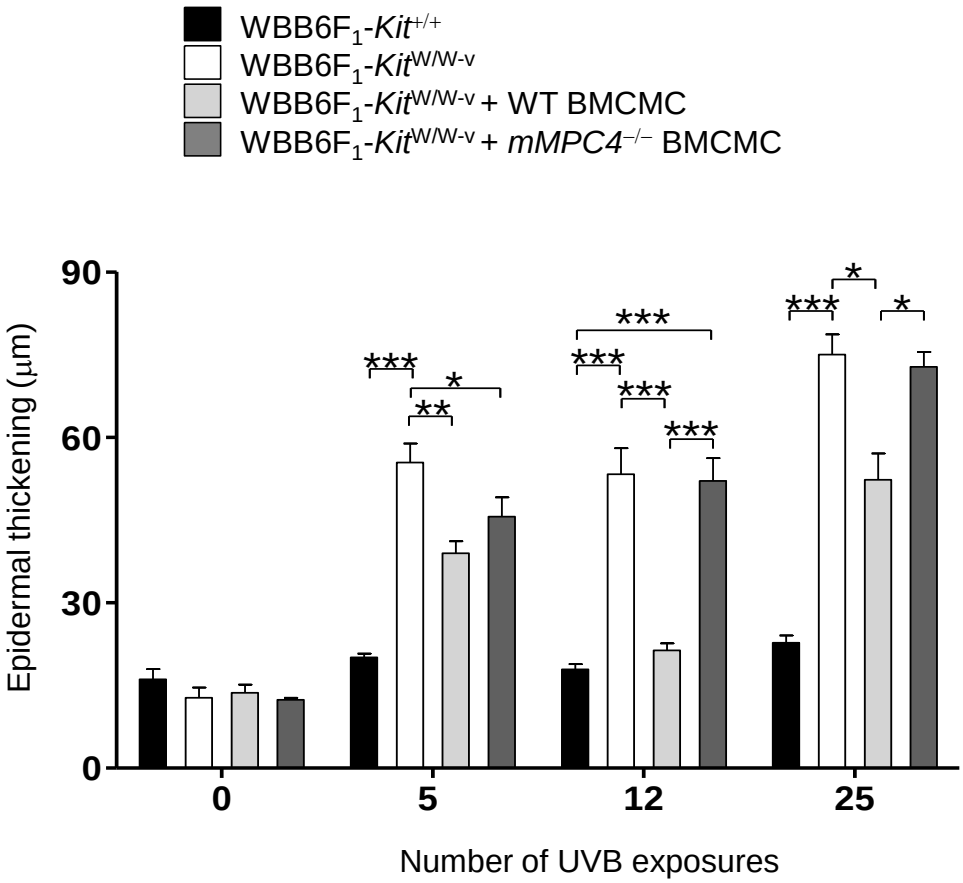

Figure 4.7. MCs and mMCP4 are important in regulating epidermal thickening when exposed to chronic UVB irradiation
Epidermal thickness was measured in cross sections of ear skin obtained from WT, WBB6F$_1$-*Kit*$^{W/W\text{-}v}$, WT BMCMC→WBB6F$_1$-*Kit*$^{W/W\text{-}v}$ and *mMCP4*$^{-/-}$ BMCMC→WBB6F$_1$-*Kit*$^{W/W\text{-}v}$ mice at 24 hours after the final exposure to 4 kJ/m^2 (5 and 12 exposures) and 8 kJ/m^2 (25 exposures). Images were taken on an Nanozoomer Technology microscope and epidermal thickness was quantified using Nanozoomer Digital Pathology software. Data are represented as mean + SEM from 2-3 independent experiments. 1-Way ANOVA with Bonferroni's post-test . *p<0.05. **p<0.01, ***p<0.001.

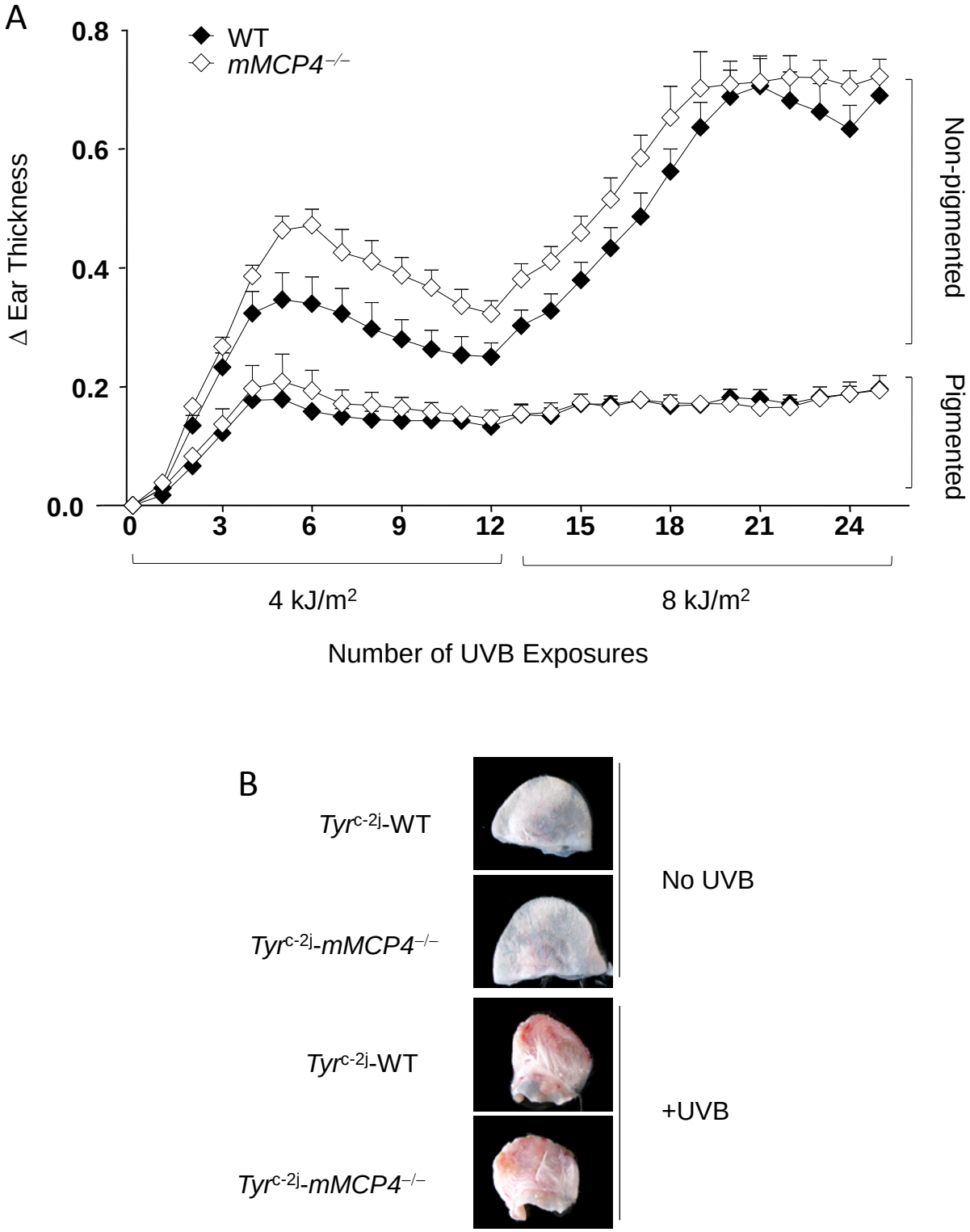

Figure 4.8. UVB-induced ear thickening response of pigmented and non-pigmented *mMCP4*$^{-/-}$ mice. (A) Ear thickness responses were measured from pigmented and non-pigmented WT and *mMCP4*$^{-/-}$ mice that were exposed to UVB every 2 days for a total of 25 (12 x 4 kJ/m^2 +13 x 8 kJ/m^2) exposures (cumulative dose 152 kJ/m^2). Data are represented as mean + SEM from 1-3 experiments. **(B)** Representative Images of gross ear pathology after 25 exposures of chronic UVB irradiation.

the importance of mMCP4 as observed in *Kit*$^{W/W\text{-}v}$ mice. However, the ear thickening response of these mice (<~0.2 mm) was greatly reduced compared to non-pigmented *Tyr*$^{c\text{-}2j}$ mice (<~0.75 mm) throughout 25 exposures to UVB. More importantly, no difference in the ear thickening response was observed in the absence of mMCP4 compared to WT mice (**Figure 4.8a**). Hence, we extended the UVB irradiation regime to 70 exposures (cumulative dose: 502 kJ/m^2) in attempt to assess any further differences in the absence of mMCP4. However, at the end of 70 exposures, the ear thickening response in these mice remains minimal despite a slight overall increase and no difference was observed between genotypes (**Figure 4.9**). Notably, no difference in MC number was observed between genotypes either (**Figure 4.10**). At the epidermal level, Toluidine blue stained ear sections showed no difference in epidermal thickness in the absence of mMCP4 in both pigmented B6 and non-pigmented *Tyr*$^{c\text{-}2j}$ mice (**Figure 4.11a, b and 4.12a, b**).

4.2.3 Increasesing mMCP4 protein expression following chronic UVB irradiation

To confirm mMCP4 expression was absent in *Kit*$^{W/W\text{-}v}$ and *mMCP4*$^{-/-}$ BMCMCs→WBB6F$_1$-*Kit*$^{W/W\text{-}v}$ mice throughout the UVB irradiation regime, QRT-PCR and western blotting analysis were utilised to measure the level of mMCP4 in the ears of mice. The analysis showed a complete absence of mMCP4 mRNA and protein in the ears of *Kit*$^{W/W\text{-}v}$ and *mMCP4*$^{-/-}$ BMCMCs→WBB6F$_1$-*Kit*$^{W/W\text{-}v}$ mice both before and after UVB irradiation. Elevated levels of mMCP4 protein was observed in WT and WT BMCMCs→WBB6F$_1$-*Kit*$^{W/W\text{-}v}$ mice, despite a decrease in mRNA as suggested by QRT-PCR (**Figure 4.13a and 4.14a**). Similar observations were also made in both pigmented B6 and non-pigmented *Tyr*$^{c\text{-}2j}$ mice, except no change was observed in the level of mMCP4 protein in *Tyr*$^{c\text{-}2j}$-WT following exposure to UVB (**Figure 4.13b, c and 4.14b**).

4.3 Discussion

It is well known that exposure to UVB not only results in recruitment of MC into the dermis in both human and mice[406-408], at the site of UVB exposure, MCs are also indirectly activated by UVB-induced mediators such as nerve growth factor and *cis*-UCA[360,361]. MCs were initially thought to be primarily pro-inflammatory and pro-carcinogenic in response to exogenous environmental agents such as UV irradiation[409]. For example, a study by Starkey *et al.,* showed that when the MC-deficient *Kit*$^{W/W\text{-}v}$ mice were either systemically or locally engrafted with B16-BL6 murine melanoma cells, these mice

Figure 4.9. Extended chronic UVB irradiation regime has no affect on pigmented B6-WT and B6-*mMCP4*$^{-/-}$ ear thickening response. Ear thickness responses were measured from pigmented B6-WT and B6-*mMCP4*$^{-/-}$ mice that were exposed to chronic high-doses of UVB every 2 days for a total of 70 exposures (12 x 4 kJ/m^2 + 8 x 58 kJ/m^2; cumulative dose 506 kJ/m^2). Data are represented as mean + SEM from 2-3 experiments.

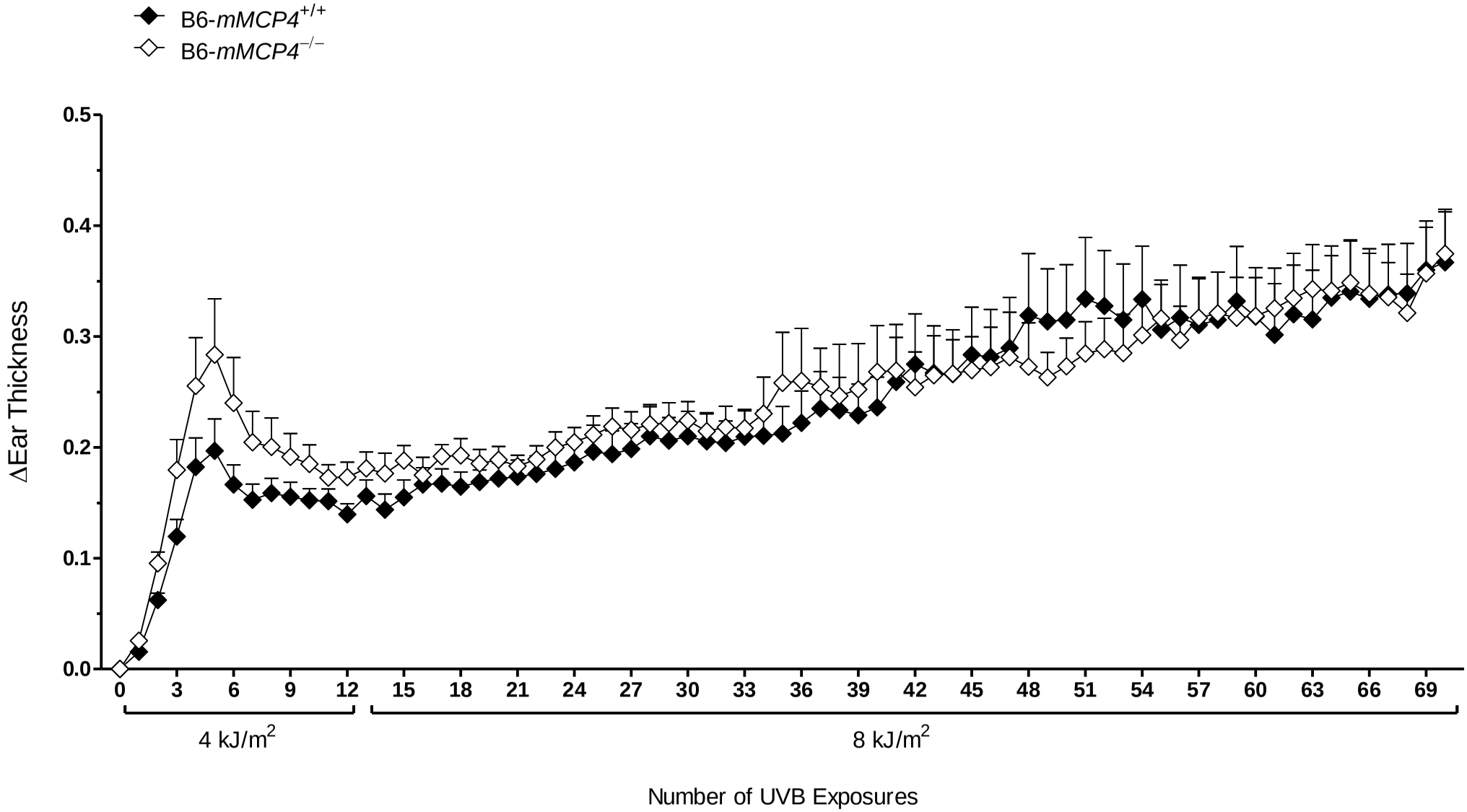
B6-mMCP4+/+
B6-mMCP4−/−
ΔEar Thickness
0.0
0.1
0.2
0.3
0.4
0.5
0 3 6 9 12 15 18 21 24 27 30 33 36 39 42 45 48 51 54 57 60 63 66 69
4 kJ/m2
8 kJ/m2
Number of UVB Exposures

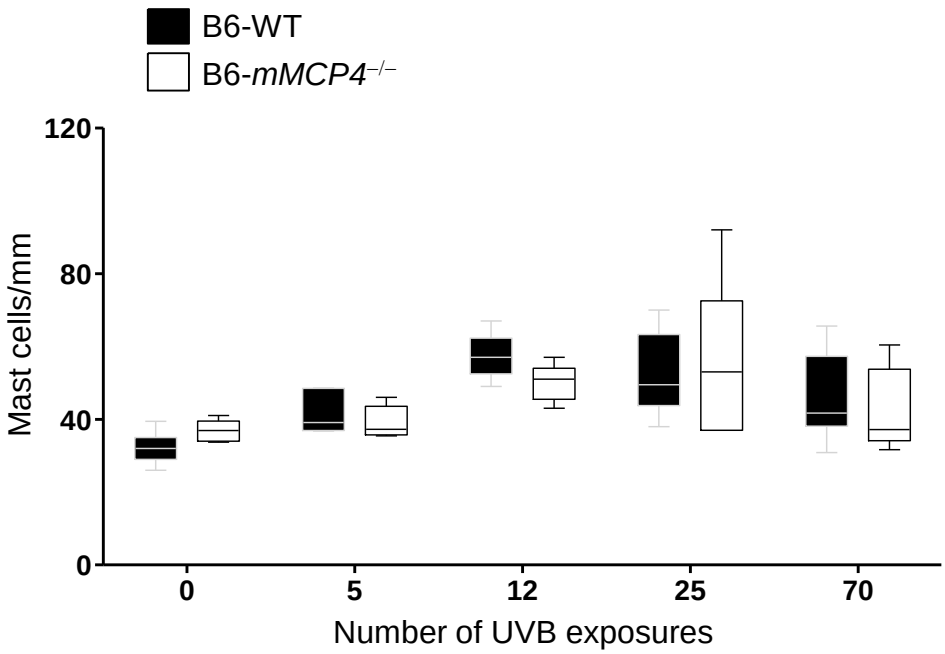

Figure 4.10. Mast cells numbers do not change in the absence of mMCP4 in response to chronic UVB irradiation. Mast cell numbers were quantified from Toluidine blue stained cross sections of the ear pinnae of untreated and UVB-treated non-pigmented B6, WT and *mMCP4*$^{-/-}$ mice (5, 12 [at 4 kJ/m^2] and 25 exposures [at 8 kJ/m^2]). Mast cell counts were normalised to length of the cartilage. Data represented as median from 2-3 experiments. Images were taken on an Nanozoomer Technology microscope and visualised using Nanozoomer Digital Pathology software.

Figure 4.11. Toluidine blue stained-cross sections of pigmented B6 and non-pigmented *Tyr*$^{c\text{-}2j}$ mice following chronic UVB exposure (A) Representative images of Toluidine blue stained cross-sections of untreated (no UVB) and UVB-treated ears from pigmented B6-WT and B6-*mMCP4*$^{-/-}$ mice at 24 h after the final exposure to 4 kJ/m^2 (5 and 12 exposures) and 8 kJ/m^2 (25 and 70 exposures). **(B)** Representative images of Toluidine blue stained-cross sections of untreated (no UVB) and UVB-treated ears from non-pigmented *Tyr*$^{c\text{-}2j}$-WT and *Tyr*$^{c\text{-}2j}$-*mMCP4*$^{-/-}$ at 24 h after the final exposure to 4 kJ/m^2 (5 and 12 exposures) and 8 kJ/m^2 (25 exposures). Scale bar: 600 μm; inset: 2 mm. All Images were taken on an Nanozoomer Technology microscope and digitised using Nanozoomer Technology software.

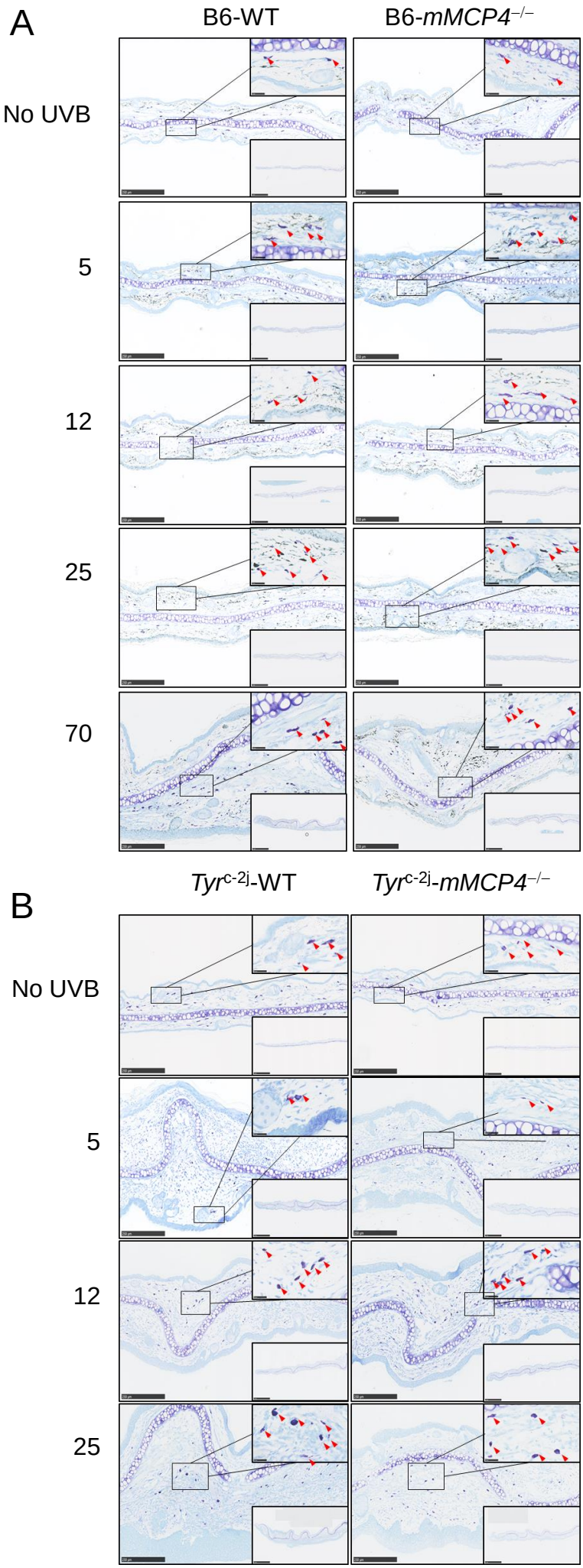
A
B6-WT
B6-mMCP4−/−
No UVB
5
12
25
70
B
Tyrc-2j-WT
Tyrc-2j-mMCP4−/−
No UVB
5
12
25

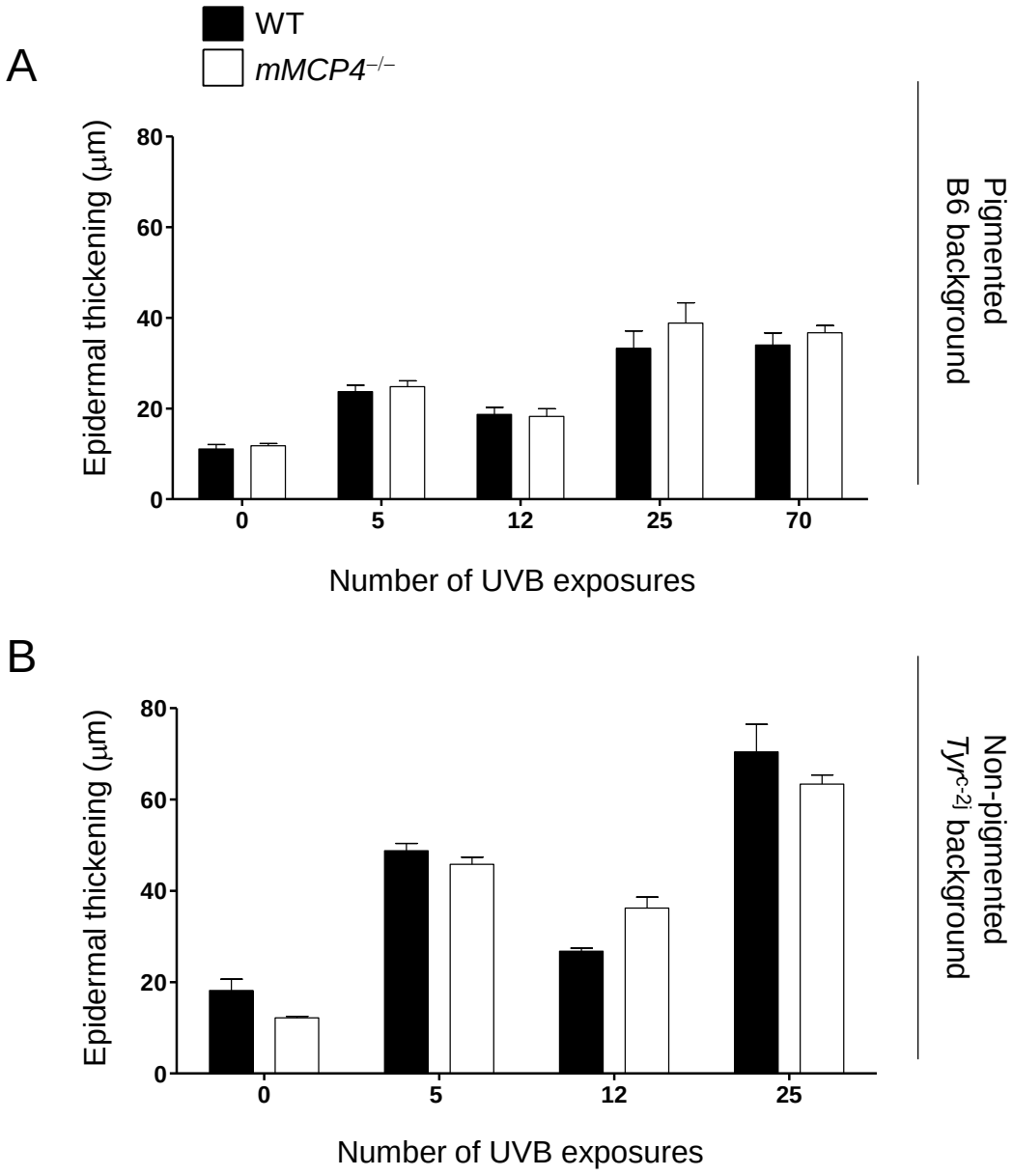

Figure 4.12. Absence of mMCP4 does not contribute to exacerbated epidermal thickening in pigmented B6 and non-pigmented *Tyr*$^{c\text{-}2j}$ mice (A) Epidermal thickness was measured from Toluidine blue stained-cross sections of ears from untreated and UVB-treated pigmented B6 and **(B)** non-pigmented *Tyr*$^{c\text{-}2j}$, WT and *mMCP4*$^{-/-}$ mice at 24 h after the final exposure to 4 kJ/m^2 (5 and 12 exposures) and 8 kJ/m^2 (25 [and 70 exposures for pigmented mice]). Scale bar: 600 μm; inset: 2 mm. All Images were taken on an Nanozoomer Technology microscope and epidermal thickness was quantified using Nanozoomer Technology software. Data are represented as mean + SEM from 2-3 experiments.

Figure 4.13. Real time qPCR to confirm the presence of mMCP4 mRNA expression in WBB6F$_1$-*Kit*$^{W/W\text{-}v}$, *mMCP4*$^{-/-}$ BMCMC→WBB6F$_1$-*Kit*$^{W/W\text{-}v}$, as well as pigmented and non-pigmented mMCP4$^{-/-}$ mice (A) RNA generated from untreated and UVB-treated ear tissues of WT, WBB6F$_1$-*Kit*$^{W/W\text{-}v}$, WT BMCMC→WBB6F$_1$-*Kit*$^{W/W\text{-}v}$ and *mMCP4*$^{-/-}$ BMCMC→WBB6F$_1$-*Kit*$^{W/W\text{-}v}$ mice were used to determine the relative mRNA expression of *mMCP4* at 0 and 25 exposures. Data are represented as mean + SEM from 1 experiment. (n=3 mice/genotype). **(B)** RNA generated from untreated and UVB-treated ear tissues of pigmented B6-WT and B6-*mMCP4*$^{-/-}$ mice were used to determine the relative mRNA expression of *mMCP4* after 0, 25 and 70 exposures of chronic UVB. Data are represented as mean + SEM from 1 experiment. (n=3 mice/genotype). **(C)** RNA generated from untreated and UVB-treated ear tissues of non-pigmented *Tyr*$^{c\text{-}2j}$-WT and *Tyr*$^{c\text{-}2j}$-*mMCP4*$^{-/-}$ mice were used to determine the relative mRNA expression of *mMCP4* at 0 and 25 exposures of chronic UVB. Data are represented as mean + SEM from 1 experiment. (n=3 mice/genotype). All relative *mMCP4* mRNA expression were quantitated by qRT-PCR and normalised to the expression of mouse *GAPDH* housekeeping gene. Relative expression was assessed using Rotorgene software using the comparative quantitation method. N.D.: not detected

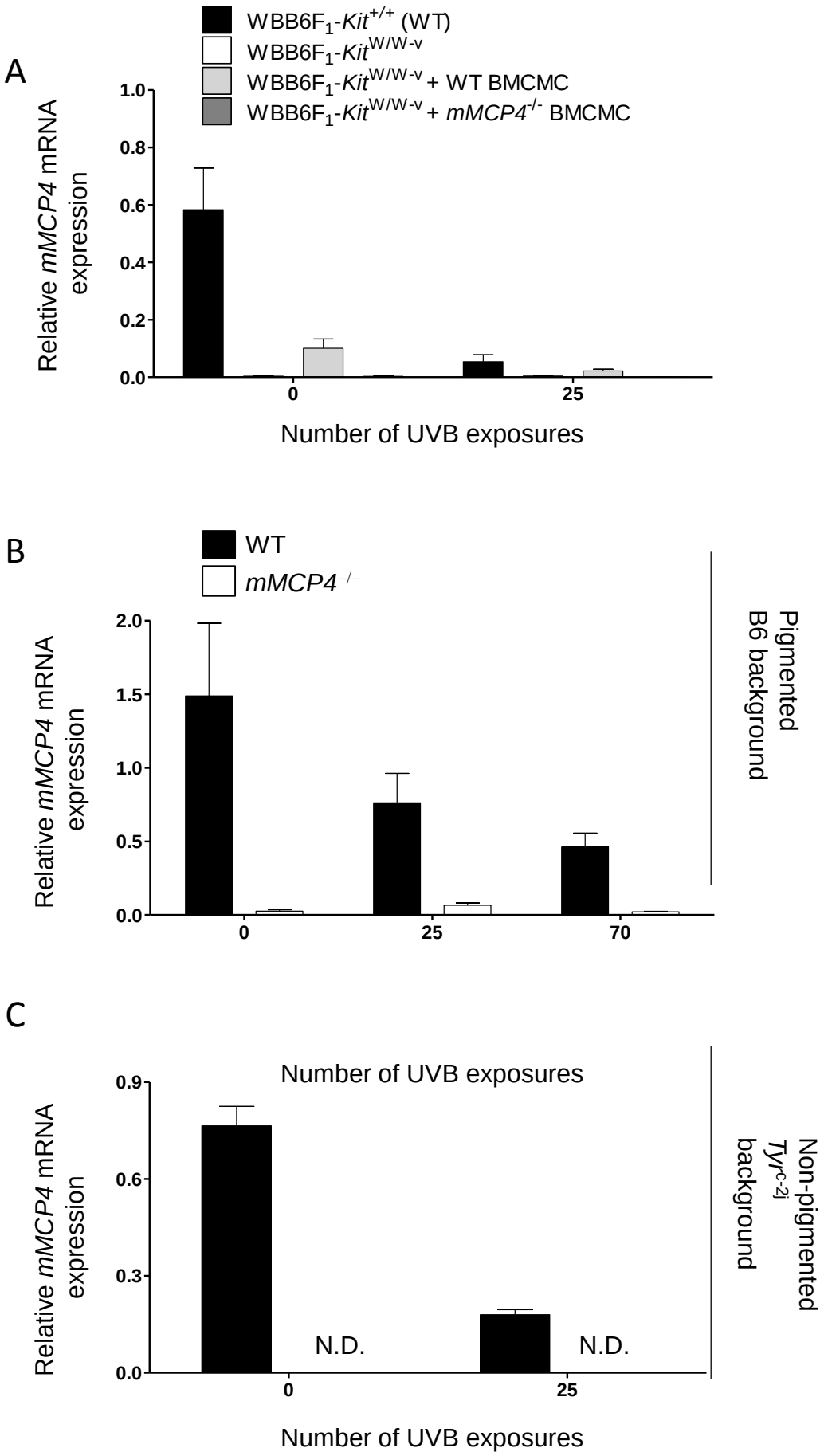
A
WBB6F1-Kit+/+ (WT)
WBB6F1-KitW/W-v
WBB6F1-KitW/W-v + WT BMCMC
WBB6F1-KitW/W-v + mMCP4-/- BMCMC
Relative mMCP4 mRNA expression
1.0
0.8
0.6
0.4
0.2
0.0
0
25
Number of UVB exposures
B
WT
mMCP4–/–
Relative mMCP4 mRNA expression
2.0
1.5
1.0
0.5
0.0
0
25
70
Pigmented B6 background
C
Number of UVB exposures
Relative mMCP4 mRNA expression
0.9
0.6
0.3
0.0
N.D.
N.D.
0
25
Number of UVB exposures
Non-pigmented Tyrc-2J background

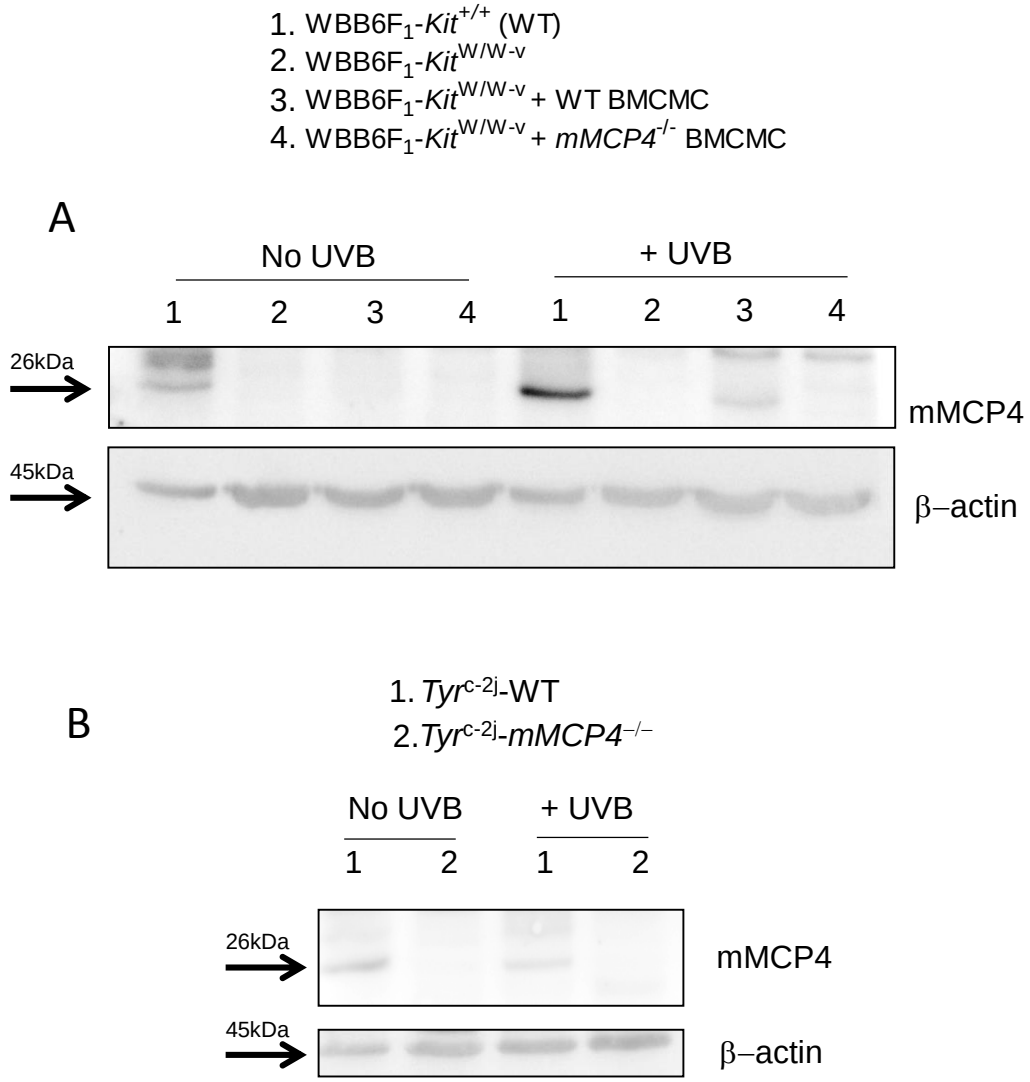

Figure 4.14. Western blotting analysis to confirm the presence of mMCP4 protein in WBB6F$_1$-*Kit*$^{W/W-v}$, *mMCP4*$^{-/-}$ BMCMC→WBB6F$_1$-*Kit*$^{W/W-v}$, as well as non-pigmented *mMCP4*$^{-/-}$ mice (A) Representative immunoblot of endogenous mMCP4 protein expression was performed on untreated (No UVB) and UVB-treated ear tissue lysates from WT, WBB6F$_1$-*Kit*$^{W/W-v}$, WT BMCMC→WBB6F$_1$-*Kit*$^{W/W-v}$ and *mMCP4*$^{-/-}$ BMCMC→WBB6F$_1$-*Kit*$^{W/W-v}$ mice**. Lane (1-4); 1)** WBB6F$_1$-*Kit*$^{+/+}$ (WT), **2)** WBB6F$_1$-*Kit*$^{W/W-v}$ **3)** WT BMCMC→WBB6F$_1$-*Kit*$^{W/W-v}$ **4)** *mMCP4*$^{-/-}$ BMCMC→WBB6F$_1$-*Kit*$^{W/W-v}$. **(B)** Representative immunoblot of endogenous mMCP4 protein expression was performed on untreated (No UVB) and UVB-treated ear tissue lysates from *Tyr*$^{c-2j}$-WT and *Tyr*$^{c-2j}$-*mMCP4*$^{-/-}$ mice**.**

showed enhanced macroscopic angiogenic responses and higher levels of spontaneous lung metastasis, compared to the animals into which MCs were reconstituted[232]. Clinically, in many cases, the number of mast cells has been correlated with disease progression and poor patient survival[230,342,410].

On the other hand, more evidence is emerging to suggest a potential protective role of MCs in skin cancers. For example, lower number of mast cells has been reported in melanoma compared to benign nevi[411]. A recent study by Siiskonen *et al*., also reported an association between reduced numbers of tryptase$^+$ and chymase$^+$ mast cells and poor patient survival and advanced tumour stage in melanoma[412]. In a model of chemical-induced skin carcinogenesis, MC-deficient *Kit*$^{W/W\text{-}v}$ mice engrafted with *ex vivo*-derived WT BMCMCs were able to curtail and control tumour growth and development compared to MC-deficient *Kit*$^{W/W\text{-}v}$ mice when chemical carcinogens TPA and DMBA were topically applied to shaven back skin[6].

The regulatory effects of MCs are typically facilitated through release of MC-specific mediators. Following the UV-induced recruitment and activation, MCs can release mediators such as histamine, which is an important rate-limiting step in UV-induced immunosuppression[105,413]. Studies have shown that histamine can alter the function of cutaneous dendritic cells to adopt an immune suppressive phenotype which can suppress Th1-mediated anti-tumour responses[414]. In addition, histamine can also promote host anti-tumour immune response through regulating the proliferation and cytokine profile of T lymphocytes residing in skin draining lymph nodes[415]. MCs are also recognised as a major source of TNFα which is known to be present at high levels in UVB-exposed skin [366]. TNFα is known to be immunosuppressive due its ability to induce epidermal Langerhan cell migration to skin draining lymph nodes and mediate activation of IL-4-producing regulatory NKT cells[416,417]. Interestingly, TNFα has also been suggested to modulate anti-tumour immune responses in human melanoma and non-melanoma skin tumours[418].

Our previous study also demonstrated the ability of MC-IL-10 in limiting UVB-induced inflammation and skin pathology following exposure to chronic low dose UVB irradiation. In response to chronic low-dose UVB, both MC-deficient *Kit*$^{W/W\text{-}v}$ and *IL-10*$^{-/-}$ BMCMCs→WBB6F$_1$-*Kit*$^{W/W\text{-}v}$ mice not only showed greater degree of skin pathology, including epidermal hyperplasia and ulceration, compared to WT and WT

BMCMCs→WBB6F$_1$-*Kit*$^{W/W\text{-}v}$ mice, but also demonstrated a reduction in inflammatory cell infiltration (including granulocytes, macrophages, CD4$^+$ and CD8$^+$ T cells, as well as CD25$^+$Foxp3$^+$ Treg cells) as well as reduced release of pro-inflammatory cytokines (IL-6, TNFα, and IL-4)[8,9].

Using the same model, our preliminary study identified mMCP4 as a novel MC-mediator that could exhibit protective properties against chronic low-dose UVB-induced ear thickening response at a similar level as MC-IL-10. In this chapter, we sought to investigate if mMCP4 could retain this protective function in a chronic high-dose UVB irradiation setting, and protect against development of UVB-induced skin carcinogenesis.

As shown by H&E staining (**Figure 4.1**), our data confirmed that both MC-IL-10 and mMCP4 were able to retain their protective function even in response to chronic high-dose UVB irradiation, and were shown to significantly limit development and progression of UVB-induced *in situ* SCCs. More importantly, utilising global mMCP4 knock-out mice (non-pigmented *Tyr*$^{c\text{-}2j}$ background), this protective role of mMCP4 was further confirmed where *Tyr*$^{c\text{-}2j}$-*mMCP4*$^{-/-}$ mice not only displayed higher rates of full-thickness epidermal necrosis indicating exacerbated inflammation of the epidermis, but more importantly mice lacking mMCP4 showed an earlier onset of *in situ* SCCs compared to the WT counterparts (**Figure 4.3**, **Table 4.1**). This is the first evidence so far showing mMCP4 as a novel MC-derived mediator that is able to limit development of UVB-induced skin carcinogenesis. Interestingly, we did observe a temporary downregulation of full-thickness epidermal necrosis after 12 exposures. This could be due to expression of the anti-inflammatory mediator IL-10, which we know is also capable of dampening inflammatory responses when exposed to chronic UVB.

Exposure to UVB irradiation is known to induce inflammation of the skin which can eventually lead to subsequent tumour development. Hence ear thickening response as well as gross pathological changes in the ears were also assessed throughout the UVB irradiation regime. As demonstrated in **Figure 4.5**, following UVB irradiation, *Kit*$^{W/W\text{-}v}$ and *mMCP4*$^{-/-}$ BMCMCs→WBB6F$_1$-*Kit*$^{W/W\text{-}v}$, and *IL-10*$^{-/-}$ BMCMCs→WBB6F$_1$-*Kit*$^{W/W\text{-}v}$ all exhibited significantly more exacerbated ear thickening response and gross damage to the ears compared to WT and WT BMCMCs→WBB6F$_1$-*Kit*$^{W/W\text{-}v}$ counterparts, further confirming the importance of mMCP4 as well as MC-IL-10 in protection against

UVB-induced skin pathology as well as precursor characteristics that can lead to ultimate skin carcinogenesis in response to chronic high-dose UVB settings.

It is worth noting that the level of ear thickening in *Kit*$^{W/W\text{-}v}$ and *IL-10*$^{-/-}$ BMCMCs→WBB6F$_1$-*Kit*$^{W/W\text{-}v}$ were identical, confirming MC-IL-10 as a crucial negative mediator in this setting. However, in comparison, the ear thickening response of *mMCP4*$^{-/-}$ BMCMCs→WBB6F$_1$-*Kit*$^{W/W\text{-}v}$ mice were slightly lower, suggesting a compensatory protective effect by other anti-inflammatory MC mediators including MC-IL-10, was playing a role. In addition, other MC-specific proteases may also compensate for the loss of mMCP4 and elicit their own protective roles. Tryptase for instance, has been demonstrated to be a regulator of skin inflammation by targeting chemokines (RANTES and eotaxin)[419], neuropeptides (CGRP)[420] and matrix metalloproteinases (MMP-3 and MMP-13)[421]. A recent study by Siiskonen *et al*., also reported a tryptase$^+$ human MCs to be protective in advanced stage melanomas and associated with limiting the metastatic spread of cancer cells[412].

Photocarcinogenesis can also be characterised by an inhibition of apoptosis coinciding with an enhancement of cell proliferation[276,422]. This inhibition of apoptosis is known to occur through the loss of expression of the apoptotic Fas-ligand during UV-induced irradiation, which leads to hyperproliferation of keratinocytes, leading to thickening of the epidermis[275,276]. It has been shown that as keratinocytes become hyperproliferative in response to chronic UVB exposure, these cells begin to accumulate *p53* mutations which could eventually lead to carcinogenesis[264]. However, epidermial thickening could also assist in protecting against deleterious effects of UVB by preventing penetration of UVB rays into the dermal layer[406]. Measurement of epidermal thickness in engrafted-*Kit*$^{W/W\text{-}v}$ mice demonstrated an increased level of epidermal thickening in *Kit*$^{W/W\text{-}v}$ and *mMCP4*$^{-/-}$ BMCMCs→WBB6F$_1$-*Kit*$^{W/W\text{-}v}$, compared to the WT and WT BMCMCs→WBB6F$_1$-*Kit*$^{W/W\text{-}v}$ counterparts (**Figure 4.7**), further confirming the importance of mMCP4 in protecting against precursor characteristics in the UVB-damaged skin which could eventually lead to development of *in situ* SCCs (**Figure 4.1**). However, it is important to note that this epidermal thickening associated with the lack of mMCP4 could either be a compensatory defensive mechanism, or an exacerbated response which eventually contributes to the development of *in situ* SCCs observed in these mice.

Interestingly, in the absence of global mMCP4 (non-pigmented *Tyr*$^{c\text{-}2j}$ background), no significant difference was observed in ear thickening response, gross pathology, or epidermal thickening throughout the UVB irradiation regime even though these mice have an earlier onset of *in situ* SCCs (**Figure 4.8, 4.11b, 4.12b**). The non-pigmented B6-*Tyr*$^{c\text{-}2j}$ mice are known to be of different genetic background compared to the *Kit*$^{W/W\text{-}v}$ mice (WB/ReJ×C57BL/6)[174], this may explain the variation observed between the two models. Note that the ear and epidermal thickening responses are the only other pathological parameters measured to assess the protective function of mMCP4 in this chapter. It is likely that mMCP4 may be involved more so in other pathways that can contribute to UVB-induced skin carcinogenesis in these mice.

Initially, the pigmented B6-*mMCP4*$^{-/-}$ mice were also applied to the same UVB irradiation regime in order to recapitulate the protective function of mMCP4 as observed in the engrafted-*Kit*$^{W/W\text{-}v}$ mice. However, as shown in **Figures 4.9, 4.11a and 4.12a** , the B6 mice not only exhibited a significantly dampened ear thickening response compared to that observed in both *Kit*$^{W/W\text{-}v}$ and B6-*Tyr*$^{c\text{-}2j}$ mice, in addition, no difference was observed in ear thickening response and epidermal thickening was observed even after an extended chronic UVB irradiation regime (70 exposures). Notably, an increased darkening of the ears of all mice were observed throughout the UVB irradiation regime, indicating an overall increase in pigmentation following exposure to UVB. These observations confirm the potent protective effect against UVB-associated skin pathology by pigmentation of the skin[313,423]. Interestingly, a study by Byrne and Sarchio showed that chronic solar simulated UV exposure could promote SCC formation on shaven back skin of pigmented B6 mice[54,424]. It is likely that this discrepancy between our current study (ears) and the observation by Byrne and Sarchio (back skin) is due to the difference in anatomical location, tissue composition but also spectra composition.

MC counts were performed on the ear sections in order to confirm the successful BMCMC engraftment into the ears of *Kit*$^{W/W\text{-}v}$ mice, and to determine whether a difference in MC number contributes to pathologies observed in response chronic UVB irradiation. As shown by **Figure 4.2**, no difference in MC number was observed between WT BMCMCs→WBB6F$_1$-*Kit*$^{W/W\text{-}v}$, *mMCP4*$^{-/-}$ BMCMCs→WBB6F$_1$-*Kit*$^{W/W\text{-}v}$, and *IL-10*$^{-/-}$ BMCMCs→WBB6F$_1$-*Kit*$^{W/W\text{-}v}$ throughout UVB irradiation regime, confirming that the protective function of these negative mediators is the main contributor to prevent the

development of skin carcinogenesis in this setting. This is also further supported in the non-pigmented B6-*Tyr*$^{c\text{-}2j}$ mice (**Figure 4.4**).

An additional noteworthy observation is the increase in MC number in *Kit*$^{W/W\text{-}v}$ mice over 25 exposures to UVB. This increase could be due to the high dosages of chronic UVB used, which could activate pathways that are able promote the proliferation of MCPs present at low numbers in the bone marrow of *Kit*$^{W/W\text{-}v}$ mice[174]. It is also possible that in response to chronic UVB, MCPs could also be recruited by mediators such as CCL2[40,41] and TNFα[51] and proliferate locally in response to growth factors such as IL-3[425]. Note that it is rather unlikely that the c-*kit*/SCF pathway is being utilised in this context, since the mutations generated in the c-*kit* receptor is known to significantly reduce tyrosine kinase signalling and subsequently perturb its ability to promote MC proliferation[426].

Interestingly, an increased level of mMCP4 protein was detected in both WT and WT BMCMCs→WBB6F$_1$-*Kit*$^{W/W\text{-}v}$ mice following 25 exposures of UVB, suggesting a protective function of mMCP4 in the chronic UVB setting (**Figure 4.14a**). Notably, no difference in mMCP4 protein was seen in *Tyr*$^{c\text{-}2j}$-WT mice following UVB irradiation (**Figure 4.14b**), this corresponds to less potent protective function of mMCP4 observed in the *Tyr*$^{c\text{-}2j}$ mouse model under UVB setting. It is likely that in the *Tyr*$^{c\text{-}2j}$-WT mice, at the end of 25 UVB exposures, the level of damage has surpassed the protective function of mMCP4, this is supported by the similar level of *in situ* SCC development between *Tyr*$^{c\text{-}2j}$-WT and *Tyr*$^{c\text{-}2j}$-mMCP4$^{-/-}$ mice at this time point (**Figure 4.3**).

To summarise, results in this chapter has demonstrated for the first time that mMCP4 is a novel MC-derived mediator which is able to elicit protective functions against chronic high-dose UVB-induced skin carcinogenesis. However, the mechanism of how mMCP4 exert this function remains unclear. Since mMCP4 is known to degrade and in some cases activate various substrates, it is likely that via targeting its known and unknown substrates, mMCP4 is able to regulate many pathways that could be attributable to the development of cancer.

Chapter 5

CHARACTERISING THE ROLE OF mMCP4 IN THE BLOOD AND LYMPHATIC VASCULATURE FOLLOWING CHRONIC UVB IRRADIATION

5.1 Introduction

As we have demonstrated in chapter 4, MCs and mMCP4 are critical in limiting the UVB-induced skin associated hallmark pathology that can lead to subsequent *in situ* SCC development. The initial findings based on gross pathological changes utilising engrafted-WBB6F$_1$–*Kit*$^{W/W\text{-}v}$ mice suggest that MCs and mMCP4 may have a role in regulating UVB-induced skin pathology but the mechanistic role of mMCP4 in chronic UVB-induced skin tumourigenesis is still not clearly defined as the pathological changes between the pigmented B6-*mMCP4*$^{-/-}$ and non-pigmented *Tyr*$^{c\text{-}2j}$-*mMCP4*$^{-/-}$ mice were not necessarily consistent with the observations in engrafted-WBB6F$_1$–*Kit*$^{W/W\text{-}v}$ mice. However, previous studies have demonstrated mMCP4 to target extracellular matrix components[7,384] and to be vital for homeostatic tissue remodelling[194]. Therefore, it is likely that mMCP4 may be more critical in the underlying pathology where its direct or indirect involvement in other pathways could lead to the changes in the tissue architecture and subsequent development of *in situ* SCCs that we observed in Chapter 4.

The stepping stones to tumourigenesis are typically associated with the attainment of multiple hallmark features which are extensively reviewed by Hanahan and Weinburg's "Hallmarks of Cancer" and "Hallmarks of cancer: the next generation"[225,427]. Exposure to the carcinogenic environmental factor UVB can influence many of the pathways reviewed by Hanahan and Weinburg, which include promoting DNA damage[320,401], pathological angiogenesis[346,347], evasion of apoptosis[276], immunosuppression[309,367] and chronic inflammation[225,428]. Ultimately, attaining these traits is required to convert normal cells to a tumourigenic state which eventually becomes malignant.

Of all of the hallmark features, the angiogenic and lymphangiogenic response in tumourigenesis is one of the major critical stepping stones[429-431]. The blood and lymphatic vasculature are indispensable for skin homeostasis and play key roles in inflammation. Blood vessels promote inflammation by allowing extravasation of leukocytes and plasma proteins to sites of inflammation, hence, leading to an overall increase interstitial fluid[432]. Subsequently, this increase in interstitial fluid at the site of inflammation leads to the opening of lymphatic capillaries, allowing the entry of inflammatory cell infiltrate and plasma proteins which drain to local lymph nodes and further promote or modulate the inflammatory response; this includes the induction of the adaptive immune response[336,433]. There has been a growing interest in the blood and lymphatic vasculature due to their

dysfunctional and aberrant characteristics in many inflammatory disorders including asthma (allergic airway inflammation)[434], lymphedema[435], rheumatoid arthritis[436] and more importantly, for the purpose of this study, tumourigenesis and metastasis[354,437,438].

As demonstrated in Chapter 4, chronic UVB exposure can promote ulceration, necrosis and scabbing, and underlying features including degradation of ECM components, elastosis, epidermal hyperplasia, erythema, vascular hyperpermeability and oedema formation[353]. UVB exposure is also known to cause an angiogenic switch whereby a pronounced increase in angiogenesis is observed in the skin of humans and mice through the up-regulation of angiogenic factors, particularly VEGF-A[346,368,439], but also other factors including fibroblast growth factor (FGF)2[440] and IL-8[441]. Moreover, UVB exposure also down-regulates the potent anti-angiogenic factor thrombospondin (TSP-1)[368,442], suggesting that blood vessels play a critical role in mediation of UVB-induced cutaneous damage.

The roles of lymphatic vessels in acute and chronic UVB settings have only begun to surface with the availability of new lymphatic vessel markers such as Prox-1[443], LYVE-1[444] and podoplanin[445]. In addition to well established roles in angiogenesis, reports also suggest that VEGF-A can induce inflammatory lymphangiogenesis. It is thought that the lymphatic vessels induced by VEGF-A are dysfunctional and unable to resolve the inflammatory response induced by both acute and chronic UVB exposure[353]. In contrast, VEGF-C and VEGF-D-mediated lymphangiogenesis is crucial in resolving UVB-induced inflammation of the skin[356]. The processes of angiogenesis and lymphangiogenesis are under strict regulatory control, based on a fine balance of positive (VEGF-A, VEGF-C, VEGF-D, FGF-2, PDGFBB)[336,341,410] and negative (thrombospondin-1[446], endostatin[447], angiostatin[448]) mediators. Aberrant angiogenesis and lymphangiogenesis contribute to a range of pathologies. MCs are typically in close proximity to the vasculature and are known to play crucial roles in the angiogenic response by releasing angiogenic factors including VEGF[358], IL-8[344] and basic fibroblast growth factor (bFGF)[449]. However, the adverse effects of UVB exposure on both the blood and lymphatic vasculature, and the role of MCs in these processes is still yet to be clearly defined. For this part of the study, the effects of MCs and mMCP4 on the blood and lymphatic vasculature following chronic UVB exposure were assessed.

5.2 Results

5.2.1 MCs and mMCP4 are important in regulating blood and lymphatic vasculature in WBB6F$_1$-Kit$^{W/W\text{-}v}$ mice in response to chronic UVB irradiation.

To assess the effects on the blood and lymphatic vasculature following UVB irradiation, triple immunofluorescence staining was conducted on frozen cryosections from engrafted-WBB6F$_1$-*Kit*$^{W/W\text{-}v}$ mice, utilising the pan-vascular endothelial cell marker, CD31 (PECAM1), vascular smooth muscle cell marker α-smooth muscle actin (SMA) and the lymphatic specific hyaluronan receptor marker (LYVE-1).

At baseline, the blood vasculature ($CD31^+SMA^-$ and $CD31^+SMA^+$ vessels) and lymphatic vasculature ($CD31^+LYVE1^+$ vessels) in the ears of WT, *Kit*$^{W/W\text{-}v}$, WT BMCMCs→WBB6F$_1$–*Kit*$^{W/W\text{-}v}$ and *mMCP4*$^{-/-}$ BMCMCs→WBB6F$_1$–*Kit*$^{W/W\text{-}v}$ mice appeared morphologically normal. However, after exposure to chronic UVB, both blood vessels and lymphatic vessels appeared more irregular and enlarged/dilated in the ears of all groups of mice (**Figure 5.1a**). Quantification of vessel number demonstrated an overall increase in the number of total and dilated blood and lymphatic vessels in the ears of all groups of mice, suggesting chronic UVB exposure is promoting an angiogenic and lymphangiogenic response (**Figure 5.1b, c** and **5.1e, f**).

After 5 exposures of chronic UVB, an overall increase in the number of total and dilated blood vessels was observed in the ears of all groups of mice, but no differences could be seen between all genotypes. It is noteworthy to point out that the increase in vessel number was more pronounced in the mice that lacked pigment compared to the pigmented WT mice (**Figure 5.1b, c**).

After 12 and 25 exposures of chronic UVB, a significant increase in the number of total blood vessels was observed in the ears of *Kit*$^{W/W\text{-}v}$ compared to their WT counterparts. A significant increase in the number of total blood vessels was also seen in *mMCP4*$^{-/-}$ BMCMCs→WBB6F$_1$–*Kit*$^{W/W\text{-}v}$ mice compared to WT BMCMCs→WBB6F$_1$–*Kit*$^{W/W\text{-}v}$ mice following 12 exposures. Whilst this increase was not significant after 25 exposures, a trend was observed (**Figure 5.1b**). The number of dilated blood vessels also appeared to be significantly greater in the ears of *Kit*$^{W/W\text{-}v}$ and *mMCP4*$^{-/-}$→WBB6F$_1$–*Kit*$^{W/W\text{-}v}$ mice compared to their WT counterparts after 12 and 25 exposures of chronic UVB (**Figure 5.1c**).

Figure 5.1 (A) Mice deficient of MCs and mMCP4 exhibit pronounced morphological changes in lymphatic or blood vessels when exposed to chronic high level doses of UVB. Representative confocal images demonstrating immunofluorescence staining of lymphatic vessels ($CD31^+/LYVE\text{-}1^+$) and blood vessels ($CD31^+/SMA^+$ or $CD31^+/SMA^-$) in UVB-treated (12 x 4 kJ/m^2 and 12 x 4 kJ/m^2 + 13 x 8 kJ/m^2) ears of WT, WBB6F$_1$-*Kit*$^{W/W\text{-}v}$ and *Kit*$^{W/W\text{-}v}$ engrafted with WT and *mMCP4*$^{-/-}$ BMCMCs. Scale bar = 100 μm. Red arrow heads; lymphatic vessels with distinct lumen (dilated/enlarged) ($CD31^+/LYVE\text{-}1^+$). **(B)** Blood vessels that were $CD31^+$ or $CD31^+/SMA^+$ were counted and quantified per field of view. **(C)** Vessels that were $CD31^+$ or $CD31^+/SMA^+$ that displayed a distinct enlarged lumen were counted and quantified per field of view. **(D)** The area of $CD31^+$ and $CD31^+/SMA^+$ vessels that displayed a distinct lumen were calculated using ImageJ. **(E)** Lymphatic vessels that were $CD31^+LYVE\text{-}1^+$ were counted and quantified per field of view. **(F)** $CD31^+LYVE\text{-}1^+$ Lymphatic vessels with a distinct lumen were counted and quantified per field of view. **(G)** The area of $CD31^+LYVE\text{-}1^+$ vessels that displayed a distinct lumen were calculated using ImageJ. All quantified vessels were assessed per field of view (639.5 x 639.5 μm); 18 images/mouse ear were assessed. All data represented as Median ± range. Mann-Whitney U Test; *p<0.05, **p<0.01; Compared to No UVB control $^{\#}p$<0.05, $^{\#\#}p$<0.01. Data from 2-3 experiments (n=5-11 mice/genotype).

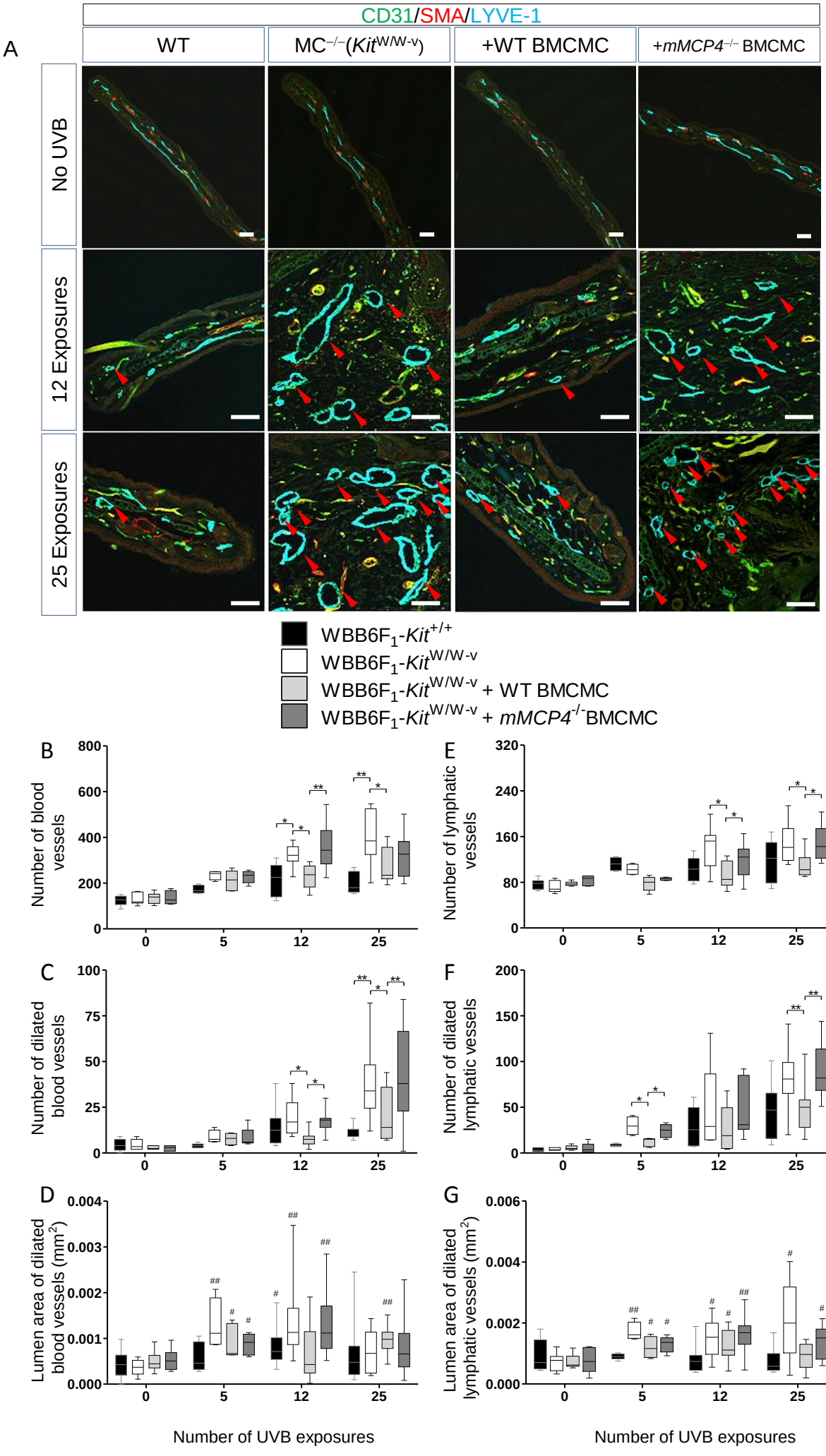
A
CD31/SMA/LYVE-1
WT
MC−/−(KitW/W-v)
+WT BMCMC
+mMCP4−/− BMCMC
No UVB
12 Exposures
25 Exposures
WBB6F1-Kit+/+
WBB6F1-KitW/W-v
WBB6F1-KitW/W-v + WT BMCMC
WBB6F1-KitW/W-v + mMCP4-/-BMCMC
B
Number of blood vessels
C
Number of dilated blood vessels
D
Lumen area of dilated blood vessels (mm2)
E
Number of lymphatic vessels
F
Number of dilated lymphatic vessels
G
Lumen area of dilated lymphatic vessels (mm2)
Number of UVB exposures
Number of UVB exposures

In regards to the lymphatic vasculature, we made similar observations where a significant increase in the number of $CD31^{+}LYVE^{+}$ lymphatic vessels in the ears of *Kit*$^{W/W\text{-}v}$ and *mMCP4*$^{-/-}$→WBB6F$_1$–*Kit*$^{W/W\text{-}v}$ mice was observed after 12 and 25 UVB exposures compared to their WT littermates (**Figure 5.1e**). Moreover, the number of dilated lymphatic vessels was also significantly higher in the ears of *Kit*$^{W/W\text{-}v}$ and *mMCP4*$^{-/-}$ BMCMCs→WBB6F$_1$–*Kit*$^{W/W\text{-}v}$ mice compared to their WT counterparts after 5 and 25 UVB exposures. A similar trend was also present after 12 exposures, although not statistically significant (**Figure 5.1f**).

The lumen area of the dilated blood and lymphatic vessels was also assessed. Overall, both types of dilated vessels showed a small increase in the lumen area in all groups of mice across the entire UVB regime, however, no differences could be seen between genotypes (**Figure 5.1d**, **g**). Taken together, the data generated from engrafted *Kit*$^{W/W\text{-}v}$ mice suggests MCs and mMCP4 do appear to play a role in regulating the architecture and potentially function of the blood and lymphatic vasculature following UVB exposure. Additionally, the changes in the vasculature appear to be more pronounced in non-pigmented mice compared to pigmented mice.

5.2.2 The role of mMCP4 appears to be more critical in regulating lymphatic vasculature in pigmented B6-mMCP4 mice.

As explained in Chapter 4, due to the phenotypic abnormalities present in WBB6F$_1$–*Kit*$^{W/W\text{-}v}$ mice, we utilised pigmented B6-*mMCP4*$^{-/-}$ mice to ensure that any changes observed were based on the deficiency of MC populations and absence of mMCP4 and independent of the other phenotypic abnormalities arising from mutations in c-*kit*^{174}. The changes in the blood and lymphatic vasculature in the absence of mMCP4 following chronic UVB irradiation were also assessed in these mice.

Based on immunofluorescence analysis, at basal levels there were no distinct irregularities or changes in the morphological features of either blood vessels or lymphatic vessels in both B6-WT and B6-*mMCP4*$^{-/-}$ mice, similar to that observed in the engrafted *Kit*$^{W/W\text{-}v}$ mice. Following exposure to UVB, enlargement of both blood vessels and lymphatic vessels was observed throughout the regime (**Figure 5.2a**).

Quantification analysis revealed an overall increase in the number of total and dilated blood vessels following UVB exposure. However, the lumen area of dilated blood vessels

Figure 5.2 (A) Pigmented B6-*mMCP4*$^{-/-}$ mice exhibit distinct changes in morphological features of lymphatic vessels after an extended chronic UVB regime. Representative confocal images demonstrating immunofluorescence staining of lymphatic vessels (CD31$^+$/LYVE-1$^+$) , blood vessels (CD31$^+$/SMA$^+$ or CD31+/SMA$^-$) in UVB-treated (5x4 kJ/m^2, 12 x 4 kJ/m^2 and 12 x 4 kJ/m^2 + 13 x 8 kJ/m^2 and 12 x 4 kJ/m^2 + 58 x 8 kJ/m^2) ears of B6-WT and B6-*mMCP4*$^{-/-}$ mice. Scale bar = 100 μm. Red Arrow; lymphatic vessels with distinct lumen (dilated/enlarged) (CD31$^+$/LYVE-1$^+$). **(B)** Blood vessels that were CD31$^+$ or CD31$^+$/SMA$^+$ were counted and quantified per field of view. **(C)** CD31$^+$ or CD31$^+$/SMA$^+$ Blood vessels that displayed a distinct enlarged lumen were counted and quantified per field of view. **(D)** The area of CD31$^+$ and CD31$^+$/SMA$^+$ vessels that displayed a distinct lumen were calculated using ImageJ. **(E)** Lymphatic vessels that were CD31$^+$LYVE-1$^+$ were counted and quantified per field of view. **(F)** CD31$^+$LYVE-1$^+$ Lymphatic vessels with a distinct lumen were counted and quantified per field of view. **(G)** The area of CD31$^+$LYVE-1$^+$ vessels that displayed a distinct lumen were calculated using ImageJ. All quantified vessels were assessed per field of view (639.5 x 639.5 μm); 18 images/mouse ear were assessed. All data represented as Median ± range. Mann-Whitney U Test; ***p<0.001. Data from 2-3 experiments. (n=5-11 mice/genotype)

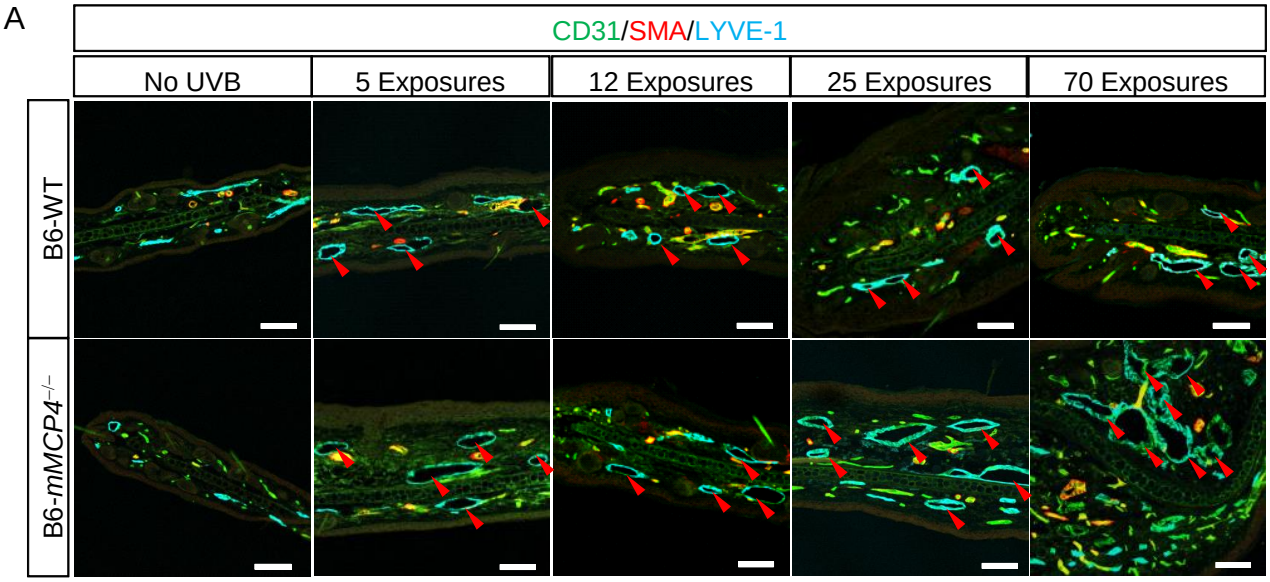
A
CD31/SMA/LYVE-1
No UVB
5 Exposures
12 Exposures
25 Exposures
70 Exposures
B6-WT
B6-mMCP4−/−

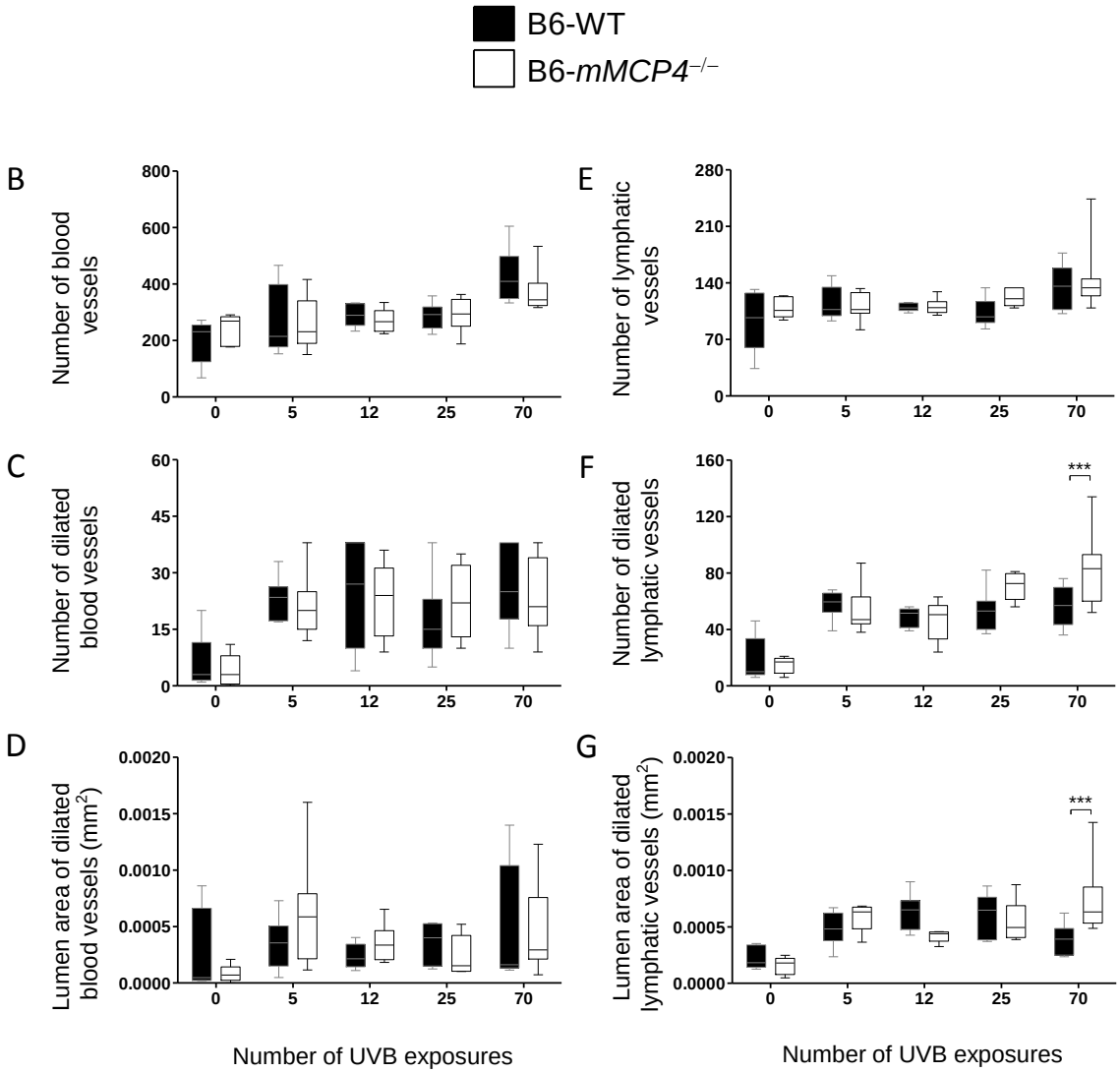
B6-WT
B6-mMCP4−/−
B
Number of blood vessels
800
600
400
200
0
0
5
12
25
70
E
Number of lymphatic vessels
280
210
140
70
0
C
Number of dilated blood vessels
60
45
30
15
F
Number of dilated lymphatic vessels
160
120
80
40
***
D
Lumen area of dilated blood vessels (mm2)
0.0020
0.0015
0.0010
0.0005
0.0000
G
Lumen area of dilated lymphatic vessels (mm2)
Number of UVB exposures
Number of UVB exposures

show no distinct changes. More importantly, no differences was observed in these parameters between B6-WT and B6-*mMCP4*$^{-/-}$ mice (**Figure 5.2b-d**).

In contrast, the number of total and dilated lymphatic vessels as well as lumen area of dilated vessels showed an increase across the chronic UVB regime in both B6-WT and B6-*mMCP4*$^{-/-}$ mice. Both the number of dilated lymphatics and lymphatic vessel lumen area were significantly increased in the absence of mMCP4 after 70 exposures (**Figure 5.2e-g**).

These data demonstrates that the impact of loss of mMCP4 on UVB-mediated effects on the lymphatic vasculature is consistent across mouse models. However, effects on the vasculature appeared to be more delayed in the pigmented B6-mice compared to non-pigmented *Kit*$^{W/W\text{-}v}$ mice. This is likely due to the presence of pigment, which can protect or limit some of the deleterious effects of UVB. Notably, although pigmentation has shielded the protective effect of mMCP4 at the gross pathological level as reported in Chapter 4, the protective effect on the underlying vasculature is still evident.

5.2.3 The role of mMCP4 is critical in regulating lymphatic vasculature in non-pigmented Tyr$^{c\text{-}2j}$-mMCP4 mice.

As the presence of pigment impacted our ability to optimally assess the function of mMCP4 in the vasculature of B6-WT and B6-*mMCP4*$^{-/-}$ mice, the effects of chronic UVB were assessed in non-pigmented *Tyr*$^{c\text{-}2j}$-*mMCP4*$^{-/-}$ mice. Based on our standard protocol, the response to chronic UVB irradiation was measured 24 h post exposure[8,9] and consistently the response to UVB irradiation in the skin has been reported to peak at 24 h following irradiation[441]. However, since mMCP4 is a pre-formed mediator found in MC dense granules, they are typically released through the process of degranulation, which is an innate immune response that normally occurs within an hour of stimulation[5]. In order to assess whether or not there were any differences in the kinetics of the response at earlier time points, changes in the vasculature 3 h post UVB irradiation were also assessed.

At steady state, no irregularities or morphological changes were evident in *Tyr*$^{c\text{-}2j}$-WT or *Tyr*$^{c\text{-}2j}$-*mMCP4*$^{-/-}$ mice. Following UVB irradiation, an overall increase in the number of total and dilated blood and lymphatic vessels was observed (**Figure 5.3b, c, e, f**). Additionally, an increase in the lumen area of dilated lymphatic vessels was also

Figure 5.3 (A) 3 hours after the final UVB exposure, non-pigmented *Tyr*$^{c\text{-}2j}$-WT and *Tyr*$^{c\text{-}2j}$-*mMCP4*$^{-/-}$ mice show pronounced changes in the architecture of blood and lymphatic vessels. Representative confocal images demonstrating immunofluorescence staining of lymphatic vessels (CD31$^+$/LYVE-1$^+$) and blood vessels (CD31$^+$/SMA$^+$ or CD31$^+$/SMA$^-$) in UVB-treated (12 x 4 kJ/m^2 and 12 x 4 kJ/m^2 + 13 x 8 kJ/m^2) ears of *Tyr*$^{c\text{-}2j}$-WT and *Tyr*$^{c\text{-}2j}$-*mMCP4*$^{-/-}$ mice. Scale bar = 100 μm. Red Arrow; lymphatic vessels with distinct lumen (dilated/enlarged). **(B)** Blood vessels that were CD31$^+$ or CD31$^+$/SMA$^+$ were counted and quantified per field of view. **(C)** CD31$^+$ or CD31$^+$/SMA$^+$ blood vessels that displayed a distinct enlarged lumen were counted and quantified per field of view. **(D)** The area of CD31$^+$ and CD31$^+$/SMA$^+$ vessels that displayed a distinct lumen were calculated using ImageJ. **(E)** Lymphatic vessels that were CD31$^+$LYVE-1$^+$ were counted and quantified per field of view. **(F)** CD31$^+$LYVE-1$^+$ Lymphatic vessels with a distinct lumen were counted and quantified per field of view. **(G)** The area of CD31$^+$LYVE-1$^+$ vessels that displayed a distinct lumen were calculated using ImageJ. All quantified vessels were assessed per field of view (639.5 x 639.5 μm); 18 images/mouse ear were assessed. All data represented as Median ± range. Mann-Whitney U Test; ****p<0.001. Data from 1 experiment (n=4-7 mice/genotype).

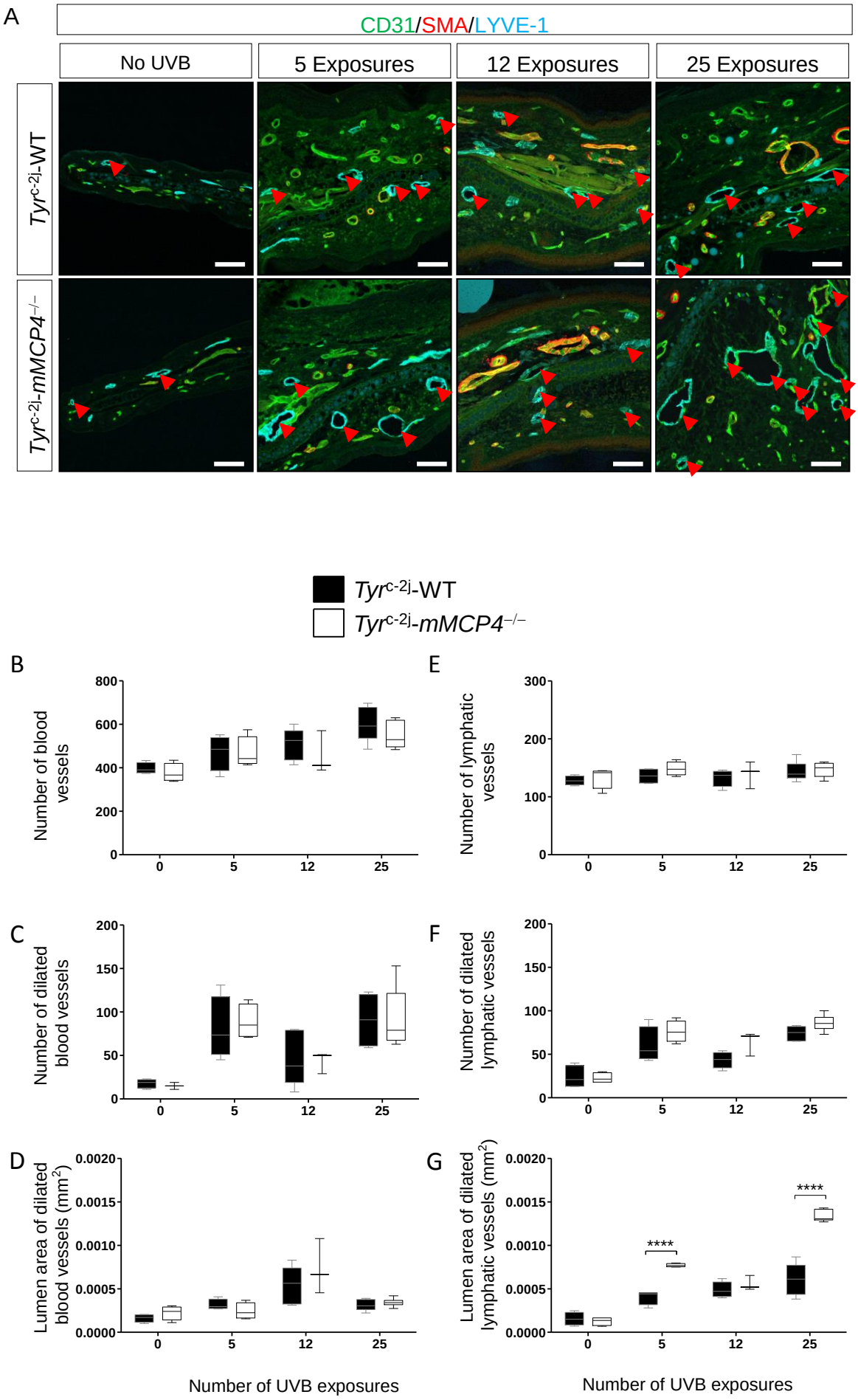
A
CD31/SMA/LYVE-1
No UVB
5 Exposures
12 Exposures
25 Exposures
Tyrc-2j-WT
Tyrc-2j-mMCP4−/−
Tyrc-2j-WT
Tyrc-2j-mMCP4−/−
B
Number of blood vessels
800
600
400
200
0
0
5
12
25
E
Number of lymphatic vessels
300
200
100
0
0
5
12
25
C
Number of dilated blood vessels
200
150
100
50
0
0
5
12
25
F
Number of dilated lymphatic vessels
200
150
100
50
0
0
5
12
25
D
Lumen area of dilated blood vessels (mm2)
0.0020
0.0015
0.0010
0.0005
0.0000
0
5
12
25
Number of UVB exposures
G
Lumen area of dilated lymphatic vessels (mm2)
0.0020
0.0015
0.0010
0.0005
0.0000
****
****
0
5
12
25
Number of UVB exposures

observed and a similar trend was seen in blood vessels within the first 5 exposures, except the lumen area was slightly reduced after 25 exposures (**Figure 5.3d, g**).

Similar to the pigmented B6-mice, no changes were observed in the number of total and dilated blood vessels as well as the lumen area of dilated blood vessels between genotypes (**Figure 5.3b-d**). No changes were observed in the number of total or dilated lymphatic vessels in the absence of mMCP4 (**Figure 5.3e, f**). However, importantly, there was a significant increase in the lumen area of dilated lymphatic vessels in *Tyr*$^{c\text{-}2j}$*-mMCP4*$^{-/-}$ mice compared to WT counterparts at 5 and 25 exposures (**Figure 5.3g**).

The same analysis was again carried out but 24 h post UVB irradiation. Again at baseline, no irregularities or morphological changes were evident in *Tyr*$^{c\text{-}2j}$-WT or *Tyr*$^{c\text{-}2j}$*-mMCP4*$^{-/-}$ mice. Following UVB irradiation, an increase in the number of total and dilated blood and lymphatic vessels was observed and the lumen areas of dilated blood and lymphatic vessels were elevated (**Figure 5.4b-g**).

Interestingly, although not significant, an increase in the number of total and dilated blood vessels was observed in *Tyr*$^{c\text{-}2j}$*-mMCP4*$^{-/-}$ mice compared to WT following UVB irradiation. The lumen area of dilated blood vessels was also increased in the absence of mMCP4 at 12 exposures (not significant) (**Figure 5.4b-d**). Similarly, in the absence of mMCP4, the total number of lymphatic vessels was not significantly elevated but an increasing trend could be observed when compared to WT mice after 12 and 25 exposures. Additionally, the number of dilated lymphatic vessels as well as the lumen area of dilated lymphatic vessels was increased (**Figure 5.4e-g**). It is important to note that the effect of mMCP4 on the vasculature appears to be more evident at 24 h post UVB irradiation compared to 3 h.

In comparison to the observations in the pigmented B6-*mMCP4*$^{-/-}$ mouse model, in non-pigmented mice, an effect of mMCP4 on the blood vasculature was also observed but the effects on lymphatic vasculature were more profound. This supports the hypothesis that pigmentation in the B6-*mMCP4*$^{-/-}$ mouse model is shielding the protective effect of mMCP4 in the UVB setting. Finally, based on the assessment of all three models, mMCP4 appears to have intermediate roles in angiogenesis but a more pronounced impact on the lymphatic vasculature.

Figure 5.4 (A) Non-pigmented *Tyr*$^{c\text{-}2j}$-WT and *Tyr*$^{c\text{-}2j}$-*mMCP4*$^{-/-}$ mice exhibit similar morphological changes in blood and lymphatic vasculature to engrafted-*Kit*$^{W/W\text{-}v}$ mice following chronic (24 hours-post final UVB) UVB irradiation. Representative confocal images demonstrating immunofluorescence staining of lymphatic vessels (CD31^{+}/LYVE-1^{+}) and blood vessels (CD31^{+}/SMA^{+} or CD31^{+}/SMA^{-}) in UVB-treated (12 x 4 kJ/m^2 and 12 x 4 kJ/m^2 + 13 x 8 kJ/m^2) ears of *Tyr*$^{c\text{-}2j}$-WT and *Tyr*$^{c\text{-}2j}$-*mMCP4*$^{-/-}$ mice. Scale bar = 100 μm. Red Arrow; lymphatic vessels with distinct lumen (dilated/enlarged). **(B)** Blood vessels that were CD31^{+} or CD31+/SMA^{+} were counted and quantified per field of view. **(C)** CD31^{+} or CD31^{+}/SMA^{+} blood vessels that were that displayed a distinct enlarged lumen were counted and quantified per field of view. **(D)** The area of CD31^{+} and CD31^{+}/SMA^{+} vessels that displayed a distinct lumen were calculated using ImageJ. **(E)** Lymphatic vessels that were CD31^{+}LYVE-1^{+} were counted and quantified per field of view. **(F)** CD31^{+}LYVE-1^{+} Lymphatic vessels with a distinct lumen were counted and quantified per field of view. **(G)** The area of CD31^{+}LYVE-1^{+} vessels that displayed a distinct lumen were calculated using ImageJ. All quantified vessels were assessed per field of view (639.5 x 639.5 μm); 18 images/mouse ear were assessed. All data represented as Median ± range. Mann-Whitney U Test *p<0.05 **p<0.01 data from 1 experiment.

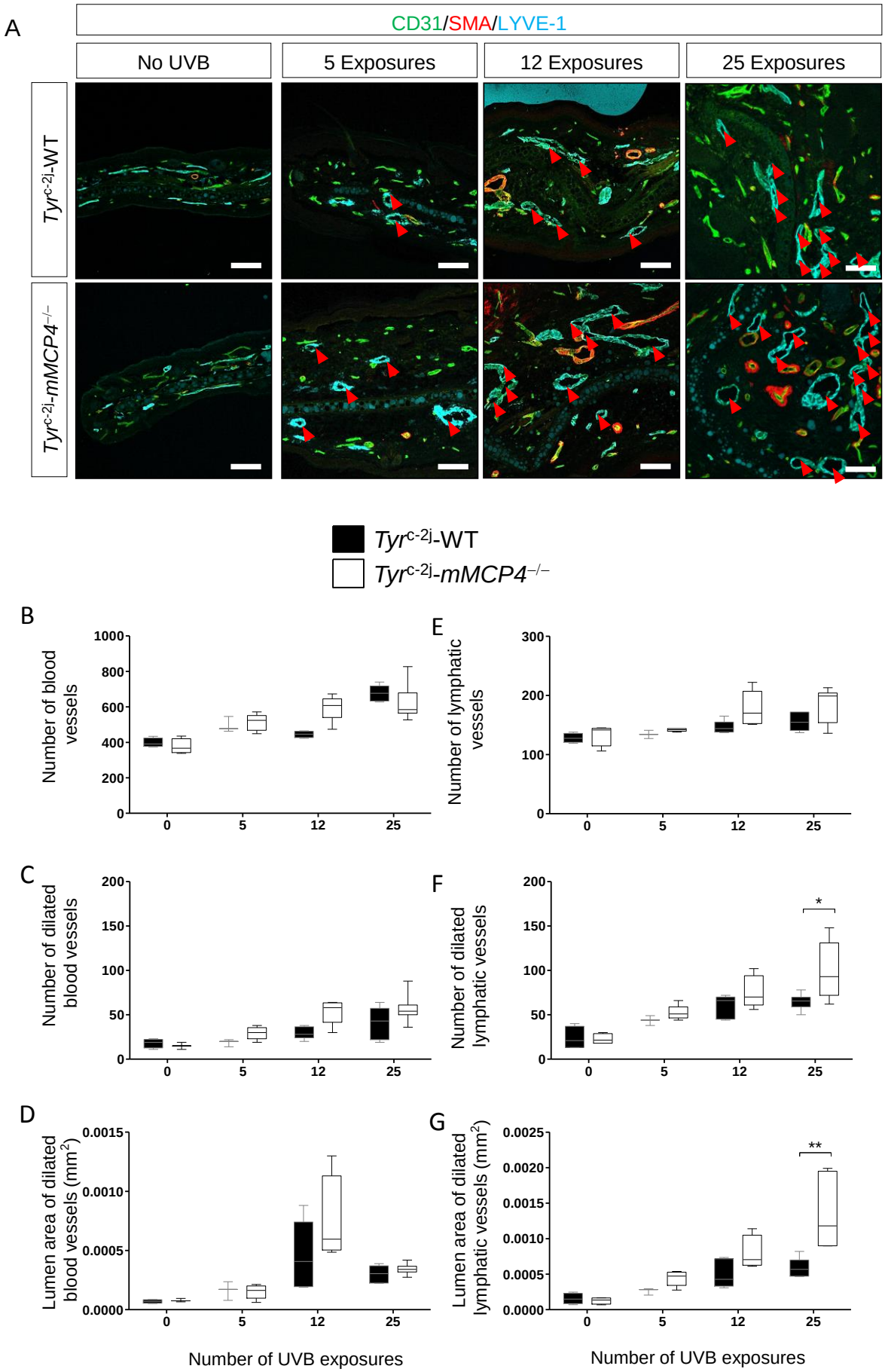
A
CD31/SMA/LYVE-1
No UVB
5 Exposures
12 Exposures
25 Exposures
Tyrc-2j-WT
Tyrc-2j-mMCP4−/−
Tyrc-2j-WT
Tyrc-2j-mMCP4−/−
B
Number of blood vessels
E
Number of lymphatic vessels
C
Number of dilated blood vessels
F
Number of dilated lymphatic vessels
D
Lumen area of dilated blood vessels (mm2)
G
Lumen area of dilated lymphatic vessels (mm2)
Number of UVB exposures
Number of UVB exposures

5.2.4 Drainage of interstitial inflammatory fluid is mediated by mMCP4 following UVB exposure.

Dilation of lymphatic vessels typically occurs in settings of inflammation and reflects elevated lymph flow[450,451]. Our findings suggest that the absence of mMCP4 results in significantly larger lumen areas of dilated lymphatic vessels. This may indicate that the loss of mMCP4 could promote or impair lymphatic drainage functions. To investigate this possibility, the functionality of lymphatic vessels in the ears of *Tyr*$^{c\text{-}2j}$-WT and *Tyr*$^{c\text{-}2j}$*-mMCP4*$^{-/-}$ mice was assessed by intradermal injection of 1% Evan's blue dye into the ears after 5 exposures of chronic UVB irradiation. The dye was then allowed to drain from the UVB-treated ears to respective draining lymph nodes for 1 hr before the ears and their respective lymph nodes were harvested and the levels of Evan's blue dye in these tissues measured by absorbance spectroscopy (610 nm absorbance); (normalised to tissue weight).

Compared to *Tyr*$^{c\text{-}2j}$-WT mice, *Tyr*$^{c\text{-}2j}$*-mMCP4*$^{-/-}$ mice had significantly more dye retained in the ears while slightly less was detected in the lymph nodes (not significant) (**Figure 5.5**). This suggests that the lymphatic vessels in the ears of *Tyr*$^{c\text{-}2j}$*-mMCP4*$^{-/-}$ mice are potentially less efficient at draining inflammatory infiltrate and plasma proteins from the site of UVB-induced damage compared to *Tyr*$^{c\text{-}2j}$-WT mice.

5.2.5 The role of mMCP4 in regulating myeloid derived suppressor cell populations at the site of UVB damage.

Based on our findings, the dilated lymphatic vessels following chronic UVB irradiation appeared to be dysfunctional, which might lead to lymphatic deficiency and the inability to efficiently drain inflammatory infiltrate from the site of UVB-induced inflammation. This suggests a potential mechanism to promote a pro-tumour microenvironment by the accumulation of dysregulated immune cell populations at the site of damage[452]. To address whether mMCP4-deficiency associated impairment of lymphatic vessel functions results in dysregulated accumulation of immune cell populations, the following populations were assessed by flow cytometric analysis: CD45$^+$ immune cells; CD3$^+$CD8$^+$ T cells, CD3$^+$CD4$^+$ T cells, B220$^+$ B cells, CD25$^+$ FoxP3$^+$ Treg cells, NK1.1$^+$CD3$^-$ NKT cells and Gr-1$^+$ granulocytes; Gr1$^+$CD11b$^+$ neutrophils, Gr-1$^+$CD11b$^-$ macrophages and CD11b$^+$ F4/80$^-$ GR-1$^+$ myeloid derived suppressor cells (MDSCs)[453,454].

Figure 5.5 (A) *Tyr*$^{c\text{-}2j}$-*mMCP4*$^{-/-}$ mice exhibit dysfunctional lymphatic drainage of Evan's blue dye from the site of UVB damage. To assess functionality of lymphatic vessels**,** 1% Evan's blue was interdermally injected into the ears of UVB-treated (5 exposures) *Tyr*$^{c\text{-}2j}$-WT and *Tyr*$^{c\text{-}2j}$-*mMCP4*$^{-/-}$ mice (24 h post final UVB irradiation). 1 h post injection, ears and draining lymph nodes were recovered and the presence of Evan's blue dye was assessed by measuring absorbance values at 610 nm. Absorbance was normalised to weight of tissue. Data shown from 2 independent experiments and represented as median. Mann-Whitney U Test *$p<0.05$ (n=9-11 mice/genotype). **(B)** Representative images of demonstrating the retainment of 1% Evan's blue dye in the ears of UVB-treated *Tyr*$^{c\text{-}2j}$-WT and *Tyr*$^{c\text{-}2j}$- *mMCP4*$^{-/-}$ mice.

Figure 5.5 (A) *Tyr*$^{c\text{-}2j}$-*mMCP4*$^{-/-}$ mice exhibit dysfunctional lymphatic drainage of Evan's blue dye from the site of UVB damage. To assess functionality of lymphatic vessels**,** 1% Evan's blue was interdermally injected into the ears of UVB-treated (5 exposures) *Tyr*$^{c\text{-}2j}$-WT and *Tyr*$^{c\text{-}2j}$-*mMCP4*$^{-/-}$ mice (24 h post final UVB irradiation). 1 h post injection, ears and draining lymph nodes were recovered and the presence of Evan's blue dye was assessed by measuring absorbance values at 610 nm. Absorbance was normalised to weight of tissue. Data shown from 2 independent experiments and represented as median. Mann-Whitney U Test *$p<0.05$ (n=9-11 mice/genotype). **(B)** Representative images of demonstrating the retainment of 1% Evan's blue dye in the ears of UVB-treated *Tyr*$^{c\text{-}2j}$-WT and *Tyr*$^{c\text{-}2j}$- *mMCP4*$^{-/-}$ mice.

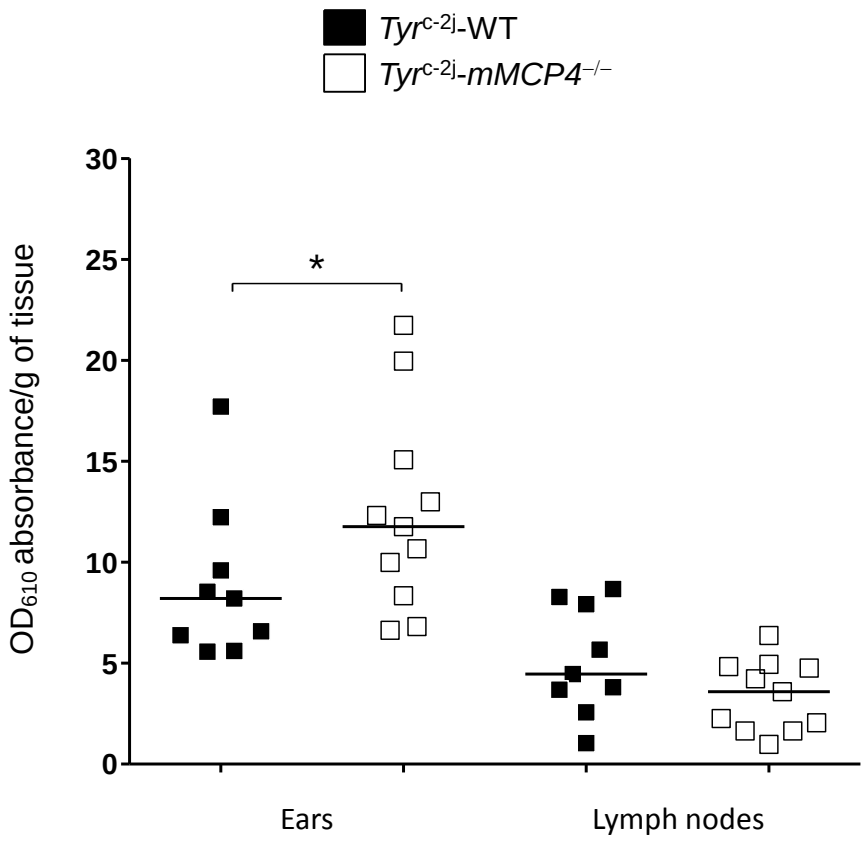
Tyrc-2j-WT
Tyrc-2j-mMCP4−/−
30
25
20
15
10
5
0
OD610 absorbance/g of tissue
*
Ears
Lymph nodes

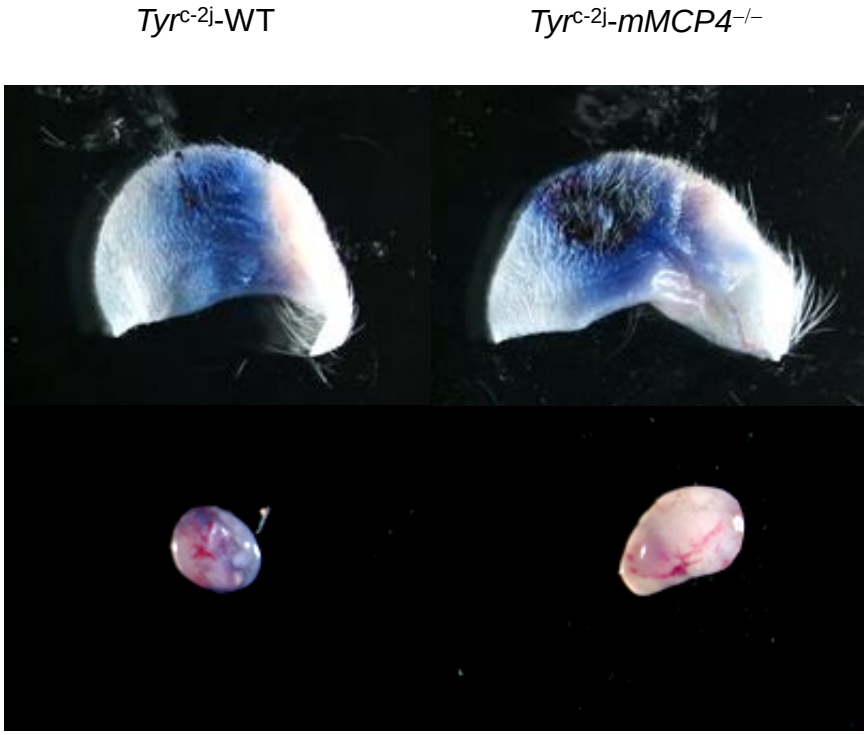
Tyrc-2j-WT
Tyrc-2j-mMCP4−/−

At baseline, no statistically significant differences between genotypes were observed in any of the immune cell populations analysed. Following UVB irradiation, an influx of all cell populations analysed was observed (**Figure 5.6**). No difference was observed between genotypes in most cell populations analysed except a slight increase in F4/80^{-}CD11b^{+}Gr-1^{+} myeloid-derived suppressor cells (**Figure 5.6g**; refer to **Supplementary Figure S5.1** for flow plots). These data suggest that the absence of mMCP4 does not have a significant influence on regulating the trafficking of distinct immune cell populations.

5.2.6 mMCP4 mediates UVB-induced hyperproliferation of lymphatic endothelial cells

The enlargement of vessels can occur through two different mechanisms; one involves stretching of the lumen walls and the other is via the proliferation of endothelial cells[455]. To assess if the vessel distension we observed is due to hyperproliferative endothelial cells, mouse-derived endothelial cells were cultured with supernatant of BMCMCs that are stimulated with ear lysates of UVB-treated *Tyr*$^{c\text{-}2j}$-WT and *Tyr*$^{c\text{-}2j}$-*mMCP4*$^{-/-}$ mice (5 exposures) and their proliferation was measured by MTS assay. However, no significant difference in proliferation status was observed in these endothelial cells (**Figure 5.7a**). We also assessed the proliferation of lymphatic vessels by staining frozen cryosections with the proliferation marker Ki67. Quantification analysis showed that after 5 exposures of chronic UVB, there were significantly more Ki67^{+} cells/enlarged lymphatic vessel in *Tyr*$^{c\text{-}2j}$-*mMCP4*$^{-/-}$ mice compared to *Tyr*$^{c\text{-}2j}$-WT mice (**Figure 5.7b**). These data suggest that increased proliferation of lymphatic endothelial cells results in the lymphatic vessel enlargement observed in mMCP4-deficient skin following UVB irradiation. To further to confirm this hypothesis, it will be ideal to examine whether blocking UVB-induced proliferation of LECs can induce failure of lymphatic vessel enlargement.

5.2.7 mMCP4 regulates the neuropeptide vasoactive intestinal peptide, and potentially VEGF-A, but not VEGF-D

As described earlier in this chapter, aberrant angiogenesis and lymphangiogenesis following exposure to chronic UVB irradiation were associated with the loss of mMCP4. In addition, hyperproliferation of endothelial cells was observed in the ears of UVB-treated *Tyr*$^{c\text{-}2j}$-*mMCP4*$^{-/-}$ mice, suggesting that there is a disrupted balance of positive

Figure 5.6 Characterisation of cell populations in the ears of *Tyr*$^{c\text{-}2j}$-WT and *Tyr*$^{c\text{-}2j}$-*mMCP4*$^{-/-}$ mice following chronic UVB irradiation. (A) Following chronic UVB irradiation (25 exposures), cell populations were extracted from the ears of *Tyr*$^{c\text{-}2j}$-WT and *Tyr*$^{c\text{-}2j}$-*mMCP4*$^{-/-}$ mice by liberase digestion. Following extraction, specific cell populations were assessed from both genotypes; **(A)** CD45^{+} immune cells, **(B)** CD4^{+} T cells, **(C)** CD8^{+} T cells, **(D)** B220^{+} B cells, **(E)** NK1.1^{+} NKT cells, **(F)** CD25^{+}FoxP3^{+} T regulatory cells, **(G)** Gr-1^{+} granulocytes, **(H)** F4/80^{+} macrophages or **(I)** F4/80^{+}CD11b^{+}Gr-1^{-} activated macrophages and **(J)** CD11b^{+}Gr-1^{+}F4/80^{-} neutrophil and MDSCs. Data from 2 independent experiments are represented as median (n=6-11 mice/genotype).

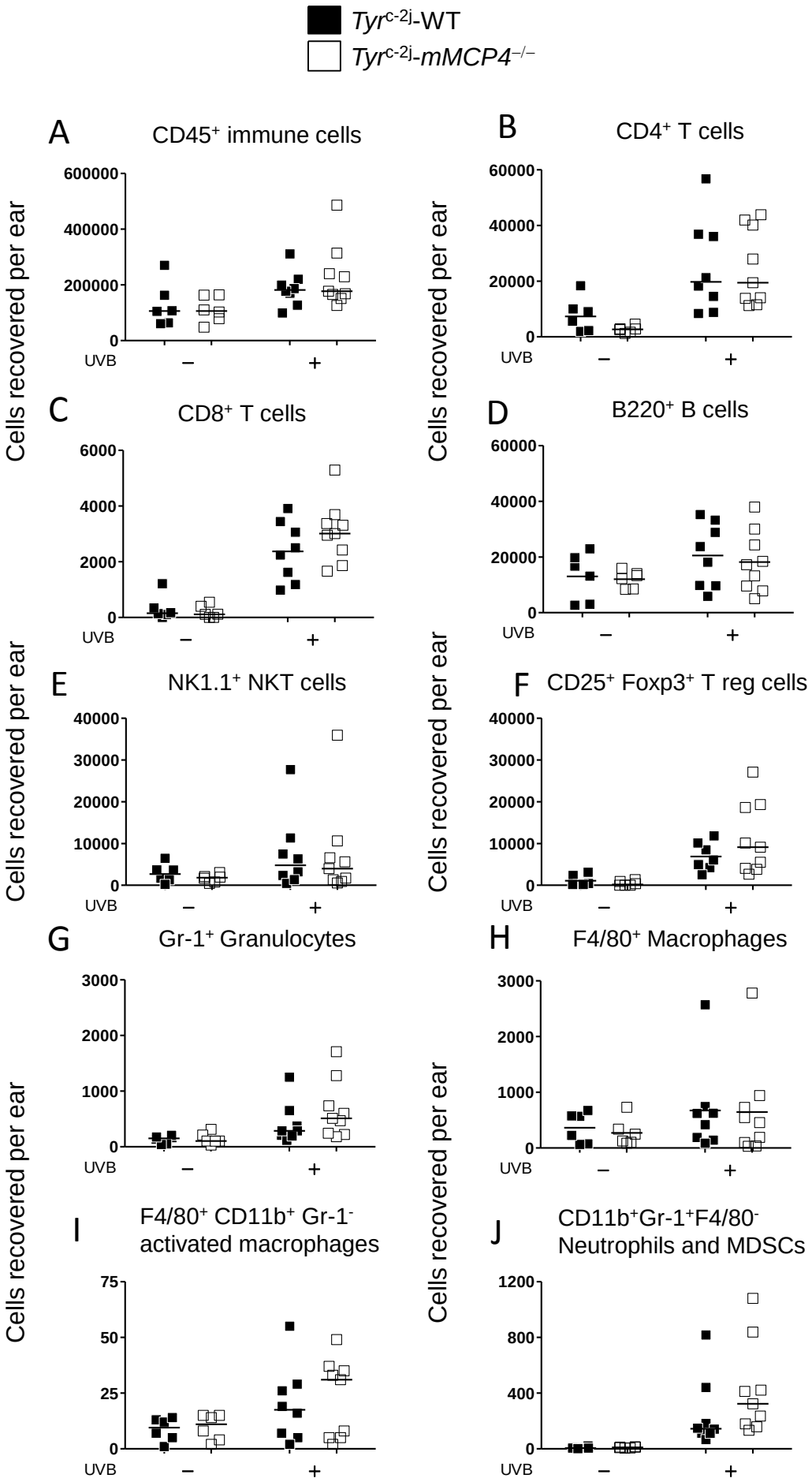
Tyrc-2j-WT
Tyrc-2j-mMCP4−/−
A
CD45+ immune cells
B
CD4+ T cells
C
CD8+ T cells
D
B220+ B cells
E
NK1.1+ NKT cells
F
CD25+ Foxp3+ T reg cells
G
Gr-1+ Granulocytes
H
F4/80+ Macrophages
I
F4/80+ CD11b+ Gr-1- activated macrophages
J
CD11b+Gr-1+F4/80- Neutrophils and MDSCs
Cells recovered per ear
UVB
–
+
600000
400000
200000
0
60000
40000
20000
6000
4000
2000
30000
10000
3000
1000
75
50
25
1200
800
400

Figure 5.7 Absence of mMCP4 causes increasing number of Ki67^{+} lymphatic endothelial cells following UVB irradiation. (A) WT and *mMCP4*$^{-/-}$ BMCMCs derived from non-pigmented B6-*Tyr*$^{c\text{-}2j}$ mice were co-cultured and activated by UVB-treated ear lysates from *Tyr*$^{c\text{-}2j}$-WT and *Tyr*$^{c\text{-}2j}$-*mMCP4*$^{-/-}$ mice (5 exposures). Supernatants were collected and added to mouse lymphatic endothelial cells (LEC)s for a period of 6 h. Following incubation, proliferation status of mLECs was assessed by MTS assay. Data from 1 experiment is represented as mean + SEM. **(B)** Proliferation status of lymphatic endothelial cells was assessed by immunofluorescence staining of UVB-treated cryosections from UVB-treated *Tyr*$^{c\text{-}2j}$-WT and *Tyr*$^{c\text{-}2j}$-*mMCP4*$^{-/-}$ mice (5 exposures). Sections were stained with Ki67 proliferation marker and counterstained with CD31, and CCL21 to detect lymphatic vessels. Data from 1 experiment are represented as median. Mann Whitney U test *$p<0.05$. **(C)** Representative confocal images taken from 1 experiment.

A

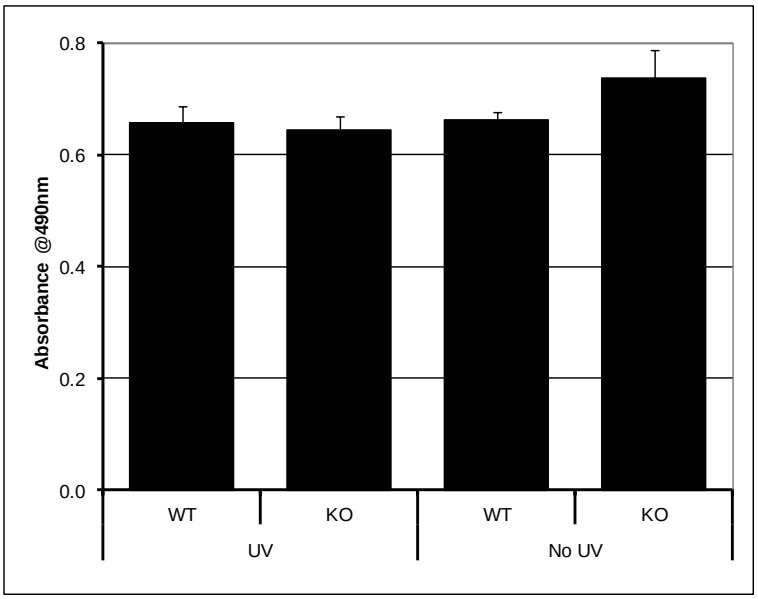
0.8
0.6
0.4
0.2
0.0
Absorbance @490nm
WT
KO
WT
KO
UV
No UV

B

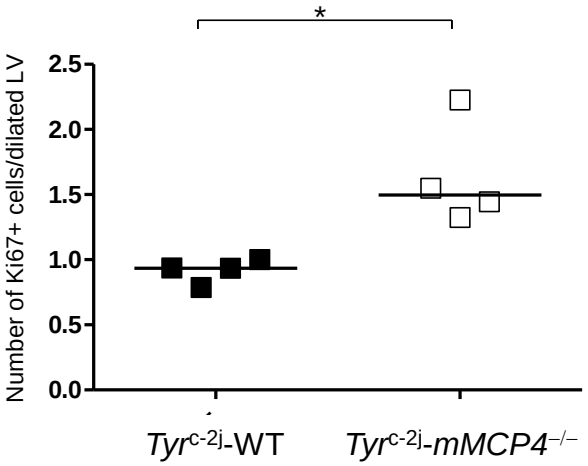
*
2.5
2.0
1.5
1.0
0.5
0.0
Number of Ki67+ cells/dilated LV
Tyrc-2j-WT
Tyrc-2j-mMCP4−/−

C

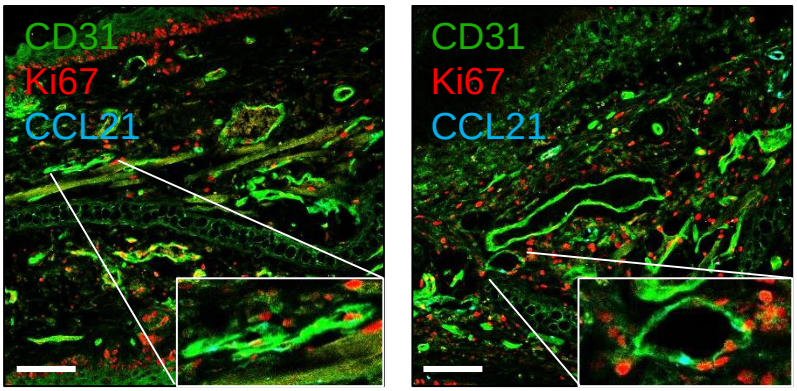
Tyrc-2j-WT
Tyrc-2j-mMCP4−/−
CD31
Ki67
CCL21
CD31
Ki67
CCL21

and negative mediators of vascular growth in these mice. The best characterised positive regulators of angiogenesis and lymphangiogenesis are VEGF-A, VEGF-C and VEGF-D. Hence we investigated the possibility that VEGF-A and VEGF-D are target substrates of mMCP4. VEGF-C is typically known to be involved in this pathway but based on our initial findings, no changes or differences in VEGF-C was observed in the absence of mMCP4 (data not shown).

The levels of mRNA expression of VEGF-A and VEGF-D were investigated as these mediators are known to promote vascular proliferation and dilation under inflammatory conditions. We assessed mRNA expression of VEGF-A and VEGF-D from UVB-treated ear lysates from WT, *Kit*$^{W/W\text{-}v}$, WT BMCMCs→WBB6F$_1$–*Kit*$^{W/W\text{-}v}$ and *mMCP4*$^{-/-}$ BMCMCs→WBB6F$_1$–*Kit*$^{W/W\text{-}v}$ mice and found that throughout all stages of the irradiation regime, the level of VEGF-A and –D mRNA expression remained unchanged, and no change was observed between genotypes (**Figure 5.8a, b**). We further investigated the level of VEGF-A and VEGF-D protein in ear lysates by ELISA. Based on ELISA analysis, VEGF-A levels increased in all genotypes except for WT over 25 exposures. Interestingly, at 5 exposures, *mMCP4*$^{-/-}$ BMCMCs→WBB6F$_1$–*Kit*$^{W/W\text{-}v}$ mice appeared to have significantly higher levels of VEGF-A compared to not only WT BMCMCs→WBB6F$_1$–*Kit*$^{W/W\text{-}v}$ but also WBB6F$_1$–*Kit*$^{W/W\text{-}v}$ mice (**Figure 5.8c**). In comparison to VEGF-A, VEGF-D levels were higher at baseline in all genotypes compared to UVB-treated mice over 25 exposures. Notably at 5 exposures, VEGF-D levels were significantly lower in *mMCP4*$^{-/-}$ BMCMCs→WBB6F$_1$–*Kit*$^{W/W\text{-}v}$ mice compared to WT BMCMCs→WBB6F$_1$–*Kit*$^{W/W\text{-}v}$ mice (**Figure 5.8d**).

Similarly, in the pigmented B6-WT and B6-*mMCP4*$^{-/-}$ mice, no difference in mRNA expression of VEGF-A or VEGF-D was observed throughout the 70 exposures, except a higher level of VEGF-D mRNA expression in B6-*mMCP4*$^{-/-}$ mice at baseline (**Figure 5.9a, b**). At the protein level, there is an overall increase of VEGF-A throughout 70 exposures in both genotypes, whereas VEGF-D peaked at 5 exposures which eventually returned to basal levels at the end of 70 exposures. Similarly no differences were observed between genotypes in either VEGF-A or –D as shown by ELISA (**Figure 5.9c, d**).

Similar to the other two models, no difference in mRNA expression of VEGF-A or VEGF-D was observed between genotypes (**Figure 5.10a, b**). At the protein level, there was an overall increase in VEGF-A observed in both genotypes throughout the UVB

Figure 5.8 mMCP4 may have a potential role in regulating VEGF-A protein in engrafted-*Kit*$^{W/W\text{-}v}$ mice following UVB irradiation. (A) Following UVB irradiation (5, 12 and 25 exposures), *vegfa* and **(B)** *vegfd* mRNA expression was assessed by qRT-PCR from ear lysates from WT, *Kit*$^{W/W\text{-}v}$, WT BMCMCs→*Kit*$^{W/W\text{-}v}$ and *mMCP4*$^{-/-}$ BMCMCs→*Kit*$^{W/W\text{-}v}$. Data from 1 experiment and represented as mean (normalised to *GAPDH*) + SEM. **(C)** VEGF-A and **(D)** VEGF-D protein was assessed by ELISA from ear lysates derived from UVB-treated and no UVB-treated WT, *Kit*$^{W/W\text{-}v}$, WT BMCMCs→*Kit*$^{W/W\text{-}v}$ and *mMCP4*$^{-/-}$ BMCMCs→*Kit*$^{W/W\text{-}v}$. Data from 1 experiment and represented as mean (normalised to total protein) + SEM. Student's unpaired T-test, *p<0.05; compared to no UVB control, $^{\#}p<0.05$, $^{\#\#}p<0.01$, $^{\#\#\#}p<0.001$

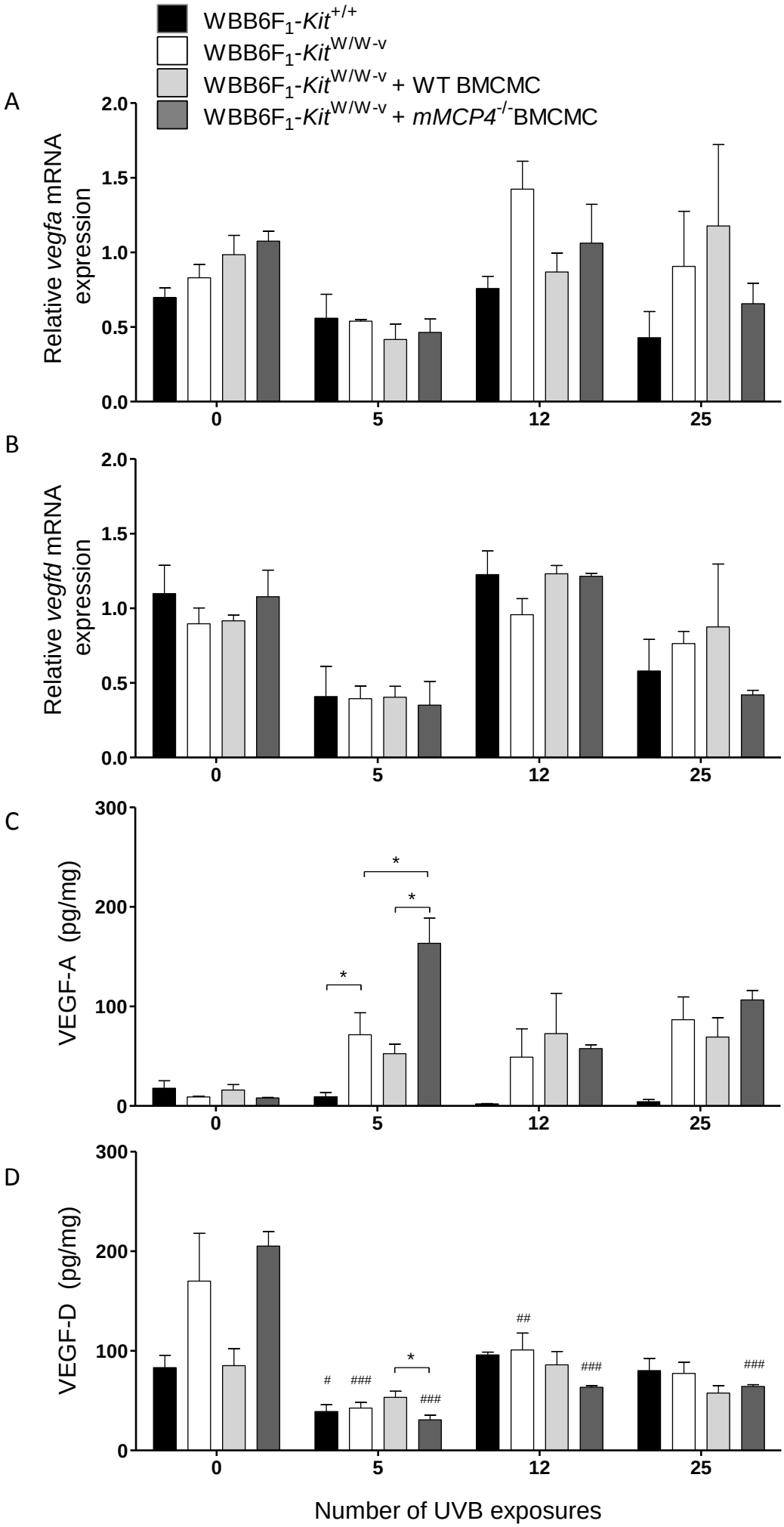
WBB6F1-Kit+/+
WBB6F1-KitW/W-v
WBB6F1-KitW/W-v + WT BMCMC
WBB6F1-KitW/W-v + mMCP4-/- BMCMC
A
Relative vegfa mRNA expression
2.0
1.5
1.0
0.5
0.0
0
5
12
25
B
Relative vegfd mRNA expression
2.0
1.5
1.0
0.5
0.0
0
5
12
25
C
VEGF-A (pg/mg)
300
200
100
0
*
*
*
0
5
12
25
D
VEGF-D (pg/mg)
300
200
100
0
#
###
*
###
##
###
###
0
5
12
25
Number of UVB exposures

Figure 5.9 The absence of mMCP4 does not influence relative mRNA expression or protein expression of VEGF-A or VEGF-D in pigmented B6 mice. (A) *vegfa* and **(B)** *vegfd* mRNA expression was assessed by qRT-PCR from no UVB-treated and UVB-treated ear lysates from B6-WT and B6-*mMCP4*$^{-/-}$ mice following an extended chronic UVB irradiation regime (5, 12, 25 and 70 exposures). Data from 1 experiment and represented as mean (normalised to *GAPDH*) + SEM. After an extended chronic UVB regime, **(C)** VEGF-A and **(D)** VEGF-D protein was assessed by ELISA from no UVB-treated and UVB-treated ear lysates from B6-WT and B6-*mMCP4*$^{-/-}$ mice. Data from 1 experiment are represented as mean (normalised to total protein) + SEM.

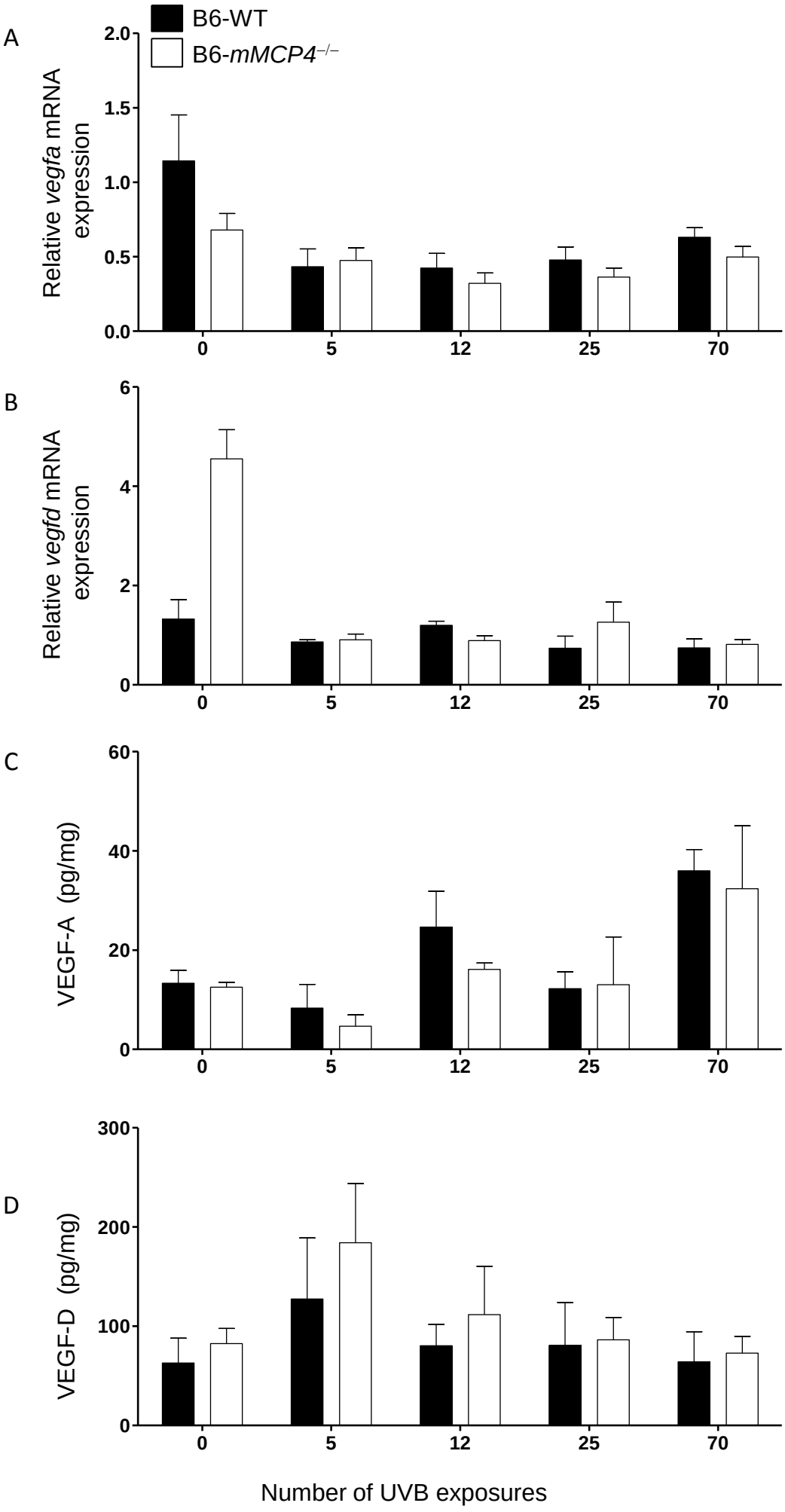
A
B6-WT
B6-mMCP4−/−
Relative vegfa mRNA expression
2.0
1.5
1.0
0.5
0.0
0
5
12
25
70
B
Relative vegfd mRNA expression
6
4
2
0
0
5
12
25
70
C
VEGF-A (pg/mg)
60
40
20
0
0
5
12
25
70
D
VEGF-D (pg/mg)
300
200
100
0
0
5
12
25
70
Number of UVB exposures

Figure 5.10 The absence of mMCP4 does not influence relative mRNA expression or protein expression of VEGF-A or VEGF-D in non-pigmented B6-*Tyr*$^{c\text{-}2j}$ mice. (A) *vegfa* and (B) *vegfd* mRNA expression was assessed by qRT-PCR from no UVB-treated and UVB-treated ear lysates from *Tyr*$^{c\text{-}2j}$-WT and *Tyr*$^{c\text{-}2j}$-*mMCP4*$^{-/-}$ mice following 5 and 25 exposures. Data from 1 experiment and represented as mean (normalised to *GAPDH*) + SEM. After exposing mice to chronic UVB, **(C)** VEGF-A and **(D)** VEGF-D protein was assessed by ELISA from no UVB-treated and UVB-treated ear lysates from *Tyr*$^{c\text{-}2j}$-WT and *Tyr*$^{c\text{-}2j}$-*mMCP4*$^{-/-}$ mice. Data from 1 experiment are represented as mean (normalised to total protein) + SEM.

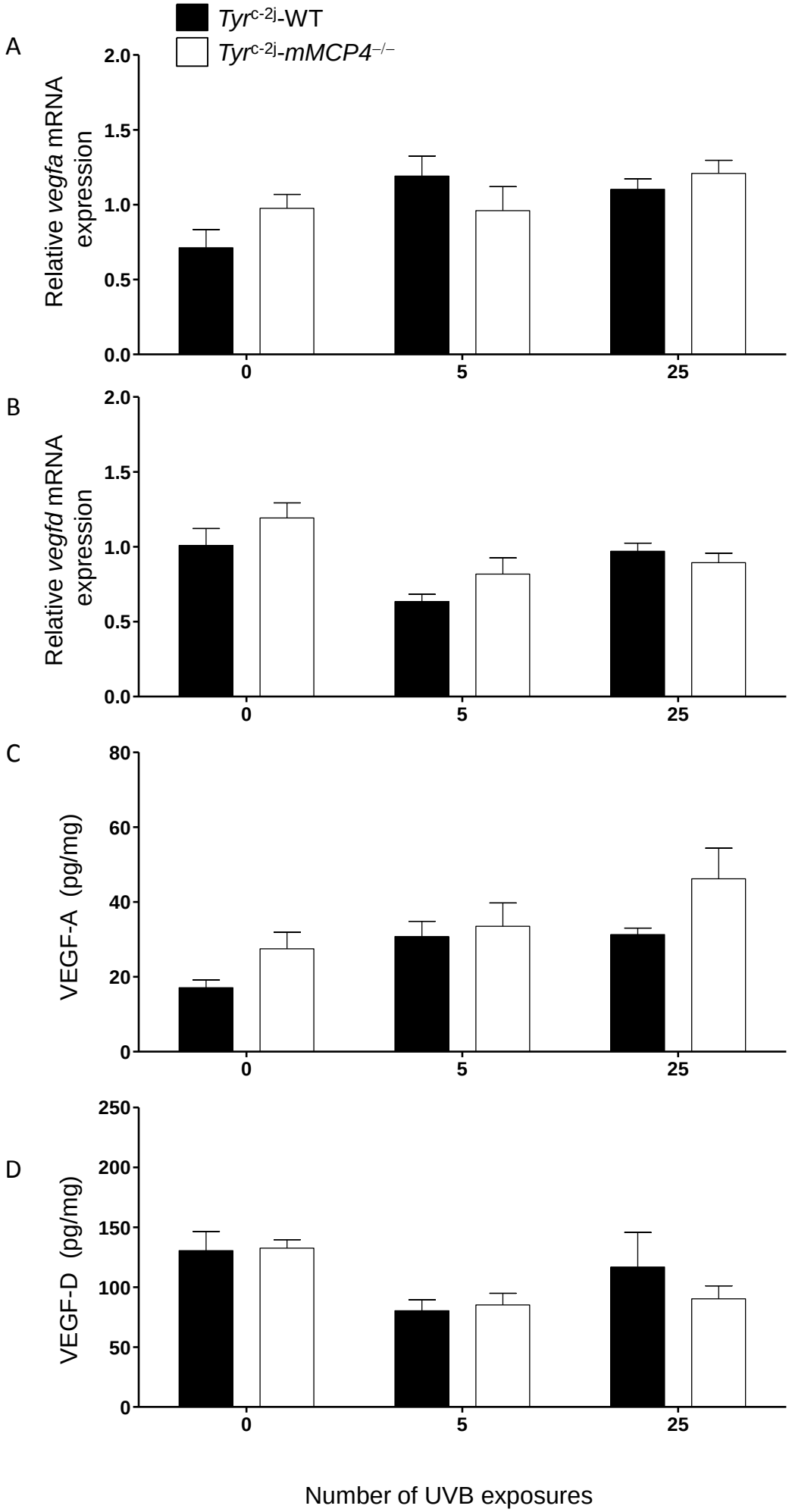
Tyrc-2j-WT
Tyrc-2j-mMCP4−/−
A
Relative vegfa mRNA expression
2.0
1.5
1.0
0.5
0.0
0
5
25
B
Relative vegfd mRNA expression
2.0
1.5
1.0
0.5
0.0
0
5
25
C
VEGF-A (pg/mg)
80
60
40
20
0
0
5
25
D
VEGF-D (pg/mg)
250
200
150
100
50
0
0
5
25
Number of UVB exposures

irradiation regime but not VEGF-D; and no difference was observed between genotypes. Interestingly, a slight increase (not significant) in VEGF-A was observed by ELISA in *Tyr*$^{c\text{-}2j}$-*mMCP4*$^{-/-}$ mice (**Figure 5.10c, d**). Altogether, the data suggests that mMCP4 may potentially target VEGF-A, but not VEGF-D.

mMCP4 has previously been shown to target and cleave to degrade the neuropeptide vasoactive intestinal peptide (VIP), which has been reported to cause toxicity especially at high concentration in mice[378]. Among other functions, VIP is also known to have a plethora of biological functions including promoting vasodilation, smooth muscle activity, epithelial cell secretion, regulating blood flow and even activating MCs[372,385,456]. Notably, VIP is also known to be abundant in the skin. In response to chronic UVB, the level of VIP was significantly increased in *Tyr*$^{c\text{-}2j}$-*mMCP4*$^{-/-}$ mice after 5 UVB exposures, but it did not further increase following 12 and 25 exposures. On the contrary, the level of VIP in *Tyr*$^{c\text{-}2j}$-WT mice remained unchanged. When comparing between *Tyr*$^{c\text{-}2j}$-WT and *Tyr*$^{c\text{-}2j}$-*mMCP4*$^{-/-}$ mice, at baseline there were no differences observed between genotypes. However, in response to chronic UVB, the level of VIP in *Tyr*$^{c\text{-}2j}$-*mMCP4*$^{-/-}$ mice was approximately 2.5-fold higher than *Tyr*$^{c\text{-}2j}$-WT mice across all exposures examined (**Figure 5.11**).

5.3 Discussion

Acute and chronic doses of UVB have been reported to induce pronounced angiogenesis of the skin but chronic UVB exposure is thought to cause a reduction of both blood and lymphatic vessels as well as ECM degradation and elastosis[353,356]. The data we showed utilising engrafted-*Kit*$^{W/W\text{-}v}$ mice demonstrates that in response to progressive chronic UVB exposure, there is a continuation of skin angiogenesis as observed by an overall increase in the number of total and dilated blood vessels. Interestingly, a significant increase in the number of total and dilated blood vessels could be seen in the absence of MCs and mMCP4 after 12 and 25 exposures. This suggests that MCs and mMCP4 are involved in regulating UVB-induced angiogenesis in this particular model, a finding supported by previous studies showing that MCs contribute to the angiogenic response by releasing VEGF-A and contributing to the release of ECM-bound angiogenic factors[357,457,458]. However, a study by Schweintzger *et al*, demonstrate that UVB-induced dermal angiogenesis was MC independent[359].

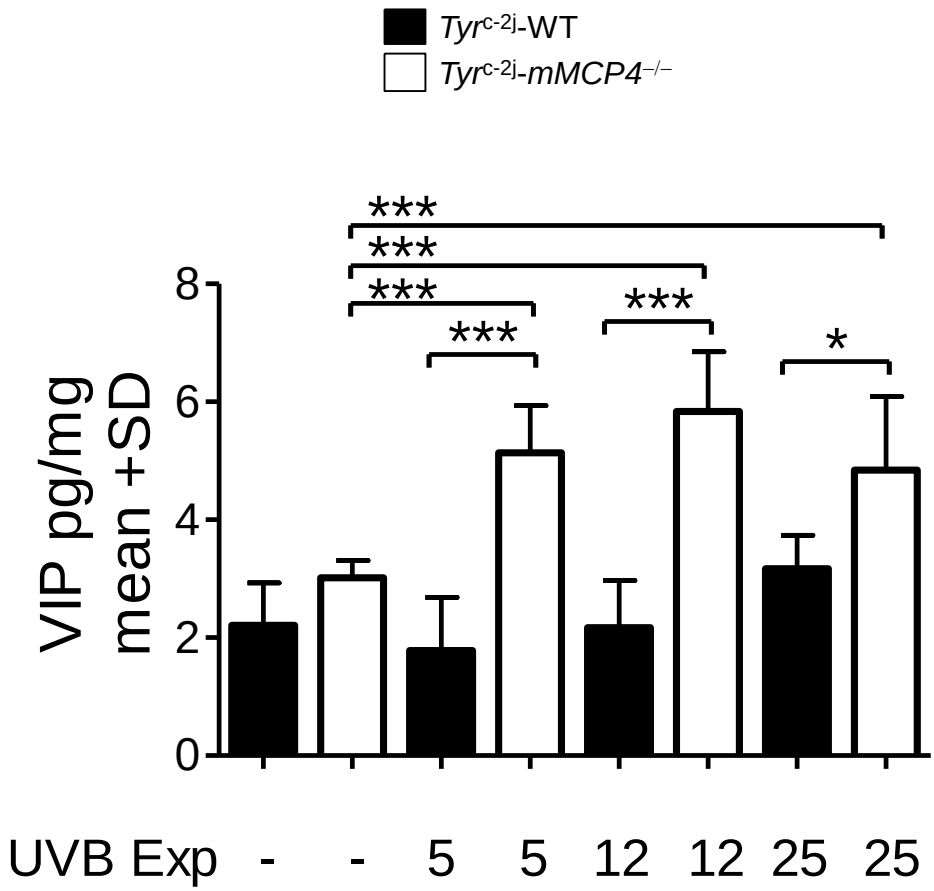

Figure 5.11 The absence of mMCP4 results in significantly greater levels of VIP in non-pigmented B6-*Tyr*$^{c\text{-}2j}$ mice following chronic UVB exposure. VIP protein was assessed by ELISA from no UVB-treated and UVB-treated (5, 12 and 25 exposures) ear lysates from *Tyr*$^{c\text{-}2j}$-WT and *Tyr*$^{c\text{-}2j}$-*mMCP4*$^{-/-}$ mice. Data from 1-3 experiments (n=5-16 mice/genotype) and represented as mean (normalised to total protein) + SD. Student's unpaired T-test, $^{*}p<0.05$, $^{***}p<0.001$

Based on ELISA data, the level of VEGF-A in *mMCP4*$^{-/-}$ BMCMCs→WBB6F$_1$–*Kit*$^{W/W\text{-}v}$ mice was significantly greater compared to WT BMCMCs→WBB6F$_1$–*Kit*$^{W/W\text{-}v}$ mice after 5 exposures of UVB. This may be correlated with the significantly higher number of total and dilated blood vessels at later time points. Interestingly, *Kit*$^{W/W\text{-}v}$ mice showed significantly lower levels of VEGF-A compared to *mMCP4*$^{-/-}$ BMCMCs→WBB6F$_1$–*Kit*$^{W/W\text{-}v}$ mice. Although MCs are the only source of mMCP4, we would expect a similar level of VEGF-A in both genotypes. Recent findings suggest that the loss of mMCP4 is associated with increased activity of MC-derived tryptases[175]. It is also known that tryptases can promote the release of VEGF-A[459], hence this could explain why we observed such a significant increase in VEGF-A in *mMCP4*$^{-/-}$ BMCMCs→WBB6F$_1$–*Kit*$^{W/W\text{-}v}$ mice. This also further confirms that MCs are indeed major contributors for the release of VEGF-A. What is also worth noticing is that this drastic difference in the level of VEGF-A between *Kit*$^{W/W\text{-}v}$ and *mMCP4*$^{-/-}$ BMCMCs→WBB6F$_1$–*Kit*$^{W/W\text{-}v}$ mice were not translated into a difference in blood vasculature pathology. This lack of difference could be associated with the release of angiogenic factors such as VEGF-A, IL-8 and FGF2 derived from other cell populations[410], such as macrophages, to compensate for the loss of MC-derived VEGF-A. Moreover, interestingly, we do not see such a high level of VEGF-A in the WT BMCMCs→WBB6F$_1$–*Kit*$^{W/W\text{-}v}$ mice compared to *mMCP4*$^{-/-}$ BMCMCs→WBB6F$_1$–*Kit*$^{W/W\text{-}v}$ mice. This could potentially be due to the specific targeting of VEGF-A by mMCP4.

The mechanistic role of how the loss of mMCP4 in engrafted-*Kit*$^{W/W\text{-}v}$ mice is contributing to the aberrant angiogenesis is not clear. It is possible that VEGF-A could be a negatively regulated substrate of mMCP4 at the early stages of chronic UVB irradiation, but this may not be the case as the levels of VEGF-A did not differ between all groups of mice later than 5 exposures.

Previous studies have shown the microenvironmental concentration of VEGF-A but not the total level can determine a threshold between normal and aberrant angiogenesis. This finding suggests a high concentration of VEGF-A can influence how blood vessels respond[460]. Studies have also suggested that expression of the antiangiogenic factor TSP-1 is dependent on the tumour suppressor gene, *p53*[461]. Since UVB exposure results in mutation of *p53*, which is the initiating factor for skin tumourigenesis[462,463], it is likely that following UVB irradiation, *p53* mutation leads to a downregulation of TSP-1,

causing an imbalance in the regulation of angiogenesis and generation of a pro-angiogenic environment. As a result of this imbalance and the absence of mMCP4, it is possible that the downregulation of TSP-1 may result in a lowered threshold for VEGF-A to promote aberrant angiogenesis. This could explain why we did see changes in blood vessels even though we did not see a consistent increase of VEGF-A concentration in the ears of *mMCP4*$^{-/-}$ BMCMCs→WBB6F$_1$–*Kit*$^{W/W\text{-}v}$ mice over 25 exposures. However, it would be beneficial to determine the specific time point when *p53* mutations take place in order to further clarify this hypothesis. It would also be worthwhile to determine whether or not the changes we observed in the lymphatic vasculature were a result of the increasing VEGF-A levels in the absence of mMCP4, as VEGF-A has been reported to induce inflammatory lymphangiogenesis[353].

Our understanding of lymphangiogenesis is still limited in comparison to our knowledge of angiogenesis. It is known that the presence of tumour cells in sentinel lymph nodes is associated with poor patient outcome[429,464,465]. This is primarily due to the presence of lymphatic vessels and their ability to efficiently transport and disseminate primary tumour cells to secondary organs, a process known as metastasis. This process typically comes about through lymphangiogenesis and enlargement of initial lymphatic vessels. Both of these processes aid the transport of tumour cells to sentinel nodes[466,467]. Lymphangiogenesis in the tumour microenvironment is primarily driven by the growth factors VEGF-C and VEGF-D, acting via VEGFR3[468-470]. Consistently, blocking VEGFR3 signalling on VEGFR3 expressing lymphatic vessels has been shown reduce the spread of tumour cells to secondary organs[466,470,471]. VEGFR-2 has also been suggested to induce inflammatory lymphangiogenesis through the angiogenic factor VEGF-A in response to UVB exposure[346,352].

Our findings suggest that in the absence of MCs and mMCP4, UVB-treated *Kit*$^{W/W\text{-}v}$ and *mMCP4*$^{-/-}$ BMCMCs→WBB6F$_1$–*Kit*$^{W/W\text{-}v}$ mice show significantly higher levels of total and dilated lymphatic vessels which implies that MCs and mMCP4 do appear to have a role in regulating lymphangiogenesis. Interestingly, lack of changes in VEGF-D at mRNA and protein levels suggest that it is not the rate limiting factor required to promote the differences we observed in our engrafted mice. This finding supports previous studies which proposed that both VEGF-C and VEGF-D are not upregulated and do not promote lymphangiogenesis in response to UVB irradiation[353]. Instead, up-regulation of VEGF-A

was suggested to be the crucial factor in promoting higher numbers of lymphatic vessels. Our findings suggest this to be partially true as *mMCP4*$^{-/-}$ BMCMCs→WBB6F$_1$–*Kit*$^{W/W-v}$ mice exhibited higher levels of VEGF-A compared to WT BMCMCs→WBB6F$_1$–*Kit*$^{W/W-v}$ mice after 5 exposures. However, it is interesting to observe that there is no difference between *mMCP4*$^{-/-}$ BMCMCs→WBB6F$_1$–*Kit*$^{W/W-v}$ and WT BMCMCs→WBB6F$_1$–*Kit*$^{W/W-v}$ mice after 12 and 25 exposures, but it would again be worthwhile to assess the influence caused by the imbalance of pro- (VEGF-A) and anti-angiogenic factors (TSP-1), as stated above. Exposure to UVB is well known to induce the production of many other growth factors that do not depend on VEGFR3 signalling, including PDGF[469], IL-8[441] and bFGF[472]. MMP2, which is another known target of mMCP4, has also been suggested to govern lymphatic vessel growth and development. Although MMP-2 can be cleaved by other proteases, it is possible that the lack of mMCP4 could influence MMP-2's ability to act as an interstitial collagenase and regulate the lymphatic vasculature[473]. Hence, it would be wise to assess other mediators that are known to promote blood and lymphatic growth. It is also noteworthy to point out that these differences in blood and lymphatic vessels were not due to differences in the number of MCs injected into each mouse, as there was no significant differences in the number of MCs in the local area in all groups of mice (**Chapter 4, Figure 4.4**).

As previously elucidated, in order to ensure that the pathology we observed in *Kit*$^{W/W-v}$ and *mMCP4*$^{-/-}$ BMCMCs→WBB6F$_1$–*Kit*$^{W/W-v}$ mice was due to the absence of MC and mMCP4 but not because of other phenotypic abnormalities, pigmented B6-*mMCP4*$^{-/-}$ mice were utilised. No differences in the number or morphology of blood and lymphatic vessels were observed prior to UVB irradiation. Following chronic UVB irradiation we again saw very little difference in the number of total or dilated blood vessels or lumen area between genotypes over 70 exposures.

Although we could not see any differences in the number of lymphatic vessels, we did see changes in the number of dilated lymphatic vessels from 25 exposures onwards. Most importantly, the lumen area was significantly larger in B6-*mMCP4*$^{-/-}$ mice compared to B6-WT mice after 70 exposures. This again suggests that mMCP4 may have a role in regulating lymphatic vessel architecture in response to chronic UVB.

We again assessed the level of VEGF-A and VEGF-D at both mRNA and protein levels in pigmented mice. An overall increase in VEGF-A protein was observed in both

genotypes over 70 exposures which correlates with an overall increase in the number of blood vessels and lymphatic vessels we observed. Although no differences were observed between B6-WT and B6-*mMCP4*$^{-/-}$ mice at any time point, this does suggest that VEGF-A or VEGF-D may not be the rate limiting factor that are promoting the differences in lymphatic vessel vasculature observed in both pigmented B6-*mMCP4*$^{-/-}$, and WBB6F$_1$–*Kit*$^{W/W\text{-}v}$ mouse models.

In comparison to engrafted–*Kit*$^{W/W\text{-}v}$ mice, where we observed drastic changes in the blood and lymphatic vasculature within the first 5 exposures of chronic UVB, it took an astonishing 70 exposures before any differences manifested in the vasculature in the pigmented B6-*mMCP4*$^{-/-}$. This is most likely due to the presence of pigment which shielded against the deleterious effects of UVB irradiation. Due to the protective properties of pigment, individuals with darker skin are less likely to have a sensitive UVB-induced angiogenic response, compared to indivduals with fairer skin. This is mainly through the release of the angiogenic factor fibromodullin which can stimulate endothelial cell proliferation through SMAD1, SMAD2, VEGF and TGFβ both *in vitro* and *in vivo*[474,475]. This could explain the lack VEGF-A production in WBB6F1-*Kit*$^{+/+}$ (WT, which are pigmented) mice compared to non-pigmented *Kit*$^{W/W\text{-}v}$ mice. Nevertheless, it is still encouraging to see that mMCP4 continues to be involved in the lymphangiogenic response following UVB irradiation.

Due to the presence of pigment, the B6-*mMCP4*$^{-/-}$ mice may not be the most beneficial or optimal model considering the reduced angiogenic and lymphangiogenic response observed in these mice.

Hence, non-pigmented *Tyr*$^{c\text{-}2j}$-*mMCP4*$^{-/-}$ mice were utilised to further investigate changes in the vasculature following UVB irradiation. In addition to assessing the changes in the vasculature 24 h post final irradiation, an earlier time point (3 h post final irradiation) was also assessed to investigate any events we have may have missed out. No differences were observed between genotypes at 3 h post irradiation. However notably, the lumen areas were significantly increased in the absence of mMCP4 at 5 and 25 exposures. This significant change could be a result of exacerbated inflammation in the ears of *Tyr*$^{c\text{-}2j}$-*mMCP4*$^{-/-}$ mice causing an influx of interstitial fluid which ultimately leads to an increase in pressure and subsequent enlargement of lymphatic vessels. Whilst we did not observe any changes at 12 exposures in the lumen area between genotypes; it

could be due to a resolution of inflammation at that particular time point. MC-IL-10 could be acting as a potential immunomodulator and dampening or even resolving the inflammatory response at 12 exposures[8], additionally this could potentially due to photohardening. Overall, it does seem that there are very little changes in the vasculature immediately following the chronic UVB irradiation regime. However, our data suggests in the absence of mMCP4 there may be a heightened level of inflammation.

On the other hand, significant changes were observed 24 h post UVB irradiation which included a significant increase in the number of total and dilated lymphatic vessels as well as the lumen area of dilated lymphatic vessels in *Tyr*$^{c\text{-}2j}$-*mMCP4*$^{-/-}$ mice compared to *Tyr*$^{c\text{-}2j}$-WT mice. In regards to the blood vasculature, although not significant, there is still a trend of a higher number of total and dilated blood vessels. This may suggest that mMCP4 could be involved in the blood vasculature but the effect could be compensated by other mechanisms. These findings provide further indication that mMCP4 does appear to have a role in regulating the lymphangiogenic response but also a potential role in angiogenic response in a setting of chronic UVB irradiation.

What was also intriguing was the significantly enlarged lymphatic vessels after 25 exposures. Typically, lymphatic vessels play an important in inflammatory conditions, where they regulate the inflammatory response by transporting extravasated fluid, inflammatory cell infiltrate and antigen-presenting cells from the site of inflammation to draining lymph nodes. This process normally occurs through signalling of VEGFR3, typically activated by binding of specific ligands VEGF-C and VEGF-D. Interestingly, Karnezis *et al*. recently showed that prostaglandins E2 and I2 are also capable of regulating lymphatic vessel dilation and promoting drainage of cell populations towards sentinel lymph nodes[450]. Based on our findings, the loss of mMCP4, particularly in our B6-*mMCP4*$^{-/-}$ and *Tyr*$^{c\text{-}2j}$-*mMCP4*$^{-/-}$ mice, resulted in significantly enlarged lymphatic vessels compared to WT counterparts. As we investigated the functional capabilities of lymphatic vessels by Evan's blue injections, in the absence of mMCP4, the lymphatic vessels appeared to be more dysfunctional as more Evan's blue dye was retained in the ears and less detected in the lymph nodes of UVB-treated *Tyr*$^{c\text{-}2j}$-*mMCP4*$^{-/-}$ mice, compared to *Tyr*$^{c\text{-}2j}$-WT mice. This suggests that the lymphatic vessels in the ears of *Tyr*$^{c\text{-}2j}$-WT mice are more efficient in draining UVB-induced fluid and inflammatory infiltrates. Based on the literature one possibility for this inefficient draining of lymphatic vessels

could be due to the overabundance of the neuropeptide and immunomodulator VIP. A study by von der Weid *et al*, has shown that VIP can alter lymphatic pumping by decreasing the frequency of lymphatic contractions and hyperpolarising the lymphatic muscle membrane potential in a concentration-dependent manner. As a result, VIP could compromise lymph drainage, oedema resolution and trafficking of immune cells to the draining lymph nodes[378,456]. Indeed, our data also shows that although no differences in the level of VIP was observed in the absence of mMCP4 at baseline, which suggests VIP is not targeted by mMCP4 at physiological conditions, but when challenged by chronic UVB, higher levels of VIP were detected only in *Tyr*$^{c\text{-}2j}$-*mMCP4*$^{-/-}$ mice, while the level of VIP in *Tyr*$^{c\text{-}2j}$-WT mice remained unchanged. This elevated level of VIP in *Tyr*$^{c\text{-}2j}$-*mMCP4*$^{-/-}$ mice is consistent with the aberrant lymphatic phenotype seen in these mice (enlarged and dysfunctional lymphatic vessels). Therefore, our data suggests that mMCP4 is likely to be required to regulate VIP levels in the skin. Particularly, mMCP4 appears to be required to remove regulate VIP levels in the local UVB exposed environment, hence preventing the lymphatic drainage from being compromised.

Taken together, our data suggests that across all models, mMCP4 is a critical mediator in the regulation of lymphangiogenesis and lymphatic vessel function, and it may also have an intermediate influence on angiogenesis. Our data also suggests that VIP is a specific target substrate of mMCP4 in this chronic UVB setting. Additionally, mMCP4 may also target VEGF-A but not VEGF-D. However, the targeting of VEGF-A by mMCP4 needs to further confirmed.

Based on the results in Chapter 4, *Tyr*$^{c\text{-}2j}$-*mMCP4*$^{-/-}$ mice appear to show earlier signs of *in situ* SCC features compared to *Tyr*$^{c\text{-}2j}$-WT mice, suggesting the loss of mMCP4 may be associated with an earlier shift towards a pro-tumour microenvironment. We showed that mice deficient of mMCP4 have more dilated and dysfunctional lymphatic vessels following UVB irradiation. We suspect if the lymphatic vessels in the ears of UVB-treated *Tyr*$^{c\text{-}2j}$-*mMCP4*$^{-/-}$ mice are unable to efficiently drain inflammatory infiltrate from the site of inflammation, the inflammatory response cannot be resolved due to an accumulation of cell populations. A balance of all immune cell population are required to maintain local tissue homeostasis. The dysregulation of one or more population of immune cells can disrupt this balance and contribute to changes in the microenvironment, subsequently promoting tumour formation. Hence, it is critical to assess whether there is

any changes in immune cell populations that is associated with the loss of mMCP4 at the site of UVB damage.

Although we did not observe any signicantly distinct difference in specific cell populations following UVB irradiation, it is noteworthy to add that the total number of CD45+ immune cells is much larger than the total number of cells combined from all of the populations assessed, suggesting that there are large number of cells that are unaccounted for. This could suggest the presnce of additional populations not measured by our FACS protocol.

Out of all of immune cell populations assessed, only $CD11b^{+}Gr\text{-}1^{+}$ myeloid-derived suppressor cells (MDSCs) was shown to be elevated in number (not significant) in the absence of mMCP4, following UVB irradiation. This cell population consists of precursors of dendritic cells, macrophages and granulocytes, and it has been reported that increased numbers of MDSCs is associated with multiple types of cancers[476-478]. The immunosuppressive functions of MDSCs have been shown to promote tumorigenesis by mechanisms such as disrupting tumour immunosurvellaince via interfering with T cell cytoxicity, antigen presentation, activation and polarisation[479-481]. As a result MDSCs are becoming better recognised as a potential target for immunotherapies for cancer patients.

Interestingly, the levels of $CD8^{+}$ T and $CD4^{+}$ T cells are also elevated in both *Tyr*$^{c\text{-}2j}$-WT and *Tyr*$^{c\text{-}2j}$-*mMCP4*$^{-/-}$ mice following 25 UVB exposures. This would suggest that indeed, the $CD8^{+}$ T and $CD4^{+}$ T cells are responding to the chronic UVB irradiation and are quite likely to be exibiting anti-tumour functions[477,482,483] as we have observed *in situ* SCC development in both *Tyr*$^{c\text{-}2j}$-WT and *Tyr*$^{c\text{-}2j}$-*mMCP4*$^{-/-}$ mice (more so in *Tyr*$^{c\text{-}2j}$-*mMCP4*$^{-/-}$ mice). Simultaneously, the presence of more MDSCs in the ears of *Tyr*$^{c\text{-}2j}$-*mMCP4*$^{-/-}$ mice is also observed and suggests that the local microenvironment at the site of UVB damage is more immunosuppressive, which would potentially counteract the anti-tumour functions of $CD4^{+}$ T cells and $CD8^{+}$ T cells[477,482,483]. Cumulative UVB irradiation is known to promote a highly immunosuppressive microenvironment, which is one of the crucial precursors leading to skin tumourigenesis. For example it is known that UVB irradiation can supress cellular immunity through serotonin and PAF-dependent activation of regulatory B cells[484,485]. Studies also showed that Langerhan cell-dependent induction of T regulatory cells is associated with supressed cellular immunity following UVB irradiation[486,487]. Hence, in *Tyr*$^{c\text{-}2j}$-*mMCP4*$^{-/-}$ mice, the accumulation of more

MDSCs at the site of UVB damage is likely to further enhance the immune suppression caused by UVB, inhibit $CD8^+$ and $CD4^+$ T cell anti-tumour functions and likely to promote earlier onset of *in situ* SCC development as we observed in Chapter 4.

But how is mMCP4 playing a role in this scenario? As shown earlier, mMCP4 may target VIP, as a greater abundance of VIP was detected in the ears of *Tyr*$^{c\text{-}2j}$-*mMCP4*$^{-/-}$ mice following chronic UVB irradiation. Interestingly, VIP has been shown to promote the differentiation of $CD14^+$ mononuclear cells into activated MDSCs[224]. The same study has also shown that VIP can also enhance MDSC function as measured by their ability to impair Th1 responses of $CD4^+$ and $CD8^+$T cell. Hence, it is likely that the loss of mMCP4 results in high levels of VIP, which causes an expansion of MDSCs at the site of UVB damage and subsequently impairing anti-tumour functions of the local microenvironment.

However, it is also noteworthy to add that the markers used to assess MDSCs in the current study was not specific enough to fully identify this population. To further confirm out findings, utilisation of markers such as $Ly6C^+Ly6G^-$ (monocytic) and $Ly6G^+Ly6C^-$ (granulocytic) will be required. To further confirm the presence of accumulating immunosuppressive MDSCs at the site of damage, it would be beneficial to assess the release of MDSC-derived mediators such as Arginase 1, inducible nitric oxide synthase, reactive oxygen species and peroxynitrite; and ability of these cells to supress T-cell responses[476].

Taken together, we have shown that MCs and mMCP4 do have a critical role in regulating lymphatic vascular structure and function following chronic UVB irradiation. We have shown that mMCP4 could be involved in the blood vasculature more so in the engrafted–*Kit*$^{W/W\text{-}v}$ mice than the non-pigmented*Tyr*$^{c\text{-}2j}$-*mMCP4*$^{-/-}$ mice. The lack of effect in pigmented B6-*mMCP4*$^{-/-}$ mice is more likely due to the presence of pigment. In regards to the lymphatic vasculature we have shown that mMCP4 does have a prevalent role in regulating the lymphatic vasculature architecture and function as well.

Furthermore, our data suggests that loss of mMCP4 results in aberrant lymphangiogenesis and impaired lymphatic vessel function. Simultaneously, we have shown for the first time that mMCP4 could potentially target VIP to allow normal drainage of inflammatory infiltrate and maintain balance of the local microenvironment in a chronic UVB setting. This is supported by the observation that loss of mMCP4 is associated with enhanced

levels of VIP following chronic UVB irradiation. Furthermore, this is potentially correlated with the presence of more immunosuppressive MDSCs which could potentially lead to earlier onset of *in situ* SCCs.

Figure S1. Characterisation of cell populations in the ears of *Tyr*$^{c\text{-}2j}$-WT and *Tyr*$^{c\text{-}2j}$- *mMCP4*$^{-/-}$ mice following chronic UVB irradiation. (A) Following chronic UVB irradiation, cell populations were extracted from the ears of *Tyr*$^{c\text{-}2j}$-WT and *Tyr*$^{c\text{-}2j}$-*mMCP4*$^{-/-}$ mice by liberase digestion. Following extraction, specific cell populations were assessed from both genotypes; representative flow plots of specific cell populations. Data from 2 independent experiments (n=6-11 mice/experiment).

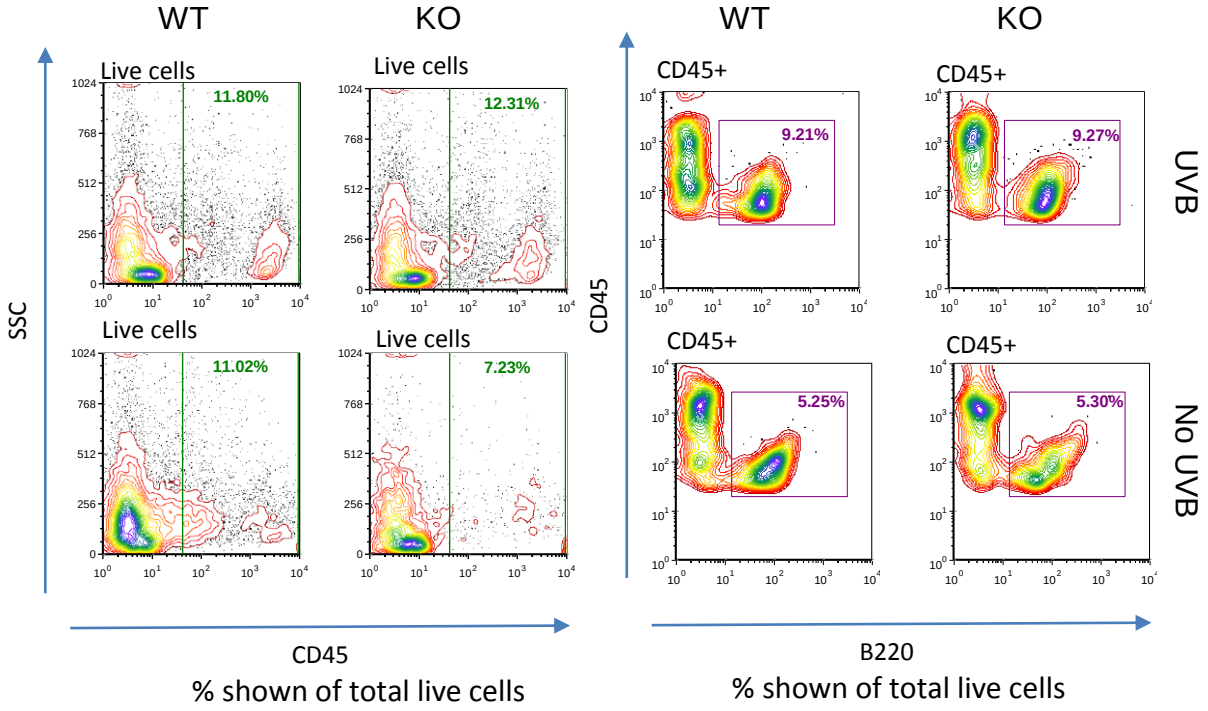
WT
KO
WT
KO
Live cells
11.80%
Live cells
12.31%
CD45+
9.21%
CD45+
9.27%
UVB
Live cells
11.02%
Live cells
7.23%
CD45+
5.25%
CD45+
5.30%
No UVB
SSC
CD45
CD45
CD45
B220
% shown of total live cells
% shown of total live cells

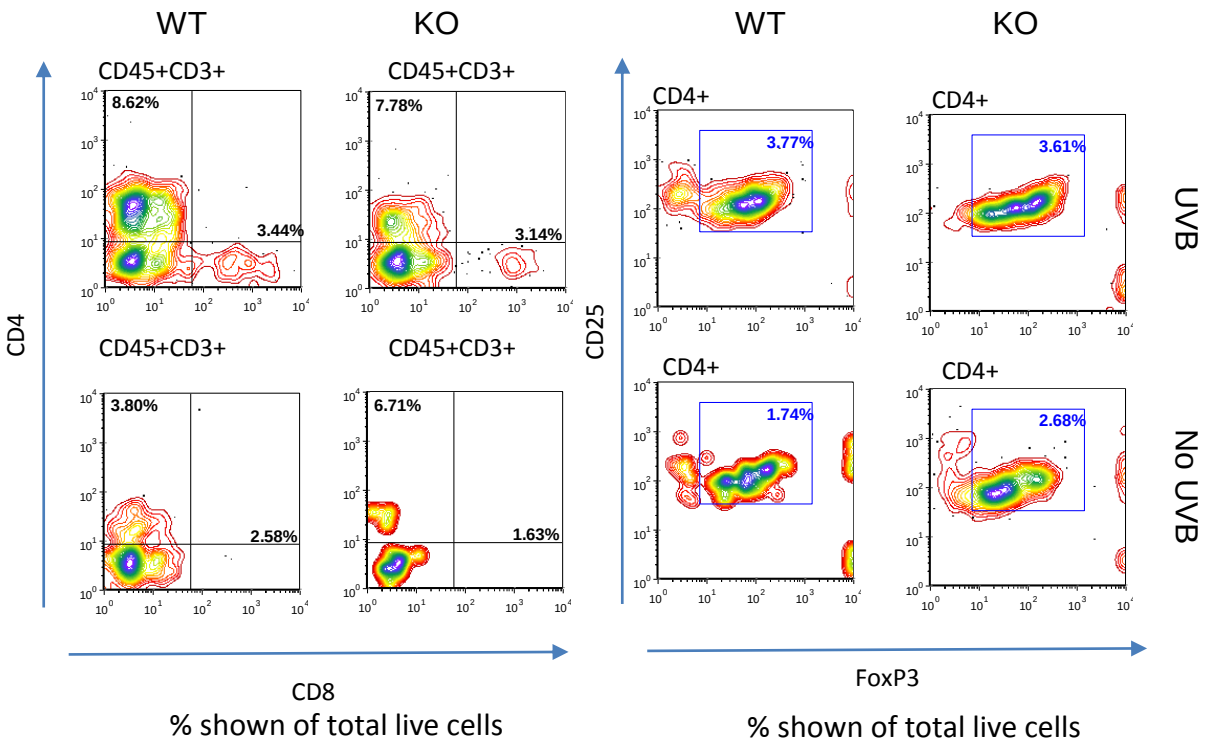
WT
KO
WT
KO
CD45+CD3+
8.62%
3.44%
CD45+CD3+
7.78%
3.14%
CD4+
3.77%
CD4+
3.61%
UVB
CD45+CD3+
3.80%
2.58%
CD45+CD3+
6.71%
1.63%
CD4+
1.74%
CD4+
2.68%
No UVB
CD4
CD25
CD8
FoxP3
% shown of total live cells
% shown of total live cells

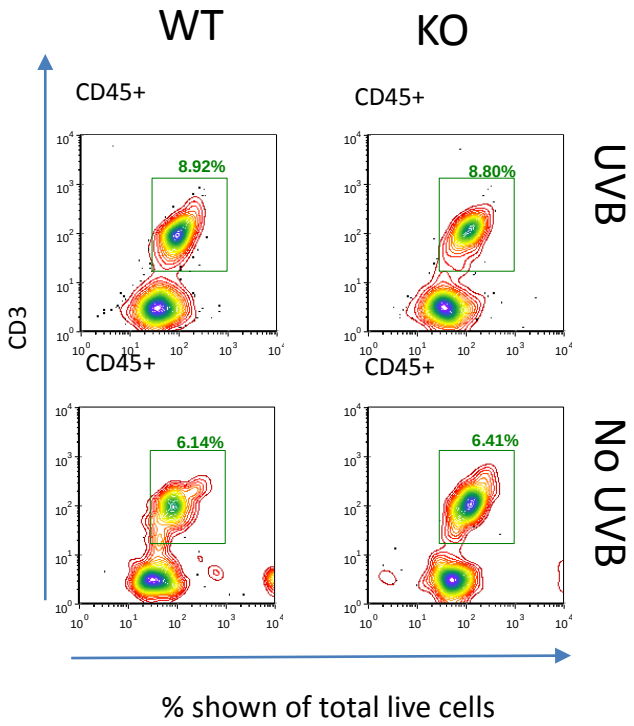
WT
KO
CD45+
CD45+
8.92%
8.80%
UVB
CD3
CD45+
CD45+
6.14%
6.41%
No UVB
% shown of total live cells

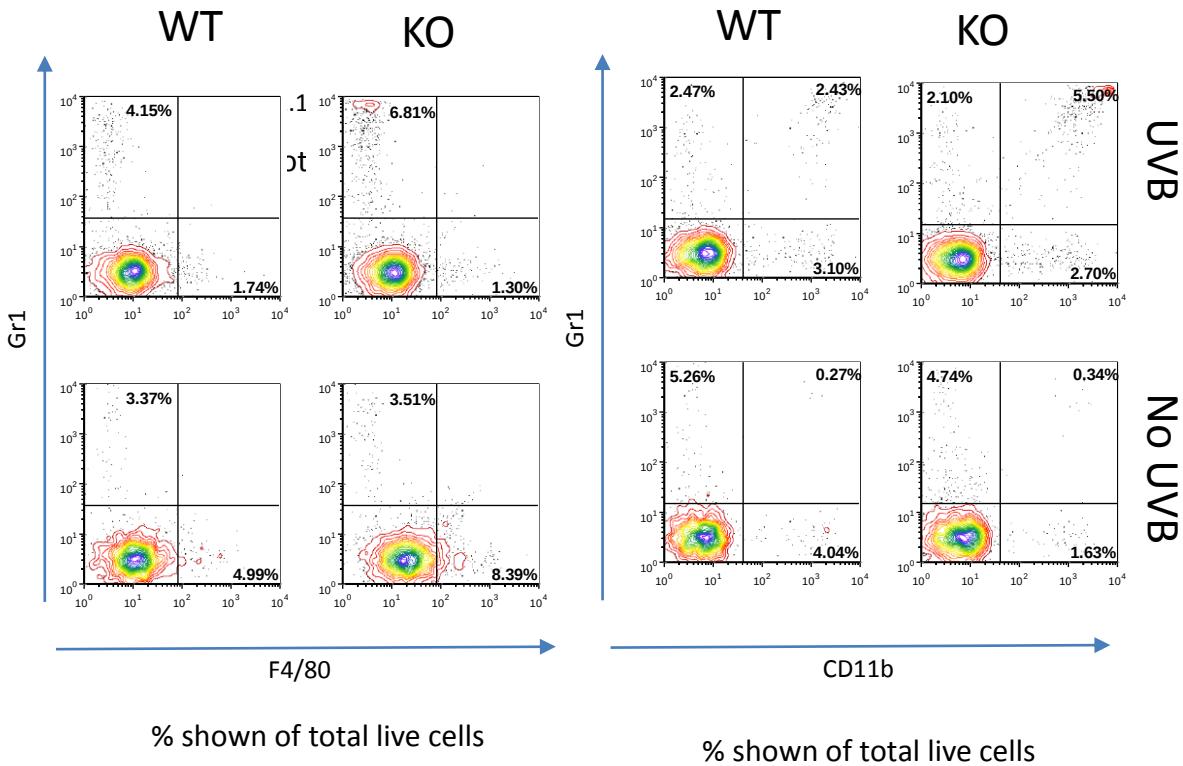
WT
KO
WT
KO
4.15%
1.74%
6.81%
1.30%
2.47%
2.43%
3.10%
2.10%
5.50%
2.70%
UVB
Gr1
3.37%
4.99%
3.51%
8.39%
5.26%
0.27%
4.04%
4.74%
0.34%
1.63%
No UVB
Gr1
F4/80
CD11b
% shown of total live cells
% shown of total live cells

Chapter 6

MICROARRAY ANALYSES SUGGESTS LOSS OF mMCP4 CAUSES ALTERATIONS IN EXTRACELLULAR MATRIX AND CELL TRAFFICKING PATHWAYS

6.1 Introduction

Proteases are known to play fundamental roles in multiple biological processes. Via highly selective cleavage of specific substrates, proteases have been well recognised as critical regulators of cellular processes, including tissue remodelling. The dysregulated functions of proteases have been associated with a wide variety of pathological conditions, including cancer[6,236]. MMP9, for example, is a well-known metalloproteinase that facilitates physiological processes such as cell migration[488,489], angiogenesis[490] and wound healing by breaking down ECM proteins such as collagen type I and IV[421]. The upregulation of MMP9 has been found in pathological conditions including angiogenic dysplasia and invasive cancer of the epidermis induced by HPV16 oncogenes[267], advanced ovarian cancer[491], as well as lung metastasis of tumour cells [492]. UVB exposure is known to induce production of cytokines which can induce local accumulation of MCs and MMP prodcution which are both known to be contributing factors in UVB-induced skin inflammation[369]. In addition, MCs are also known to release MMP's such as MMP2 and MMP9[384], as well as their own mast cell-specific proteases. As noted in earlier chapters of this thesis, mast cell-specific proteases can play important roles the initiation as well as the resolution of inflammation in certain contexts of inflammation[57], functions that are also shared by some MMPs, including MMP2[493,494] and MMP9[267,494,495].

mMCP4 is thought to be involved in multiple pathways including, collagen turnover, chemokine-induced trafficking of cells, and inflammation, through targeting substrates such as fibronectin[194,381], CCL2[380], and TNFα[5]. However, these findings currently appear to be disease and context dependent. More importantly, no study has investigated the role of mMCP4 in UVB-induced skin tumourigenesis. As discussed in chapters 4 and 5, we have clearly demonstrated mMCP4 is a protective factor against the development of skin tumourigenesis following chronic UVB irradiation. mMCP4 also appears to be required for functional lymphatic drainage and potentially trafficking of inflammatory infiltrates in this disease model. Although we have identified VIP as a potential substrate of mMCP4 in mediating normal lymphatic function, other direct or indirect targets that may facilitate mMCP4 function in this setting remains to be further elucidated.

ECM provide a scaffold for all cell types in the tumour microenvironment and they are important in initiating the development of tumours and assisting the spread of cancer cells[496]. MMPs that are secreted and activated by tumour cells, tumour-associated

macrophages, and cancer-associated fibroblasts are able to remodel ECM by degradation. As a result of ECM remodelling, factors including chemokines, growth and angiogenic factors are released and made readily available not only to structural cells, but also resident and infiltrating immune cells[497]. As a result, modulation of the infiltrating immune cells and local microenvironment can activate downstream pathways including chronic inflammation, angiogenesis and metastasis[498]. This relationship between the ECM and tumour microenvironment is critical for the progression of malignancies[499-501]. Although the role of mMCP4 in UVB-induced skin carcinogenesis is not yet fully elucidated, a study by Siiskonen *et al*., reported an association between the expression of chymases and tryptases and metastasis of melanoma[412]. This further suggests a role of mMCP4 in regulating other pathways in the tumour microenvironment. Therefore, in this chapter, we sought to explore other pathways regulated by mMCP4 via examining the global effect of mMCP4 deficiency in the context of UVB-induced skin carcinogenesis.

6.2 Results

6.2.1 Deficiency in mMCP4 causes global changes in mRNA expression of multiple pathways

In order to study the global effects of MCs and the consequences associated with the loss of mMCP4 in the chronic UVB setting, mRNA microarray was utilised. The RNA integrity was confirmed via BioAnalyzer assessment and was shown to be adequate for further assessment. To maximise the coverage of potential genes and pathways being affected, tissue samples from the mouse model (engrafted-*Kit*$^{W/W\text{-}v}$ mice) and the time point (12 exposures) that were previously found to produce the most pronounced response was selected. Based on our microarray analyses, a large number of genes were differentially regulated in UVB-treated skin that lacked MCs or mMCP4. More importantly, based on pathways analysis using INGENUITY PATHWAY ANALYSIS software, several genes involved in the ECM (p-value=1.82 x 10^{-16}) and cell migration (p-value=1.69 x 10^{-3}) pathways appeared to be upregulated in the absence of both MCs and mMCP4 (**Figure 6.1a, b**), suggesting that these genes may be direct or indirect downstream targets of mMCP4. These findings were then further verified by qRT-PCR.

Figure 6.1 Signalling pathway analysis of WBB6F$_1$-*Kit*$^{W/W\text{-}v}$ mice in response to chronic UVB irradiation (A) Pathway analysis produced by Ingenuity Pathway Analyser indicating potential pathways that were affected by the loss of mMCP4. **(B) Genes involved in chemokine trafficking and ECM.**

A

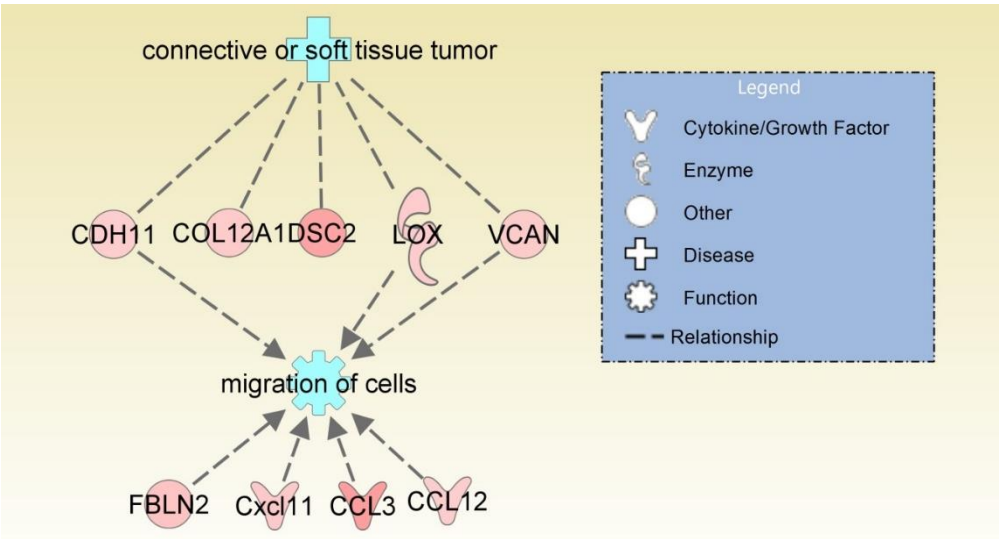

B

Loss of MCs and/or mMCP4

ECM

cdh11
dsc2
lox
Vcan
fbln2

Cell Trafficking

ccl12
ccl3
cxcl11

6.2.2 Loss of MCs and mMCP4 causes up-regulation of genes involved in chemokine-dependent cell trafficking

Although not much is known about the targeting of chemokines by mMCP4, previous studies have demonstrated that CCL2 can be targeted and degrade by mMCP4 in a mouse model of post-traumatic spinal cord damage[380]. In the absence of mMCP4, it is likely that the loss of this protease will result in alterations of various pathways, potentially including cell trafficking that ultimately contribute to changes in the skin. Based on the mRNA microarray data, we observed non-significant up-regulation of chemokines *ccl3*, *ccl12* and *cxcl11* in the absence of mMCP4. By qRT-PCR analysis, in agreement with the microarray data, *ccl3* expression was elevated in both *Kit*$^{W/W\text{-}v}$ and *mMCP4*$^{-/-}$ BMCMCs→*Kit*$^{W/W\text{-}v}$ mice (**Figure 6.2a**), while mRNA transcript of *ccl12* and *cxcl11* were up-regulated only in *mMCP4*$^{-/-}$ BMCMCs→*Kit*$^{W/W\text{-}v}$ mice (**Figure 6.2b, c**).

6.2.3 Loss of mMCP4 causes dysregulation in genes involved in the extracellular matrix

ECM and cell-cell junction proteins are crucial for both tissue homeostasis and patholigcal conditions such as cancer. ECM proteins such as fibronectin is a direct target of mMCP4[194,381]. Our microarray data, validated by qRT-PCR analysis, also demonstrated that in the absence of MCs and mMCP4, other ECM components such as fibulin 2 (*fbln2*), Versican (*Vcan*), collagen XII (*col12a1*), cell-cell junction molecules desmocollin2 (*dsc2*), integrin cadherin11 (*cdh11*), and collagen cross linking enzyme lysl oxidase (*lox*), were all up-regulated transcriptionally after 12 exposures of UVB (12 x 4 kJ/m^2) in *mMCP4*$^{-/-}$ BMCMCs→*Kit*$^{W/W\text{-}v}$ mice, and also in some cases, in *Kit*$^{W/W\text{-}v}$ mice (**Figure 6.3a-f**).

6.2.4 Loss of mMCP4 potentially causes loss of the anti-angiogenic factor tumstatin

Next, we wanted to investigate whether expression of other ECM genes that are involved in tumour progression were affected by the loss of mMCP4. A study by Hamano *et al.*, demonstrated that MMP9 is required to generate the anti-angiogenic factor tumstatin through cleavage of collagen type IVαV3. By assessing the presence of the active (cleaved) and inactive (uncleaved) form of MMP9 in naïve WT and *mMCP4*$^{-/-}$ BMCMC, we found that, in agreement with the literature, the loss of mMCP4 is associated with the absence of active MMP9 (**Figure 6.4a**). We therefore hypothesised that mMCP4 could

Figure 6.2. Quantitative real-time PCR analysis suggests the importance of mMCP4 in regulating *ccl3*, and *cxcl11* mRNA expression in engrafted-*Kit*$^{W/W\text{-}v}$ mice following 12 exposures of chronic UVB. (A) Following UVB irradiation (12 exposures), *ccl3*, **(B)** *ccl12 and* **(C)** *cxcl11* mRNA expression was assessed by qRT-PCR from ears of WT, *Kit*$^{W/W\text{-}v}$, WT BMCMCs→*Kit*$^{W/W\text{-}v}$ and *mMCP4*$^{-/-}$ BMCMCs→*Kit*$^{W/W\text{-}v}$ mice. Data from 1 experiment (n=3 mice/genotype) and represented as fold change in gene expression compared to non-UVB treated samples (normalised to *GAPDH*) + SEM. Student's unpaired T test *p<0.05, **p<0.01, ***p<0.001, n.s.: not significant.

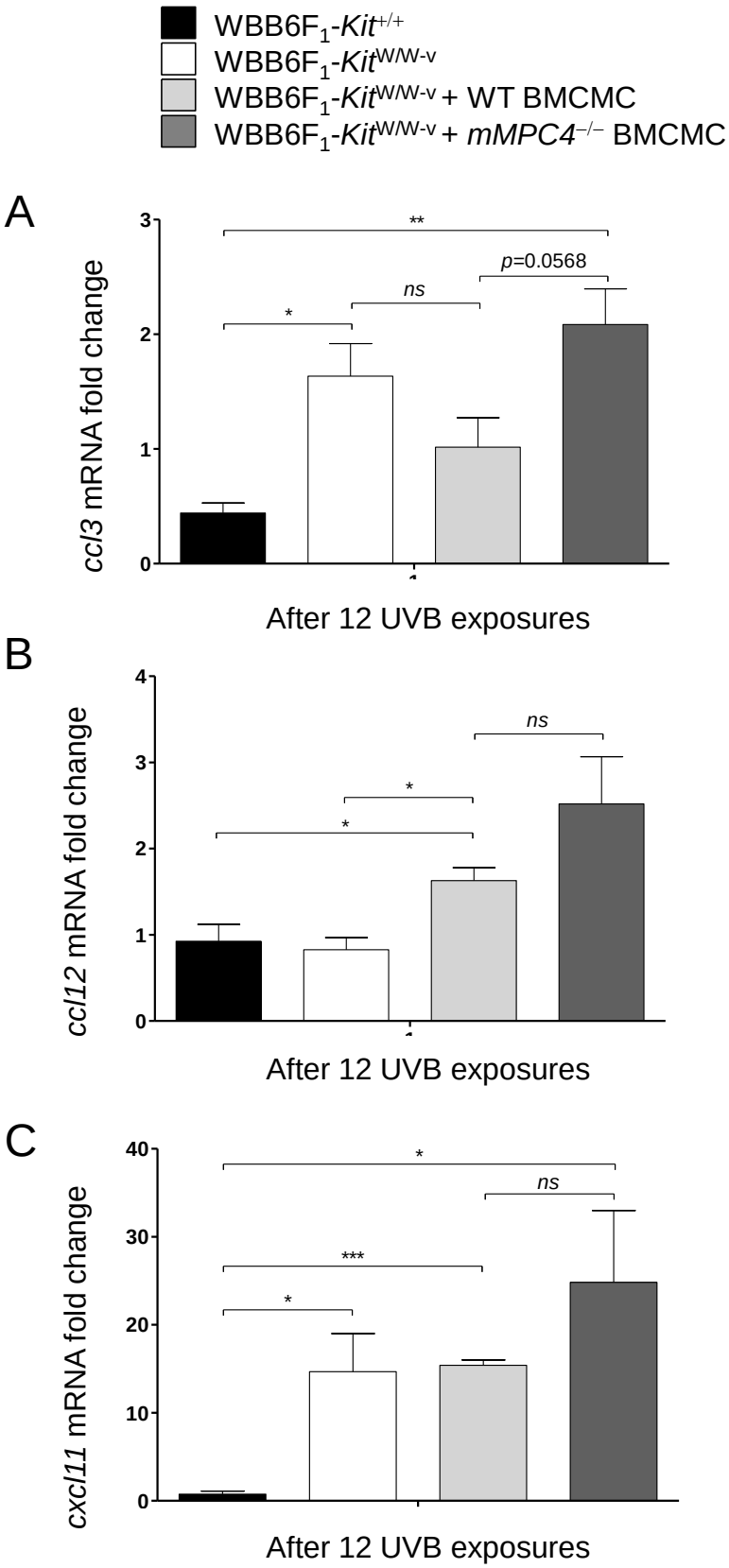
WBB6F1-Kit+/+
WBB6F1-KitW/W-v
WBB6F1-KitW/W-v + WT BMCMC
WBB6F1-KitW/W-v + mMPC4−/− BMCMC
A
ccl3 mRNA fold change
**
p=0.0568
ns
*
After 12 UVB exposures
B
ccl12 mRNA fold change
ns
*
*
After 12 UVB exposures
C
cxcl11 mRNA fold change
*
ns
***
*
After 12 UVB exposures

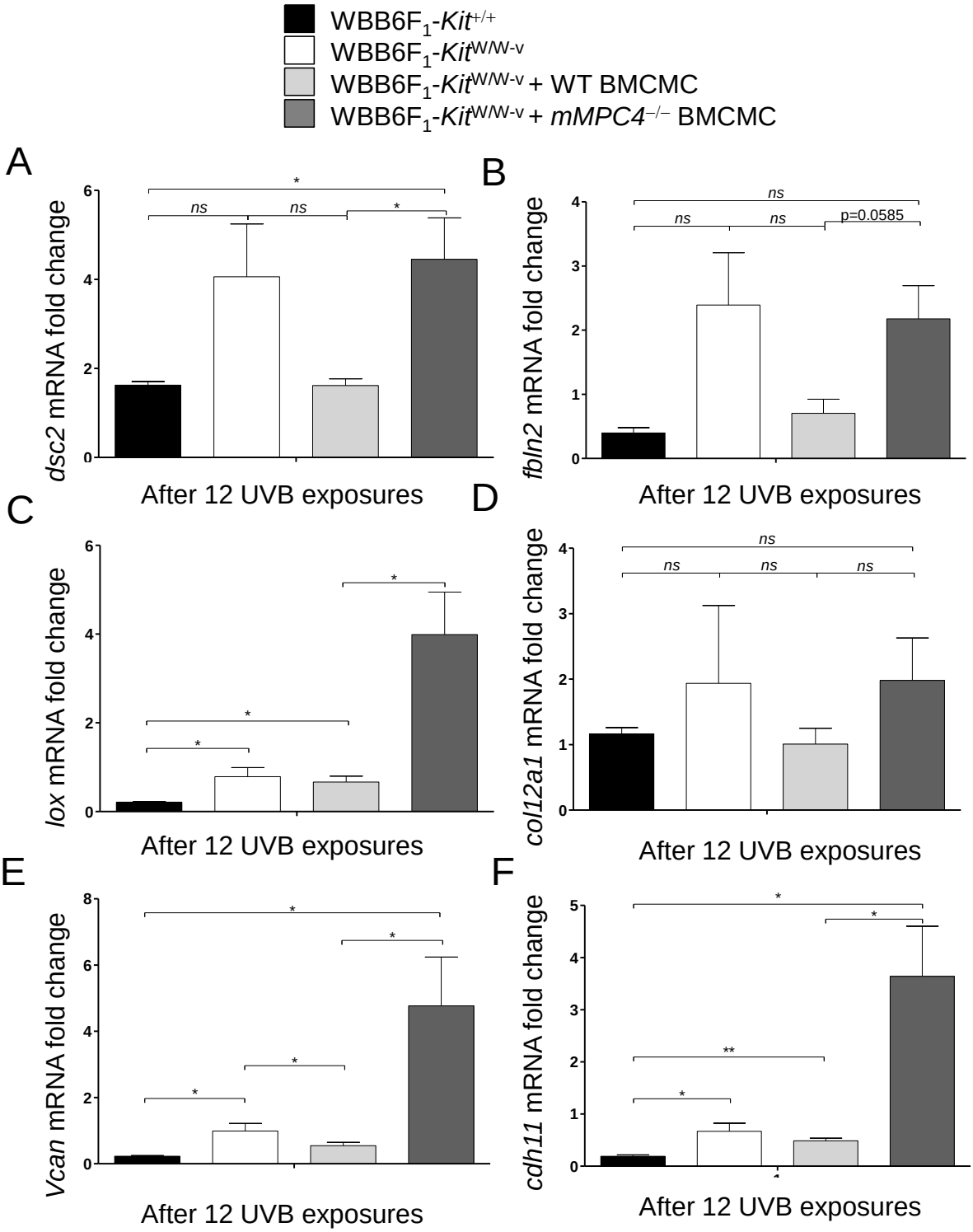

Figure 6.3 Quantitative real-time PCR analysis suggests the importance of mMCP4 in regulating mRNA expression of ECM components in engrafted-*Kit*$^{W/W\text{-}v}$ mice following 12 exposures of chronic UVB. (A) Following UVB irradiation (12 exposures), *dsc2*, **(B)** *fbln2*, **(C)** *lox*, **(D)** *col12a1*, **(E)** *Vcan*, and **(F)** *cdh11* mRNA expression was assessed by qRT-PCR from ears of WT, *Kit*$^{W/W\text{-}v}$, WT BMCMCs→*Kit*$^{W/W\text{-}v}$ and *mMCP4*$^{-/-}$ BMCMCs→*Kit*$^{W/W\text{-}v}$ mice. Data from 1 experiment (n=3 mice/genotype) and represented as fold change in gene expression compared to non-UVB treated samples (normalised to *GAPDH*) + SEM. Student's unpaired T test *p<0.05, **p<0.01, n.s.: not significant.

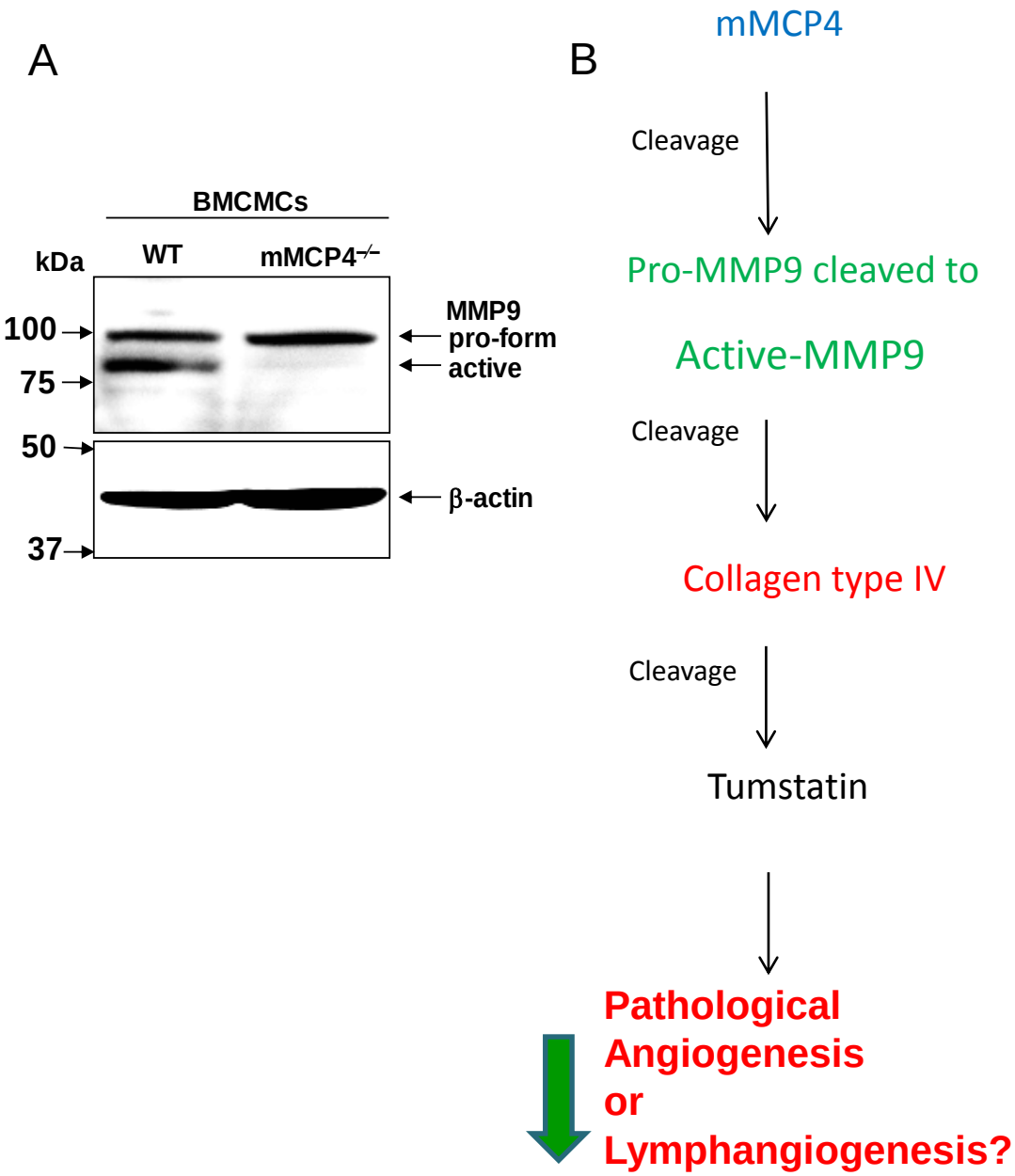

Figure 6.4 Western blot analysis confirms that *mMCP4*$^{-/-}$ BMCMCs exhibit low levels of the activated form of MMP9. (A) Immunoblot of endogenous MMP9 protein expression in naive WT and *mMCP4*$^{-/-}$ BMCMCs. Data from 1 experiment. **(B)** Hypothetical mechanism whereby mMCP4 exhibits protective function through targeting the MMP9/ c*olIV*α*V3* /tumstatin pathway.

elicit its anti-tumourigenic functions through targeting the MMP9/collagenIVαV3/tumstatin pathway (**Figure 6.4b**). To clarify, we initially assessed mRNA expression of collagen IVαV3 following 12 exposures of UVB, however, we did not observe any changes (data not shown). Following 25 exposures of UVB (12 x 4 kJ/m2 + 13 x 8 kJ/m^2), the mRNA expression of collagen IVαV3 was elevated in WT and WT BMCMCs→*Kit*$^{W/W\text{-}v}$ mice, whereas no change was observed in *Kit*$^{W/W\text{-}v}$ or *mMCP4*$^{-/-}$ BMCMCs→*Kit*$^{W/W\text{-}v}$ mice, suggesting that lack of MCs and mMCP4 results in deficient turnover of this collagen (**Figure 6.5a**). Similar results were observed in pigmented B6 mice (**Figure 6.5b**), even though the protective effect of mMCP4 was not as pronounced as the *Kit*$^{W/W\text{-}v}$ model, consistent with previous observations described in Chapters 4 and 5.

6.3 Discussion

Determining the array of specific substrates of proteases *in vivo* continues to be a difficult task due to many technical limitations. Therefore we used mRNA microarray as an alternative approach to assess global effects of mMCP4 in chronic UVB setting. This is because changes in mRNAs can provide potential indications of what pathways mMCP4 may be influencing, irrespective of whether it reflects a direct or indirect effect of mMCP4 proteolytic activity. As suggested by the microarray, and later confirmed by qRT-PCR, some genes involved in chemokine/cell trafficking and ECM/cell-cell junction are upregulated by the loss of both MCs and mMCP4 following UVB irradiation.

CCL3 can regulate intra-tumoural accumulation of leukocytes and fibroblasts and promote angiogenesis in the murine lung-metastasis process[502], and it has been reported to recruit monocytic myeloid derived suppressor cells (monocytic MDSCs) to the tumour tissue[454,503]. Our observation of higher levels of *ccl3* in the ears of both *Kit*$^{W/W\text{-}v}$ and *mMCP4*$^{-/-}$ BMCMCs→*Kit*$^{W/W\text{-}v}$ mice following UVB irradiation suggests that there may be an increasing abundance of cell populations at the site of UVB irradiation that can assist in development of local tumourigenic microenvironment. Interestingly, considering CCL3 can recruit certain populations of MDSCs[454,503], this could correlate with our previous data in Chapter 5 where there were elevated levels of MDSC populations detected in the UVB treated ears in the absence of mMCP4.

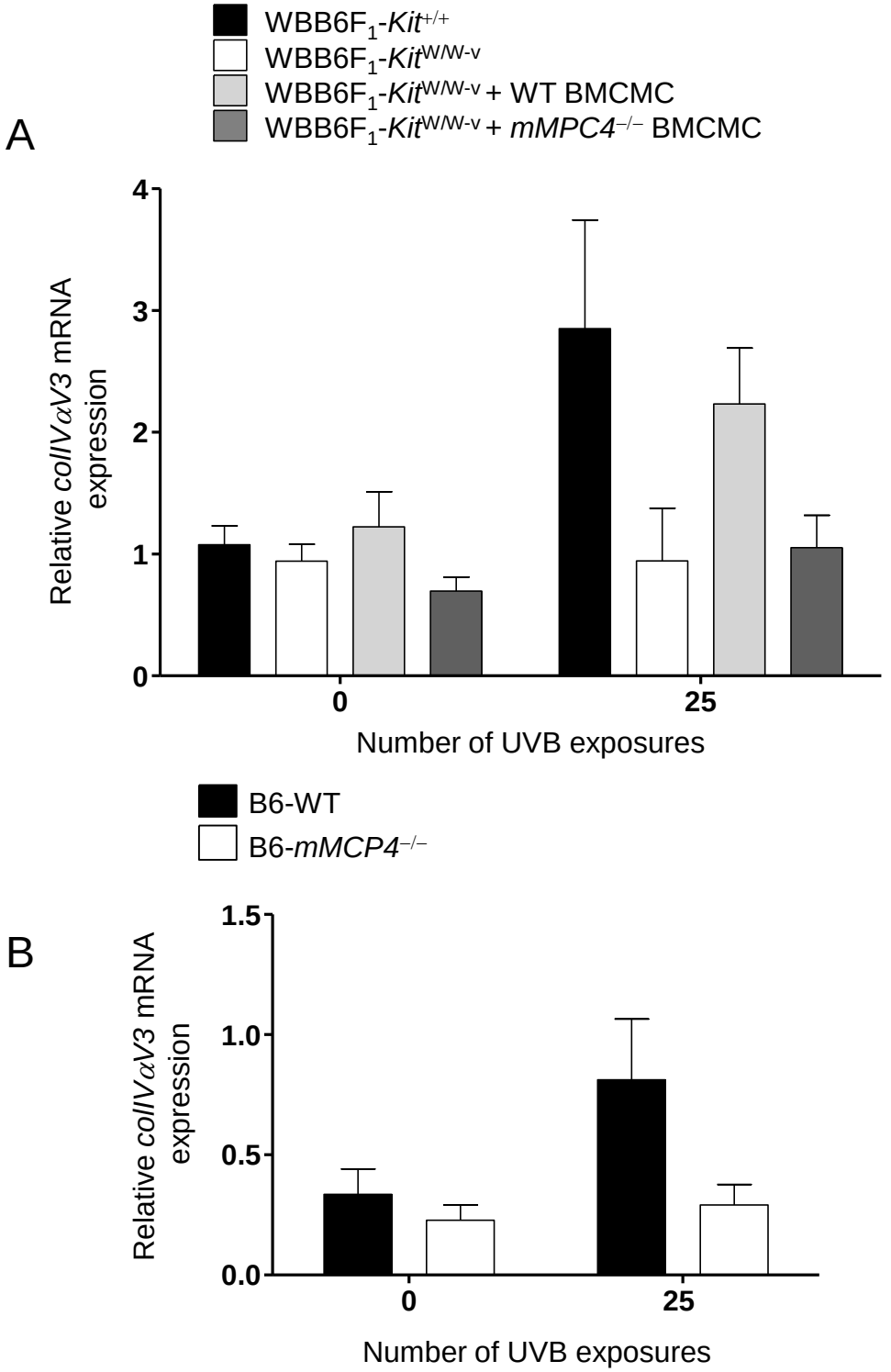

Figure 6.5 Quantitative real-time PCR analysis suggests the importance of mMCP4 in regulating mRNA expression of ECM components in engrafted-*Kit*$^{W/W\text{-}v}$ mice following 12 exposures of chronic UVB. (A) Following UVB irradiation (12 exposures), mRNA expression of c*olIVαV3* in engrafted-*Kit*$^{W/W\text{-}v}$ mice and **(B)** pigmented B6-mice was assessed by qRT-PCR from ears of WT, *Kit*$^{W/W\text{-}v}$, WT BMCMCs→*Kit*$^{W/W\text{-}v}$ and *mMCP4*$^{-/-}$ BMCMCs→*Kit*$^{W/W\text{-}v}$ mice. Data from 1 experiment (n=3-5 mice/genotype) and represented as mean (normalised to *GAPDH*) + SEM.

On the contrary, CCL12, is not as well-studied. However, CCL12 is a homologue of CCL2, and they both bind to the same receptor CCR2[504]. Therefore, CCL12 may have redundant functions with CCL2 in terms of recruiting monocytes, macrophages, MCs[40], MDSCs[505] as well as activating T and B cells[506]. As a result, it is difficult to differentiate the true function between these two chemokines. Interestingly, CCL2 is a bona fide substrate for mMCP4 and is indicated to be involved in promoting cancer[505,507]. Hence it is likely that the potential regulation of CCL12 by mMCP4 indicates a novel mechanism whereby mMCP4 exerts its protective role in chronic UVB-induced skin carcinogenesis. Although our results suggest that the levels of both *ccl3* and *ccl12* can be up-regulated in the absence of mMCP4, further verification, ideally via ELISA, is required to determine whether this targeting effect is direct.

CXCL11 is another chemokine that has been demonstrated to be involved in cancers including ovarian[508] and colorectal cancer[509]. The poposed roles of CXCL11 include facilitating tumour growth, as well as promoting cancer cell migration and metastasis, potentially through regulation of MMPs[508,509]. Based on our findings, although not signifcant, we did observe a trend in elevated mRNA expression of *cxcl11* in *mMCP4*$^{-/-}$ BMCMCs→*Kit*$^{W/W\text{-}v}$ mice. Notably, overexpression of CXCR3, the receptor for CXCL11, has been associated with tumour grade and lymph node mestastises in ovarian cancer[508]. Hence it is likely that the expression level of CXCL11 could also act as a prognostic marker and provide insights into tumour progression. Further stuies will be required to fully elucidate this hypothesis, and whether mMCP4 is involved in its regulation will also need to be addressed, which will add valuable knowledge to this field.

Notably, the mRNA up regulation of the above mentioned chemokine genes in the absence of mMCP4 are not signficant. A larger sample will be required to further confirm these hypotheses.

The ECM is composed of many structural components that play important roles in regulating cancer cell metastasis[496]. Fibulin2 is an ECM protein component of the basement membranes and elastic fibre matrix. It is known to be associated with fibronectin and has also been reported to assist the adherence of cells to ECM via its interaction with β3 integrins[510,511]. Apart from their structural function, ECM components are important in both anti- and pro-tumourigenic roles[512,513]. Based on our data, we observed elevated levels of *fbln2* gene expression in both *Kit*$^{W/W\text{-}v}$ and *mMCP4*$^{-/-}$

BMCMCs→*Kit*$^{W/W\text{-}v}$ mice following 12 exposures of chronic UVB. It is difficult to conclude whether fibulin 2 is promoting or limiting tumourigenesis. Some studies suggest that overexpression of fibulin 2 can initiate tumourigenic properties particularly in the presence of collagen. Interestingly, it has also been reported that fibulin 2 is preferentially expressed in highly metastatic cells[513,514]. On the other hand, fibulin2, interacts with the protease ADAMTS12, by which it can also exhibit tumour suppressive functions via reducing cell migration, invasion and other tumourigenic properties in breast cancer cell lines[512]. Nevertheless, it would be worthwhile to assess the overall protein expression of fibulin2 in UVB-treated tissue to provide a better understanding of how it is regulated by mMCP4 at the protein level. This can also indicate the potential role of fibulin2 in the current disease setting.

DSC2 is a desmosomal cadherin protein that is involved in maintaining epithelial homeostasis by reinforcing adhesion of epithelial cells[515]. Although its roles in cancer is yet to be fully elucidated, recent studies have suggested that DSC2 acts as a tumour suppressor. It has been reported that loss of DSC2 expression confers a tumourigenic phenotype in colon[516], oesophageal SCCs[517] as well as skin cancers. The loss of DSC2 in epithelial cancers such as skin cancers also correlates with advanced tumour grade and poor prognosis[518,519]. Interestingly, in some cases, an increase in expression of other desmosomal components such as desmoglein 2 (DSG2) have also been suggested to be associated with enhanced tumour growth and reduced patient survival[520,521]. Based on our data, elevated levels of *dsc2* gene expression was observed in the ears of both *Kit*$^{W/W\text{-}v}$ and *mMCP4*$^{-/-}$ BMCMCs→*Kit*$^{W/W\text{-}v}$ mice following 12 exposures to chronic UVB. It is likely that at this particular time point, this up-regulation of *dsc2* gene expression could be a result of a loss of the protective functions of MCs and mMCP4. By up-regulating *dsc2* expression, UVB-treated tissues may be attempting to compensate for the loss of anti-tumour functions elicited by MCs and mMCP4 as a repair or rescue mechanism. Similarly, fibulin2 can also act as a tumour suppressor[522]. The elevated levels of fibulin2 may also be an attempt to compensate for the loss of MCs and mMCP4 and promote their tumour suppressive properties to prevent further damage.

Versican is a proteoglycan and has been implicated in a number of malignancies including brain, ovarian, colon, breast, and pancreatic cancers[523-527]. Also found playing a role in melanoma, versican is upregulated upon exposure to UVB[528]. Based on current studies, versican can regulate a number of different pathways and promote tumourigenesis. For

example, overexpressing the functional domains of versican induces *in vitro* proliferation of NIH-3T3 mouse fibroblasts and astrocytoma cells[529]; and it is able to promote tumour growth by breast cancer[530] and melanoma cells[531]. Versican has also been shown to promote motility and invasion of various cancer cell lines[532,533] and promote metastasis of melanoma as well as lung and breast cancer cells[530,531]. Furthermore, angiogenesis is enhanced by the addition of the G3 functional domain of versican, leading to the increase in blood vessel formation in nude mouse tumours[529]. In our study, we observed a significant increase in versican mRNA transcript in the absence of mMCP4 following UVB irradiation, suggesting that versican and its functional domains are potential substrate for mMCP4. In the absence of mMCP4, the abnormal accumulation of versican could contribute to the initiation and progression of the skin tumourigenesis as we observed in these mice. Proteomic analysis will be critical to confirm this hypothesis.

Cadherin11, also known as osteoblast-cadherin, is expressed in breast, prostate, colon and stomach cancers[534-537]. The high expression of cadherin 11, particularly in breast and prostate cancers, is associated with increased invasiveness and poor patient survival[536,537]. However, the underlying mechanism for the expression of cadherin 11 and its involvement in cancers has not been elucidated until recently. Epithelial-mesenchymal transition (EMT) is a critical process required in the invasion and metastasis of cancer cells and it is characterised by the expression of epithelial markers (E-cadherin) and the induction of the mesenchymal marker ZEB2 that drives EMT. A study by Nam *et al*. recently demonstrated that ZEB2 can also trans-activate the promoter of cadherin 11, suggesting that cadherin 11 may also be involved in EMT dependent invasion[538]. Additional studies also suggested that the expression of cadherin 11, particularly early in breast and ductal carcinomas, is crucial in malignant progression. This is supported by the observation that knocking down cadherin 11 or blocking it with antibodies can suppress colony formation and tumour growth by breast cancer, glioblastoma and prostate cancer cells[539]. Based on our findings, mRNA expression of *cdh11* is significantly up regulated in the absence of mMCP4 following UVB irradiation. However, whether this is directly contributing to the observed pathology of these mice is not entirely clear, since this upregulation was observed at a relatively early stage of tumour development. Validation of this effect at the protein level, especially at later stages of tumourigenesis will allow us to further confirm whether mMCP4 is involved in regulating cadherin-11 mediated tumourigenic properties.

Lysyl oxidases (Lox) enzymes are key contributors of tissue stiffening by initiating crosslinking of collagens and elastins[540]. They were well studied due to their established involvement in tumour progression[540,541]. Tumours are typically stiffer compared to normal tissues. Increased Lox activity results in increased stiffness of the ECM and this is suggested to increase the invasiveness of many cancer cells[540,542-546]. Further, elevated Lox expression has been correlated with metastasis and decreased survival in cancer patients. A similar correlation was also observed in mouse models of various cancer types[543,547]. To further verify the upregulation of *lox* transcripts we observed in the UVB-treated *mMCP4*$^{-/-}$ BMCMCs→*Kit*$^{W/W\text{-}v}$ mice, it will be ideal to measure the enzymatic activity of Lox, but also the stiffness of the ECM in these mice at different stages of the disease development. Collagens are also critical in tumour progression, particularly due to their roles as scaffolding proteins. They regulate ECM remodelling through collagen degradation and re-deposition. Additionally they also promote tumour infiltration, angiogenesis, migration and invasion[548-550]. Collagens I, III and IV are typically the most abundant, hence are normally one of the most well studied collagens particularly in cancers[550-553]. Collagen XII belongs to a subgroup of non-fibrillar collagens that has been suggested to be involved in basement membrane regulation by providing molecular bridges between collagen I fibrils[554] and other ECM components such as fibromodulin and lumican[555]. Although the understanding of collagen XII and its roles in cancer are limited, a recent study by Yen *et al*., suggest collagen XII to be a potential biomarker in the malignant breast cancer cell line MCF10CA1a[556]. Collagen XII was also suggested as a marker of myofibroblastic differentiation in a setting of colorectal cancer metastasis according to a proteomic study[557]. In our study, an increase in mRNA expression of *col12a1* was observed in the absence of mMCP4 following chronic UVB exposure. It would be interesting to investigate their protein expression levels as well its degradation/deposition following UVB irradiation, in order to determine whether their roles may correlate with the previous studies, as outlined above.

Simiarly, the sample size used in these qRT-PCR validations are still insufficient to draw any concrete conclusions. Therefore, it would be advisable to further validate these findings using a larger sample size. Furthermore, we observed differences in the level of mRNA modulation between *mMCP4*$^{-/-}$ BMCMCs→*Kit*$^{W/W\text{-}v}$ mice and *Kit*$^{W/W\text{-}v}$ mice. This suggests the absence of mMCP4 may not be responsible for direct regulation of the genes including; *Vcan*, *lox* and *cdh11*. This also suggests that other MC mediators (i.e.

other MC-specific protease that can also regulate ECM genes[558,559] may be involved, that are counter regulating mMCP4 induced effects. Similarly, this also applied to the observations regarding the chemokine genes, considering other MC-specific proteases are also known to regulate chemokine expression[560-563]

Additionally, mMCP4 can target substrates that are involved in processing other extracellular matrix proteins, particularly MMP9[384]. Previous studies have shown that mMCP4 can cleave and activate MMP9 to its active state. MMP9 is responsible for cleavage of collagen IVαV3 and the subsequent generation of the bioactive fragment, tumstatin. Based on our data, in both engrafted *Kit*$^{W/W\text{-}v}$ and pigmented B6 mouse models, we observed a significant upregulation of *tumstatin* gene expression in WT controls, while this gene upregulation was abolished in the absence of mMCP4. This lack of *tumstatin* gene upregulation is likely to suggest a lack of collagen IVαV3 turnover, which could be due to a reduced MMP9 activity. And this correlates with the literature and our own observation that MMP9 is a direct target of mMCP4. Based on the findings of Hamano *et al*.[495], tumstatin inhibits tumour growth in xenografted mouse models, by inhibiting pathological $CD31^+VEGFR2^+$ angiogenesis, but not physiological angiogenesis, via an αVβ3 integrin-dependent pathway[495]. This could correlate with our findings from Chapter 5 where we observed a significant increase in the number of blood vessels in the absence of mMCP4 in multiple mouse models following UVB irradiation. Interestingly, it has been reported that tumstatin can also target lymphatic vessels [564]. This may also correlate with our findings where the absence of mMCP4 also promotes aberrant lymphangiogenesis following chronic UVB irradiation. Although our findings have provided the first link between mMCP4 and tumstatin, qRT-PCR is not an optimal method to measure the presence of bioactive fragments. It would therefore be ideal to utilise ELISA or immunohistochemistry staining to confirm our hypothesis.

Tumor development is a complex, dynamic and progressive process that involves both cellular and environmental cues. The tumour microenvironment is mechanically and biologically active and, more importantly, is dynamic, as is highlighted by the fact that it is continuously and progressively remodelled[565]. It is well known that interactions between cells and an altered microenvironment can drive malignancy. Conversely, tumour cells can manipulate their microenvironment to enhance their own survival, thereby creating a positive tumorigenic feedback loop. Based on our findings in this chapter, the absence of mMCP4 appears to have substantial impact on not only the blood and lymphatic vasculature (Chapter

5) but also on the ECM and the migration of immune cells. These findings further demonstrate the requirement of multiple pathways to be affected in order to promote a microenvironment that is capable of inducing tumourigenesis. Furthermore, this also suggests that mMCP4 is a key negative regulator of UVB-induced skin tumourigenesis and is required to mediate multiple cellular and environmental pathways.

Chapter 7

CONCLUDING REMARKS AND FUTURE DIRECTIONS

While MC's typically have a reputation as notorious promoters of tumourigenesis, recent advances in the field have resulted in a paradigm shift such that we now know that MCs are capable of tumour-suppressive functions in conditions including skin cancers. In Australia, exposure to UVB is a critical contributing factor in the development of non-melanoma skin cancers. Following our previous studies which showed that MC's, MC-IL-10, and a MC-specific protease, mMCP4, play an important protective role against chronic low dose UVB-induced skin inflammation, this study aimed to investigate whether MCs and mMCP4 continue to be protective against chronic high dose UVB induced skin tumourigenesis.

In the first part of the study, we characterised *mMCP4*$^{-/-}$ mice and MC's derived from these mice. Following confirmation of the absence of mMCP4 transcript and protein, we also confirmed that the *mMCP4*$^{-/-}$ BMCMC are phenotypically and functionally normal, which allowed us to re-engraft these MCs into MC-deficient *Kit*$^{W/W\text{-}v}$ mice in order to assess the function of mast cell derived mMCP4 in chronic high dose UVB irradiation. Using this model, we have shown for the first time that MCs and mMCP4 have critical tumour-suppressing functions and protect against the development of *in situ* SCCs. This finding was also supported by the use of non-pigmented *Tyr*$^{c\text{-}2j}$-*mMCP4*$^{-/-}$ mice, which also showed higher rates of *in situ* SCC development compared to WT counterparts, further confirming the protective function of mMCP4 in this disease setting. To investigate the underlying mechanism of this protective function of mMCP4, we focused on the influence of mMCP4 on the vasculature following chronic high dose UVB in both *Kit*$^{W/W\text{-}v}$ and *Tyr*$^{c\text{-}2j}$-*mMCP4*$^{-/-}$ models. Interestingly, our results revealed that mMCP4 is a potential regulator of lymphatic vessel function in the chronic high dose UVB setting, via regulating vasoactive intestinal peptide (VIP) activity.

As described in Chapter 3, we were able to show that the neuropeptide, substance P, could induce degranulation of BMCMCs cultured with IL-3 and SCF. However, this finding remains to be further characterised. In our study, BMCMC degranulation was observed following 24 h of stimulation, as opposed to the study by van der Kleij *et al*, which reported a more immediate effect on MCs cultured in the presence of IL-3, IL-4 and SCF[393]. It has been recently reported that substance P can induce MC degranulation through the binding of substance P (SP) receptor Mrgprb2[93] in peritoneal-derived MCs. Hence, this discrepancy could reflect the difference in tissue origin of the MC populations

used in our study, compared to McNeil *et al*. Although we observed degranulation following SP stimulation, further investigation is required to assess whether SP can induce selective release of mMCP4. It is known that UVB can induce production of neuropeptides like SP[360], but other UVB-induced mediators (such as vitamin D[9], CGRP[360,385], PAF[566], NGF[361], and α-MSH[363]) are also known to be able to activate MCs. Hence it will be worthwhile investigating and determining whether these factors can also induce the release of mMCP4 in a chronic UVB-induced context. A complete understanding of the mechanism of MC activation and especially release of mMCP4 will be beneficial for the future manipulation of MCs and mMCP4, with an ultimate goal of utilising them for therapeutic interventions.

As shown in Chapter 4, using the MC-deficient *Kit*$^{W/W-v}$ mouse model, we demonstrated that MC-IL-10 and mMCP4 retained their protective function in chronic high-dose UVB irradiation. This shows for the first time that MCs can secrete protective mediators that suppress the formation of UVB-induced *in situ* SCCs. Based on these findings, the next question would be to determine whether knocking out both MC-IL-10 and mMCP4 will induce an additive damage response beyond that observed in the normal MC-deficient *Kit*$^{W/W-v}$ mice. This would shed light on whether MC-IL-10 and mMCP4 function simultaneously, or in an independent manner. We previously published that the active form of vitamin D3 (1α25-dihydroxyvitamin D3) could induce the release of MC-IL-10[9]. In addition, we have also shown *in vivo* that topically applied 1α25-dihydroxyvitamin D3 could reduce IgE-dependent passive cutaneous anaphylaxis ear thickening responses[10]. In the context of chronic UVB irradiation, 1α25-dihydroxyvitamin D3 has been shown to protect against UVB-induced cell loss, DNA damage, immunosuppression and skin carcinogenesis[251,252,256,257]. Hence it will be interesting to investigate whether topical application of 1α25-dihydroxyvitamin D3 on UVB-treated ears could enhance MC-mediated protection and rescue some of the damage observed in the absence of mMCP4.

As described in Chapter 4, the protective function of mMCP4 observed in MC-deficient *Kit*$^{W/W-v}$ mice was also evident in non-pigmented *Tyr*$^{c-2j}$ mice. However, it is worth noting that there was a difference in the overall level of gross pathology between these two models, despite the association of higher level of *in situ* SCC and the absence of mMCP4 observed in both models. This difference in observations is likely due to the difference in genetic background of the mice, where the WBB6F$_1$-*Kit*$^{W/W-v}$ mice consist of a mixed

background of C57BL6J and WB/ReJ whereas *Tyr*$^{c\text{-}2j}$ mice are derived from purely C57BL6J background. It is known that different genetic background between mouse strains is associated with variations in both physiological and pathological processes in these animals, hence it is likely that these mice will respond differently in response to UVB-induced skin damage. Additionally, these discrepancies could also relate to the difference in the nature of the two models, with *Kit*$^{W/W\text{-}v}$ model based on mutations of the c-*kit* receptor followed by reconstitution of BMCMCs, while *Tyr*$^{c\text{-}2j}$ model is based on global knockout of the mMCP4 gene, without affecting specific MC populations. Additionally, to further confirm these findings it would be beneficial to reassess this data, but by engrafting WT or *mMCP4*$^{-/-}$ BMCMCs into the back skin of the mice, as the architeture of back skin is more physiologically relevant compared to ear skin.

Although our data has shown a role of MCs and mMCP4 using the WBB6F$_1$-*Kit*$^{W/W\text{-}v}$ mice, determining the role of MCs using this mouse model is becoming more complicated due to the phenotypic abnormalities associated with mutations of the *c-kit* receptor in these mice, such as deficiencies in melanocyte populations, macrocytic anaemia, sterility, reduced numbers of BM and blood neutrophils, and lack of interstitial cells of Cajal as well as T cell receptor (TCR)γδ cells in the small intestine; and, for the latter, enlarged spleen, mild cardiomegaly, and increased numbers of BM and blood neutrophils[174]. Since the reconstitution of syngeneic BMCMCs is critical to exclude the major impact of genetic alterations independent of the deficiency in MC populations, an alternative way to achieve this without affecting the c-*kit* receptor would be using CPA3;Cre-Mcl-1$^{fl/fl}$ or 'Hello Kitty' mice, which introduce MC-deficiency through deletion of the anti-apoptotic factor Mcl-1 in CPA3 expressing MCs. The use of these mice has confirmed previously published roles of MCs that were initially found through the use of WBB6F$_1$-*Kit*$^{W/W\text{-}v}$ mice[175]. It is well documented that global knockout mouse models are widely used to study the function of MC proteases. As shown by our data, the use of *Tyr*$^{c\text{-}2j}$-*mMCP4*$^{-/-}$ mouse models indeed allow confirmation of the protective function of mMCP4 against UVB-induced *in situ* SCC development. However, there are also limitations associated with global knockout mouse models, similar to the WBB6F$_1$-*Kit*$^{W/W\text{-}v}$ mice. Knockout of a gene globally can have systemic effects on the animal, leading to other changes accumulated throughout pre- and post-natal development, which could complicate the assessment of direct effects due to the loss of this particular gene. Although no significant physiological abnormalities were observed in the *Tyr*$^{c\text{-}2j}$-

mMCP4$^{-/-}$ mice, it is likely that there are changes in these animals that only become evidence upon challenge. Hence, it would also be beneficial to utilise a tissue-specific knockout mouse model. It has been previously shown in mMCP5-Cre:IL-10$^{fl/fl}$, i.e. mice that express Cre recombinase under the mMCP5 promoter gene crossed with IL-10 floxed mice, were able to delete the IL-10 gene specifically in MCs that express mMCP5, which are typically CTMCs localised in the peritoneum and the skin[182,183]. Hence a similar model engineered to remove mMCP4 under control of promoters exclusively expressed in CTMCs in the skin could provide a model for future studies.

Notably, multiple MC-specific proteases are expressed in mice, some of which are likely to share similar substrate specificities with mMCP4[63]. This poses the question whether the loss of mMCP4 could be compensated for by other MC-specific proteases. Furthermore, although it has been reported that the absence of mMCP4 does not cause any changes in endogenous protein levels of mMCP5, 6 and MC-CPA3, the change in activities of these proteases in response to the loss of mMCP4 is yet to be elucidated. It is also possible that the loss of mMCP4 may cause an imbalance of protease activity from mMCP5 or mMCP6, and this effect may only be evident in response to stress or physiological challenge. In addition to regulation of mMCP function via its level of expression and activity, the storage of MC proteases can also play a role. For example, studies have reported that mMCP4, 5, 6 and MC-CPA3 are closely associated through the glycoamniprotein Serglycin (Srg). *Srg*$^{-/-}$ mice exhibit instability in the storage of these proteases [36]. Hence, to address the above mentioned questions, it would be ideal to quantify the intracellular and extracellular levels of additional MC proteases as well as assessing their activities, both under basal and challenged conditions as described in Chapters 3 and 4.

Consistent with the effect of mMCP4 on the gross pathology associated with chronic UVB irradiation, the vasculature was also affected in the absence of mMCP4. Our data presented in Chapter 5 showed that the loss of mMCP4 is associated with aberrant lymphatic vessel function. Our investigation of *Kit*$^{W/W-v}$ mice demonstrated a profound increase in the total number, as well as number of dilated lymphatic vessels, in the absence of MCs and mMCP4. Blood vessel number and dilation was similarly increased in *Kit*$^{W/W-v}$ mice. Notably, a similar trend was observed in *Tyr*$^{c-2j}$-*mMCP4*$^{-/-}$ mice, though only the lymphatic vessel lumen area was statistically significantly elevated in mMCP4 deficient

mice. Importantly, we showed that lymphatic vessels had deficient drainage functions in the absence of mMCP4. Nevertheless, it would be beneficial to also investigate the functional capabilities of lymphatic vessels in the MC-deficient *Kit*$^{W/W\text{-}v}$ and the *mMCP4*$^{-/-}$ BMCMC→*Kit*$^{W/W\text{-}v}$ mice to ensure this coincides with our findings in the *Tyr*$^{c\text{-}2j}$-*mMCP4*$^{-/-}$ mice. Alternatively, when assessing lymphatic drainage functions, the use of fluorescent dyes such as FITC-Dextran in combination with intravital microscopy may be beneficial to allow real time assessment of leakiness of lymphatic vessels. Coinciding, labelling lymphocytes with CFSE could also assist in tracking specific cell populations within the lymphatic system. Together, this will not only show whether the lymphatic vessels are functional, but also provide information on whether certain cell populations are draining efficiently to their sentinel lymph nodes. As we have also shown that a deficiency in the drainage of the myeloid derived suppressor cells (MDSC) cell population may be associated with the loss of mMCP4. Importantly, this finding needs to be further validated by the use of more cell surface markers such as Ly6C^{+}Ly6G^{-} (monocytic) and Ly6G^{+}Ly6C^{-} (granulocytic) to identify specific subtypes of this population. Moreover, if the gross pathology we observed was associated with this abundance of MDSC populations at the site of UVB damage, it would be critical to assess the actual function of these cells by isolating these cells and assessing their immunosuppressive properties *in vitro*[224,454,483].

This study has revealed a potential correlation between dysfunctional lymphatics and UVB-induced skin carcinogenesis. However, this could either be a contributing factor to the damage, or a process that occurs in parallel, and this remains to be further investigated. In aged individuals (>60 years old), Conway and colleagues found a distinct trend of dysfunctional lymphatic vessels, coinciding with a higher rate of melanoma and poorer prognosis. However, interestingly, a lower rate of sentinel lymph node metastasis was observed in this patient cohort[567]. Notably, another study also found larger lesions at the primary site of melanoma in the elderly patient cohort[568]. In comparison, younger patients exhibit better lymphatic vessel function but show higher rates of sentinel lymph node metastases. This suggests a similar correlation to what we observed in Chapter 4 and 5, but in a different context. Elderly patients have poorer physiological and immune functions, and also accumulate more DNA damage and mutations due to a lifetime of exposure to deleterious environmental factors, particularly UVB exposure. These could all contribute to development of malignancies more easily. However, it is possible that

the dysfunction lymphatic vessels is responsible for the lack of metastasis, leading to further accumulation of local ulceration and damage at the primary tumour site. This could explain why an opposite trend was observed in the younger cohorts. Based on the protective function of MCs in UVB-induced skin damage observed by this study [412], it will be of interest to investigate whether MCs and MC-specific proteases are also protective in either patients with lymphatic function deficiency, especially among the elderly individuals. Even though the dynamics of immune responses and interaction between different cell populations and microenvironment differs between elderly and younger patients, this could still provide vital clues as to whether MCs are crucial in regulating lymphatic vessel function in cutaneous malignancies. Interestingly, human chymase polymorphisms have been described associated with various pathological conditions including gastric cancer[569].

Previous studies have shown that mMCP4 can limit morbidity and mortality induced by scorpion venoms, which are structurally similar to VIP[378]. VIP is a neuro- and immunological modulator and has been implicated in negatively regulating lymphatic vessel pumping[456]. As described in Chapter 5, our data, in agreement with the literature, demonstrated that in the absence of mMCP4, high concentrations of VIP result in deficient lymphatic vessel drainage. Surprisingly, although an inefficient lymphatic drainage was observed in the *Tyr*$^{c\text{-}2j}$*-mMCP4*$^{-/-}$ mice, the MDSCs was the only cell population that was differentially affected in these mice. This raises the question whether VIP is specifically targeting this population, or is this mediated through other factors that were also targeted by mMCP4.

It is also worth noting that we observed an increase in the number of Ki67^{+} lymphatic endothelial cells in the UVB-treated ears of *Tyr*$^{c\text{-}2j}$*-mMCP4*$^{-/-}$ compared to WT littermates after 5 exposures of UVB, suggesting a potential mechanism by which the lack of mMCP4 is promoting a deficiency in lymphatic vessel drainage. Hyperproliferation of lymphatic endothelial cells has been correlated with enlargement of lymphatic vessels, which has been suggested to lead to inefficient lymphatic vessel drainage. It is known that mMCP4 can specifically target and degrade endothelial growth factors such as FGF2 and PDGFBB[7], both of which have roles in promoting lymphatic vessel proliferation [455,570,571]. Hence it is possible that the loss of mMCP4 results in accumulation of endothelial growth factors, which leads to hyperproliferation of lymphatic endothelial

cells, and contributes to the enlargement of lymphatic vessels observed in mast cell deficient mice.

mMCP4 is known to target a wide range of substrates that are involved in multiple biological processes. Consistently, as shown by the microarray analysis in Chapter 6, we demonstrated that the loss of mMCP4 results in global changes in various cellular and physiological pathways, particularly in the recruitment of immune cell populations and tissue homeostasis. This supports some previous studies which have shown that mMCP4 can specifically target chemokines such as CCL2[379] and ECM-related factors including MMP-2, MMP-9[384] and fibronectin[7,381]. However, we did not observe changes in other signalling pathways which mMCP4 is known to regulate in various other models. These include TNFα[5], IL-6, IL-13[379], IL-33[572], FGF2 and PDGFBB[7]. Hence it is important to confirm the involvement of these other substrates and their related biological processes in our chronic UVB model, preferably through proteomic analysis.

As processing enzymes with highly specific cleavage of selective substrates, proteases play fundamental roles in various biological and pathological processes, including cancer. Proteases have long been known to aid in all aspects of cancer progression through targeting a diversity of substrates. However, a number of studies have also revealed tumour-suppressive functions of various proteases. By utilising multiple mouse models, this study has demonstrated a protective function of a MC-specific protease, mMCP4, against chronic UVB-induced skin tumourigenesis. The protective function of mMCP4 revealed by this study might imply potential novel strategies for therapeutic interventions against this disease. In order to further exploit the tumour-suppressive function of mMCP4 as a means of either early prevention or tumour intervention, elevating the amount of accessible mMCP4 or enhancing the enzymatic activity of mMCP4 could both be beneficial. A potential approach could include introducing recombinant mMCP4 via nanoparticle delivery system, specifically targeting this enzyme to tumoural microenvironment. It is also possible, via gene therapy and other interventional approaches, to directly increase the gene expression or enhance the enzyme activity of mMCP4. However, each of these potential approaches has their own limitations and will require further investigations and refinement.

As suggested by growing evidence accumulated in the recent decades, the function of MCs is more complicated than originally anticipated. In addition to their roles in host

defence against infections[5,208,374]and toxins[378,375], MCs are well known to positively regulate inflammatory responses[416,573,574]. Moreover, MCs are also known to play a role in negative immunomodulation via supressing the initiation, magnitude and/or duration of immune responses in certain disease settings[8,9,53,184,424]. More importantly, this plasticity of MCs has now attracted growing attention due to their potential therapeutic applications. In order to optimally exploit the protective function of mMCP4 in chronic UVB-induced skin tumourigenesis as revealed in this study, in addition to the direct manipulation of mMCP4 expression/activity as we previously suggested, a more physiological approach could be through manipulation of MCs. By manipulating MCs to produce more mMCP4 at critical time points of UVB-induced skin tumourigenesis, we may be able to limit the potentiation of tumour development at early stages. However, our study did not identify which factors are critical in promoting mMCP4 release, which requires further investigation.

Taken together, this study constitutes a new body of work indicating the protective function of MCs and mMCP4 against chronic UVB-induced development of *in situ* SCCs *in vivo*. Overall, the outcome of this project highlights and confirms the complexity of MC functions in cancer, and importantly, the therapeutic potential of MCs and mMCP4 for the prevention and intervention of UVB-induced skin tumourigenesis.

References

1 el Sayed, S. O. & Dyson, M. Histochemical heterogeneity of mast cells in rat dermis. *Biotech Histochem* **68**, 326-332 (1993).
2 Schulman, E. S., Pollack, R. B., Post, T. J. & Peters, S. P. Histochemical heterogeneity of dispersed human lung mast cells. *Journal of immunology* **144**, 4195-4201 (1990).
3 Galli, S. J. & Tsai, M. IgE and mast cells in allergic disease. *Nature medicine* **18**, 693-704, doi:10.1038/nm.2755 (2012).
4 Theoharides, T. C. & Conti, P. Mast cells: the Jekyll and Hyde of tumor growth. *Trends in immunology* **25**, 235-241, doi:10.1016/j.it.2004.02.013 (2004).
5 Piliponsky, A. M. *et al.* The Chymase Mouse Mast Cell Protease 4 Degrades TNF, Limits Inflammation, and Promotes Survival in a Model of Sepsis. *The American journal of pathology* **181**, 875-886, doi:10.1016/j.ajpath.2012.05.013 (2012).
6 Siebenhaar, F., Metz, M. & Maurer, M. Mast cells protect from skin tumor development and limit tumor growth during cutaneous de novo carcinogenesis in a Kit-dependent mouse model. *Experimental dermatology* **23**, 159-164, doi:10.1111/exd.12328 (2014).
7 Waern, I. *et al.* Mouse mast cell protease 4 is the major chymase in murine airways and has a protective role in allergic airway inflammation. *Journal of immunology* **183**, 6369-6376, doi:10.4049/jimmunol.0900180 (2009).
8 Grimbaldeston, M. A., Nakae, S., Kalesnikoff, J., Tsai, M. & Galli, S. J. Mast cell-derived interleukin 10 limits skin pathology in contact dermatitis and chronic irradiation with ultraviolet B. *Nature immunology* **8**, 1095-1104, doi:10.1038/ni1503 (2007).
9 Biggs, L. *et al.* Evidence that vitamin D(3) promotes mast cell-dependent reduction of chronic UVB-induced skin pathology in mice. *The Journal of experimental medicine* **207**, 455-463, doi:10.1084/jem.20091725 (2010).
10 Yip, K. H. *et al.* Mechanisms of vitamin D(3) metabolite repression of IgE-dependent mast cell activation. *The Journal of allergy and clinical immunology* **133**, 1356-1364, 1364 e1351-1314, doi:10.1016/j.jaci.2013.11.030 (2014).
11 Kirshenbaum, A. S. *et al.* Demonstration that human mast cells arise from a progenitor cell population that is CD34(+), c-kit(+), and expresses aminopeptidase N (CD13). *Blood* **94**, 2333-2342 (1999).
12 Metcalfe, A. D. & Ferguson, M. W. Skin stem and progenitor cells: using regeneration as a tissue-engineering strategy. *Cellular and molecular life sciences : CMLS* **65**, 24-32, doi:10.1007/s00018-007-7427-x (2008).
13 Chen, C. C., Grimbaldeston, M. A., Tsai, M., Weissman, I. L. & Galli, S. J. Identification of mast cell progenitors in adult mice. *Proceedings of the National Academy of Sciences of the United States of America* **102**, 11408-11413, doi:10.1073/pnas.0504197102 (2005).
14 Akashi, K., Traver, D., Miyamoto, T. & Weissman, I. L. A clonogenic common myeloid progenitor that gives rise to all myeloid lineages. *Nature* **404**, 193-197, doi:10.1038/35004599 (2000).
15 Akashi, K., Traver, D. & Zon, L. I. The complex cartography of stem cell commitment. *Cell* **121**, 160-162, doi:10.1016/j.cell.2005.04.005 (2005).
16 Arinobu, Y. *et al.* Developmental checkpoints of the basophil/mast cell lineages in adult murine hematopoiesis. *Proceedings of the National Academy of Sciences of the United States of America* **102**, 18105-18110, doi:10.1073/pnas.0509148102 (2005).
17 Ohmori, K. *et al.* IL-3 induces basophil expansion in vivo by directing granulocyte-monocyte progenitors to differentiate into basophil lineage-restricted progenitors in the bone marrow and by increasing the number of basophil/mast cell progenitors in the spleen. *Journal of immunology* **182**, 2835-2841, doi:10.4049/jimmunol.0802870 (2009).
18 Gurish, M. F. & Austen, K. F. Developmental origin and functional specialization of mast cell subsets. *Immunity* **37**, 25-33, doi:10.1016/j.immuni.2012.07.003 (2012).
19 Franco, C. B., Chen, C. C., Drukker, M., Weissman, I. L. & Galli, S. J. Distinguishing mast cell and granulocyte differentiation at the single-cell level. *Cell stem cell* **6**, 361-368, doi:10.1016/j.stem.2010.02.013 (2010).
20 Maaninka, K., Lappalainen, J. & Kovanen, P. T. Human mast cells arise from a common circulating progenitor. *The Journal of allergy and clinical immunology* **132**, 463-469 e463, doi:10.1016/j.jaci.2013.02.011 (2013).

21 Gurish, M. F. *et al.* Intestinal mast cell progenitors require CD49dbeta7 (alpha4beta7 integrin) for tissue-specific homing. *The Journal of experimental medicine* **194**, 1243-1252 (2001).
22 Hamawy, M. M., Mergenhagen, S. E. & Siraganian, R. P. Adhesion molecules as regulators of mast-cell and basophil function. *Immunology today* **15**, 62-66, doi:10.1016/0167-5699(94)90135-X (1994).
23 Abonia, J. P. *et al.* Constitutive homing of mast cell progenitors to the intestine depends on autologous expression of the chemokine receptor CXCR2. *Blood* **105**, 4308-4313, doi:10.1182/blood-2004-09-3578 (2005).
24 Weller, C. L. *et al.* Leukotriene B4, an activation product of mast cells, is a chemoattractant for their progenitors. *The Journal of experimental medicine* **201**, 1961-1971, doi:10.1084/jem.20042407 (2005).
25 Gurish, M. F. & Boyce, J. A. Mast cells: ontogeny, homing, and recruitment of a unique innate effector cell. *The Journal of allergy and clinical immunology* **117**, 1285-1291, doi:10.1016/j.jaci.2006.04.017 (2006).
26 Jagels, M. A. & Hugli, T. E. Neutrophil chemotactic factors promote leukocytosis. A common mechanism for cellular recruitment from bone marrow. *Journal of immunology* **148**, 1119-1128 (1992).
27 Palframan, R. T. *et al.* Mechanisms of acute eosinophil mobilization from the bone marrow stimulated by interleukin 5: the role of specific adhesion molecules and phosphatidylinositol 3-kinase. *The Journal of experimental medicine* **188**, 1621-1632 (1998).
28 Hart, A. L. *et al.* Homing of immune cells: role in homeostasis and intestinal inflammation. *Inflammatory bowel diseases* **16**, 1969-1977, doi:10.1002/ibd.21304 (2010).
29 Abonia, J. P. *et al.* Alpha-4 integrins and VCAM-1, but not MAdCAM-1, are essential for recruitment of mast cell progenitors to the inflamed lung. *Blood* **108**, 1588-1594, doi:10.1182/blood-2005-12-012781 (2006).
30 Boyce, J. A., Mellor, E. A., Perkins, B., Lim, Y. C. & Luscinskas, F. W. Human mast cell progenitors use alpha4-integrin, VCAM-1, and PSGL-1 E-selectin for adhesive interactions with human vascular endothelium under flow conditions. *Blood* **99**, 2890-2896 (2002).
31 Rosenkranz, A. R. *et al.* Impaired mast cell development and innate immunity in Mac-1 (CD11b/CD18, CR3)-deficient mice. *Journal of immunology* **161**, 6463-6467 (1998).
32 Berlanga, O., Emambokus, N. & Frampton, J. GPIIb (CD41) integrin is expressed on mast cells and influences their adhesion properties. *Experimental hematology* **33**, 403-412, doi:10.1016/j.exphem.2005.01.011 (2005).
33 Poglio, S. *et al.* Adipose tissue as a dedicated reservoir of functional mast cell progenitors. *Stem cells* **28**, 2065-2072, doi:10.1002/stem.523 (2010).
34 Collmann, E. *et al.* Transient targeting of phosphoinositide 3-kinase acts as a roadblock in mast cells' route to allergy. *The Journal of allergy and clinical immunology* **132**, 959-968, doi:10.1016/j.jaci.2013.03.008 (2013).
35 Ronnberg, E., Melo, F. R. & Pejler, G. Mast Cell Proteoglycans. *The journal of histochemistry and cytochemistry : official journal of the Histochemistry Society*, doi:10.1369/0022155412458927 (2012).
36 Ronnberg, E. & Pejler, G. Serglycin: the master of the mast cell. *Methods in molecular biology* **836**, 201-217, doi:10.1007/978-1-61779-498-8_14 (2012).
37 Georgin-Lavialle, S. *et al.* Mast cell leukemia. *Blood* **121**, 1285-1295, doi:10.1182/blood-2012-07-442400 (2013).
38 Nagata, H. *et al.* Identification of a point mutation in the catalytic domain of the protooncogene c-kit in peripheral blood mononuclear cells of patients who have mastocytosis with an associated hematologic disorder. *Proceedings of the National Academy of Sciences of the United States of America* **92**, 10560-10564 (1995).

39 Longley, B. J. *et al.* Somatic c-KIT activating mutation in urticaria pigmentosa and aggressive mastocytosis: establishment of clonality in a human mast cell neoplasm. *Nature genetics* **12**, 312-314, doi:10.1038/ng0396-312 (1996).

40 Collington, S. J. *et al.* The role of the CCL2/CCR2 axis in mouse mast cell migration in vitro and in vivo. *Journal of immunology* **184**, 6114-6123, doi:10.4049/jimmunol.0904177 (2010).

41 Bergot, A. S. *et al.* HPV16-E7 expression in squamous epithelium creates a local immune suppressive environment via CCL2- and CCL5- mediated recruitment of mast cells. *PLoS pathogens* **10**, e1004466, doi:10.1371/journal.ppat.1004466 (2014).

42 Juremalm, M., Olsson, N. & Nilsson, G. Selective CCL5/RANTES-induced mast cell migration through interactions with chemokine receptors CCR1 and CCR4. *Biochemical and biophysical research communications* **297**, 480-485 (2002).

43 Nilsson, G. *et al.* C3a and C5a are chemotaxins for human mast cells and act through distinct receptors via a pertussis toxin-sensitive signal transduction pathway. *Journal of immunology* **157**, 1693-1698 (1996).

44 Hartmann, K. *et al.* C3a and C5a stimulate chemotaxis of human mast cells. *Blood* **89**, 2863-2870 (1997).

45 Weller, C. L. *et al.* Chemotactic action of prostaglandin E2 on mouse mast cells acting via the PGE2 receptor 3. *Proceedings of the National Academy of Sciences of the United States of America* **104**, 11712-11717, doi:10.1073/pnas.0701700104 (2007).

46 Boehme, S. A. *et al.* Murine bone marrow-derived mast cells express chemoattractant receptor-homologous molecule expressed on T-helper class 2 cells (CRTh2). *International immunology* **21**, 621-632, doi:10.1093/intimm/dxp031 (2009).

47 Gruber, B. L., Marchese, M. J. & Kew, R. R. Transforming growth factor-beta 1 mediates mast cell chemotaxis. *Journal of immunology* **152**, 5860-5867 (1994).

48 Olsson, N., Piek, E., ten Dijke, P. & Nilsson, G. Human mast cell migration in response to members of the transforming growth factor-beta family. *Journal of leukocyte biology* **67**, 350-356 (2000).

49 Huang, B. *et al.* SCF-mediated mast cell infiltration and activation exacerbate the inflammation and immunosuppression in tumor microenvironment. *Blood* **112**, 1269-1279, doi:10.1182/blood-2008-03-147033 (2008).

50 Wang, H. W., Tedla, N., Lloyd, A. R., Wakefield, D. & McNeil, P. H. Mast cell activation and migration to lymph nodes during induction of an immune response in mice. *The Journal of clinical investigation* **102**, 1617-1626, doi:10.1172/JCI3704 (1998).

51 Misiak-Tloczek, A. & Brzezinska-Blaszczyk, E. IL-6, but not IL-4, stimulates chemokinesis and TNF stimulates chemotaxis of tissue mast cells: involvement of both mitogen-activated protein kinases and phosphatidylinositol 3-kinase signalling pathways. *APMIS : acta pathologica, microbiologica, et immunologica Scandinavica* **117**, 558-567, doi:10.1111/j.1600-0463.2009.02518.x (2009).

52 Brzezinska-Blaszczyk, E., Pietrzak, A. & Misiak-Tloczek, A. H. Tumor necrosis factor (TNF) is a potent rat mast cell chemoattractant. *Journal of interferon & cytokine research : the official journal of the International Society for Interferon and Cytokine Research* **27**, 911-919, doi:10.1089/jir.2006.0158 (2007).

53 Byrne, S. N., Limon-Flores, A. Y. & Ullrich, S. E. Mast cell migration from the skin to the draining lymph nodes upon ultraviolet irradiation represents a key step in the induction of immune suppression. *Journal of immunology* **180**, 4648-4655 (2008).

54 Byrne, S. N. & Sarchio, S. N. AMD3100 protects from UV-induced skin cancer. *Oncoimmunology* **3**, e27562, doi:10.4161/onci.27562 (2014).

55 Gurish, M. F. & Boyce, J. A. Mast cell growth, differentiation, and death. *Clinical reviews in allergy & immunology* **22**, 107-118, doi:10.1385/CRIAI:22:2:107 (2002).

56 Yokoi, H. *et al.* Comparison of human tonsillar mast cell localization and ultrastructural observations between IgE-mediated allergic and nonallergic donors. *Allergy and asthma proceedings : the official journal of regional and state allergy societies* **27**, 415-421 (2006).

57 Pejler, G., Ronnberg, E., Waern, I. & Wernersson, S. Mast cell proteases: multifaceted regulators of inflammatory disease. *Blood* **115**, 4981-4990, doi:10.1182/blood-2010-01-257287 (2010).
58 McNeil, H. P. *et al.* The mouse mast cell-restricted tetramer-forming tryptases mouse mast cell protease 6 and mouse mast cell protease 7 are critical mediators in inflammatory arthritis. *Arthritis and rheumatism* **58**, 2338-2346, doi:10.1002/art.23639 (2008).
59 Heavey, D. J. *et al.* Generation of leukotriene C4, leukotriene B4, and prostaglandin D2 by immunologically activated rat intestinal mucosa mast cells. *Journal of immunology* **140**, 1953-1957 (1988).
60 Mrabet-Dahbi, S., Metz, M., Dudeck, A., Zuberbier, T. & Maurer, M. Murine mast cells secrete a unique profile of cytokines and prostaglandins in response to distinct TLR2 ligands. *Experimental dermatology* **18**, 437-444 (2009).
61 Andersson, M. K., Enoksson, M., Gallwitz, M. & Hellman, L. The extended substrate specificity of the human mast cell chymase reveals a serine protease with well-defined substrate recognition profile. *International immunology* **21**, 95-104, doi:10.1093/intimm/dxn128 (2009).
62 Andersson, M. K., Karlson, U. & Hellman, L. The extended cleavage specificity of the rodent beta-chymases rMCP-1 and mMCP-4 reveal major functional similarities to the human mast cell chymase. *Molecular immunology* **45**, 766-775, doi:10.1016/j.molimm.2007.06.360 (2008).
63 Pejler, G., Abrink, M., Ringvall, M. & Wernersson, S. Mast cell proteases. *Advances in immunology* **95**, 167-255, doi:10.1016/S0065-2776(07)95006-3 (2007).
64 Freeland, H. S., Schleimer, R. P., Schulman, E. S., Lichtenstein, L. M. & Peters, S. P. Generation of leukotriene B4 by human lung fragments and purified human lung mast cells. *The American review of respiratory disease* **138**, 389-394, doi:10.1164/ajrccm/138.2.389 (1988).
65 Anderson, D. F. *et al.* The relative contribution of mast cell subsets to conjunctival TH2-like cytokines. *Investigative ophthalmology & visual science* **42**, 995-1001 (2001).
66 Moon, T. C. *et al.* Advances in mast cell biology: new understanding of heterogeneity and function. *Mucosal immunology* **3**, 111-128, doi:10.1038/mi.2009.136 (2010).
67 Lee, Y. M. *et al.* Alteration of protease expression phenotype of mouse peritoneal mast cells by changing the microenvironment as demonstrated by in situ hybridization histochemistry. *The American journal of pathology* **153**, 931-936, doi:10.1016/S0002-9440(10)65634-9 (1998).
68 Lennartsson, J. & Ronnstrand, L. Stem cell factor receptor/c-Kit: from basic science to clinical implications. *Physiological reviews* **92**, 1619-1649, doi:10.1152/physrev.00046.2011 (2012).
69 Sawai, N. *et al.* Thrombopoietin augments stem cell factor-dependent growth of human mast cells from bone marrow multipotential hematopoietic progenitors. *Blood* **93**, 3703-3712 (1999).
70 Galli, S. J., Tsai, M. & Wershil, B. K. The c-kit receptor, stem cell factor, and mast cells. What each is teaching us about the others. *The American journal of pathology* **142**, 965-974 (1993).
71 Chabot, B., Stephenson, D. A., Chapman, V. M., Besmer, P. & Bernstein, A. The proto-oncogene c-kit encoding a transmembrane tyrosine kinase receptor maps to the mouse W locus. *Nature* **335**, 88-89, doi:10.1038/335088a0 (1988).
72 Copeland, N. G. *et al.* Mast cell growth factor maps near the steel locus on mouse chromosome 10 and is deleted in a number of steel alleles. *Cell* **63**, 175-183 (1990).
73 Nakano, T., Kanakura, Y., Nakahata, T., Matsuda, H. & Kitamura, Y. Genetically mast cell-deficient W/Wv mice as a tool for studies of differentiation and function of mast cells. *Federation proceedings* **46**, 1920-1923 (1987).
74 Besmer, P. *et al.* The kit-ligand (steel factor) and its receptor c-kit/W: pleiotropic roles in gametogenesis and melanogenesis. *Dev Suppl*, 125-137 (1993).
75 Halaban, R. & Moellmann, G. White mutants in mice shedding light on humans. *The Journal of investigative dermatology* **100**, 176S-185S (1993).

76 Ezoe, K. *et al.* Novel mutations and deletions of the KIT (steel factor receptor) gene in human piebaldism. *American journal of human genetics* **56**, 58-66 (1995).
77 Ma, Y. *et al.* The c-KIT mutation causing human mastocytosis is resistant to STI571 and other KIT kinase inhibitors; kinases with enzymatic site mutations show different inhibitor sensitivity profiles than wild-type kinases and those with regulatory-type mutations. *Blood* **99**, 1741-1744 (2002).
78 Xu, Z. *et al.* Frequent KIT mutations in human gastrointestinal stromal tumors. *Sci Rep* **4**, 5907, doi:10.1038/srep05907 (2014).
79 Xuan, H. *et al.* Somatic mutation of KIT is rare in small cell lung cancer patients from Northeast China. *Histology and histopathology* **29**, 273-278 (2014).
80 Hamaguchi, Y. *et al.* Interleukin 4 as an essential factor for in vitro clonal growth of murine connective tissue-type mast cells. *The Journal of experimental medicine* **165**, 268-273 (1987).
81 Takagi, M. *et al.* Stimulation of mouse connective tissue-type mast cells by hemopoietic stem cell factor, a ligand for the c-kit receptor. *Journal of immunology* **148**, 3446-3453 (1992).
82 Tsuji, K. *et al.* Synergistic action of interleukin-10 (IL-10) with IL-3, IL-4 and stem cell factor on colony formation from murine mast cells in culture. *International journal of hematology* **61**, 51-60 (1995).
83 Kinoshita, T., Sawai, N., Hidaka, E., Yamashita, T. & Koike, K. Interleukin-6 directly modulates stem cell factor-dependent development of human mast cells derived from CD34(+) cord blood cells. *Blood* **94**, 496-508 (1999).
84 Rottem, M., Okada, T., Goff, J. P. & Metcalfe, D. D. Mast cells cultured from the peripheral blood of normal donors and patients with mastocytosis originate from a CD34+/Fc epsilon RI- cell population. *Blood* **84**, 2489-2496 (1994).
85 Wernersson, S. & Pejler, G. Mast cell secretory granules: armed for battle. *Nature reviews. Immunology*, doi:10.1038/nri3690 (2014).
86 Dvorak, A. M. Piecemeal degranulation of basophils and mast cells is effected by vesicular transport of stored secretory granule contents. *Chemical immunology and allergy* **85**, 135-184, doi:10.1159/000086516 (2005).
87 Taylor, A. M., Galli, S. J. & Coleman, J. W. Stem-cell factor, the kit ligand, induces direct degranulation of rat peritoneal mast cells in vitro and in vivo: dependence of the in vitro effect on period of culture and comparisons of stem-cell factor with other mast cell-activating agents. *Immunology* **86**, 427-433 (1995).
88 Subramanian, N. & Bray, M. A. Interleukin 1 releases histamine from human basophils and mast cells in vitro. *Journal of immunology* **138**, 271-275 (1987).
89 Alam, R., Welter, J. B., Forsythe, P. A., Lett-Brown, M. A. & Grant, J. A. Comparative effect of recombinant IL-1, -2, -3, -4, and -6, IFN-gamma, granulocyte-macrophage-colony-stimulating factor, tumor necrosis factor-alpha, and histamine-releasing factors on the secretion of histamine from basophils. *Journal of immunology* **142**, 3431-3435 (1989).
90 Alam, R., Kumar, D., Anderson-Walters, D. & Forsythe, P. A. Macrophage inflammatory protein-1 alpha and monocyte chemoattractant peptide-1 elicit immediate and late cutaneous reactions and activate murine mast cells in vivo. *Journal of immunology* **152**, 1298-1303 (1994).
91 Andoh, A. *et al.* Role of complement activation and mast cell degranulation in the pathogenesis of rapid intestinal ischemia/reperfusion injury in rats. *Digestion* **63 Suppl 1**, 103-107, doi:51920 (2001).
92 Ali, H. Regulation of human mast cell and basophil function by anaphylatoxins C3a and C5a. *Immunology letters* **128**, 36-45, doi:10.1016/j.imlet.2009.10.007 (2010).
93 McNeil, B. D. *et al.* Identification of a mast-cell-specific receptor crucial for pseudo-allergic drug reactions. *Nature*, doi:10.1038/nature14022 (2015).
94 Papadopoulou, N. G. *et al.* Regulation of corticotropin-releasing hormone receptor-2 expression in human cord blood-derived cultured mast cells. *Journal of molecular endocrinology* **35**, R1-8, doi:10.1677/jme.1.01833 (2005).

95 Rychter, J. W. *et al.* CGRP1 receptor activation induces piecemeal release of protease-1 from mouse bone marrow-derived mucosal mast cells. *Neurogastroenterology and motility : the official journal of the European Gastrointestinal Motility Society* **23**, e57-68, doi:10.1111/j.1365-2982.2010.01617.x (2011).
96 Varadaradjalou, S. *et al.* Toll-like receptor 2 (TLR2) and TLR4 differentially activate human mast cells. *European journal of immunology* **33**, 899-906, doi:10.1002/eji.200323830 (2003).
97 Kulka, M. & Metcalfe, D. D. TLR3 activation inhibits human mast cell attachment to fibronectin and vitronectin. *Molecular immunology* **43**, 1579-1586, doi:10.1016/j.molimm.2005.09.019 (2006).
98 Matsushima, H., Yamada, N., Matsue, H. & Shimada, S. TLR3-, TLR7-, and TLR9-mediated production of proinflammatory cytokines and chemokines from murine connective tissue type skin-derived mast cells but not from bone marrow-derived mast cells. *Journal of immunology* **173**, 531-541 (2004).
99 Kandere-Grzybowska, K. *et al.* IL-1 induces vesicular secretion of IL-6 without degranulation from human mast cells. *Journal of immunology* **171**, 4830-4836 (2003).
100 Nakayama, T., Mutsuga, N., Yao, L. & Tosato, G. Prostaglandin E2 promotes degranulation-independent release of MCP-1 from mast cells. *Journal of leukocyte biology* **79**, 95-104, doi:10.1189/jlb.0405226 (2006).
101 Kalesnikoff, J. *et al.* Monomeric IgE stimulates signaling pathways in mast cells that lead to cytokine production and cell survival. *Immunity* **14**, 801-811 (2001).
102 Riley, J. F. Histamine in tissue mast cells. *Science* **118**, 332 (1953).
103 Sjoerdsma, A., Waalkes, T. P. & Weissbach, H. Serotonin and histamine in mast cells. *Science* **125**, 1202-1203 (1957).
104 Thurmond, R. L. Histamine inflammation. Preface. *Advances in experimental medicine and biology* **709**, vii-viii (2010).
105 Hart, P. H. *et al.* Dermal mast cells determine susceptibility to ultraviolet B-induced systemic suppression of contact hypersensitivity responses in mice. *The Journal of experimental medicine* **187**, 2045-2053 (1998).
106 Mohammad-Zadeh, L. F., Moses, L. & Gwaltney-Brant, S. M. Serotonin: a review. *Journal of veterinary pharmacology and therapeutics* **31**, 187-199, doi:10.1111/j.1365-2885.2008.00944.x (2008).
107 Fang, K. C. *et al.* Mast cell expression of gelatinases A and B is regulated by kit ligand and TGF-beta. *Journal of immunology* **162**, 5528-5535 (1999).
108 Pallaoro, M., Fejzo, M. S., Shayesteh, L., Blount, J. L. & Caughey, G. H. Characterization of genes encoding known and novel human mast cell tryptases on chromosome 16p13.3. *The Journal of biological chemistry* **274**, 3355-3362 (1999).
109 Caughey, G. H. *et al.* Characterization of human gamma-tryptases, novel members of the chromosome 16p mast cell tryptase and prostasin gene families. *Journal of immunology* **164**, 6566-6575 (2000).
110 Caughey, G. H. Mast cell tryptases and chymases in inflammation and host defense. *Immunological reviews* **217**, 141-154, doi:10.1111/j.1600-065X.2007.00509.x (2007).
111 Urata, H., Karnik, S. S., Graham, R. M. & Husain, A. Dipeptide processing activates recombinant human prochymase. *The Journal of biological chemistry* **268**, 24318-24322 (1993).
112 Pemberton, A. D. *et al.* Purification and characterization of mouse mast cell proteinase-2 and the differential expression and release of mouse mast cell proteinase-1 and -2 in vivo. *Clinical and experimental allergy : journal of the British Society for Allergy and Clinical Immunology* **33**, 1005-1012 (2003).
113 Schneider, L. A., Schlenner, S. M., Feyerabend, T. B., Wunderlin, M. & Rodewald, H. R. Molecular mechanism of mast cell mediated innate defense against endothelin and snake venom sarafotoxin. *The Journal of experimental medicine* **204**, 2629-2639, doi:10.1084/jem.20071262 (2007).

114 de Souza, D. A., Jr. *et al.* Expression of mast cell proteases correlates with mast cell maturation and angiogenesis during tumor progression. *PloS one* **7**, e40790, doi:10.1371/journal.pone.0040790 (2012).
115 Reynolds, D. S., Gurley, D. S. & Austen, K. F. Cloning and characterization of the novel gene for mast cell carboxypeptidase A. *The Journal of clinical investigation* **89**, 273-282, doi:10.1172/JCI115571 (1992).
116 Reynolds, D. S. *et al.* Cloning of cDNAs that encode human mast cell carboxypeptidase A, and comparison of the protein with mouse mast cell carboxypeptidase A and rat pancreatic carboxypeptidases. *Proceedings of the National Academy of Sciences of the United States of America* **86**, 9480-9484 (1989).
117 Yamagishi, H. *et al.* Basophil-derived mouse mast cell protease 11 induces microvascular leakage and tissue edema in a mast cell-independent manner. *Biochemical and biophysical research communications* **415**, 709-713, doi:10.1016/j.bbrc.2011.10.150 (2011).
118 Ugajin, T. *et al.* Basophils preferentially express mouse Mast Cell Protease 11 among the mast cell tryptase family in contrast to mast cells. *Journal of leukocyte biology* **86**, 1417-1425, doi:10.1189/jlb.0609400 (2009).
119 Lunderius, C. & Hellman, L. Characterization of the gene encoding mouse mast cell protease 8 (mMCP-8), and a comparative analysis of hematopoietic serine protease genes. *Immunogenetics* **53**, 225-232 (2001).
120 Lee, V. *et al.* Cleavage of the carboxyl tail from the G3 domain of aggrecan but not versican and identification of the amino acids involved in the degradation. *The Journal of biological chemistry* **277**, 22279-22288, doi:10.1074/jbc.M110227200 (2002).
121 Chen, L., Yang, B. L., Wu, Y., Yee, A. & Yang, B. B. G3 domains of aggrecan and PG-M/versican form intermolecular disulfide bonds that stabilize cell-matrix interaction. *Biochemistry* **42**, 8332-8341, doi:10.1021/bi034335f (2003).
122 Meen, A. J. *et al.* Serglycin is a major proteoglycan in polarized human endothelial cells and is implicated in the secretion of the chemokine GROalpha/CXCL1. *The Journal of biological chemistry* **286**, 2636-2647, doi:10.1074/jbc.M110.151944 (2011).
123 Kolset, S. O. & Pejler, G. Serglycin: a structural and functional chameleon with wide impact on immune cells. *Journal of immunology* **187**, 4927-4933, doi:10.4049/jimmunol.1100806 (2011).
124 Pejler, G., Abrink, M. & Wernersson, S. Serglycin proteoglycan: regulating the storage and activities of hematopoietic proteases. *BioFactors* **35**, 61-68, doi:10.1002/biof.11 (2009).
125 Gordon, J. R. & Galli, S. J. Release of both preformed and newly synthesized tumor necrosis factor alpha (TNF-alpha)/cachectin by mouse mast cells stimulated via the Fc epsilon RI. A mechanism for the sustained action of mast cell-derived TNF-alpha during IgE-dependent biological responses. *The Journal of experimental medicine* **174**, 103-107 (1991).
126 Kalesnikoff, J. & Galli, S. J. New developments in mast cell biology. *Nature immunology* **9**, 1215-1223, doi:10.1038/ni.f.216 (2008).
127 Kumar, V. & Sharma, A. Mast cells: emerging sentinel innate immune cells with diverse role in immunity. *Molecular immunology* **48**, 14-25, doi:10.1016/j.molimm.2010.07.009 (2010).
128 Nagata, K. *et al.* CRTH2, an orphan receptor of T-helper-2-cells, is expressed on basophils and eosinophils and responds to mast cell-derived factor(s). *FEBS letters* **459**, 195-199 (1999).
129 Hirai, H. *et al.* Prostaglandin D2 selectively induces chemotaxis in T helper type 2 cells, eosinophils, and basophils via seven-transmembrane receptor CRTH2. *The Journal of experimental medicine* **193**, 255-261 (2001).
130 Marone, G., Triggiani, M., Genovese, A. & De Paulis, A. Role of human mast cells and basophils in bronchial asthma. *Advances in immunology* **88**, 97-160, doi:10.1016/S0065-2776(05)88004-6 (2005).

131 Lam, B. K., Penrose, J. F., Freeman, G. J. & Austen, K. F. Expression cloning of a cDNA for human leukotriene C4 synthase, an integral membrane protein conjugating reduced glutathione to leukotriene A4. *Proceedings of the National Academy of Sciences of the United States of America* **91**, 7663-7667 (1994).
132 Ford-Hutchinson, A. W., Bray, M. A., Doig, M. V., Shipley, M. E. & Smith, M. J. Leukotriene B, a potent chemokinetic and aggregating substance released from polymorphonuclear leukocytes. *Nature* **286**, 264-265 (1980).
133 Huang, W. W. *et al.* Molecular and biological characterization of the murine leukotriene B4 receptor expressed on eosinophils. *The Journal of experimental medicine* **188**, 1063-1074 (1998).
134 Serhan, C. N. & Prescott, S. M. The scent of a phagocyte: Advances on leukotriene b(4) receptors. *The Journal of experimental medicine* **192**, F5-8 (2000).
135 Tsai, M., Grimbaldeston, M. & Galli, S. J. Mast cells and immunoregulation/immunomodulation. *Advances in experimental medicine and biology* **716**, 186-211, doi:10.1007/978-1-4419-9533-9_11 (2011).
136 Galli, S. J. *et al.* Mast cells as "tunable" effector and immunoregulatory cells: recent advances. *Annual review of immunology* **23**, 749-786, doi:10.1146/annurev.immunol.21.120601.141025 (2005).
137 Hershko, A. Y. *et al.* Mast cell interleukin-2 production contributes to suppression of chronic allergic dermatitis. *Immunity* **35**, 562-571, doi:10.1016/j.immuni.2011.07.013 (2011).
138 Tsai, M., Tam, S. Y. & Galli, S. J. Distinct patterns of early response gene expression and proliferation in mouse mast cells stimulated by stem cell factor, interleukin-3, or IgE and antigen. *European journal of immunology* **23**, 867-872, doi:10.1002/eji.1830230415 (1993).
139 Castellani, M. L. *et al.* Expression and secretion of CXCL8 (IL-8), release of tryptase and transcription of histidine decarboxylase mRNA by anti-IgE-activated human umbilical cord blood-derived cultured mast cells. *Neuroimmunomodulation* **14**, 97-104, doi:10.1159/000107425 (2007).
140 Johnson, S. A. *et al.* Phosphorylated immunoreceptor signaling motifs (ITAMs) exhibit unique abilities to bind and activate Lyn and Syk tyrosine kinases. *Journal of immunology* **155**, 4596-4603 (1995).
141 Jabril-Cuenod, B. *et al.* Syk-dependent phosphorylation of Shc. A potential link between FcepsilonRI and the Ras/mitogen-activated protein kinase signaling pathway through SOS and Grb2. *The Journal of biological chemistry* **271**, 16268-16272 (1996).
142 Damen, J. E., Ware, M. D., Kalesnikoff, J., Hughes, M. R. & Krystal, G. SHIP's C-terminus is essential for its hydrolysis of PIP3 and inhibition of mast cell degranulation. *Blood* **97**, 1343-1351 (2001).
143 Shenker, B. J. *et al.* Inhibition of mast cell degranulation by a chimeric toxin containing a novel phosphatidylinositol-3,4,5-triphosphate phosphatase. *Molecular immunology* **48**, 203-210, doi:10.1016/j.molimm.2010.08.009 (2010).
144 Galli, S. J., Grimbaldeston, M. & Tsai, M. Immunomodulatory mast cells: negative, as well as positive, regulators of immunity. *Nature reviews. Immunology* **8**, 478-486, doi:10.1038/nri2327 (2008).
145 Kraft, S. & Kinet, J. P. New developments in FcepsilonRI regulation, function and inhibition. *Nature reviews. Immunology* **7**, 365-378, doi:10.1038/nri2072 (2007).
146 Armstrong, S. C. Analysis of mitogen-activated protein kinase activation. *Methods in molecular biology* **315**, 151-163 (2006).
147 Kopec, A., Panaszek, B. & Fal, A. M. Intracellular signaling pathways in IgE-dependent mast cell activation. *Archivum immunologiae et therapiae experimentalis* **54**, 393-401, doi:10.1007/s00005-006-0049-4 (2006).
148 Hata, D. *et al.* Involvement of Bruton's tyrosine kinase in FcepsilonRI-dependent mast cell degranulation and cytokine production. *The Journal of experimental medicine* **187**, 1235-1247 (1998).

149 Kawakami, Y. *et al.* Redundant and opposing functions of two tyrosine kinases, Btk and Lyn, in mast cell activation. *Journal of immunology* **165**, 1210-1219 (2000).
150 Metcalfe, D. D. Mast cells and mastocytosis. *Blood* **112**, 946-956, doi:10.1182/blood-2007-11-078097 (2008).
151 Tsai, M. *et al.* Induction of mast cell proliferation, maturation, and heparin synthesis by the rat c-kit ligand, stem cell factor. *Proceedings of the National Academy of Sciences of the United States of America* **88**, 6382-6386 (1991).
152 Ronnstrand, L. Signal transduction via the stem cell factor receptor/c-Kit. *Cellular and molecular life sciences : CMLS* **61**, 2535-2548, doi:10.1007/s00018-004-4189-6 (2004).
153 Linnekin, D. Early signaling pathways activated by c-Kit in hematopoietic cells. *The international journal of biochemistry & cell biology* **31**, 1053-1074 (1999).
154 Shivakrupa, R. & Linnekin, D. Lyn contributes to regulation of multiple Kit-dependent signaling pathways in murine bone marrow mast cells. *Cellular signalling* **17**, 103-109, doi:10.1016/j.cellsig.2004.06.004 (2005).
155 Samayawardhena, L. A., Hu, J., Stein, P. L. & Craig, A. W. Fyn kinase acts upstream of Shp2 and p38 mitogen-activated protein kinase to promote chemotaxis of mast cells towards stem cell factor. *Cellular signalling* **18**, 1447-1454, doi:10.1016/j.cellsig.2005.11.005 (2006).
156 Iwaki, S. *et al.* Btk plays a crucial role in the amplification of Fc epsilonRI-mediated mast cell activation by kit. *The Journal of biological chemistry* **280**, 40261-40270, doi:10.1074/jbc.M506063200 (2005).
157 Hundley, T. R. *et al.* Kit and FcepsilonRI mediate unique and convergent signals for release of inflammatory mediators from human mast cells. *Blood* **104**, 2410-2417, doi:10.1182/blood-2004-02-0631 (2004).
158 Polajeva, J. *et al.* Mast cell accumulation in glioblastoma with a potential role for stem cell factor and chemokine CXCL12. *PloS one* **6**, e25222, doi:10.1371/journal.pone.0025222 (2011).
159 Gilfillan, A. M. & Rivera, J. The tyrosine kinase network regulating mast cell activation. *Immunological reviews* **228**, 149-169, doi:10.1111/j.1600-065X.2008.00742.x (2009).
160 Hachiya, A., Kobayashi, A., Ohuchi, A., Takema, Y. & Imokawa, G. The paracrine role of stem cell factor/c-kit signaling in the activation of human melanocytes in ultraviolet-B-induced pigmentation. *The Journal of investigative dermatology* **116**, 578-586, doi:10.1046/j.1523-1747.2001.01290.x (2001).
161 Schieven, G. L. & Ledbetter, J. A. Ultraviolet radiation induces differential calcium signals in human peripheral blood lymphocyte subsets. *J Immunother Emphasis Tumor Immunol* **14**, 221-225 (1993).
162 Dickinson, S. E. *et al.* p38 MAP kinase plays a functional role in UVB-induced mouse skin carcinogenesis. *Molecular carcinogenesis* **50**, 469-478, doi:10.1002/mc.20734 (2011).
163 Liu, K. *et al.* Sunlight UV-induced skin cancer relies upon activation of the p38alpha signaling pathway. *Cancer research* **73**, 2181-2188, doi:10.1158/0008-5472.CAN-12-3408 (2013).
164 Hafner, C., Landthaler, M. & Vogt, T. Activation of the PI3K/AKT signalling pathway in non-melanoma skin cancer is not mediated by oncogenic PIK3CA and AKT1 hotspot mutations. *Experimental dermatology* **19**, e222-227, doi:10.1111/j.1600-0625.2009.01056.x (2010).
165 Butterfield, J. H., Weiler, D., Dewald, G. & Gleich, G. J. Establishment of an immature mast cell line from a patient with mast cell leukemia. *Leukemia research* **12**, 345-355 (1988).
166 Kirshenbaum, A. S. *et al.* Characterization of novel stem cell factor responsive human mast cell lines LAD 1 and 2 established from a patient with mast cell sarcoma/leukemia; activation following aggregation of FcepsilonRI or FcgammaRI. *Leukemia research* **27**, 677-682 (2003).
167 Boesiger, J. *et al.* Mast cells can secrete vascular permeability factor/ vascular endothelial cell growth factor and exhibit enhanced release after immunoglobulin E-dependent

upregulation of fc epsilon receptor I expression. *The Journal of experimental medicine* **188**, 1135-1145 (1998).

168 Razin, E. *et al.* Interleukin 3: A differentiation and growth factor for the mouse mast cell that contains chondroitin sulfate E proteoglycan. *Journal of immunology* **132**, 1479-1486 (1984).

169 Levi-Schaffer, F. *et al.* Mouse bone marrow-derived mast cells cocultured with fibroblasts. Morphology and stimulation-induced release of histamine, leukotriene B4, leukotriene C4, and prostaglandin D2. *Journal of immunology* **139**, 3431-3441 (1987).

170 Dvorak, A. M., Seder, R. A., Paul, W. E., Morgan, E. S. & Galli, S. J. Effects of interleukin-3 with or without the c-kit ligand, stem cell factor, on the survival and cytoplasmic granule formation of mouse basophils and mast cells in vitro. *The American journal of pathology* **144**, 160-170 (1994).

171 Haig, D. M. *et al.* Effects of stem cell factor (kit-ligand) and interleukin-3 on the growth and serine proteinase expression of rat bone-marrow-derived or serosal mast cells. *Blood* **83**, 72-83 (1994).

172 Rottem, M., Goff, J. P., Albert, J. P. & Metcalfe, D. D. The effects of stem cell factor on the ultrastructure of Fc epsilon RI+ cells developing in IL-3-dependent murine bone marrow-derived cell cultures. *Journal of immunology* **151**, 4950-4963 (1993).

173 Galli, S. J. & Kitamura, Y. Genetically mast-cell-deficient W/Wv and Sl/Sld mice. Their value for the analysis of the roles of mast cells in biologic responses in vivo. *The American journal of pathology* **127**, 191-198 (1987).

174 Grimbaldeston, M. A. *et al.* Mast cell-deficient W-sash c-kit mutant Kit W-sh/W-sh mice as a model for investigating mast cell biology in vivo. *The American journal of pathology* **167**, 835-848, doi:10.1016/S0002-9440(10)62055-X (2005).

175 Reber, L. L., Marichal, T. & Galli, S. J. New models for analyzing mast cell functions in vivo. *Trends in immunology* **33**, 613-625, doi:10.1016/j.it.2012.09.008 (2012).

176 Tsai, M., Grimbaldeston, M. A., Yu, M., Tam, S. Y. & Galli, S. J. Using mast cell knock-in mice to analyze the roles of mast cells in allergic responses in vivo. *Chemical immunology and allergy* **87**, 179-197, doi:10.1159/000087644 (2005).

177 Kawakami, T. A crucial door to the mast cell mystery knocked in. *Journal of immunology* **183**, 6861-6862, doi:10.4049/jimmunol.0990101 (2009).

178 Lilla, J. N. *et al.* Reduced mast cell and basophil numbers and function in Cpa3-Cre; Mcl-1fl/fl mice. *Blood* **118**, 6930-6938, doi:10.1182/blood-2011-03-343962 (2011).

179 Steimer, D. A. *et al.* Selective roles for antiapoptotic MCL-1 during granulocyte development and macrophage effector function. *Blood* **113**, 2805-2815, doi:10.1182/blood-2008-05-159145 (2009).

180 Feyerabend, T. B. *et al.* Loss of histochemical identity in mast cells lacking carboxypeptidase A. *Molecular and cellular biology* **25**, 6199-6210, doi:10.1128/MCB.25.14.6199-6210.2005 (2005).

181 Feyerabend, T. B. *et al.* Cre-mediated cell ablation contests mast cell contribution in models of antibody- and T cell-mediated autoimmunity. *Immunity* **35**, 832-844, doi:10.1016/j.immuni.2011.09.015 (2011).

182 Scholten, J. *et al.* Mast cell-specific Cre/loxP-mediated recombination in vivo. *Transgenic research* **17**, 307-315, doi:10.1007/s11248-007-9153-4 (2008).

183 Dudeck, A. *et al.* Mast cells are key promoters of contact allergy that mediate the adjuvant effects of haptens. *Immunity* **34**, 973-984, doi:10.1016/j.immuni.2011.03.028 (2011).

184 Chan, C. Y., St John, A. L. & Abraham, S. N. Mast cell interleukin-10 drives localized tolerance in chronic bladder infection. *Immunity* **38**, 349-359, doi:10.1016/j.immuni.2012.10.019 (2013).

185 Reber, L. L. *et al.* Selective ablation of mast cells or basophils reduces peanut-induced anaphylaxis in mice. *The Journal of allergy and clinical immunology* **132**, 881-888 e881-811, doi:10.1016/j.jaci.2013.06.008 (2013).

186 Ronnberg, E. *et al.* Mast cells are activated by Staphylococcus aureus in vitro but do not influence the outcome of intraperitoneal S. aureus infection in vivo. *Immunology* **143**, 155-163, doi:10.1111/imm.12297 (2014).

187 Ronnberg, E., Guss, B. & Pejler, G. Infection of mast cells with live streptococci causes a toll-like receptor 2- and cell-cell contact-dependent cytokine and chemokine response. *Infection and immunity* **78**, 854-864, doi:10.1128/IAI.01004-09 (2010).
188 Heger, K. *et al.* A20-deficient mast cells exacerbate inflammatory responses in vivo. *PLoS biology* **12**, e1001762, doi:10.1371/journal.pbio.1001762 (2014).
189 Noli, C. & Miolo, A. The mast cell in wound healing. *Veterinary dermatology* **12**, 303-313 (2001).
190 Egozi, E. I., Ferreira, A. M., Burns, A. L., Gamelli, R. L. & Dipietro, L. A. Mast cells modulate the inflammatory but not the proliferative response in healing wounds. *Wound repair and regeneration : official publication of the Wound Healing Society [and] the European Tissue Repair Society* **11**, 46-54 (2003).
191 Weller, K., Foitzik, K., Paus, R., Syska, W. & Maurer, M. Mast cells are required for normal healing of skin wounds in mice. *FASEB journal : official publication of the Federation of American Societies for Experimental Biology* **20**, 2366-2368, doi:10.1096/fj.06-5837fje (2006).
192 Ng, M. F. The role of mast cells in wound healing. *Int Wound J* **7**, 55-61, doi:10.1111/j.1742-481X.2009.00651.x (2010).
193 Willenborg, S. *et al.* Genetic ablation of mast cells redefines the role of mast cells in skin wound healing and bleomycin-induced fibrosis. *The Journal of investigative dermatology* **134**, 2005-2015, doi:10.1038/jid.2014.12 (2014).
194 Tchougounova, E., Pejler, G. & Abrink, M. The chymase, mouse mast cell protease 4, constitutes the major chymotrypsin-like activity in peritoneum and ear tissue. A role for mouse mast cell protease 4 in thrombin regulation and fibronectin turnover. *The Journal of experimental medicine* **198**, 423-431, doi:10.1084/jem.20030671 (2003).
195 Hagaman, D. D. *et al.* Secretion of interleukin-1 receptor antagonist from human mast cells after immunoglobulin E-mediated activation and after segmental antigen challenge. *American journal of respiratory cell and molecular biology* **25**, 685-691 (2001).
196 Bradding, P., Walls, A. F. & Holgate, S. T. The role of the mast cell in the pathophysiology of asthma. *J Allergy Clin Immun* **117**, 1277-1284, doi:DOI 10.1016/j.jaci.2006.02.039 (2006).
197 Wershil, B. K., Furuta, G. T., Wang, Z. S. & Galli, S. J. Mast cell-dependent neutrophil and mononuclear cell recruitment in immunoglobulin E-induced gastric reactions in mice. *Gastroenterology* **110**, 1482-1490 (1996).
198 Biedermann, T. *et al.* Mast cells control neutrophil recruitment during T cell-mediated delayed-type hypersensitivity reactions through tumor necrosis factor and macrophage inflammatory protein 2. *The Journal of experimental medicine* **192**, 1441-1452 (2000).
199 Velin, D., Bachmann, D., Bouzourene, H. & Michetti, P. Mast cells are critical mediators of vaccine-induced Helicobacter clearance in the mouse model. *Gastroenterology* **129**, 142-155 (2005).
200 Jolly, S., Detilleux, J. & Desmecht, D. Extensive mast cell degranulation in bovine respiratory syncytial virus-associated paroxystic respiratory distress syndrome. *Veterinary immunology and immunopathology* **97**, 125-136 (2004).
201 Lantz, C. S. *et al.* Role for interleukin-3 in mast-cell and basophil development and in immunity to parasites. *Nature* **392**, 90-93, doi:10.1038/32190 (1998).
202 Lantz, C. S. *et al.* IL-3 is required for increases in blood basophils in nematode infection in mice and can enhance IgE-dependent IL-4 production by basophils in vitro. *Laboratory investigation; a journal of technical methods and pathology* **88**, 1134-1142, doi:10.1038/labinvest.2008.88 (2008).
203 Ha, T. Y., Reed, N. D. & Crowle, P. K. Delayed expulsion of adult Trichinella spiralis by mast cell-deficient W/Wv mice. *Infection and immunity* **41**, 445-447 (1983).
204 Anthony, R. M., Rutitzky, L. I., Urban, J. F., Jr., Stadecker, M. J. & Gause, W. C. Protective immune mechanisms in helminth infection. *Nature reviews. Immunology* **7**, 975-987, doi:10.1038/nri2199 (2007).

205 Roediger, B. *et al.* Cutaneous immunosurveillance and regulation of inflammation by group 2 innate lymphoid cells. *Nature immunology* **14**, 564-573, doi:10.1038/ni.2584 (2013).
206 Lawrence, C. E., Paterson, Y. Y., Wright, S. H., Knight, P. A. & Miller, H. R. Mouse mast cell protease-1 is required for the enteropathy induced by gastrointestinal helminth infection in the mouse. *Gastroenterology* **127**, 155-165 (2004).
207 McDermott, J. R. *et al.* Mast cells disrupt epithelial barrier function during enteric nematode infection. *Proceedings of the National Academy of Sciences of the United States of America* **100**, 7761-7766, doi:10.1073/pnas.1231488100 (2003).
208 Shin, K. *et al.* Mouse mast cell tryptase mMCP-6 is a critical link between adaptive and innate immunity in the chronic phase of Trichinella spiralis infection. *Journal of immunology* **180**, 4885-4891 (2008).
209 Wei, O. L., Hilliard, A., Kalman, D. & Sherman, M. Mast cells limit systemic bacterial dissemination but not colitis in response to Citrobacter rodentium. *Infection and immunity* **73**, 1978-1985, doi:10.1128/IAI.73.4.1978-1985.2005 (2005).
210 Malaviya, R., Ikeda, T., Ross, E. & Abraham, S. N. Mast cell modulation of neutrophil influx and bacterial clearance at sites of infection through TNF-alpha. *Nature* **381**, 77-80, doi:10.1038/381077a0 (1996).
211 Mannel, D. N., Hultner, L. & Echtenacher, B. Critical protective role of mast cell-derived tumour necrosis factor in bacterial infection. *Research in immunology* **147**, 491-493 (1996).
212 Di Nardo, A., Yamasaki, K., Dorschner, R. A., Lai, Y. & Gallo, R. L. Mast cell cathelicidin antimicrobial peptide prevents invasive group A Streptococcus infection of the skin. *Journal of immunology* **180**, 7565-7573 (2008).
213 Orinska, Z. *et al.* TLR3-induced activation of mast cells modulates CD8+ T-cell recruitment. *Blood* **106**, 978-987, doi:10.1182/blood-2004-07-2656 (2005).
214 Cho, J. J., Vliagoftis, H., Rumsaeng, V., Metcalfe, D. D. & Oh, C. K. Identification and categorization of inducible mast cell genes in a subtraction library. *Biochemical and biophysical research communications* **242**, 226-230, doi:10.1006/bbrc.1997.7644 (1998).
215 Kulka, M., Alexopoulou, L., Flavell, R. A. & Metcalfe, D. D. Activation of mast cells by double-stranded RNA: evidence for activation through Toll-like receptor 3. *The Journal of allergy and clinical immunology* **114**, 174-182, doi:10.1016/j.jaci.2004.03.049 (2004).
216 St John, A. L. *et al.* Immune surveillance by mast cells during dengue infection promotes natural killer (NK) and NKT-cell recruitment and viral clearance. *Proceedings of the National Academy of Sciences of the United States of America* **108**, 9190-9195, doi:10.1073/pnas.1105079108 (2011).
217 Bannert, N. *et al.* Human Mast cell progenitors can be infected by macrophagetropic human immunodeficiency virus type 1 and retain virus with maturation in vitro. *Journal of virology* **75**, 10808-10814, doi:10.1128/JVI.75.22.10808-10814.2001 (2001).
218 Marone, G. *et al.* Are mast cells MASTers in HIV-1 infection? *International archives of allergy and immunology* **125**, 89-95, doi:53802 (2001).
219 Li, Y. *et al.* Mast cells/basophils in the peripheral blood of allergic individuals who are HIV-1 susceptible due to their surface expression of CD4 and the chemokine receptors CCR3, CCR5, and CXCR4. *Blood* **97**, 3484-3490 (2001).
220 Lu, L. F. *et al.* Mast cells are essential intermediaries in regulatory T-cell tolerance. *Nature* **442**, 997-1002, doi:10.1038/nature05010 (2006).
221 Boerma, M. *et al.* Influence of mast cells on outcome after heterotopic cardiac transplantation in rats. *Transplant international : official journal of the European Society for Organ Transplantation* **20**, 256-265, doi:10.1111/j.1432-2277.2006.00420.x (2007).
222 de Vries, V. C. *et al.* Mast cell degranulation breaks peripheral tolerance. *American journal of transplantation : official journal of the American Society of Transplantation and the American Society of Transplant Surgeons* **9**, 2270-2280, doi:10.1111/j.1600-6143.2009.02755.x (2009).
223 Chacon-Salinas, R., Limon-Flores, A. Y., Chavez-Blanco, A. D., Gonzalez-Estrada, A. & Ullrich, S. E. Mast cell-derived IL-10 suppresses germinal center formation by

affecting T follicular helper cell function. *Journal of immunology* **186**, 25-31, doi:10.4049/jimmunol.1001657 (2011).

224 Li, G. *et al.* Vasoactive intestinal peptide induces CD14+HLA-DR/low myeloid-derived suppressor cells in gastric cancer. *Mol Med Rep* **12**, 760-768, doi:10.3892/mmr.2015.3374 (2015).

225 Hanahan, D. & Weinberg, R. A. Hallmarks of cancer: the next generation. *Cell* **144**, 646-674, doi:10.1016/j.cell.2011.02.013 (2011).

226 Hanahan, D. & Coussens, L. M. Accessories to the crime: functions of cells recruited to the tumor microenvironment. *Cancer cell* **21**, 309-322, doi:10.1016/j.ccr.2012.02.022 (2012).

227 Rigoni, A., Colombo, M. P. & Pucillo, C. The Role of Mast Cells in Molding the Tumor Microenvironment. *Cancer Microenviron* **8**, 167-176, doi:10.1007/s12307-014-0152-8 (2015).

228 Galli, S. J., Borregaard, N. & Wynn, T. A. Phenotypic and functional plasticity of cells of innate immunity: macrophages, mast cells and neutrophils. *Nature immunology* **12**, 1035-1044, doi:10.1038/ni.2109 (2011).

229 Blair, R. J. *et al.* Human mast cells stimulate vascular tube formation. Tryptase is a novel, potent angiogenic factor. *The Journal of clinical investigation* **99**, 2691-2700, doi:10.1172/JCI119458 (1997).

230 Duncan, L. M., Richards, L. A. & Mihm, M. C., Jr. Increased mast cell density in invasive melanoma. *Journal of cutaneous pathology* **25**, 11-15 (1998).

231 Diaconu, N. C. *et al.* Increase in CD30 ligand/CD153 and TNF-alpha expressing mast cells in basal cell carcinoma. *Cancer immunology, immunotherapy : CII* **56**, 1407-1415, doi:10.1007/s00262-007-0290-7 (2007).

232 Starkey, J. R., Crowle, P. K. & Taubenberger, S. Mast-cell-deficient W/Wv mice exhibit a decreased rate of tumor angiogenesis. *International journal of cancer. Journal international du cancer* **42**, 48-52 (1988).

233 Wedemeyer, J. & Galli, S. J. Decreased susceptibility of mast cell-deficient Kit(W)/Kit(W-v) mice to the development of 1, 2-dimethylhydrazine-induced intestinal tumors. *Laboratory investigation; a journal of technical methods and pathology* **85**, 388-396, doi:10.1038/labinvest.3700232 (2005).

234 Soucek, L. *et al.* Mast cells are required for angiogenesis and macroscopic expansion of Myc-induced pancreatic islet tumors. *Nature medicine* **13**, 1211-1218, doi:10.1038/nm1649 (2007).

235 Pittoni, P. *et al.* Mast cell targeting hampers prostate adenocarcinoma development but promotes the occurrence of highly malignant neuroendocrine cancers. *Cancer research* **71**, 5987-5997, doi:10.1158/0008-5472.CAN-11-1637 (2011).

236 Coussens, L. M. *et al.* Inflammatory mast cells up-regulate angiogenesis during squamous epithelial carcinogenesis. *Genes & development* **13**, 1382-1397 (1999).

237 Sinnamon, M. J. *et al.* A protective role of mast cells in intestinal tumorigenesis. *Carcinogenesis* **29**, 880-886, doi:10.1093/carcin/bgn040 (2008).

238 Feoktistov, I., Ryzhov, S., Goldstein, A. E. & Biaggioni, I. Mast cell-mediated stimulation of angiogenesis: cooperative interaction between A2B and A3 adenosine receptors. *Circulation research* **92**, 485-492, doi:10.1161/01.RES.0000061572.10929.2D (2003).

239 Diaconu, N. C., Kaminska, R., Naukkarinen, A., Harvima, R. J. & Harvima, I. T. The increase in tryptase- and chymase-positive mast cells is associated with partial inactivation of chymase and increase in protease inhibitors in basal cell carcinoma. *Journal of the European Academy of Dermatology and Venereology : JEADV* **21**, 908-915, doi:10.1111/j.1468-3083.2006.02100.x (2007).

240 Medina, V. *et al.* Histamine-mediated signaling processes in human malignant mammary cells. *Cancer biology & therapy* **5**, 1462-1471 (2006).

241 Blaya, B. *et al.* Histamine and histamine receptor antagonists in cancer biology. *Inflammation & allergy drug targets* **9**, 146-157 (2010).

242 Hart, P. H., Grimbaldeston, M. A., Swift, G. J., Hosszu, E. K. & Finlay-Jones, J. J. A critical role for dermal mast cells in cis-urocanic acid-induced systemic suppression of contact hypersensitivity responses in mice. *Photochemistry and photobiology* **70**, 807-812 (1999).
243 Hart, P. H., Townley, S. L., Grimbaldeston, M. A., Khalil, Z. & Finlay-Jones, J. J. Mast cells, neuropeptides, histamine, and prostaglandins in UV-induced systemic immunosuppression. *Methods* **28**, 79-89 (2002).
244 Hart, P. H., Grimbaldeston, M. A. & Finlay-Jones, J. J. Sunlight, immunosuppression and skin cancer: role of histamine and mast cells. *Clinical and experimental pharmacology & physiology* **28**, 1-8 (2001).
245 Ribatti, D. & Crivellato, E. Mast cells, angiogenesis and cancer. *Advances in experimental medicine and biology* **716**, 270-288, doi:10.1007/978-1-4419-9533-9_14 (2011).
246 Samoszuk, M., Kanakubo, E. & Chan, J. K. Degranulating mast cells in fibrotic regions of human tumors and evidence that mast cell heparin interferes with the growth of tumor cells through a mechanism involving fibroblasts. *BMC cancer* **5**, 121, doi:10.1186/1471-2407-5-121 (2005).
247 Yang, X. D. *et al.* Histamine deficiency promotes inflammation-associated carcinogenesis through reduced myeloid maturation and accumulation of CD11b+Ly6G+ immature myeloid cells. *Nature medicine* **17**, 87-95, doi:10.1038/nm.2278 (2011).
248 Oldford, S. A. *et al.* A critical role for mast cells and mast cell-derived IL-6 in TLR2-mediated inhibition of tumor growth. *Journal of immunology* **185**, 7067-7076, doi:10.4049/jimmunol.1001137 (2010).
249 Maltby, S., Khazaie, K. & McNagny, K. M. Mast cells in tumor growth: angiogenesis, tissue remodelling and immune-modulation. *Biochimica et biophysica acta* **1796**, 19-26, doi:10.1016/j.bbcan.2009.02.001 (2009).
250 Lazar-Molnar, E. *et al.* Inhibition of human primary melanoma cell proliferation by histamine is enhanced by interleukin-6. *European journal of clinical investigation* **32**, 743-749 (2002).
251 Dixon, K. M. *et al.* Differential photoprotective effects of 1,25-dihydroxyvitamin D3 and a low calcaemic deltanoid. *Photochemical & photobiological sciences : Official journal of the European Photochemistry Association and the European Society for Photobiology* **11**, 1825-1830, doi:10.1039/c2pp25208b (2012).
252 Dixon, K. M. *et al.* 1alpha,25(OH)(2)-vitamin D and a nongenomic vitamin D analogue inhibit ultraviolet radiation-induced skin carcinogenesis. *Cancer prevention research* **4**, 1485-1494, doi:10.1158/1940-6207.CAPR-11-0165 (2011).
253 Gupta, R. *et al.* Photoprotection by 1,25 dihydroxyvitamin D3 is associated with an increase in p53 and a decrease in nitric oxide products. *The Journal of investigative dermatology* **127**, 707-715, doi:10.1038/sj.jid.5700597 (2007).
254 Tongkao-On, W. *et al.* CYP11A1 in skin: An alternative route to photoprotection by vitamin D compounds. *The Journal of steroid biochemistry and molecular biology* **148**, 72-78, doi:10.1016/j.jsbmb.2014.11.015 (2015).
255 Song, E. J. *et al.* 1alpha,25-Dihydroxyvitamin D3 reduces several types of UV-induced DNA damage and contributes to photoprotection. *The Journal of steroid biochemistry and molecular biology* **136**, 131-138, doi:10.1016/j.jsbmb.2012.11.003 (2013).
256 Dixon, K. M. *et al.* Skin cancer prevention: a possible role of 1,25dihydroxyvitamin D3 and its analogs. *The Journal of steroid biochemistry and molecular biology* **97**, 137-143, doi:10.1016/j.jsbmb.2005.06.006 (2005).
257 Dixon, K. M. *et al.* In vivo relevance for photoprotection by the vitamin D rapid response pathway. *The Journal of steroid biochemistry and molecular biology* **103**, 451-456, doi:10.1016/j.jsbmb.2006.11.016 (2007).
258 McGee, H., Scott, D. K. & Woods, G. M. Neonatal exposure to UV-B radiation leads to a large reduction in Langerhans cell density, but by maturity, there is an enhanced ability of dendritic cells to stimulate T cells. *Immunology and cell biology* **84**, 259-266, doi:10.1111/j.1440-1711.2006.01429.x (2006).

259 Muller, H. K. *et al.* Effect of UV radiation on the neonatal skin immune system-implications for melanoma. *Photochemistry and photobiology* **84**, 47-54, doi:10.1111/j.1751-1097.2007.00246.x (2008).
260 Nakazawa, H. *et al.* UV and skin cancer: specific p53 gene mutation in normal skin as a biologically relevant exposure measurement. *Proceedings of the National Academy of Sciences of the United States of America* **91**, 360-364 (1994).
261 Ren, Z. P., Ponten, F., Nister, M. & Ponten, J. Two distinct p53 immunohistochemical patterns in human squamous-cell skin cancer, precursors and normal epidermis. *International journal of cancer. Journal international du cancer* **69**, 174-179, doi:10.1002/(SICI)1097-0215(19960621)69:3<174::AID-IJC4>3.0.CO;2-X (1996).
262 Kanjilal, S. *et al.* p53 mutations in nonmelanoma skin cancer of the head and neck: molecular evidence for field cancerization. *Cancer research* **55**, 3604-3609 (1995).
263 Brash, D. E. *et al.* Sunlight and sunburn in human skin cancer: p53, apoptosis, and tumor promotion. *The journal of investigative dermatology. Symposium proceedings / the Society for Investigative Dermatology, Inc. [and] European Society for Dermatological Research* **1**, 136-142 (1996).
264 Melnikova, V. O., Pacifico, A., Chimenti, S., Peris, K. & Ananthaswamy, H. N. Fate of UVB-induced p53 mutations in SKH-hr1 mouse skin after discontinuation of irradiation: relationship to skin cancer development. *Oncogene* **24**, 7055-7063, doi:10.1038/sj.onc.1208863 (2005).
265 Hufbauer, M. *et al.* Human papillomavirus mediated inhibition of DNA damage sensing and repair drives skin carcinogenesis. *Molecular cancer* **14**, 183, doi:10.1186/s12943-015-0453-7 (2015).
266 Masset, A. *et al.* Unimpeded skin carcinogenesis in K14-HPV16 transgenic mice deficient for plasminogen activator inhibitor. *International journal of cancer. Journal international du cancer* **128**, 283-293, doi:10.1002/ijc.25326 (2011).
267 Coussens, L. M., Tinkle, C. L., Hanahan, D. & Werb, Z. MMP-9 supplied by bone marrow-derived cells contributes to skin carcinogenesis. *Cell* **103**, 481-490 (2000).
268 Abel, E. L., Angel, J. M., Kiguchi, K. & DiGiovanni, J. Multi-stage chemical carcinogenesis in mouse skin: fundamentals and applications. *Nature protocols* **4**, 1350-1362, doi:10.1038/nprot.2009.120 (2009).
269 Boshart, M. *et al.* A new type of papillomavirus DNA, its presence in genital cancer biopsies and in cell lines derived from cervical cancer. *The EMBO journal* **3**, 1151-1157 (1984).
270 Walboomers, J. M. *et al.* Human papillomavirus is a necessary cause of invasive cervical cancer worldwide. *The Journal of pathology* **189**, 12-19, doi:10.1002/(SICI)1096-9896(199909)189:1<12::AID-PATH431>3.0.CO;2-F (1999).
271 Pfister, H. & Ter Schegget, J. Role of HPV in cutaneous premalignant and malignant tumors. *Clinics in dermatology* **15**, 335-347 (1997).
272 Boxman, I. L. *et al.* Transduction of the E6 and E7 genes of epidermodysplasia-verruciformis-associated human papillomaviruses alters human keratinocyte growth and differentiation in organotypic cultures. *The Journal of investigative dermatology* **117**, 1397-1404, doi:10.1046/j.0022-202x.2001.01602.x (2001).
273 Giampieri, S., Garcia-Escudero, R., Green, J. & Storey, A. Human papillomavirus type 77 E6 protein selectively inhibits p53-dependent transcription of proapoptotic genes following UV-B irradiation. *Oncogene* **23**, 5864-5870, doi:10.1038/sj.onc.1207711 (2004).
274 Billecke, C. A. *et al.* Lack of functional pRb results in attenuated recovery of mRNA synthesis and increased apoptosis following UV radiation in human breast cancer cells. *Oncogene* **21**, 4481-4489, doi:10.1038/sj.onc.1205546 (2002).
275 Ananthaswamy, H. N. *et al.* Persistence of p53 mutations and resistance of keratinocytes to apoptosis are associated with the increased susceptibility of mice lacking the XPC gene to UV carcinogenesis. *Oncogene* **18**, 7395-7398, doi:10.1038/sj.onc.1203147 (1999).

276 Ouhtit, A. *et al.* Loss of Fas-ligand expression in mouse keratinocytes during UV carcinogenesis. *The American journal of pathology* **157**, 1975-1981, doi:10.1016/S0002-9440(10)64836-5 (2000).
277 Daniel, D. *et al.* Immune enhancement of skin carcinogenesis by CD4+ T cells. *The Journal of experimental medicine* **197**, 1017-1028, doi:10.1084/jem.20021047 (2003).
278 Boccardo, E., Lepique, A. P. & Villa, L. L. The role of inflammation in HPV carcinogenesis. *Carcinogenesis* **31**, 1905-1912, doi:10.1093/carcin/bgq176 (2010).
279 Loeb, L. A. & Harris, C. C. Advances in chemical carcinogenesis: a historical review and prospective. *Cancer research* **68**, 6863-6872, doi:10.1158/0008-5472.CAN-08-2852 (2008).
280 Rundhaug, J. E. & Fischer, S. M. Molecular mechanisms of mouse skin tumor promotion. *Cancers* **2**, 436-482, doi:10.3390/cancers2020436 (2010).
281 Luch, A. Nature and nurture - lessons from chemical carcinogenesis. *Nature reviews. Cancer* **5**, 113-125, doi:10.1038/nrc1546 (2005).
282 Spalding, J. W., Momma, J., Elwell, M. R. & Tennant, R. W. Chemically induced skin carcinogenesis in a transgenic mouse line (TG.AC) carrying a v-Ha-ras gene. *Carcinogenesis* **14**, 1335-1341 (1993).
283 Hennings, H. & Boutwell, R. K. Studies on the mechanism of skin tumor promotion. *Cancer research* **30**, 312-320 (1970).
284 Griner, E. M. & Kazanietz, M. G. Protein kinase C and other diacylglycerol effectors in cancer. *Nature reviews. Cancer* **7**, 281-294, doi:10.1038/nrc2110 (2007).
285 Blumberg, P. M. Protein kinase C as the receptor for the phorbol ester tumor promoters: sixth Rhoads memorial award lecture. *Cancer research* **48**, 1-8 (1988).
286 Cohen, E. E. *et al.* Protein kinase C zeta mediates epidermal growth factor-induced growth of head and neck tumor cells by regulating mitogen-activated protein kinase. *Cancer research* **66**, 6296-6303, doi:10.1158/0008-5472.CAN-05-3139 (2006).
287 Rho, O., Beltran, L. M., Gimenez-Conti, I. B. & DiGiovanni, J. Altered expression of the epidermal growth factor receptor and transforming growth factor-alpha during multistage skin carcinogenesis in SENCAR mice. *Molecular carcinogenesis* **11**, 19-28 (1994).
288 Xian, W. *et al.* Activation of the epidermal growth factor receptor by skin tumor promoters and in skin tumors from SENCAR mice. *Cell growth & differentiation : the molecular biology journal of the American Association for Cancer Research* **6**, 1447-1455 (1995).
289 Fischer, S. M., Baldwin, J. K. & Adams, L. M. Effects of anti-promoters and strain of mouse on tumor promoter-induced oxidants in murine epidermal cells. *Carcinogenesis* **7**, 915-918 (1986).
290 Perchellet, E. M. & Perchellet, J. P. Characterization of the hydroperoxide response observed in mouse skin treated with tumor promoters in vivo. *Cancer research* **49**, 6193-6201 (1989).
291 Murakawa, M., Yamaoka, K., Tanaka, Y. & Fukuda, Y. Involvement of tumor necrosis factor (TNF)-alpha in phorbol ester 12-O-tetradecanoylphorbol-13-acetate (TPA)-induced skin edema in mice. *Biochemical pharmacology* **71**, 1331-1336, doi:10.1016/j.bcp.2006.01.005 (2006).
292 Moore, R. J. *et al.* Mice deficient in tumor necrosis factor-alpha are resistant to skin carcinogenesis. *Nature medicine* **5**, 828-831, doi:10.1038/10552 (1999).
293 Lee, W. Y., Lockniskar, M. F. & Fischer, S. M. Interleukin-1 alpha mediates phorbol ester-induced inflammation and epidermal hyperplasia. *FASEB journal : official publication of the Federation of American Societies for Experimental Biology* **8**, 1081-1087 (1994).
294 Langowski, J. L. *et al.* IL-23 promotes tumour incidence and growth. *Nature* **442**, 461-465, doi:10.1038/nature04808 (2006).
295 Karen, J. *et al.* 12-O-tetradecanoylphorbol-13-acetate induces clonal expansion of potentially malignant keratinocytes in a tissue model of early neoplastic progression. *Cancer research* **59**, 474-481 (1999).

296 Hennings, H., Michael, D., Lichti, U. & Yuspa, S. H. Response of carcinogen-altered mouse epidermal cells to phorbol ester tumor promoters and calcium. *The Journal of investigative dermatology* **88**, 60-65 (1987).
297 Woodworth, C. D. *et al.* Strain-dependent differences in malignant conversion of mouse skin tumors is an inherent property of the epidermal keratinocyte. *Carcinogenesis* **25**, 1771-1778, doi:10.1093/carcin/bgh170 (2004).
298 Gimenez-Conti, I. B. *et al.* Dissociation of sensitivities to tumor promotion and progression in outbred and inbred SENCAR mice. *Cancer research* **52**, 3432-3435 (1992).
299 Hennings, H. *et al.* FVB/N mice: an inbred strain sensitive to the chemical induction of squamous cell carcinomas in the skin. *Carcinogenesis* **14**, 2353-2358 (1993).
300 Popp, S., Waltering, S., Herbst, C., Moll, I. & Boukamp, P. UV-B-type mutations and chromosomal imbalances indicate common pathways for the development of Merkel and skin squamous cell carcinomas. *International journal of cancer. Journal international du cancer* **99**, 352-360, doi:10.1002/ijc.10321 (2002).
301 Lieu, F. M., Yamanishi, K., Konishi, K., Kishimoto, S. & Yasuno, H. Low incidence of Ha-ras oncogene mutations in human epidermal tumors. *Cancer letters* **59**, 231-235 (1991).
302 Campbell, C., Quinn, A. G. & Rees, J. L. Codon 12 Harvey-ras mutations are rare events in non-melanoma human skin cancer. *The British journal of dermatology* **128**, 111-114 (1993).
303 Daya-Grosjean, L., Robert, C., Drougard, C., Suarez, H. & Sarasin, A. High mutation frequency in ras genes of skin tumors isolated from DNA repair deficient xeroderma pigmentosum patients. *Cancer research* **53**, 1625-1629 (1993).
304 Littlepage, L. E., Egeblad, M. & Werb, Z. Coevolution of cancer and stromal cellular responses. *Cancer cell* **7**, 499-500, doi:10.1016/j.ccr.2005.05.019 (2005).
305 Swartz, M. A. *et al.* Tumor microenvironment complexity: emerging roles in cancer therapy. *Cancer research* **72**, 2473-2480, doi:10.1158/0008-5472.CAN-12-0122 (2012).
306 Wasiuk, A., de Vries, V. C., Hartmann, K., Roers, A. & Noelle, R. J. Mast cells as regulators of adaptive immunity to tumours. *Clinical and experimental immunology* **155**, 140-146, doi:10.1111/j.1365-2249.2008.03840.x (2009).
307 Ch'ng, S., Wallis, R. A., Yuan, L., Davis, P. F. & Tan, S. T. Mast cells and cutaneous malignancies. *Modern pathology : an official journal of the United States and Canadian Academy of Pathology, Inc* **19**, 149-159, doi:10.1038/modpathol.3800474 (2006).
308 Walker, S. L. & Young, A. R. Sunscreens offer the same UVB protection factors for inflammation and immunosuppression in the mouse. *The Journal of investigative dermatology* **108**, 133-138 (1997).
309 Halliday, G. M. Inflammation, gene mutation and photoimmunosuppression in response to UVR-induced oxidative damage contributes to photocarcinogenesis. *Mutation research* **571**, 107-120, doi:10.1016/j.mrfmmm.2004.09.013 (2005).
310 Noonan, F. P. *et al.* Melanoma induction by ultraviolet A but not ultraviolet B radiation requires melanin pigment. *Nat Commun* **3**, 884, doi:10.1038/ncomms1893 (2012).
311 De Fabo, E. C., Noonan, F. P., Fears, T. & Merlino, G. Ultraviolet B but not ultraviolet A radiation initiates melanoma. *Cancer research* **64**, 6372-6376, doi:10.1158/0008-5472.CAN-04-1454 (2004).
312 De Fabo, E. C. Ultraviolet-B radiation and stratospheric ozone loss: potential impacts on human health in the arctic. *International journal of circumpolar health* **59**, 4-8 (2000).
313 Brenner, M. & Hearing, V. J. The protective role of melanin against UV damage in human skin. *Photochemistry and photobiology* **84**, 539-549, doi:10.1111/j.1751-1097.2007.00226.x (2008).
314 Lehmann, B., Genehr, T., Knuschke, P., Pietzsch, J. & Meurer, M. UVB-induced conversion of 7-dehydrocholesterol to 1alpha,25-dihydroxyvitamin D3 in an in vitro human skin equivalent model. *The Journal of investigative dermatology* **117**, 1179-1185, doi:10.1046/j.0022-202x.2001.01538.x (2001).

315 Young, A. R. Chromophores in human skin. *Physics in medicine and biology* **42**, 789-802 (1997).
316 Kinley, J. S., Brunborg, G., Moan, J. & Young, A. R. Photoprotection by furocoumarin-induced melanogenesis against DNA photodamage in mouse epidermis in vivo. *Photochemistry and photobiology* **65**, 486-491 (1997).
317 Juzeniene, A. & Moan, J. Beneficial effects of UV radiation other than via vitamin D production. *Dermato-endocrinology* **4**, 109-117, doi:10.4161/derm.20013 (2012).
318 Dinkova-Kostova, A. T. Phytochemicals as protectors against ultraviolet radiation: versatility of effects and mechanisms. *Planta medica* **74**, 1548-1559, doi:10.1055/s-2008-1081296 (2008).
319 Johnson, T. M., Yu, Z. X., Ferrans, V. J., Lowenstein, R. A. & Finkel, T. Reactive oxygen species are downstream mediators of p53-dependent apoptosis. *Proceedings of the National Academy of Sciences of the United States of America* **93**, 11848-11852 (1996).
320 Wolfle, U. *et al.* UVB-induced DNA damage, generation of reactive oxygen species, and inflammation are effectively attenuated by the flavonoid luteolin in vitro and in vivo. *Free radical biology & medicine* **50**, 1081-1093, doi:10.1016/j.freeradbiomed.2011.01.027 (2011).
321 Villiotou, V. & Deliconstantinos, G. Nitric oxide, peroxynitrite and nitroso-compounds formation by ultraviolet A (UVA) irradiated human squamous cell carcinoma: potential role of nitric oxide in cancer prognosis. *Anticancer research* **15**, 931-942 (1995).
322 Deliconstantinos, G., Villiotou, V. & Stavrides, J. C. Increase of particulate nitric oxide synthase activity and peroxynitrite synthesis in UVB-irradiated keratinocyte membranes. *The Biochemical journal* **320 (Pt 3)**, 997-1003 (1996).
323 Deliconstantinos, G., Villiotou, V. & Stavrides, J. C. Alterations of nitric oxide synthase and xanthine oxidase activities of human keratinocytes by ultraviolet B radiation. Potential role for peroxynitrite in skin inflammation. *Biochemical pharmacology* **51**, 1727-1738 (1996).
324 Melnikova, V. O. & Ananthaswamy, H. N. Cellular and molecular events leading to the development of skin cancer. *Mutation research* **571**, 91-106, doi:10.1016/j.mrfmmm.2004.11.015 (2005).
325 Bikle, D. D. Protective actions of vitamin D in UVB induced skin cancer. *Photochemical & photobiological sciences : Official journal of the European Photochemistry Association and the European Society for Photobiology*, doi:10.1039/c2pp25251a (2012).
326 Freeman, S. E. *et al.* Wavelength dependence of pyrimidine dimer formation in DNA of human skin irradiated in situ with ultraviolet light. *Proceedings of the National Academy of Sciences of the United States of America* **86**, 5605-5609 (1989).
327 Hussein, M. R. Ultraviolet radiation and skin cancer: molecular mechanisms. *Journal of cutaneous pathology* **32**, 191-205, doi:10.1111/j.0303-6987.2005.00281.x (2005).
328 Wood, R. D., Mitchell, M., Sgouros, J. & Lindahl, T. Human DNA repair genes. *Science* **291**, 1284-1289, doi:10.1126/science.1056154 (2001).
329 Wood, R. D. *et al.* DNA damage recognition and nucleotide excision repair in mammalian cells. *Cold Spring Harbor symposia on quantitative biology* **65**, 173-182 (2000).
330 Peus, D. & Pittelkow, M. R. Reactive oxygen species as mediators of UVB-induced mitogen-activated protein kinase activation in keratinocytes. *Current problems in dermatology* **29**, 114-127 (2001).
331 Daya-Grosjean, L. & Sarasin, A. The role of UV induced lesions in skin carcinogenesis: an overview of oncogene and tumor suppressor gene modifications in xeroderma pigmentosum skin tumors. *Mutation research* **571**, 43-56, doi:10.1016/j.mrfmmm.2004.11.013 (2005).
332 Ziegler, A. *et al.* Mutation hotspots due to sunlight in the p53 gene of nonmelanoma skin cancers. *Proceedings of the National Academy of Sciences of the United States of America* **90**, 4216-4220 (1993).
333 Brash, D. E. *et al.* A role for sunlight in skin cancer: UV-induced p53 mutations in squamous cell carcinoma. *Proceedings of the National Academy of Sciences of the United States of America* **88**, 10124-10128 (1991).

334 Sander, C. S., Chang, H., Hamm, F., Elsner, P. & Thiele, J. J. Role of oxidative stress and the antioxidant network in cutaneous carcinogenesis. *International journal of dermatology* **43**, 326-335, doi:10.1111/j.1365-4632.2004.02222.x (2004).
335 Marongiu, F., Doratiotto, S., Sini, M., Serra, M. P. & Laconi, E. Cancer as a disease of tissue pattern formation. *Progress in histochemistry and cytochemistry*, doi:10.1016/j.proghi.2012.08.001 (2012).
336 Huggenberger, R. & Detmar, M. The cutaneous vascular system in chronic skin inflammation. *The journal of investigative dermatology. Symposium proceedings / the Society for Investigative Dermatology, Inc. [and] European Society for Dermatological Research* **15**, 24-32, doi:10.1038/jidsymp.2011.5 (2011).
337 Tammela, T. & Alitalo, K. Lymphangiogenesis: Molecular mechanisms and future promise. *Cell* **140**, 460-476, doi:10.1016/j.cell.2010.01.045 (2010).
338 Wang, Y. & Oliver, G. Current views on the function of the lymphatic vasculature in health and disease. *Genes & development* **24**, 2115-2126, doi:10.1101/gad.1955910 (2010).
339 Sawane, M. & Kajiya, K. Ultraviolet light-induced changes of lymphatic and blood vasculature in skin and their molecular mechanisms. *Experimental dermatology* **21 Suppl 1**, 22-25, doi:10.1111/j.1600-0625.2012.01498.x (2012).
340 Grutzkau, A. *et al.* Synthesis, storage, and release of vascular endothelial growth factor/vascular permeability factor (VEGF/VPF) by human mast cells: implications for the biological significance of VEGF206. *Molecular biology of the cell* **9**, 875-884 (1998).
341 Sitohy, B., Nagy, J. A. & Dvorak, H. F. Anti-VEGF/VEGFR therapy for cancer: reassessing the target. *Cancer research* **72**, 1909-1914, doi:10.1158/0008-5472.CAN-11-3406 (2012).
342 Sawatsubashi, M. *et al.* Association of vascular endothelial growth factor and mast cells with angiogenesis in laryngeal squamous cell carcinoma. *Virchows Archiv : an international journal of pathology* **436**, 243-248 (2000).
343 Toth-Jakatics, R., Jimi, S., Takebayashi, S. & Kawamoto, N. Cutaneous malignant melanoma: correlation between neovascularization and peritumor accumulation of mast cells overexpressing vascular endothelial growth factor. *Human pathology* **31**, 955-960 (2000).
344 Aoki, M., Pawankar, R., Niimi, Y. & Kawana, S. Mast cells in basal cell carcinoma express VEGF, IL-8 and RANTES. *International archives of allergy and immunology* **130**, 216-223, doi:69515 (2003).
345 Imada, A., Shijubo, N., Kojima, H. & Abe, S. Mast cells correlate with angiogenesis and poor outcome in stage I lung adenocarcinoma. *The European respiratory journal : official journal of the European Society for Clinical Respiratory Physiology* **15**, 1087-1093 (2000).
346 Yano, K., Kadoya, K., Kajiya, K., Hong, Y. K. & Detmar, M. Ultraviolet B irradiation of human skin induces an angiogenic switch that is mediated by upregulation of vascular endothelial growth factor and by downregulation of thrombospondin-1. *The British journal of dermatology* **152**, 115-121, doi:10.1111/j.1365-2133.2005.06368.x (2005).
347 Yano, K. *et al.* Ultraviolet B-induced skin angiogenesis is associated with a switch in the balance of vascular endothelial growth factor and thrombospondin-1 expression. *The Journal of investigative dermatology* **122**, 201-208, doi:10.1046/j.0022-202X.2003.22101.x (2004).
348 Carmeliet, P. & Jain, R. K. Angiogenesis in cancer and other diseases. *Nature* **407**, 249-257, doi:10.1038/35025220 (2000).
349 Detmar, M. & Hirakawa, S. The formation of lymphatic vessels and its importance in the setting of malignancy. *The Journal of experimental medicine* **196**, 713-718 (2002).
350 Beasley, N. J. *et al.* Intratumoral lymphangiogenesis and lymph node metastasis in head and neck cancer. *Cancer research* **62**, 1315-1320 (2002).
351 Hirakawa, S. *et al.* VEGF-C-induced lymphangiogenesis in sentinel lymph nodes promotes tumor metastasis to distant sites. *Blood* **109**, 1010-1017, doi:10.1182/blood-2006-05-021758 (2007).

352 Hirakawa, S. *et al.* VEGF-A induces tumor and sentinel lymph node lymphangiogenesis and promotes lymphatic metastasis. *The Journal of experimental medicine* **201**, 1089-1099, doi:10.1084/jem.20041896 (2005).

353 Kajiya, K., Hirakawa, S. & Detmar, M. Vascular endothelial growth factor-A mediates ultraviolet B-induced impairment of lymphatic vessel function. *The American journal of pathology* **169**, 1496-1503, doi:10.2353/ajpath.2006.060197 (2006).

354 Karnezis, T. *et al.* VEGF-D promotes tumor metastasis by regulating prostaglandins produced by the collecting lymphatic endothelium. *Cancer cell* **21**, 181-195, doi:10.1016/j.ccr.2011.12.026 (2012).

355 Kajiya, K., Sawane, M., Huggenberger, R. & Detmar, M. Activation of the VEGFR-3 pathway by VEGF-C attenuates UVB-induced edema formation and skin inflammation by promoting lymphangiogenesis. *The Journal of investigative dermatology* **129**, 1292-1298, doi:10.1038/jid.2008.351 (2009).

356 Kajiya, K. & Detmar, M. An important role of lymphatic vessels in the control of UVB-induced edema formation and inflammation. *The Journal of investigative dermatology* **126**, 919-921, doi:10.1038/sj.jid.5700126 (2006).

357 Sismanopoulos, N. *et al.* IL-9 induces VEGF secretion from human mast cells and IL-9/IL-9 receptor genes are overexpressed in atopic dermatitis. *PloS one* **7**, e33271, doi:10.1371/journal.pone.0033271 (2012).

358 Detoraki, A. *et al.* Vascular endothelial growth factors synthesized by human lung mast cells exert angiogenic effects. *The Journal of allergy and clinical immunology* **123**, 1142-1149, 1149 e1141-1145, doi:10.1016/j.jaci.2009.01.044 (2009).

359 Schweintzger, N. A. *et al.* Mast cells are required for phototolerance induction and scratching abatement. *Experimental dermatology* **24**, 491-496, doi:10.1111/exd.12687 (2015).

360 Khalil, Z., Townley, S. L., Grimbaldeston, M. A., Finlay-Jones, J. J. & Hart, P. H. cis-Urocanic acid stimulates neuropeptide release from peripheral sensory nerves. *The Journal of investigative dermatology* **117**, 886-891, doi:10.1046/j.0022-202x.2001.01466.x (2001).

361 Townley, S. L. *et al.* Nerve growth factor, neuropeptides, and mast cells in ultraviolet-B-induced systemic suppression of contact hypersensitivity responses in mice. *The Journal of investigative dermatology* **118**, 396-401, doi:10.1046/j.0022-202x.2001.01679.x (2002).

362 Byrne, S. N., Beaugie, C., O'Sullivan, C., Leighton, S. & Halliday, G. M. The immune-modulating cytokine and endogenous Alarmin interleukin-33 is upregulated in skin exposed to inflammatory UVB radiation. *The American journal of pathology* **179**, 211-222, doi:10.1016/j.ajpath.2011.03.010 (2011).

363 Sarkar, A., Sreenivasan, Y. & Manna, S. K. alpha-Melanocyte-stimulating hormone induces cell death in mast cells: involvement of NF-kappaB. *FEBS letters* **549**, 87-93 (2003).

364 Wolf, P. *et al.* Platelet-activating factor is crucial in psoralen and ultraviolet A-induced immune suppression, inflammation, and apoptosis. *The American journal of pathology* **169**, 795-805, doi:10.2353/ajpath.2006.060079 (2006).

365 Endoh, I. *et al.* Ultraviolet B irradiation selectively increases the production of interleukin-8 in human cord blood-derived mast cells. *Clinical and experimental immunology* **148**, 161-167, doi:10.1111/j.1365-2249.2007.03332.x (2007).

366 Alard, P., Niizeki, H., Hanninen, L. & Streilein, J. W. Local ultraviolet B irradiation impairs contact hypersensitivity induction by triggering release of tumor necrosis factor-alpha from mast cells. Involvement of mast cells and Langerhans cells in susceptibility to ultraviolet B. *The Journal of investigative dermatology* **113**, 983-990, doi:10.1046/j.1523-1747.1999.00772.x (1999).

367 Hart, P. H. *et al.* Histamine involvement in UVB- and cis-urocanic acid-induced systemic suppression of contact hypersensitivity responses. *Immunology* **91**, 601-608 (1997).

368 Yano, K., Oura, H. & Detmar, M. Targeted overexpression of the angiogenesis inhibitor thrombospondin-1 in the epidermis of transgenic mice prevents ultraviolet-B-induced

angiogenesis and cutaneous photo-damage. *The Journal of investigative dermatology* **118**, 800-805, doi:10.1046/j.1523-1747.2002.01752.x (2002).

369 Van Nguyen, H. *et al.* Ultraviolet radiation-induced cytokines promote mast cell accumulation and matrix metalloproteinase production: potential role in cutaneous lupus erythematosus. *Scandinavian journal of rheumatology* **40**, 197-204, doi:10.3109/03009742.2010.528020 (2011).

370 Imamura, T., Dubin, A., Moore, W., Tanaka, R. & Travis, J. Induction of vascular permeability enhancement by human tryptase: dependence on activation of prekallikrein and direct release of bradykinin from kininogens. *Laboratory investigation; a journal of technical methods and pathology* **74**, 861-870 (1996).

371 Tam, E. K. & Caughey, G. H. Degradation of airway neuropeptides by human lung tryptase. *American journal of respiratory cell and molecular biology* **3**, 27-32, doi:10.1165/ajrcmb/3.1.27 (1990).

372 Caughey, G. H., Leidig, F., Viro, N. F. & Nadel, J. A. Substance P and vasoactive intestinal peptide degradation by mast cell tryptase and chymase. *The Journal of pharmacology and experimental therapeutics* **244**, 133-137 (1988).

373 Huang, C. *et al.* The tryptase, mouse mast cell protease 7, exhibits anticoagulant activity in vivo and in vitro due to its ability to degrade fibrinogen in the presence of the diverse array of protease inhibitors in plasma. *The Journal of biological chemistry* **272**, 31885-31893 (1997).

374 Thakurdas, S. M. *et al.* The mast cell-restricted tryptase mMCP-6 has a critical immunoprotective role in bacterial infections. *The Journal of biological chemistry* **282**, 20809-20815, doi:10.1074/jbc.M611842200 (2007).

375 Maurer, M. *et al.* Mast cells promote homeostasis by limiting endothelin-1-induced toxicity. *Nature* **432**, 512-516, doi:10.1038/nature03085 (2004).

376 Metz, M. *et al.* Mast cells can enhance resistance to snake and honeybee venoms. *Science* **313**, 526-530, doi:10.1126/science.1128877 (2006).

377 Abonia, J. P. *et al.* Mast cell protease 5 mediates ischemia-reperfusion injury of mouse skeletal muscle. *Journal of immunology* **174**, 7285-7291 (2005).

378 Akahoshi, M. *et al.* Mast cell chymase reduces the toxicity of Gila monster venom, scorpion venom, and vasoactive intestinal polypeptide in mice. *The Journal of clinical investigation* **121**, 4180-4191, doi:10.1172/JCI46139 (2011).

379 Hendrix, S. *et al.* Mast cells protect from post-traumatic brain inflammation by the mast cell-specific chymase mouse mast cell protease-4. *FASEB journal : official publication of the Federation of American Societies for Experimental Biology* **27**, 920-929, doi:10.1096/fj.12-204800 (2013).

380 Nelissen, S. *et al.* Mast cells protect from post-traumatic spinal cord damage in mice by degrading inflammation-associated cytokines via mouse mast cell protease 4. *Neurobiology of disease* **62**, 260-272, doi:10.1016/j.nbd.2013.09.012 (2014).

381 Beghdadi, W. *et al.* Mast cell chymase protects against renal fibrosis in murine unilateral ureteral obstruction. *Kidney international* **84**, 317-326, doi:10.1038/ki.2013.98 (2013).

382 Younan, G. *et al.* The inflammatory response after an epidermal burn depends on the activities of mouse mast cell proteases 4 and 5. *Journal of immunology* **185**, 7681-7690, doi:10.4049/jimmunol.1002803 (2010).

383 Hart, P. H., Grimbaldeston, M. A. & Finlay-Jones, J. J. Mast cells in UV-B-induced immunosuppression. *Journal of photochemistry and photobiology. B, Biology* **55**, 81-87 (2000).

384 Tchougounova, E. *et al.* A key role for mast cell chymase in the activation of pro-matrix metalloprotease-9 and pro-matrix metalloprotease-2. *The Journal of biological chemistry* **280**, 9291-9296, doi:10.1074/jbc.M410396200 (2005).

385 Kulka, M., Sheen, C. H., Tancowny, B. P., Grammer, L. C. & Schleimer, R. P. Neuropeptides activate human mast cell degranulation and chemokine production. *Immunology* **123**, 398-410, doi:10.1111/j.1365-2567.2007.02705.x (2008).

386 Coelho, S. G. *et al.* Photobiological implications of melanin photoprotection after UVB-induced tanning of human skin but not UVA-induced tanning. *Pigment cell & melanoma research* **28**, 210-216, doi:10.1111/pcmr.12331 (2015).
387 Kaidbey, K. H., Agin, P. P., Sayre, R. M. & Kligman, A. M. Photoprotection by melanin--a comparison of black and Caucasian skin. *Journal of the American Academy of Dermatology* **1**, 249-260 (1979).
388 Kobayashi, N. *et al.* Supranuclear melanin caps reduce ultraviolet induced DNA photoproducts in human epidermis. *The Journal of investigative dermatology* **110**, 806-810, doi:10.1046/j.1523-1747.1998.00178.x (1998).
389 Kennedy, C. *et al.* Melanocortin 1 receptor (MC1R) gene variants are associated with an increased risk for cutaneous melanoma which is largely independent of skin type and hair color. *The Journal of investigative dermatology* **117**, 294-300, doi:10.1046/j.0022-202x.2001.01421.x (2001).
390 Streutker, C. J., McCready, D., Jimbow, K. & From, L. Malignant melanoma in a patient with oculocutaneous albinism. *Journal of cutaneous medicine and surgery* **4**, 149-152 (2000).
391 An, S. M., Koh, J. S. & Boo, Y. C. Inhibition of melanogenesis by tyrosinase siRNA in human melanocytes. *BMB reports* **42**, 178-183 (2009).
392 Wershil, B. K. & Galli, S. J. Gastrointestinal mast cells. New approaches for analyzing their function in vivo. *Gastroenterol Clin North Am* **20**, 613-627 (1991).
393 van der Kleij, H. P. *et al.* Functional expression of neurokinin 1 receptors on mast cells induced by IL-4 and stem cell factor. *Journal of immunology* **171**, 2074-2079 (2003).
394 Hill, P. B. *et al.* Stem cell factor enhances immunoglobulin E-dependent mediator release from cultured rat bone marrow-derived mast cells: activation of previously unresponsive cells demonstrated by a novel ELISPOT assay. *Immunology* **87**, 326-333 (1996).
395 Gagari, E., Tsai, M., Lantz, C. S., Fox, L. G. & Galli, S. J. Differential release of mast cell interleukin-6 via c-kit. *Blood* **89**, 2654-2663 (1997).
396 Kendall, J. C., Li, X. H., Galli, S. J. & Gordon, J. R. Promotion of mouse fibroblast proliferation by IgE-dependent activation of mouse mast cells: role for mast cell tumor necrosis factor-alpha and transforming growth factor-beta 1. *The Journal of allergy and clinical immunology* **99**, 113-123 (1997).
397 Ito, T. *et al.* Stem cell factor programs the mast cell activation phenotype. *Journal of immunology* **188**, 5428-5437, doi:10.4049/jimmunol.1103366 (2012).
398 Liu, F. T. *et al.* Monoclonal dinitrophenyl-specific murine IgE antibody: preparation, isolation, and characterization. *Journal of immunology* **124**, 2728-2737 (1980).
399 McNeil, B. D. *et al.* Identification of a mast-cell-specific receptor crucial for pseudo-allergic drug reactions. *Nature*, doi:10.1038/nature14022 (2014).
400 Bryce, P. J. *et al.* Immune sensitization in the skin is enhanced by antigen-independent effects of IgE. *Immunity* **20**, 381-392 (2004).
401 Ichihashi, M. *et al.* UV-induced skin damage. *Toxicology* **189**, 21-39 (2003).
402 Halliday, G. M. & Lyons, J. G. Inflammatory doses of UV may not be necessary for skin carcinogenesis. *Photochemistry and photobiology* **84**, 272-283, doi:10.1111/j.1751-1097.2007.00247.x (2008).
403 Ribatti, D. *et al.* Tumor vascularity and tryptase-positive mast cells correlate with a poor prognosis in melanoma. *European journal of clinical investigation* **33**, 420-425 (2003).
404 Junankar, S. R., Eichten, A., Kramer, A., de Visser, K. E. & Coussens, L. M. Analysis of immune cell infiltrates during squamous carcinoma development. *The journal of investigative dermatology. Symposium proceedings / the Society for Investigative Dermatology, Inc. [and] European Society for Dermatological Research* **11**, 36-43 (2006).
405 Marichal, T., Tsai, M. & Galli, S. J. Mast cells: potential positive and negative roles in tumor biology. *Cancer Immunol Res* **1**, 269-279, doi:10.1158/2326-6066.CIR-13-0119 (2013).
406 Kligman, L. H. The hairless mouse model for photoaging. *Clinics in dermatology* **14**, 183-195 (1996).

407 Grimbaldeston, M. A. *et al.* Susceptibility to basal cell carcinoma is associated with high dermal mast cell prevalence in non-sun-exposed skin for an Australian populations. *Photochemistry and photobiology* **78**, 633-639 (2003).
408 Grimbaldeston, M. A., Simpson, A., Finlay-Jones, J. J. & Hart, P. H. The effect of ultraviolet radiation exposure on the prevalence of mast cells in human skin. *The British journal of dermatology* **148**, 300-306 (2003).
409 Metz, M., Lammel, V., Gibbs, B. F. & Maurer, M. Inflammatory murine skin responses to UV-B light are partially dependent on endothelin-1 and mast cells. *The American journal of pathology* **169**, 815-822, doi:10.2353/ajpath.2006.060037 (2006).
410 Ribatti, D. *et al.* Neovascularisation, expression of fibroblast growth factor-2, and mast cells with tryptase activity increase simultaneously with pathological progression in human malignant melanoma. *European journal of cancer* **39**, 666-674 (2003).
411 Biswas, A., Richards, J. E., Massaro, J. & Mahalingam, M. Mast cells in cutaneous tumors: innocent bystander or maestro conductor? *International journal of dermatology* **53**, 806-811, doi:10.1111/j.1365-4632.2012.05745.x (2014).
412 Siiskonen, H. *et al.* Low numbers of tryptase+ and chymase+ mast cells associated with reduced survival and advanced tumor stage in melanoma. *Melanoma Res* **25**, 479-485, doi:10.1097/CMR.0000000000000192 (2015).
413 Hart, P. H. *et al.* TNF modulates susceptibility to UVB-induced systemic immunomodulation in mice by effects on dermal mast cell prevalence. *European journal of immunology* **28**, 2893-2901, doi:10.1002/(SICI)1521-4141(199809)28:09<2893::AID-IMMU2893>3.0.CO;2-U (1998).
414 Mazzoni, A., Young, H. A., Spitzer, J. H., Visintin, A. & Segal, D. M. Histamine regulates cytokine production in maturing dendritic cells, resulting in altered T cell polarization. *The Journal of clinical investigation* **108**, 1865-1873, doi:10.1172/JCI13930 (2001).
415 Lagier, B., Lebel, B., Bousquet, J. & Pene, J. Different modulation by histamine of IL-4 and interferon-gamma (IFN-gamma) release according to the phenotype of human Th0, Th1 and Th2 clones. *Clinical and experimental immunology* **108**, 545-551 (1997).
416 Suto, H. *et al.* Mast cell-associated TNF promotes dendritic cell migration. *Journal of immunology* **176**, 4102-4112 (2006).
417 Fukunaga, A., Khaskhely, N. M., Sreevidya, C. S., Byrne, S. N. & Ullrich, S. E. Dermal dendritic cells, and not Langerhans cells, play an essential role in inducing an immune response. *Journal of immunology* **180**, 3057-3064 (2008).
418 Artuc, M. *et al.* Mast cell-derived TNF-alpha and histamine modify IL-6 and IL-8 expression and release from cutaneous tumor cells. *Experimental dermatology* **20**, 1020-1022, doi:10.1111/j.1600-0625.2011.01377.x (2011).
419 Pang, L., Nie, M., Corbett, L., Sutcliffe, A. & Knox, A. J. Mast cell beta-tryptase selectively cleaves eotaxin and RANTES and abrogates their eosinophil chemotactic activities. *Journal of immunology* **176**, 3788-3795 (2006).
420 Walls, A. F. *et al.* Human mast cell tryptase attenuates the vasodilator activity of calcitonin gene-related peptide. *Biochemical pharmacology* **43**, 1243-1248 (1992).
421 Iddamalgoda, A. *et al.* Mast cell tryptase and photoaging: possible involvement in the degradation of extra cellular matrix and basement membrane proteins. *Archives of dermatological research* **300 Suppl 1**, S69-76, doi:10.1007/s00403-007-0806-1 (2008).
422 Ouhtit, A. *et al.* Temporal events in skin injury and the early adaptive responses in ultraviolet-irradiated mouse skin. *The American journal of pathology* **156**, 201-207, doi:10.1016/S0002-9440(10)64720-7 (2000).
423 Seagle, B. L. *et al.* Melanin photoprotection in the human retinal pigment epithelium and its correlation with light-induced cell apoptosis. *Proceedings of the National Academy of Sciences of the United States of America* **102**, 8978-8983, doi:10.1073/pnas.0501971102 (2005).
424 Sarchio, S. N. *et al.* Pharmacologically antagonizing the CXCR4-CXCL12 chemokine pathway with AMD3100 inhibits sunlight-induced skin cancer. *The Journal of investigative dermatology* **134**, 1091-1100, doi:10.1038/jid.2013.424 (2014).

425 Reed, J. A., McNutt, N. S., Bogdany, J. K. & Albino, A. P. Expression of the mast cell growth factor interleukin-3 in melanocytic lesions correlates with an increased number of mast cells in the perilesional stroma: implications for melanoma progression. *Journal of cutaneous pathology* **23**, 495-505 (1996).
426 Galli, S. J., Tsai, M., Wershil, B. K., Tam, S. Y. & Costa, J. J. Regulation of mouse and human mast cell development, survival and function by stem cell factor, the ligand for the c-kit receptor. *International archives of allergy and immunology* **107**, 51-53 (1995).
427 Hanahan, D. & Weinberg, R. A. The hallmarks of cancer. *Cell* **100**, 57-70 (2000).
428 Coussens, L. M. & Werb, Z. Inflammation and cancer. *Nature* **420**, 860-867, doi:10.1038/nature01322 (2002).
429 Karatzanis, A. D., Koudounarakis, E., Papadakis, I. & Velegrakis, G. Molecular pathways of lymphangiogenesis and lymph node metastasis in head and neck cancer. *European archives of oto-rhino-laryngology : official journal of the European Federation of Oto-Rhino-Laryngological Societies* **269**, 731-737, doi:10.1007/s00405-011-1809-2 (2012).
430 Holopainen, T., Bry, M., Alitalo, K. & Saaristo, A. Perspectives on lymphangiogenesis and angiogenesis in cancer. *Journal of surgical oncology* **103**, 484-488, doi:10.1002/jso.21808 (2011).
431 Holmgren, L., O'Reilly, M. S. & Folkman, J. Dormancy of micrometastases: balanced proliferation and apoptosis in the presence of angiogenesis suppression. *Nature medicine* **1**, 149-153 (1995).
432 Feng, D. *et al.* Pathways of macromolecular extravasation across microvascular endothelium in response to VPF/VEGF and other vasoactive mediators. *Microcirculation* **6**, 23-44 (1999).
433 Carmeliet, P. & Jain, R. K. Principles and mechanisms of vessel normalization for cancer and other angiogenic diseases. *Nature reviews. Drug discovery* **10**, 417-427, doi:10.1038/nrd3455 (2011).
434 Baluk, P. *et al.* Pathogenesis of persistent lymphatic vessel hyperplasia in chronic airway inflammation. *The Journal of clinical investigation* **115**, 247-257, doi:10.1172/JCI22037 (2005).
435 Rutkowski, J. M., Moya, M., Johannes, J., Goldman, J. & Swartz, M. A. Secondary lymphedema in the mouse tail: Lymphatic hyperplasia, VEGF-C upregulation, and the protective role of MMP-9. *Microvascular research* **72**, 161-171, doi:10.1016/j.mvr.2006.05.009 (2006).
436 van Zonneveld, A. J., de Boer, H. C., van der Veer, E. P. & Rabelink, T. J. Inflammation, vascular injury and repair in rheumatoid arthritis. *Annals of the rheumatic diseases* **69 Suppl 1**, i57-60, doi:10.1136/ard.2009.119495 (2010).
437 Stacker, S. A. & Achen, M. G. From anti-angiogenesis to anti-lymphangiogenesis: emerging trends in cancer therapy. *Lymphatic research and biology* **6**, 165-172, doi:10.1089/lrb.2008.1015 (2008).
438 Nishida, N., Yano, H., Nishida, T., Kamura, T. & Kojiro, M. Angiogenesis in cancer. *Vascular health and risk management* **2**, 213-219 (2006).
439 Li, Y., Bi, Z., Yan, B. & Wan, Y. UVB radiation induces expression of HIF-1alpha and VEGF through the EGFR/PI3K/DEC1 pathway. *International journal of molecular medicine* **18**, 713-719 (2006).
440 Kramer, M., Sachsenmaier, C., Herrlich, P. & Rahmsdorf, H. J. UV irradiation-induced interleukin-1 and basic fibroblast growth factor synthesis and release mediate part of the UV response. *The Journal of biological chemistry* **268**, 6734-6741 (1993).
441 Strickland, I., Rhodes, L. E., Flanagan, B. F. & Friedmann, P. S. TNF-alpha and IL-8 are upregulated in the epidermis of normal human skin after UVB exposure: correlation with neutrophil accumulation and E-selectin expression. *The Journal of investigative dermatology* **108**, 763-768 (1997).
442 Howell, B. G. *et al.* Microarray analysis of UVB-regulated genes in keratinocytes: downregulation of angiogenesis inhibitor thrombospondin-1. *J Dermatol Sci* **34**, 185-194, doi:10.1016/j.jdermsci.2004.01.004 (2004).

443 Wilting, J. *et al.* The transcription factor Prox1 is a marker for lymphatic endothelial cells in normal and diseased human tissues. *FASEB journal : official publication of the Federation of American Societies for Experimental Biology* **16**, 1271-1273, doi:10.1096/fj.01-1010fje (2002).
444 Gordon, E. J., Gale, N. W. & Harvey, N. L. Expression of the hyaluronan receptor LYVE-1 is not restricted to the lymphatic vasculature; LYVE-1 is also expressed on embryonic blood vessels. *Developmental dynamics : an official publication of the American Association of Anatomists* **237**, 1901-1909, doi:10.1002/dvdy.21605 (2008).
445 Oliver, G. & Detmar, M. The rediscovery of the lymphatic system: old and new insights into the development and biological function of the lymphatic vasculature. *Genes & development* **16**, 773-783, doi:10.1101/gad.975002 (2002).
446 Dameron, K. M., Volpert, O. V., Tainsky, M. A. & Bouck, N. The p53 tumor suppressor gene inhibits angiogenesis by stimulating the production of thrombospondin. *Cold Spring Harbor symposia on quantitative biology* **59**, 483-489 (1994).
447 Jia, Y. T. *et al.* [Endostar reduces the growth and metastasis by inhibiting angiogenesis and lymphangiogenesis in nude mouse models of human cervical cancer]. *Zhonghua zhong liu za zhi [Chinese journal of oncology]* **31**, 254-257 (2009).
448 Kim, J. M. *et al.* Angiostatin gene transfer as an effective treatment strategy in murine collagen-induced arthritis. *Arthritis and rheumatism* **46**, 793-801, doi:10.1002/art.10113 (2002).
449 Esposito, I. *et al.* Inflammatory cells contribute to the generation of an angiogenic phenotype in pancreatic ductal adenocarcinoma. *Journal of clinical pathology* **57**, 630-636 (2004).
450 Karnezis, T., Shayan, R., Fox, S., Achen, M. G. & Stacker, S. A. The connection between lymphangiogenic signalling and prostglandin biology: A missing link in the metastatsic pathway. *Oncotarget* **3**, 893-906 (2012).
451 Huggenberger, R. *et al.* An important role of lymphatic vessel activation in limiting acute inflammation. *Blood* **117**, 4667-4678, doi:10.1182/blood-2010-10-316356 (2011).
452 Quail, D. F. & Joyce, J. A. Microenvironmental regulation of tumor progression and metastasis. *Nature medicine* **19**, 1423-1437, doi:10.1038/nm.3394 (2013).
453 Youn, J. I., Nagaraj, S., Collazo, M. & Gabrilovich, D. I. Subsets of myeloid-derived suppressor cells in tumor-bearing mice. *Journal of immunology* **181**, 5791-5802 (2008).
454 Schlecker, E. *et al.* Tumor-infiltrating monocytic myeloid-derived suppressor cells mediate CCR5-dependent recruitment of regulatory T cells favoring tumor growth. *Journal of immunology* **189**, 5602-5611, doi:10.4049/jimmunol.1201018 (2012).
455 Gordon, E. J. *et al.* Macrophages define dermal lymphatic vessel calibre during development by regulating lymphatic endothelial cell proliferation. *Development* **137**, 3899-3910, doi:10.1242/dev.050021 (2010).
456 von der Weid, P. Y. *et al.* Mechanisms of VIP-induced inhibition of the lymphatic vessel pump. *The Journal of physiology* **590**, 2677-2691, doi:10.1113/jphysiol.2012.230599 (2012).
457 Norrby, K. Mast cells and angiogenesis. *APMIS : acta pathologica, microbiologica, et immunologica Scandinavica* **110**, 355-371 (2002).
458 Sperr, W. R. *et al.* Specific activation of human mast cells by the ligand for c-kit: comparison between lung, uterus and heart mast cells. *International archives of allergy and immunology* **102**, 170-175 (1993).
459 Ammendola, M. *et al.* Targeting mast cells tryptase in tumor microenvironment: a potential antiangiogenetic strategy. *BioMed research international* **2014**, 154702, doi:10.1155/2014/154702 (2014).
460 Ozawa, C. R. *et al.* Microenvironmental VEGF concentration, not total dose, determines a threshold between normal and aberrant angiogenesis. *The Journal of clinical investigation* **113**, 516-527, doi:10.1172/JCI18420 (2004).
461 Dameron, K. M., Volpert, O. V., Tainsky, M. A. & Bouck, N. Control of angiogenesis in fibroblasts by p53 regulation of thrombospondin-1. *Science* **265**, 1582-1584 (1994).

462 Solomon, H., Madar, S. & Rotter, V. Mutant p53 gain of function is interwoven into the hallmarks of cancer. *The Journal of pathology* **225**, 475-478, doi:10.1002/path.2988 (2011).
463 van Kranen, H. J. & de Gruijl, F. R. Mutations in cancer genes of UV-induced skin tumors of hairless mice. *Journal of epidemiology / Japan Epidemiological Association* **9**, S58-65 (1999).
464 Wang, C. A. *et al.* SIX1 induces lymphangiogenesis and metastasis via upregulation of VEGF-C in mouse models of breast cancer. *The Journal of clinical investigation* **122**, 1895-1906, doi:10.1172/JCI59858 (2012).
465 Cunnick, G. H. *et al.* Lymphangiogenesis and lymph node metastasis in breast cancer. *Molecular cancer* **7**, 23, doi:10.1186/1476-4598-7-23 (2008).
466 Zhao, Y. C. *et al.* Tumor-derived VEGF-C, but not VEGF-D, promotes sentinel lymph node lymphangiogenesis prior to metastasis in breast cancer patients. *Medical oncology*, doi:10.1007/s12032-012-0205-0 (2012).
467 Yu, J. W. *et al.* Study on lymph node metastasis correlated to lymphangiogenesis, lymphatic vessel invasion, and lymph node micrometastasis in gastric cancer. *The Journal of surgical research* **168**, 188-196, doi:10.1016/j.jss.2009.10.030 (2011).
468 Dupuy, E. & Tobelem, G. [Mechanisms and role of lymphangiogenesis in cancer metastasis]. *Bulletin du cancer* **90**, 595-599 (2003).
469 Bahram, F. & Claesson-Welsh, L. VEGF-mediated signal transduction in lymphatic endothelial cells. *Pathophysiology : the official journal of the International Society for Pathophysiology / ISP* **17**, 253-261, doi:10.1016/j.pathophys.2009.10.004 (2010).
470 Min, Y. *et al.* C/EBP-delta regulates VEGF-C autocrine signaling in lymphangiogenesis and metastasis of lung cancer through HIF-1alpha. *Oncogene* **30**, 4901-4909, doi:10.1038/onc.2011.187 (2011).
471 Feng, Y. *et al.* Expression of VEGF-C and VEGF-D as significant markers for assessment of lymphangiogenesis and lymph node metastasis in non-small cell lung cancer. *Anatomical record* **293**, 802-812, doi:10.1002/ar.21096 (2010).
472 Halaban, R., Kwon, B. S., Ghosh, S., Delli Bovi, P. & Baird, A. bFGF as an autocrine growth factor for human melanomas. *Oncogene research* **3**, 177-186 (1988).
473 Detry, B. *et al.* Matrix metalloproteinase-2 governs lymphatic vessel formation as an interstitial collagenase. *Blood* **119**, 5048-5056, doi:10.1182/blood-2011-12-400267 (2012).
474 Kontos, C. D. More than skin deep: connecting melanocyte pigmentation and angiogenic diseases. *The Journal of clinical investigation* **124**, 76-79, doi:10.1172/JCI73559 (2014).
475 Adini, I. *et al.* Melanocyte pigmentation inversely correlates with MCP-1 production and angiogenesis-inducing potential. *FASEB journal : official publication of the Federation of American Societies for Experimental Biology* **29**, 662-670, doi:10.1096/fj.14-255398 (2015).
476 Gabrilovich, D. I. & Nagaraj, S. Myeloid-derived suppressor cells as regulators of the immune system. *Nature reviews. Immunology* **9**, 162-174, doi:10.1038/nri2506 (2009).
477 Corzo, C. A. *et al.* HIF-1alpha regulates function and differentiation of myeloid-derived suppressor cells in the tumor microenvironment. *The Journal of experimental medicine* **207**, 2439-2453, doi:10.1084/jem.20100587 (2010).
478 Diaz-Montero, C. M. *et al.* Increased circulating myeloid-derived suppressor cells correlate with clinical cancer stage, metastatic tumor burden, and doxorubicin-cyclophosphamide chemotherapy. *Cancer immunology, immunotherapy : CII* **58**, 49-59, doi:10.1007/s00262-008-0523-4 (2009).
479 Rodriguez, P. C. *et al.* Arginase I in myeloid suppressor cells is induced by COX-2 in lung carcinoma. *The Journal of experimental medicine* **202**, 931-939, doi:10.1084/jem.20050715 (2005).
480 Zea, A. H. *et al.* Arginase-producing myeloid suppressor cells in renal cell carcinoma patients: a mechanism of tumor evasion. *Cancer research* **65**, 3044-3048, doi:10.1158/0008-5472.CAN-04-4505 (2005).

481 Rodriguez, P. C. *et al.* Regulation of T cell receptor CD3zeta chain expression by L-arginine. *The Journal of biological chemistry* **277**, 21123-21129, doi:10.1074/jbc.M110675200 (2002).
482 Kusmartsev, S., Nefedova, Y., Yoder, D. & Gabrilovich, D. I. Antigen-specific inhibition of CD8+ T cell response by immature myeloid cells in cancer is mediated by reactive oxygen species. *Journal of immunology* **172**, 989-999 (2004).
483 Lesokhin, A. M. *et al.* Monocytic CCR2(+) myeloid-derived suppressor cells promote immune escape by limiting activated CD8 T-cell infiltration into the tumor microenvironment. *Cancer research* **72**, 876-886, doi:10.1158/0008-5472.CAN-11-1792 (2012).
484 Byrne, S. N. & Halliday, G. M. B cells activated in lymph nodes in response to ultraviolet irradiation or by interleukin-10 inhibit dendritic cell induction of immunity. *The Journal of investigative dermatology* **124**, 570-578, doi:10.1111/j.0022-202X.2005.23615.x (2005).
485 Matsumura, Y., Byrne, S. N., Nghiem, D. X., Miyahara, Y. & Ullrich, S. E. A role for inflammatory mediators in the induction of immunoregulatory B cells. *Journal of immunology* **177**, 4810-4817 (2006).
486 Schwarz, A. *et al.* Langerhans cells are required for UVR-induced immunosuppression. *The Journal of investigative dermatology* **130**, 1419-1427, doi:10.1038/jid.2009.429 (2010).
487 Loser, K. *et al.* Epidermal RANKL controls regulatory T-cell numbers via activation of dendritic cells. *Nature medicine* **12**, 1372-1379, doi:10.1038/nm1518 (2006).
488 Rolli, M., Fransvea, E., Pilch, J., Saven, A. & Felding-Habermann, B. Activated integrin alphavbeta3 cooperates with metalloproteinase MMP-9 in regulating migration of metastatic breast cancer cells. *Proceedings of the National Academy of Sciences of the United States of America* **100**, 9482-9487, doi:10.1073/pnas.1633689100 (2003).
489 Harvima, I. T. Induction of matrix metalloproteinase-9 in keratinocytes by histamine. *The Journal of investigative dermatology* **128**, 2748-2750, doi:10.1038/jid.2008.331 (2008).
490 Jodele, S. *et al.* The contribution of bone marrow-derived cells to the tumor vasculature in neuroblastoma is matrix metalloproteinase-9 dependent. *Cancer research* **65**, 3200-3208, doi:10.1158/0008-5472.CAN-04-3770 (2005).
491 Schmalfeldt, B. *et al.* Increased expression of matrix metalloproteinases (MMP)-2, MMP-9, and the urokinase-type plasminogen activator is associated with progression from benign to advanced ovarian cancer. *Clinical cancer research : an official journal of the American Association for Cancer Research* **7**, 2396-2404 (2001).
492 van Kempen, L. C. & Coussens, L. M. MMP9 potentiates pulmonary metastasis formation. *Cancer cell* **2**, 251-252 (2002).
493 Lee, B. K. *et al.* A high concentration of MMP-2/gelatinase A and MMP-9/gelatinase B reduce NK cell-mediated cytotoxicity against an oral squamous cell carcinoma cell line. *In vivo* **22**, 593-597 (2008).
494 Chakrabarti, S. & Patel, K. D. Matrix metalloproteinase-2 (MMP-2) and MMP-9 in pulmonary pathology. *Experimental lung research* **31**, 599-621, doi:10.1080/019021490944232 (2005).
495 Hamano, Y. *et al.* Physiological levels of tumstatin, a fragment of collagen IV alpha3 chain, are generated by MMP-9 proteolysis and suppress angiogenesis via alphaV beta3 integrin. *Cancer cell* **3**, 589-601 (2003).
496 Lu, P., Weaver, V. M. & Werb, Z. The extracellular matrix: a dynamic niche in cancer progression. *The Journal of cell biology* **196**, 395-406, doi:10.1083/jcb.201102147 (2012).
497 Sorokin, L. The impact of the extracellular matrix on inflammation. *Nature reviews. Immunology* **10**, 712-723, doi:10.1038/nri2852 (2010).
498 Werb, Z., Vu, T. H., Rinkenberger, J. L. & Coussens, L. M. Matrix-degrading proteases and angiogenesis during development and tumor formation. *APMIS : acta pathologica, microbiologica, et immunologica Scandinavica* **107**, 11-18 (1999).

499 Edovitsky, E., Elkin, M., Zcharia, E., Peretz, T. & Vlodavsky, I. Heparanase gene silencing, tumor invasiveness, angiogenesis, and metastasis. *Journal of the National Cancer Institute* **96**, 1219-1230, doi:10.1093/jnci/djh230 (2004).
500 Lerner, I. *et al.* Heparanase powers a chronic inflammatory circuit that promotes colitis-associated tumorigenesis in mice. *The Journal of clinical investigation* **121**, 1709-1721, doi:10.1172/JCI43792 (2011).
501 Balkwill, F. R., Capasso, M. & Hagemann, T. The tumor microenvironment at a glance. *Journal of cell science* **125**, 5591-5596, doi:10.1242/jcs.116392 (2012).
502 Wu, Y., Li, Y. Y., Matsushima, K., Baba, T. & Mukaida, N. CCL3-CCR5 axis regulates intratumoral accumulation of leukocytes and fibroblasts and promotes angiogenesis in murine lung metastasis process. *Journal of immunology* **181**, 6384-6393 (2008).
503 Sevko, A. & Umansky, V. Myeloid-derived suppressor cells interact with tumors in terms of myelopoiesis, tumorigenesis and immunosuppression: thick as thieves. *J Cancer* **4**, 3-11, doi:10.7150/jca.5047 (2013).
504 Tsui, P. *et al.* Generation, characterization and biological activity of CCL2 (MCP-1/JE) and CCL12 (MCP-5) specific antibodies. *Hum Antibodies* **16**, 117-125 (2007).
505 Xie, J. The hedgehog's trick for escaping immunosurveillance: The molecular mechanisms driving myeloid-derived suppressor cell recruitment in hedgehog signaling-dependent tumors. *Oncoimmunology* **3**, e29180, doi:10.4161/onci.29180 (2014).
506 Mukaida, N., Sasaki, S. & Baba, T. Chemokines in cancer development and progression and their potential as targeting molecules for cancer treatment. *Mediators of inflammation* **2014**, 170381, doi:10.1155/2014/170381 (2014).
507 Loberg, R. D. *et al.* CCL2 is a potent regulator of prostate cancer cell migration and proliferation. *Neoplasia* **8**, 578-586, doi:10.1593/neo.06280 (2006).
508 Lau, T. S. *et al.* Cancer cell-derived lymphotoxin mediates reciprocal tumour-stromal interactions in human ovarian cancer by inducing CXCL11 in fibroblasts. *The Journal of pathology* **232**, 43-56, doi:10.1002/path.4258 (2014).
509 Rupertus, K. *et al.* Interaction of the chemokines I-TAC (CXCL11) and SDF-1 (CXCL12) in the regulation of tumor angiogenesis of colorectal cancer. *Clin Exp Metastasis* **31**, 447-459, doi:10.1007/s10585-014-9639-4 (2014).
510 Gu, Y. C., Nilsson, K., Eng, H. & Ekblom, M. Association of extracellular matrix proteins fibulin-1 and fibulin-2 with fibronectin in bone marrow stroma. *British journal of haematology* **109**, 305-313 (2000).
511 Gu, Y. C., Talts, J. F., Gullberg, D., Timpl, R. & Ekblom, M. Glucocorticoids down-regulate the extracellular matrix proteins fibronectin, fibulin-1 and fibulin-2 in bone marrow stroma. *European journal of haematology* **67**, 176-184 (2001).
512 Fontanil, T. *et al.* Interaction between the ADAMTS-12 metalloprotease and fibulin-2 induces tumor-suppressive effects in breast cancer cells. *Oncotarget* **5**, 1253-1264, doi:10.18632/oncotarget.1690 (2014).
513 Baird, B. N. *et al.* Fibulin-2 is a driver of malignant progression in lung adenocarcinoma. *PloS one* **8**, e67054, doi:10.1371/journal.pone.0067054 (2013).
514 Schliekelman, M. J. *et al.* Targets of the tumor suppressor miR-200 in regulation of the epithelial-mesenchymal transition in cancer. *Cancer research* **71**, 7670-7682, doi:10.1158/0008-5472.CAN-11-0964 (2011).
515 Kobielak, A. & Fuchs, E. Alpha-catenin: at the junction of intercellular adhesion and actin dynamics. *Nat Rev Mol Cell Biol* **5**, 614-625, doi:10.1038/nrm1433 (2004).
516 Kolegraff, K., Nava, P., Helms, M. N., Parkos, C. A. & Nusrat, A. Loss of desmocollin-2 confers a tumorigenic phenotype to colonic epithelial cells through activation of Akt/beta-catenin signaling. *Molecular biology of the cell* **22**, 1121-1134, doi:10.1091/mbc.E10-10-0845 (2011).
517 Fang, W. K. *et al.* Down-regulated desmocollin-2 promotes cell aggressiveness through redistributing adherens junctions and activating beta-catenin signalling in oesophageal squamous cell carcinoma. *The Journal of pathology* **231**, 257-270, doi:10.1002/path.4236 (2013).

518 Harada, T., Shinohara, M., Nakamura, S., Shimada, M. & Oka, M. Immunohistochemical detection of desmosomes in oral squamous cell carcinomas: correlation with differentiation, mode of invasion, and metastatic potential. *International journal of oral and maxillofacial surgery* **21**, 346-349 (1992).
519 Hiraki, A. *et al.* Immunohistochemical staining of desmosomal components in oral squamous cell carcinomas and its association with tumour behaviour. *British journal of cancer* **73**, 1491-1497 (1996).
520 Brennan, D. & Mahoney, M. G. Increased expression of Dsg2 in malignant skin carcinomas: A tissue-microarray based study. *Cell Adh Migr* **3**, 148-154 (2009).
521 Chen, Y. J. *et al.* DSG3 is overexpressed in head neck cancer and is a potential molecular target for inhibition of oncogenesis. *Oncogene* **26**, 467-476, doi:10.1038/sj.onc.1209802 (2007).
522 Missan, D. S., Chittur, S. V. & DiPersio, C. M. Regulation of fibulin-2 gene expression by integrin alpha3beta1 contributes to the invasive phenotype of transformed keratinocytes. *The Journal of investigative dermatology* **134**, 2418-2427, doi:10.1038/jid.2014.166 (2014).
523 Ricciardelli, C. *et al.* Regulation of stromal versican expression by breast cancer cells and importance to relapse-free survival in patients with node-negative primary breast cancer. *Clinical cancer research : an official journal of the American Association for Cancer Research* **8**, 1054-1060 (2002).
524 Ricciardelli, C. *et al.* Elevated levels of versican but not decorin predict disease progression in early-stage prostate cancer. *Clinical cancer research : an official journal of the American Association for Cancer Research* **4**, 963-971 (1998).
525 Arslan, F. *et al.* The role of versican isoforms V0/V1 in glioma migration mediated by transforming growth factor-beta2. *British journal of cancer* **96**, 1560-1568, doi:10.1038/sj.bjc.6603766 (2007).
526 Serra, M. *et al.* V3 versican isoform expression alters the phenotype of melanoma cells and their tumorigenic potential. *International journal of cancer. Journal international du cancer* **114**, 879-886, doi:10.1002/ijc.20813 (2005).
527 Voutilainen, K. *et al.* Versican in epithelial ovarian cancer: relation to hyaluronan, clinicopathologic factors and prognosis. *International journal of cancer. Journal international du cancer* **107**, 359-364, doi:10.1002/ijc.11423 (2003).
528 Kunisada, M. *et al.* Increased expression of versican in the inflammatory response to UVB- and reactive oxygen species-induced skin tumorigenesis. *The American journal of pathology* **179**, 3056-3065, doi:10.1016/j.ajpath.2011.08.042 (2011).
529 Zheng, P. S. *et al.* Versican/PG-M G3 domain promotes tumor growth and angiogenesis. *FASEB journal : official publication of the Federation of American Societies for Experimental Biology* **18**, 754-756, doi:10.1096/fj.03-0545fje (2004).
530 Yee, A. J. *et al.* The effect of versican G3 domain on local breast cancer invasiveness and bony metastasis. *Breast cancer research : BCR* **9**, R47, doi:10.1186/bcr1751 (2007).
531 Miquel-Serra, L. *et al.* V3 versican isoform expression has a dual role in human melanoma tumor growth and metastasis. *Laboratory investigation; a journal of technical methods and pathology* **86**, 889-901, doi:10.1038/labinvest.3700449 (2006).
532 Ang, L. C. *et al.* Versican enhances locomotion of astrocytoma cells and reduces cell adhesion through its G1 domain. *J Neuropathol Exp Neurol* **58**, 597-605 (1999).
533 Paris, S., Sesboue, R., Chauzy, C., Maingonnat, C. & Delpech, B. Hyaluronectin modulation of lung metastasis in nude mice. *European journal of cancer* **42**, 3253-3259, doi:10.1016/j.ejca.2006.06.012 (2006).
534 Munro, S. B., Turner, I. M., Farookhi, R., Blaschuk, O. W. & Jothy, S. E-cadherin and OB-cadherin mRNA levels in normal human colon and colon carcinoma. *Exp Mol Pathol* **62**, 118-122 (1995).
535 Shibata, T., Ochiai, A., Gotoh, M., Machinami, R. & Hirohashi, S. Simultaneous expression of cadherin-11 in signet-ring cell carcinoma and stromal cells of diffuse-type gastric cancer. *Cancer letters* **99**, 147-153 (1996).

536 Pishvaian, M. J. *et al.* Cadherin-11 is expressed in invasive breast cancer cell lines. *Cancer research* **59**, 947-952 (1999).
537 Tomita, K. *et al.* Cadherin switching in human prostate cancer progression. *Cancer research* **60**, 3650-3654 (2000).
538 Nam, E. H. *et al.* ZEB2-Sp1 cooperation induces invasion by upregulating cadherin-11 and integrin alpha5 expression. *Carcinogenesis* **35**, 302-314, doi:10.1093/carcin/bgt340 (2014).
539 Assefnia, S. *et al.* Cadherin-11 in poor prognosis malignancies and rheumatoid arthritis: common target, common therapies. *Oncotarget* **5**, 1458-1474, doi:10.18632/oncotarget.1538 (2014).
540 Levental, K. R. *et al.* Matrix crosslinking forces tumor progression by enhancing integrin signaling. *Cell* **139**, 891-906, doi:10.1016/j.cell.2009.10.027 (2009).
541 Wong, C. C. *et al.* Hypoxia-inducible factor 1 is a master regulator of breast cancer metastatic niche formation. *Proceedings of the National Academy of Sciences of the United States of America* **108**, 16369-16374, doi:10.1073/pnas.1113483108 (2011).
542 Kirschmann, D. A. *et al.* A molecular role for lysyl oxidase in breast cancer invasion. *Cancer research* **62**, 4478-4483 (2002).
543 Erler, J. T. & Giaccia, A. J. Lysyl oxidase mediates hypoxic control of metastasis. *Cancer research* **66**, 10238-10241, doi:10.1158/0008-5472.CAN-06-3197 (2006).
544 Granchi, C. *et al.* Bioreductively activated lysyl oxidase inhibitors against hypoxic tumours. *ChemMedChem* **4**, 1590-1594, doi:10.1002/cmdc.200900247 (2009).
545 Le, Q. T. *et al.* Validation of lysyl oxidase as a prognostic marker for metastasis and survival in head and neck squamous cell carcinoma: Radiation Therapy Oncology Group trial 90-03. *Journal of clinical oncology : official journal of the American Society of Clinical Oncology* **27**, 4281-4286, doi:10.1200/JCO.2008.20.6003 (2009).
546 Erler, J. T. *et al.* Hypoxia-induced lysyl oxidase is a critical mediator of bone marrow cell recruitment to form the premetastatic niche. *Cancer cell* **15**, 35-44, doi:10.1016/j.ccr.2008.11.012 (2009).
547 Cox, T. R. & Erler, J. T. Remodeling and homeostasis of the extracellular matrix: implications for fibrotic diseases and cancer. *Disease models & mechanisms* **4**, 165-178, doi:10.1242/dmm.004077 (2011).
548 Fang, M., Yuan, J., Peng, C. & Li, Y. Collagen as a double-edged sword in tumor progression. *Tumour biology : the journal of the International Society for Oncodevelopmental Biology and Medicine* **35**, 2871-2882, doi:10.1007/s13277-013-1511-7 (2014).
549 Gilkes, D. M. *et al.* Collagen prolyl hydroxylases are essential for breast cancer metastasis. *Cancer research* **73**, 3285-3296, doi:10.1158/0008-5472.CAN-12-3963 (2013).
550 Xiong, G., Deng, L., Zhu, J., Rychahou, P. G. & Xu, R. Prolyl-4-hydroxylase alpha subunit 2 promotes breast cancer progression and metastasis by regulating collagen deposition. *BMC cancer* **14**, 1, doi:10.1186/1471-2407-14-1 (2014).
551 Zhu, G. G. *et al.* Immunohistochemical study of type I collagen and type I pN-collagen in benign and malignant ovarian neoplasms. *Cancer* **75**, 1010-1017 (1995).
552 Huijbers, I. J. *et al.* A role for fibrillar collagen deposition and the collagen internalization receptor endo180 in glioma invasion. *PloS one* **5**, e9808, doi:10.1371/journal.pone.0009808 (2010).
553 Cao, X. L. *et al.* Expression of type IV collagen, metalloproteinase-2, metalloproteinase-9 and tissue inhibitor of metalloproteinase-1 in laryngeal squamous cell carcinomas. *Asian Pac J Cancer Prev* **12**, 3245-3249 (2011).
554 Young, B. B., Zhang, G., Koch, M. & Birk, D. E. The roles of types XII and XIV collagen in fibrillogenesis and matrix assembly in the developing cornea. *Journal of cellular biochemistry* **87**, 208-220, doi:10.1002/jcb.10290 (2002).
555 Font, B., Eichenberger, D., Rosenberg, L. M. & van der Rest, M. Characterization of the interactions of type XII collagen with two small proteoglycans from fetal bovine tendon, decorin and fibromodulin. *Matrix Biol* **15**, 341-348 (1996).

556 Yen, T. Y. *et al.* Using a cell line breast cancer progression system to identify biomarker candidates. *J Proteomics* **96**, 173-183, doi:10.1016/j.jprot.2013.11.006 (2014).
557 Karagiannis, G. S. *et al.* Proteomic signatures of the desmoplastic invasion front reveal collagen type XII as a marker of myofibroblastic differentiation during colorectal cancer metastasis. *Oncotarget* **3**, 267-285, doi:10.18632/oncotarget.451 (2012).
558 Liu, X. *et al.* Induction of Mast Cell Accumulation by Tryptase via a Protease Activated Receptor-2 and ICAM-1 Dependent Mechanism. *Mediators of inflammation* **2016**, 6431574, doi:10.1155/2016/6431574 (2016).
559 Cui, Y. *et al.* Mouse mast cell protease-6 and MHC are involved in the development of experimental asthma. *Journal of immunology* **193**, 4783-4789, doi:10.4049/jimmunol.1302947 (2014).
560 de Vries, V. C., Elgueta, R., Lee, D. M. & Noelle, R. J. Mast cell protease 6 is required for allograft tolerance. *Transplantation proceedings* **42**, 2759-2762, doi:10.1016/j.transproceed.2010.05.168 (2010).
561 Zeng, X., Zhang, S., Xu, L., Yang, H. & He, S. Activation of protease-activated receptor 2-mediated signaling by mast cell tryptase modulates cytokine production in primary cultured astrocytes. *Mediators of inflammation* **2013**, 140812, doi:10.1155/2013/140812 (2013).
562 Orinska, Z. *et al.* IL-15 constrains mast cell-dependent antibacterial defenses by suppressing chymase activities. *Nature medicine* **13**, 927-934, doi:10.1038/nm1615 (2007).
563 Mirghomizadeh, F. *et al.* Transcriptional regulation of mouse mast cell protease-2 by interleukin-15. *The Journal of biological chemistry* **284**, 32635-32641, doi:10.1074/jbc.M109.015446 (2009).
564 Chung, I. S. *et al.* Peritumor injections of purified tumstatin delay tumor growth and lymphatic metastasis in an orthotopic oral squamous cell carcinoma model. *Oral Oncol* **44**, 1118-1126, doi:10.1016/j.oraloncology.2008.01.017 (2008).
565 Yu, H. M., Mouw, J. K. & Weaver, V. M. Forcing form and function: biomechanical regulation of tumor evolution. *Trends in cell biology* **21**, 47-56, doi:10.1016/j.tcb.2010.08.015 (2011).
566 Nilsson, G., Metcalfe, D. D. & Taub, D. D. Demonstration that platelet-activating factor is capable of activating mast cells and inducing a chemotactic response. *Immunology* **99**, 314-319 (2000).
567 Conway, W. C. *et al.* Age-related lymphatic dysfunction in melanoma patients. *Ann Surg Oncol* **16**, 1548-1552, doi:10.1245/s10434-009-0420-x (2009).
568 Macdonald, J. B. *et al.* Malignant melanoma in the elderly: different regional disease and poorer prognosis. *J Cancer* **2**, 538-543 (2011).
569 Sugimoto, M. *et al.* Influences of chymase and angiotensin I-converting enzyme gene polymorphisms on gastric cancer risks in Japan. *Cancer epidemiology, biomarkers & prevention : a publication of the American Association for Cancer Research, cosponsored by the American Society of Preventive Oncology* **15**, 1929-1934, doi:10.1158/1055-9965.EPI-06-0339 (2006).
570 Kazenwadel, J., Secker, G. A., Betterman, K. L. & Harvey, N. L. In vitro assays using primary embryonic mouse lymphatic endothelial cells uncover key roles for FGFR1 signalling in lymphangiogenesis. *PloS one* **7**, e40497, doi:10.1371/journal.pone.0040497 (2012).
571 Miyazaki, H. *et al.* Expression of platelet-derived growth factor receptor beta is maintained by Prox1 in lymphatic endothelial cells and is required for tumor lymphangiogenesis. *Cancer science* **105**, 1116-1123, doi:10.1111/cas.12476 (2014).
572 Waern, I., Lundequist, A., Pejler, G. & Wernersson, S. Mast cell chymase modulates IL-33 levels and controls allergic sensitization in dust-mite induced airway inflammation. *Mucosal immunology* **6**, 911-920, doi:10.1038/mi.2012.129 (2013).
573 Jawdat, D. M., Albert, E. J., Rowden, G., Haidl, I. D. & Marshall, J. S. IgE-mediated mast cell activation induces Langerhans cell migration in vivo. *Journal of immunology* **173**, 5275-5282 (2004).

574 Chen, R. *et al.* Mast cells play a key role in neutrophil recruitment in experimental bullous pemphigoid. *The Journal of clinical investigation* **108**, 1151-1158, doi:10.1172/JCI11494 (2001).